“One who makes no mistakes makes nothing at all.”

Giacomo Casanova

University of Alberta

Characterization of NFκB Inhibition by Poxviral Ankryin/F-box Proteins

by

Kristin Alison Burles

A thesis submitted to the Faculty of Graduate Studies and Research
in partial fulfillment of the requirements for the degree of

Master of Science

in

Virology

Medical Microbiology and Immunology

Fall 2012
Edmonton, Alberta

ABSTRACT

One of the most notable features of poxviruses is their ability to regulate cellular signaling pathways, including the ubiquitin-proteasome system. Ubiquitin plays a crucial role in the fate of a protein. Typically poly-ubiquitinated proteins are degraded by the 26S proteasome. The Skp1, culllin-1, F-box (SCF) ubiquitin ligase links ubiquitin to a substrate through a family of proteins possessing F-box domains. Recently, our lab has determined that ectromelia virus, the causative agent of lethal mousepox, encodes four F-box-containing proteins, ECTV002, ECTV005, ECTV154, and ECTV165, that interact with the SCF ubiquitin ligase. Many cellular pathways are tightly controlled by the SCF ubiquitin ligase, including the nuclear factor kappa B (NFκB) pathway, which mediates an antiviral immune response. We have shown that the ectromelia ankyrin/F-box proteins inhibit NFκB activation. Our data also suggest that ECTV002 and ECTV154 mediate virion release or spread.

ACKNOWLEDGMENTS

I would first off like to thank my supervisor, Dr. Michele Barry, for all of her support and encouragement during the course of my graduate degree. Michele has been supportive in ways that go beyond being a mentor and our relationship has developed into something that I think is very special. I remember the first time we met. I had no confidence and I definitely didn't feel smart enough to be sitting in her office. I would like to thank Michele for taking a chance on me.

There are many members of the lab who I would also like to thank. I was lucky enough to join Barry lab 2.0, which was filled with a fantastic group of people who have become really close friends. Nick van Buuren and Katie Fagan-Garcia were such great mentors, and without their supervision I would still be lysing cells in PBS. Nick has helped me navigate through of a lot of the science valleys, and if it weren't for him I would probably still be spinning my wheels and staring up at the peaks. Stephanie Campbell and Logan Banadyga have also taught me so much - a little about science and a lot about life. Stephanie and Logan both exemplify the type of person that I want to be; they are fun, thoughtful, intelligent, and interesting. I would also like to thank two members of Barry lab 3.0, Robyn Burton and John Thibault. Robyn and John are super fun and they have made the days go easy. As well, Chad Irwin, an inaugural member of our lab, has been a great friend. Chad is a bright, hard-working individual and I know that he will become a fantastic scientist.

Finally, I would like to thank my family. I'm not sure if any of them really know what I've actually been doing for the past three years, however they have given me love and support in their own unique ways. It is because of my parents, Wes and Kathy Burles, that I have become independent and hard working - two characteristics that have allowed me to complete a master's degree that I can say I'm proud of. My second parents, Wes and Karen Perry, have shown me that there are more important things in life than just working and studying - this has helped me to finally be on a life path that I'm excited to be on.

TABLE OF CONTENTS

TABLE OF CONTENTS

TABLE OF CONTENTS

TABLE OF CONTENTS

LIST OF TABLES

LIST OF FIGURES

CHAPTER 1

CHAPTER 2

CHAPTER 3

LIST OF FIGURES

CHAPTER 4

APPENDIX

LIST OF ABBREVIATIONS

AcNPV	*Autographa californica* nuclear polyhedrosis
ALR	AIM2-like receptor
APC/C	anaphase promoting complex/cyclosome
Ank	ankyrin
AraC	cytosine β-D-arabinofuransoside hydrochloride
ATCC	American Type Culture Collection
Bcl-2	B-cell lymphoma 2
Bcl-3	B-cell lymphoma 3
BLAST	Basic Local Alignment Search Tool
BTB	Bric-a-Brac, Tramtrack, Broad complex
βTrCP	transducin repeat-containing protein
CBP	CREB-binding protein
cIAP	cellular inhibitor of apoptosis protein
CK1α	casein kinase 1α
CMC	carboxymethylcellulose
CMPV	campelpox virus
CO	codon optimized
Cop	Copenhagen
CPXV	cowpox virus
Crm	cytokine response modifier
DAG	diacyglycerol
DAPI	4,6-diamino-2-phenylindole
DEPC	diethylpyrocarbonate
DIGE	2D difference in gel electrophoresis
dNTPs	deoxyribonucleotide triphosphate
dsDNA	double-stranded DNA
DTT	dithiothreitol
EBV	Epstein-Barr virus
ECL	enhanced chemiluminescence
E. coli	*Escherichia coli*
ECTV	ectromelia virus
EDTA	ethylenediaminetetraacetic acid
eIF2	eukaryotic initiation factor 2
EV	extracellular virion
GPT	guanine phosphoribosyltransferase
GSK3β	glycogen synthase kinase 3β
HBV	hepatitis B virus
HCV	hepatatis C virus
HECT	homologous to E6AP C-terminus
HI-FBS	heat inactivate fetal bovine serum
HIV-1	human immunodeficiency virus 1
HRP	horse-radish peroxidase

LIST OF ABBREVIATIONS

HTLV-1	human T-lymphotrophic virus 1
IκB	inhibitors of κB
IKK	IκB kinase
IL-1β	interleukin-1 beta
IL-1R	interleukin-1 receptor
IPTG	isopropyl β-D-1-thiogalactopyranoside
IRAK	IL-1R associated kinase
IRF	interferon regulatory transcription factor
IV	immature virion
K	lysine
κB	kappa B
KSHV	Kaposi's sarcoma-associated herpesvirus
LB	Luria Bertani
LMP	low melting point
LRR	leucine rich repeat
LZ	leucine zipper
MAPK	mitogen-activated protein
MARCH	membrane-associated RING-CH
MNF	MYXV nuclear factor
MOCV	molluscm contagiosum virus
MOI	multiplicity of infection
MPA	mycophenolic acid
MPXV	monkeypox virus
mRNA	messenger ribonucleic acid
MSK1	mitogen- and stress-activated protein kinase
MV	mature virion
MVA	Modified Vaccinia strain Ankara
MyD88	myeloid differentiation primary response gene 88
MYXV	myxoma virus
NCBI	National Centre for Biotechnology Information
NCS	newborn calf serum
NEMO	NFκB essential modulator
NFκB	nuclear factor kappa-light-chain enhancer of activated B cells
NIK	NFκB-inducing kinase
NLR	nod-like receptor
NP-40	Nonident P-40
ORF	open reading frame
PACR	poxvirus APC/cyclosome regulator
PBS	phosphate-buffered saline
PCR	polymerase chain reactions
PFU	plaque forming units
PKA	protein kinase A

LIST OF ABBREVIATIONS

PKR	protein kinase R
PP6	protein phosphatase 6
PRANC	pox proteins repeats of ankyrin C-terminal
PRR	pattern recognition receptor
RING	really interesting new gene
RIP1	Receptor-interacting protein 1
RHD	Rel homology domain
RSV	respiratory syncytial virus
RT-PCR	reverse transcription PCR
SDD	scaffold/dimerization domain
SDS	sodium dodecyl sulphate
SDS-PAGE	sodium dodecyl sulphate polyacrylamide gel electrophoresis
SILAC	stable isotope labeling with amino acids in culture
SOC	super optimal broth with calabolite repression
SSC	standard saline citrate
TAD	transcription activation domain
TAE	Tris-acetate-EDTA
TAK1	TGFβ-activated kinase-1
TBS-T	Tris-buffered saline with Tween 20
TE	Tris-EDTA
TIR	Toll IL-1R
TIRAP	Toll/interleukin-1 receptor adapter protein
TLR	Toll-like receptor
TNF	tumor necrosis factor
TNFR	TNF receptor
TRADD	TNFR1-associated DEATH domain protein
TRAF2	TNF receptor-associated factor 2
TRIF	TIR domain-containing adapter-inducing IFN-β
VARV	variola virus
VACV811	vaccinia virus strain 811
VACV	vaccinia virus
V	volts
WD40	tryptophan-aspartic 40 amino acid
WV	wrapped virion
YFP	yellow fluorescent protein
X-gal	5-bromo-4-chloro-3-indoyl-β-galactopyranoside

Chapter 1: Introduction

1.1 POXVIRUSES

The *Poxviridae* comprise a unique family of viruses distinguished by a single linear double-stranded DNA (dsDNA) genome, a large brick-shaped virion, and the ability to replicate exclusively in the cytoplasm of an infected cell (197). The most notorious member of the *Poxviridae* family, variola virus, is the causative agent of smallpox, a disease that has killed more humans in recorded history than all other infectious diseases combined (89). Although smallpox was eradicated in 1977 through a dedicated effort by the World Health Organization (89), other poxviruses cause clinically relevant diseases in animals and humans, and recent outbreaks of monkeypox virus underline the importance of studying these viruses (224). In addition to the threat of emerging poxvirus outbreaks in humans, the use of poxviruses for gene-delivery and vaccine vectors, and oncolytic therapies has generated a renewed interest in studying poxvirus modulation of immune signalling pathways (35, 244, 272).

1.1.1 Classification

Members of the *Poxviridae* are divided into the subfamilies *Chordopoxvirinae* and *Entomopoxvirina*e, which infect vertebrates and insects respectively (197) (Table 1-1). The *Chordopoxvirinae* is further divided into nine genera based on genetic similarity: *Avipoxvirus, Capripoxvirus, Cervidpoxvirus, Leporipoxvirus, Molluscipoxvirus, Orthopoxvirus, Parapoxvirus, Suipoxvirus,* and *Yatapoxvirus*. Interestingly, members of the *Molluscipoxvirus, Orthopoxvirus, Parapoxvirus,* and *Yatapoxvirus* genera contain viruses that cause disease in humans by zoonoses (63). However, only Molluscum contagiosum, a molluscipoxvirus, and variola virus and vaccinia virus, two orthopoxviruses, are natural pathogens of humans (63). The *Orthopoxvirus* genus is the best studied, and includes camelpox virus (CMPV), cowpox virus (CPXV), ectromelia virus (ECTV), monkeypox virus (MPXV), taterapox virus, variola virus (VARV), and vaccinia virus (VACV).

Table 1-1. The *Poxviridae* family

Subfamily	Genus	Member viruses
Chordopoxvirinae	*Avipoxvirus*	Canarypox virus Fowlpox virus
	Capripoxvirus	Goatpox virus Lumpy skin disease virus Sheeppox virus
	Cervidpoxvirus	Deerpox virus
	Leporipoxvirus	Myxoma virus Shope fibroma virus
	Molluscipoxvirus	Mollusm contagiosum virus
	Orthopoxvirus	Camelpox virus Cowpox virus Ectromelia virus Monkeypox virus Taterapox virus Vaccinia virus Variola virus
	Parapoxvirus	Bovine papular stomatitis virus Orf virus
	Suipoxvirus	Swinepox virus
	Yatapoxvirus	Tanapox virus Yaba-like disease virus Yaba monkey tumour virus
Entomopoxvirinae	*Entomopoxvirus* α	*Melontha melontha*
	Entomopoxvirus β	*Amsacta moorei* *Melanoplus sanguinipes*
	Entomopoxvirus γ	*Chrionimus luridus*

Poxviruses are a large family of viruses that infect vertebrates and invertebrates. The *Entomopoxvirina*e infect invertebrates, including insects, and are divided into three genera. The *Chordopoxvirinae* infect a wide range of vertebrates, and are divided into nine genera: members of the *Avipoxvirus* genus infect birds*;* members of the *Capripoxvirus* genus infect goats, sheep, and cattle; members of the *Cervipoxvirus* genus infect deer; members of the *Leporipoxvirus* genus infect rabbits and hares; members of the *Molluscipoxvirus* genus infect humans; members of the *Orthopoxvirus* genus infect humans, monkeys, cows, mice, camels, and a variety of other small mammals; members of the *Parapoxvirus* genus infect goats, sheep, cattle*,* and humans; members of the *Suipoxvirus* genus infect swine; and members of the *Yatapoxvirus* genus infect humans and non-human primates (127).

Work in our lab focuses on two members of the *Orthopoxvirus* genera, VACV and ECTV. VACV was used to vaccinate against smallpox (89, 197). Although the origins of VACV are unknown, the genomes of VACV and VARV are genetically similar (197). VACV is the most well studied member of the *Poxviridae*, and serves as an excellent model for studying virus-host interactions (138, 198, 244). ECTV is highly related to VARV and causes mousepox, a smallpox-like infection, in susceptible mouse strains, making ECTV a good model to study poxvirus infection *in vivo* (83, 84).

1.1.2 Genome

Poxviruses possess a single linear dsDNA genome that ranges from approximately 150 to 300 kilobase pairs in length. The DNA strands are connected by hairpin loops, which consist of AT-rich inverted terminal repeats (17). The genome encodes approximately 150 to 350 open reading frames (ORFs) (197), which are identified by a numerical designation, assigned successively from one end of the genome to the other (197). The exception to this designation is the Copenhagen strain of VACV (66). Prior to whole genome sequencing, *HindIII* restriction enzyme digestion was used to identify genomic fragments. Consequently, ORFs in the Copenhagen strain of VACV are named by *HindIII* restriction enzyme DNA fragment letter (letters A to P), followed by a number (assigned successively from left to right), and either "L" or "R" (left or right; depending on the direction that the gene is transcribed) (Figure 1-1). The genome possesses a central conserved region and variable regions at both ends. The conserved region contains close to 100 ORFS that are common to many chordopoxviruses and encode virion structural proteins, replication machinery, and immune evasion functions (102, 284). The variable regions encode many non-essential ORFs dedicated to regulating cellular signalling pathways and evading the host immune response (138, 191, 244); however, a few essential genes are also located in the variable ends of the genome (197). Many ORFs in

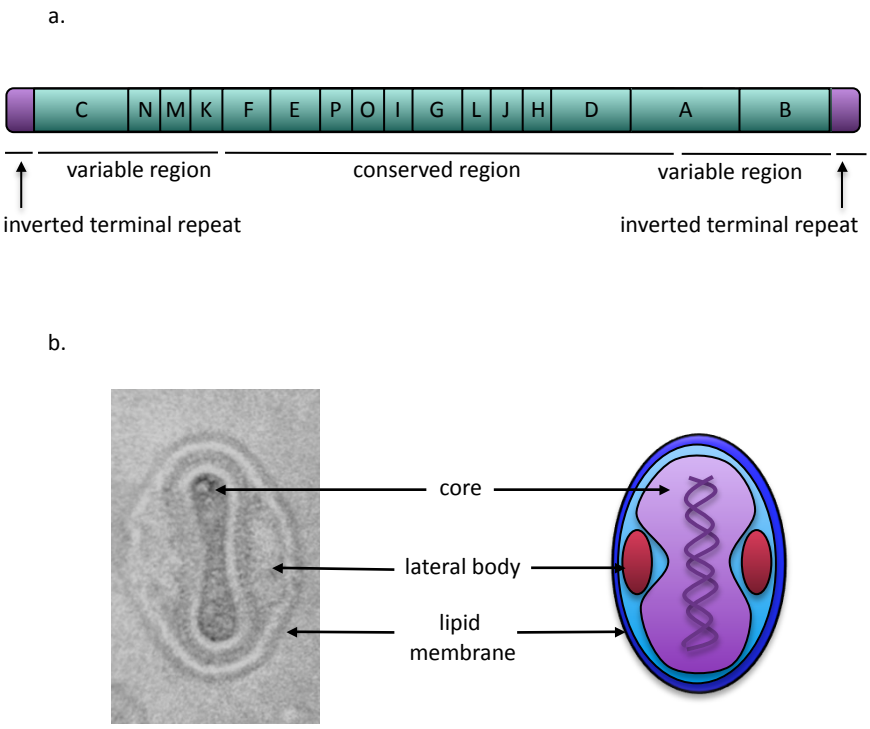

Figure 1-1. Poxvirus genome organization and structure. (a.) The poxvirus genome contains a central conserved region flanked by variable regions. At the ends of the genome, inverted terminal repeat form hairpin loops that connect the two DNA strands. The letters correspond to the genomic fragments in VACVCop that were identified by *HindIII* restriction enzyme digestion (66). **(b.)** The basic poxvirus infectious unit is characterized by its dumbell-shaped protein core and lateral bodies, which are easily visualized by electron microscopy. Pictured above is the mature virion, which contains a single lipid membrane (123).

the variable region are unique to different members of the *Poxviridae* and these dictate host-range. Interestingly, deletion of genes from the variable regions does not usually alter virus growth *in vitro*; however, genes involved in immune evasion are usually important for virulence *in vivo* (102, 197).

1.1.3 Life cycle

1.1.3.1 Entry. Poxviruses form two types of infectious particles, mature virions (MV; also known as intracellular mature virus, IMV), and extracellular virions (EV; also known as extracellular enveloped virus, EEV) (56, 197) (Figure 1-1). The MV, which is the basic infectious particle, contains a single lipid bilayer surrounding a dumbbell-shaped protein capsid that encapsulates the dsDNA genome and numerous enzymes required for early gene expression. The single lipid bilayer contains at least twenty-five viral proteins that are important for virion maturation or virion entry (197, 246). EVs are distinguished from MVs by an additional lipid membrane containing at least six unique viral proteins that are important for virion spread through actin projectiles (147, 197). The mechanism driving virus entry has generated much controversy within the poxvirus field. It has been demonstrated that MVs bind a number of different cell surface molecules, including glycosaminglycans, heparin sulfate, chondroitin sulfate, and laminin, depending on cell type, virus strain, and experimental conditions (22, 226, 241, 298). However, no cell surface molecules have been identified for EV (241). A fusion event is necessary for MV and EV internalization. Fusion is mediated by the so-called entry-fusion complex, a large viral protein complex consisting of at least twelve virally-encoded proteins contained in the MV lipid membrane (246). For EV fusion, disruption of the outer lipid membrane must occur in order to expose the entry-fusion complex contained in the primary lipid membrane (161). The location of the fusion event has generated controversy, since fusion of MVs and EVs has been demonstrated both at the cell surface and after endocytic uptake of the virus particles (81, 250). However, there is

increasing evidence suggesting that most virus particles undergo fusion with an endosome (185, 233, 240, 277) (Figure 1-2).

1.1.3.2 Gene expression and DNA replication. Poxvirus genes are expressed temporally and fall into early, intermediate, and late expression groups based on the promoter (7, 29). Some genes are under the control of both an early and a late promoter and these genes are categorized as early/late genes (7). Fusion between the virion and cell membranes leads to the release of the virion core into the cytoplasm, where it is transported along microtubules to the site of transcription outside of the nucleus, termed the "virus factory" (36, 62, 146). The viral RNA polymerase and transcription factors contained within the virion core initialize synthesis of early viral mRNAs, which encode proteins involved in DNA replication (139, 164, 253), enhanced nucleotide biosynthesis (124, 254), immune evasion, and intermediate gene transcription (2, 140, 234). DNA replication begins within a few hours after the cell has been infected, corresponding with the expression of early genes involved in this process. Termination of early mRNA synthesis occurs as the core disassembles, most likely because the early mRNA transcription complex becomes disrupted (12). Intermediate genes are expressed after DNA replication but before late gene expression (29). The requirement for DNA replication to occur before intermediate mRNAs are synthesized is likely because the genome within the core is inaccessible to the newly synthesized intermediate transcription factors (149). Intermediate genes typically encode regulators of late gene transcription. Late genes are transcribed following intermediate gene transcription, and typically encode structural proteins that make up new infectious particles and enzymes that are packaged in the virion and are required to initiate early mRNA transcription during the next round of infection (228).

1.1.3.3 Virion assembly and egress. Production of infectious virions begins in the virus factories with the formation of crescent-shaped structures, comprised of lipids and virion core proteins, which surround the newly replicated DNA

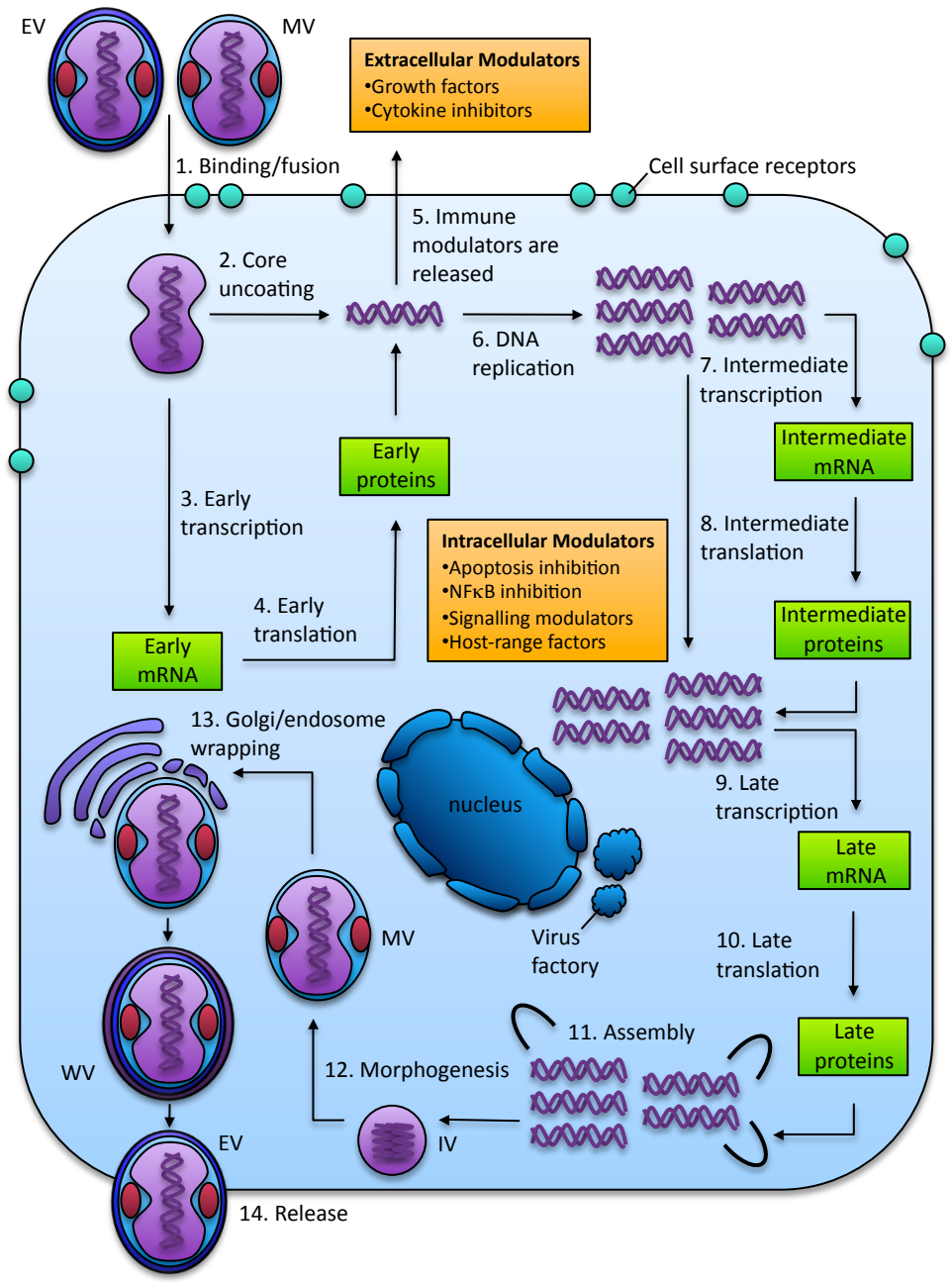
EV
MV
Extracellular Modulators
•Growth factors
•Cytokine inhibitors
1. Binding/fusion
Cell surface receptors
5. Immune modulators are released
2. Core uncoating
6. DNA replication
7. Intermediate transcription
Intermediate mRNA
Early proteins
3. Early transcription
Intracellular Modulators
•Apoptosis inhibition
•NFκB inhibition
•Signalling modulators
•Host-range factors
8. Intermediate translation
Intermediate proteins
4. Early translation
Early mRNA
13. Golgi/endosome wrapping
nucleus
9. Late transcription
Late mRNA
MV
Virus factory
10. Late translation
11. Assembly
Late proteins
WV
12. Morphogenesis
IV
EV
14. Release

Figure 1-2. Poxvirus lifecycle. Mature virions (MVs) and extracellular virions (EVs) bind to the cell surface receptors, followed by a fusion event that releases the virion core into the cytoplasm **(1)**. As the core uncoats **(2)**, early genes are transcribed **(3)**, resulting in production of proteins that are important for immune defense, DNA replication, and intermediate gene expression **(4)**. Extracellular modulators that enhance poxvirus lifecycle are also released from the cell **(5)**. Following uncoating of the core, DNA replication occurs **(6)** and intermediate genes are expressed **(7 and 8)**, followed by expression of late genes **(9 and 10)**. Immature virions (IVs) are assembled in crescent-shaped membranes with unknown origins **(11)**. Following morphogenesis when the genome is packaged into the core **(12)**, MVs are either released following cell lysis, or acquire an additional membrane from the endosome or Golgi-complex to become a wrapped virion (WV) **(13)**. These virions are released by exocytosis as EVs **(14)**. Uncoating of the core and and transcription occur in perinuclear regions called virus factories (adapted from 182).

genome (61, 197). Poxviruses encode a scaffold protein that provides a stable structure for a lipid bilayer to form (115, 266), and proteins synthesized in the endoplasmic reticulum can be transported to the growing lipid bilayer, bringing with them additional lipids (128, 129). An immature virion (IV) is formed once the lipid bilayer fully encloses the core. Transition to a MV occurs when the dsDNA genome gets packaged into the IV, resulting in proteolytic cleavage and loss of the scaffold, association of additional membrane proteins, and core rearrangement. Most MVs are released during cell lysis; however, some acquire two additional lipid membranes from endosomes and the trans-Golgi network to form wrapped virions (WV) (238). During their release by excocytosis, WVs fuse with the plasma membrane and lose one of their two additional membranes to become EVs. EVs are immediately released, or remain associated with the outside of the plasma membrane and are propelled by actin polymerization to infect adjacent cells (24, 59). MVs mediate host-to-host transmission, while EVs, the less abundant of the two, mediate spread within an infected host (255).

1.1.4 Poxviruses and the immune response

Poxvirus infection activates a potent immune response that includes both innate and adaptive immunity (138, 191, 244); however, members of the *Poxviridae* have evolved a number of mechanisms to counteract the immune response (138, 198, 244). Poxviruses encode secreted receptor homologues and binding proteins that block complement (131, 154-156, 190, 229), chemokine (10, 99, 159, 160, 207, 283), and cytokine responses (3, 4, 25, 55, 126, 175, 235, 252, 256, 262, 265, 281, 306) (Table 1-2). In addition, myxoma virus (MYXV) encodes a protein that enhances blood coagulation, thus preventing motility of immune factors and lymphocytes in the blood (174, 177, 203, 282). Members of the *Poxviridae* also encode a number of intracellular proteins that down regulate immune receptors (19, 103, 181), inhibit inflammation (79, 137, 150, 221, 223, 278, 279), inhibit the interferon response (38, 39, 64, 201, 242), and prevent

Table 1-2. Secreted poxviral proteins that inhibit the immune response

Virus	Viral Factor	Mechanism	References
Inhibitors of complement			
VACV	C21L (VCP)	Binds complement; inactivates complement proteins	(131, 154, 156)
CPXV	IMP	Binds complement; inactivates complement proteins	(155, 190)
VARV	SPICE	Binds complement; inactivates complement proteins	(229)
Inhibitors of chemokines			
VACV	CrmB, C, D, E	Binds chemokines; inhibits activity of chemokines	(10, 207)
MYXV	M-T2	Binds chemokines; inhibits activity of chemokines	(99, 160)
MYXV	B15R	Binds chemokines; inhibits activity of chemokines	(159, 283)
Inhibitors of cytokine receptor stimulation			
CPXV	D7L	Soluble TNF receptor; inhibits stimulation of the TNF receptor	(126, 175, 235, 252)
MYXV	B8R	Soluble TNF receptor; inhibits stimulation of the TNF receptor	(281)
VACV	B18R	Souluble IL-1β receptor; inhibits stimulation of the IL-1β receptor	(3, 262)
Molluscm contagiosum	CrmB, C, D, E	Binds IL-18; prevents stimulation of the IL-18 receptor	(25, 306)
ECTV	M-T2	Binds IL-18; prevents stimulation of the IL-18 receptor	(256)
VACV	B15R	Soluble IFN-γ receptor; inhibits IFNγ signalling	(4)
VACV	MC45L	Soluble IFN α/β receptor; inhibits IFNγ signalling	(55, 265)
Inhibitors of the inflammatory response			
MYXV	SERP-1	Extracellular protease inhibitor; cleaves proteins important for blood coagulation, acts as a substrate for proteins that mediate coagulation, resulting in decreased mobility of immune cells to the site of infection	(174, 177, 203, 282)

Poxviruses encode many secreted proteins that modulate the immune response. VCP, vaccinia complement control protein; IMP, inflammation modulatory protein; SPICE, smallpox inhibitor of complement enzymes; Crm, cytokine response modifier; TNF, tumour necrosis factor; IL-1β, interleukin-1 beta; IL-18, interleukin-18; IFN-γ, interferon γ.

Table 1-3. Intracellular poxviral proteins that inhibit the immune response

Virus	Viral Factor	Mechanism	References
Downregulation of receptors			
MYXV	M153R	Ubiquitin ligase; downregulates MHC class I, CD4, ALCAM (CD166), CD95	(19, 103, 181)
Inhibitors of the inflammatory response			
CPXV	SPI-3	Serine protease inhibitor; cleaves proteins important for blood coagulation, resulting in decreased mobility of immune cells to the site of infection	(278)
VACV	K2L (SPI-3)	Serine protease inhibitor; cleaves proteins important for blood coagulation, resulting in decreased mobility of immune cells to the site of infection	(279)
MYXV	M013L	Pyrin protein; binds ASC and prevents inflammasome activation	(137, 221)
Shope fibroma virus	gp013L	Pyrin protein; binds ASC and prevents inflammasome activation	(79)
VACV(WR)	B13R (SPI-2)	Serine protease inhibitor; prevents cleavage of pro-IL-1β and subsequent secretion of mature IL-1β	(150)
CPXV	CrmA	Serine protease inhibitor; prevents cleavage of pro-IL-1β and subsequent secretion of mature IL-1β	(223)
Inhibitors of interferon Induction			
VACV	E3L	Binds dsRNA, inhibits PKR-induced IFN response	(38, 39)
VACV	H1L	Dephosphorylates STAT1; prevents IFN response	(201)
VACV	K3L (CrmD)	eIF-2 decoy; competes for phosphorylation with cellular eIF-2; prevents PKR-induced IFN response	(64)
VACV	K7L	Prevents TBK1/IKKε activation of IFN	(242)
Inhibitors of apoptosis			
Molluscm contagiosum	MC159	Prevents PKR-induced apoptosis; binds FADD and pro-caspase 8 and inhibits apoptosis	(96, 249)
VACV(WR)	B13R (SPI-2)	Serine protease inhibitor; inhibits granzyme B-mediated apoptosis	(75, 150)
CPXV	CrmA	Serine protease inhibitor; inhibits granzyme B-mediated apoptosis; inhibits caspases 1 and 8	(82, 219)
MYXV	Serp2	Serine protease inhibitor; inhibits granzyme B-mediated apoptosis	(186)
VACV	F1L	Folds like a Bcl-2 protein; mitochondrial inhibitor of apoptosis	(295)
VACV	N1L	Folds like a Bcl-2 protein; inhibits apoptosis through an unknown mechanism	(58)
MYXV	M11L	Folds like a Bcl-2 protein; mitochondrial inhibitor of apoptosis	(85, 264)
Fowlpox virus	FPV039	Folds like a Bcl-2 protein; mitochondrial inhibitor of apoptosis	(14, 16)
Deerpox virus	DPV022	Folds like a Bcl-2 protein; mitochondrial inhibitor of apoptosis	(15)

Poxviruses encode many intracellular proteins that modulate the immune response. MHC, major histocompatibility complex; CD4, cluster of differentiation 4; ALCAM, activated leukocyte cell adhesion molecule; CD95, cluster of differentiation 95; ASC, apoptotic speck protein; IL-1β, interleukin-1 beta; dsRNA, double stranded ribonucleic acid; PKR, dsRNA-dependent protein kinase; IFN, interferon; STAT1, signal transducers and activators of transcription; eIF-2, eukaryotic initiation factor 2; TBK1, TANK-binding kinase 1; IKKε, IkappaB kinase epsilon; FADD, Fas-associated protein with death domain; WR, western reserve; Bcl-2, B-cell lymphoma 2.

apoptosis (14-16, 58, 75, 82, 85, 96, 150, 186, 219, 249, 264, 295) (Table 1-3). Importantly, the NFκB transcription factor controls the production of many of the important moderators of the immune response that are described above, and poxviruses also encode many proteins that inhibit the NFκB pathway (121, 286).

1.2 THE NFκB PATHWAY

The nuclear factor kappa-light-chain enhancer of activated B cells (NFκB) transcription factors play an essential role in regulating inflammation, innate immunity, and the immune response (121, 286). The NFκB pathway can be activated by a number of stimuli, including the pro-inflammatory cytokines tumor necrosis factor alpha (TNFα) and interleukin-1 beta (IL-1β) (212), and pathogen-associated molecular patterns, including double-stranded RNA (292). In general, the NFκB pathway is activated when ligands engage the appropriate receptors at the cell surface, resulting in the recruitment of adapter proteins and ubiquitin ligases that ultimately activate the regulatory kinase complex, the inhibitor of κB (IκB) kinase (IKK) complex (Figure 1-3). Following activation, the IKK complex phosphorylates the IκB protein that binds the NFκB transcription factor in the cytoplasm, resulting in degradation of IκB (110, 157, 260). Left unsequestered by its inhibitor, the free NFκB transcription factor translocates into the nucleus, where it regulates gene transcription. This section will highlight information pertaining to the NFκB transcription factor family, the IκB family, and the IKK complex. It will also describe the classical and non-classical NFκB signalling pathways.

1.2.1 The NFκB family of transcription factors

The mammalian family of NFκB transcription factors includes five members: p50 (also known as NFκB1), p52 (also known as NFκB2), p65 (also known as RelA), c-

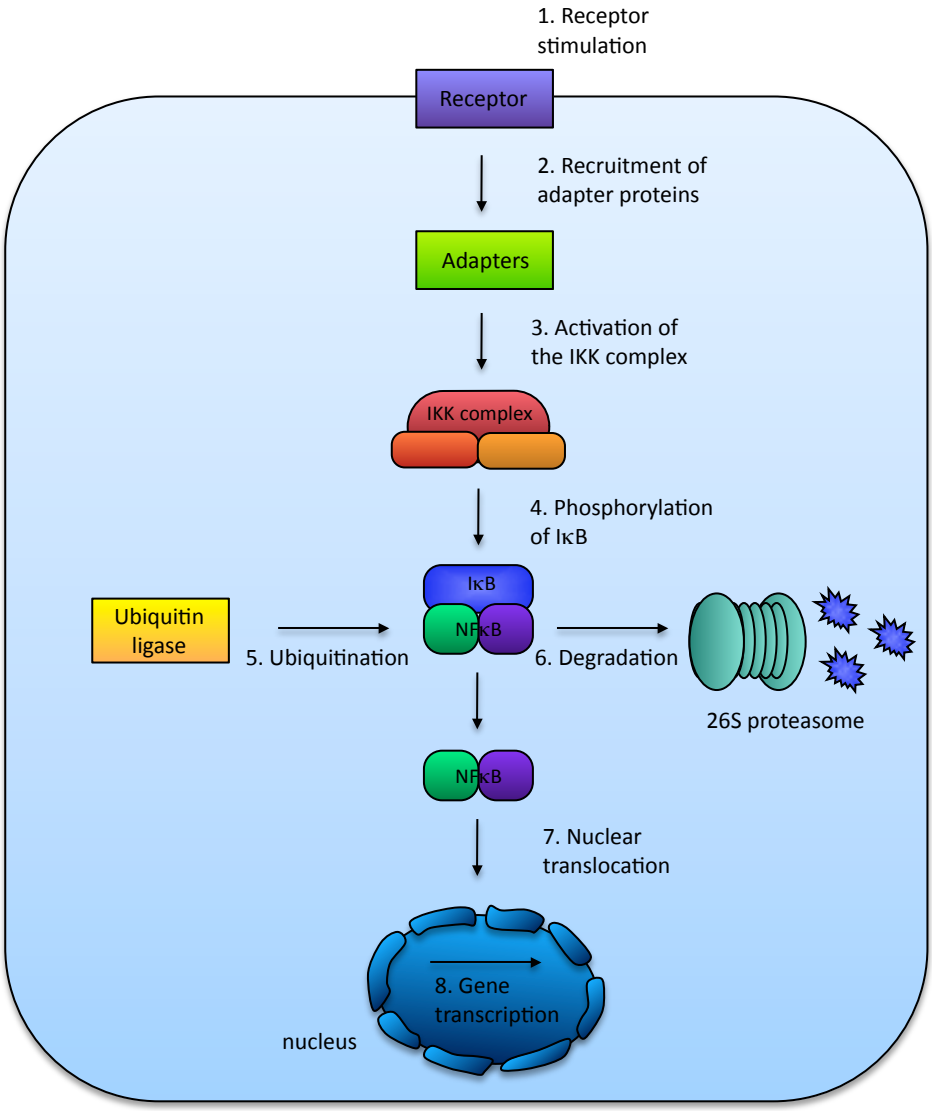

Figure 1-3. Simplified NFκB activation pathway. The NFκB pathway can be activated by a variety of stimuli. Upon stimulation of receptors at the cell surface **(1)**, a signaling cascade is induced that results in recruitment of adapter proteins and kinases **(2)** that activate the IKK complex **(3)**. The role of the IKK complex is to phosphorylate IκB **(4)**, which allows for its subsequent ubiquitination **(5)** and degradation by the 26S proteosome **(6)**. This leaves the NFκB dimer free to translocate into the nucleus **(7)**, where it activates gene transcription **(8)**.

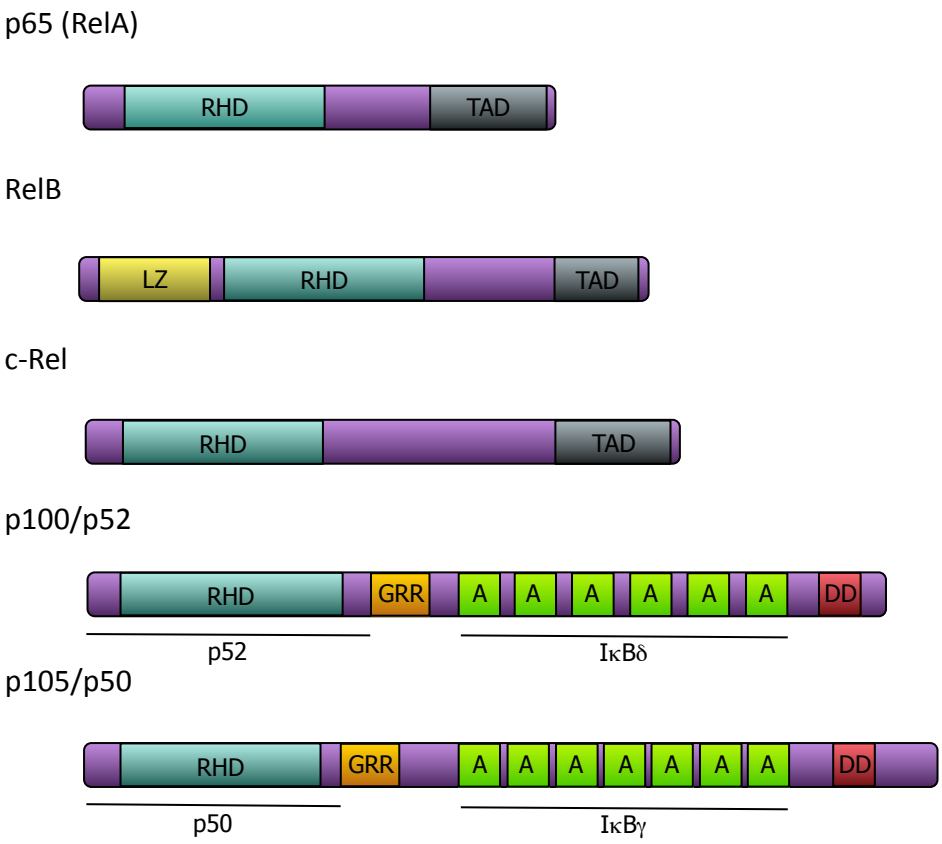

Figure 1-4. Schematic representation of the NFκB family of transcription factors. The NFκB family of transcription factors is composed of five members: p65 (RelA), RelB, c-Rel, and the precursor proteins p100 and p105, which behave as NFκB subunits when they are processed into p52 and p50, respectively. Members of this family share a common Rel homology domain (RHD) at the N-terminus, which is responsible for homo- and heterodimerization and for binding to specific κB sites on DNA. p65, RelB, and c-Rel contain transactivation domain (TAD) that mediates gene transcription, and RelB also contains a leucine zipper (LZ) that is important for transcriptional regulation. p105 and p100 contain glycine-rich regions (GRR) that act as proteolytic stop signals, as well as death domain (DD). The ankyrin (A) domains in p105/p50 and p100/p52 mediate binding to NFκB transcription factors (adapted from 112).

Rel, and RelB (Figure 1-4). p50 and p52 are unique because they are first expressed as the precursor proteins p105 and p100, respectively (112). The C-termini of p105 and p100 are structurally homologous to the IκB family, thus these proteins behave as IκBs when unprocessed, but yield NFκB proteins upon processing (23, 114). NFκB proteins form homodimers or heterodimers through their Rel-homology domain (RHDs) and regulate transcription by binding to kappa B (κB) sites in promoters and enhancers of target genes. p65, RelB, and c-Rel possess a TAD (transcription activation domain) at the C-terminus that positively regulates gene transcription (13, 238). Since p50 and p52 lack a TAD, they repress transcription by competing with TAD-containing dimers for κB sites, unless they heterodimerize with a TAD-containing NFκB family member (112). Interestingly, members of the NFκB family are non-redundant since different combinations of NFκB dimers regulate transcription of different genes (121). For instance, NFκB dimers containing p65 or c-Rel are important inducers of inflammatory genes as well as those possessing innate immune or anti-apoptotic functions (121). In contrast, NFκB dimers containing RelB regulate transcription of genes important for lymphoid organ development and development of B cells (121).

In addition to being associated with an IκB protein in unstimulated cells, NFκB dimers are also in complex with protein kinase A (PKA). Following IκB degradation, p65-containing dimers are phosphorylated by PKA, which promotes their interaction with the transcriptional coactivators CREB-binding protein (CBP) and p300 (322). Mitogen- and stress-activated protein kinases, MSK1 and MSK2, as well as IKKα and IKKβ, have also been implicated in direct phosphorylation of p65-containing dimers; however, the mechanistic details remain unclear (42). Following phosphorylation, the NFκB dimer is transported into the nucleus, where it is acetylated on multiple lysine residues before it can initiate gene transcription (42). Genes regulated by NFκB can be divided based on their

requirement for chromatin modification, and genes transcribed early in the NFκB response do not require modification, while it is a necessity for those transcribed late (204).

1.2.2 Inhibitors of NFκB: the IκB family

Members of the IκB family are a critical component of the NFκB signalling cascade, since they retain NFκB dimers in the cytoplasm of unstimulated cells (8, 112). While cytoplasmic retention of NFκB is the most important role of the IκB proteins, they are also important for stabilizing otherwise unstable NFκB dimers, aiding gene transcription in the nucleus, and for mediating crosstalk between the NFκB pathway and other cell signalling pathways (112). Members of the IκB family are characterized by the presence of multiple ankyrin (Ank) repeats that mediate the interaction with the NFκB dimers (196) (Figure 1-5). The Ank domain is a 33 amino acid sequence that is one of the most common protein-protein interaction motifs in nature (196). Although members of the IκB family are structurally similar, they bind preferentially to different members of the NFκB family and exert different effects on gene transcription in the cell (299). The IκB family is composed of eight members: three classical members, IκBα, IκBβ, IκBε, the two NFκB precursor proteins, p100 (IκBδ) and p105 (IκBγ), and three atypical members, B-cell lymphoma 3 (Bcl-3), IκBζ, and IκBNS. Unlike other members of the IκB family, the three atypical members only become upregulated during the NFκB response (112); however, the importance of these proteins is not well understood.

IκBα, IκBβ, and IκBε are most important for sequestering NFκB dimers in the cytoplasm. The most-extensively studied of the three is IκBα, which regulates the p65/p50 NFκB dimer (145). IκBα interacts with p65 and p50 through multiple Ank repeats, masking the nuclear localization signal in p65. The complex formed between IκBα, p65, and p50 is constantly shuttled into the nucleus since

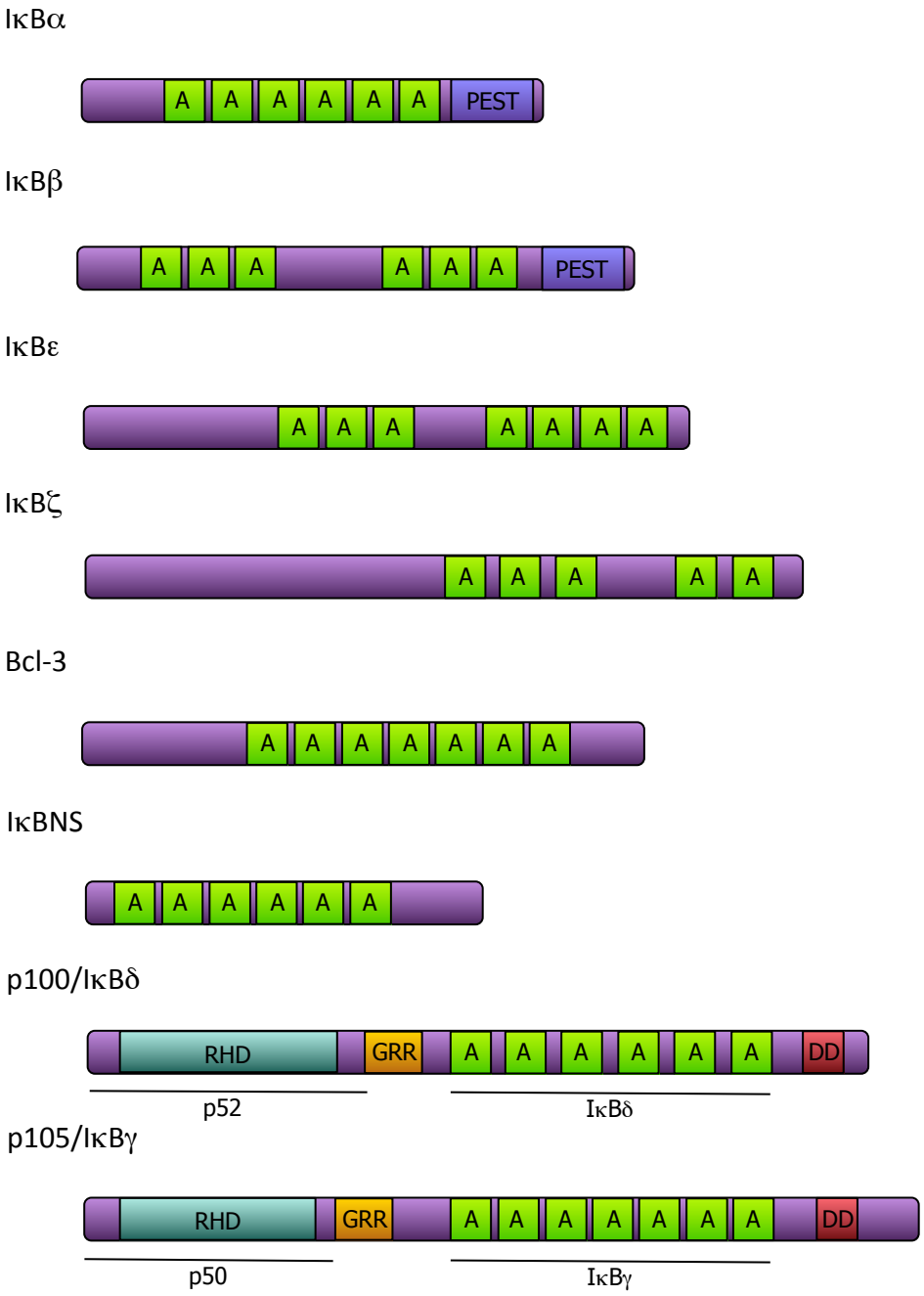

Figure 1-5. Schematic representation of the inhibitor of κB family. The IκB family is composed of eight members: IκBα, IκBβ, IκBε, IκBζ, Bcl-3, IκBNS, p100 (IκBδ), and p105 (IκBγ). Members of the IκB family are characterized multiple ankyrin (A) domains, that mediate binding to NFκB transcription factor. IκBα and IκBβ also contain a proline-rich, glutamic acid-rich, serine-rich, threonine-rich (PEST) domain that can be phosphorylated, however the importance of these domains is unclear. RHD, Rel homology domain; GRR, glycine rich region; DD, death domain (adapted from 112).

the nuclear localization signal of p50 remains exposed (34). However, since IκBα possesses a nuclear export signal, the complex is quickly shuttled back to the cytoplasm, thus resulting in the majority of the p65/p50 heterodimers being located in the cytoplasm (34). Unlike IκBα and IκBβ, which are expressed in all tissues, IκBε is expressed only in hematopoietic cells. However, it acts in a similar manner to IκBα, though it predominantly binds to p65/p65 and c-Rel/p65 NFκB dimers, and its degradation and resynthesis is delayed in comparison to IκBα (170). IκBβ, the third classical member of the IκB family, binds to p65- and c-Rel-containing NFκB dimers in the cytoplasm (222, 236). Like IκBε, IκBβ is degraded at a slower rate compared to IκBα (122). Interestingly, newly synthesized, hypophosphorylated IκBβ binds to NFκB dimers in complex with κB sites on DNA and promotes continued binding and prolonged gene transcription (222). However, the details of how IκBβ functions in this manner have not been elucidated.

The two NFκB precursor proteins, p100 and p105, act as IκB proteins when they are unprocessed since they possess Ank repeats in their C-termini (76, 172). p105 binds to p50-, p65-, and c-Rel-containing NFκB dimers in the cytoplasm (172). When p105 is in complex with an NFκB dimer, complete proteasomal degradation of the protein is preferred to processing (54). However, this degradation event occurs only during activation of the NFκB pathway (53). If p105 does not bind an NFκB dimer, p105 is processed by the proteasome and the C-terminus is removed, yielding p50 (213). Consequently, whether p105 acts as an IκB protein or yields p50 is determined by the amount of NFκB dimers in the cell shortly after p105 is translated; if a lot of NFκB dimers are available for p105 to bind, less p50 will be produced. Like p105, p100 also exerts a dual effect in the cell by either acting as a classical IκB by sequestering p65- and RelB-containing NFκB dimers in the cytoplasm (20, 247), or by contributing to the pool of NFκB dimers in the cell. In stimulated cells, phosphorylation of p100 results in

processing by the proteasome to yield p52. p52 forms a heterodimer with RelB that immediately translocates into the nucleus to activate gene transcription (257). The pathway leading to p100 processing is discussed more in section 1.2.5.

1.2.3 The IKK complex

The IKK complex can be composed of three possible subunits: IKKα, IKKβ, and NFκB essential modulator (NEMO; also known as IKKγ) (189) (Figure 1-6). IKKα and IKKβ are homologous serine/threonine kinases that share an N-terminal kinase domain (316, 317). The interaction between IKKα and IKKβ is mediated through the α-helical scaffold/dimerization domain (SDD) in each of the proteins (309). In contrast to its kinase counterparts in the complex, NEMO is a regulatory subunit that contains a C-terminal zinc finger-like domain, a leucine zipper, and coiled domains at the N- and C-termini. NEMO interacts with the IKK subunits through its N-terminus, while the ubiquitin-binding domain in the C-terminus mediates interaction with upstream signalling adapters (179, 231). There are two classes of IKK complex, classical and non-classical (237). Classical IKK complexes are defined as those that are bound and regulated by NEMO. Most often, the classical complex is composed of IKKα, IKKβ, and NEMO; however, it can also be composed of two IKKβ subunits and a single NEMO, or two IKKα subunits and a single NEMO (237). Non-canonical complexes are composed of two IKKα subunits that function independently of NEMO, but require NFκB-inducing kinase (NIK) for activation (237).

During cell stimulation, canonical IKK complexes are activated by phosphorylation of NEMO, which subsequently phosphorylates IKKα and IKKβ, resulting in their activation (67). Though the NFκB pathway has been studied extensively for the past twenty-five years, how NEMO is activated in the canonical pathways is highly debated and is discussed in more detail in section 1.2.4 (112). Once activated, IKKα or IKKβ in classical IKK complexes

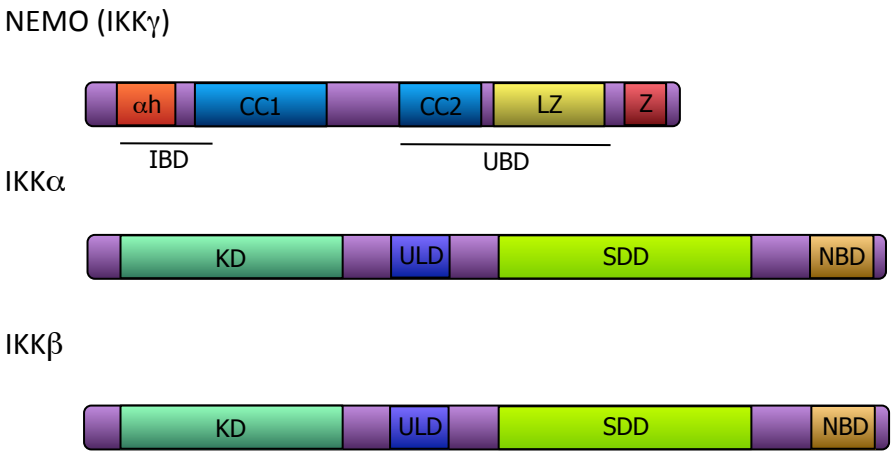

Figure 1-6. Schematic representation of the components of the IKK complex. The IKK complex is be composed of three members, NEMO (IKKγ), IKKα, and IKKβ. IKKα and IKKβ posses a kinase domain (KD) that is responsible for kinase activity, and a ubiquitin-like domain (ULD) with unknown significance. The interaction between IKKα and IKKβ is mediated by the scaffold/dimerization domain (SDD), and the NEMO-binding domain (NBD) in IKKα and IKKβ mediate interaction with NEMO. NEMO contains an IKK binding domain (IBD) at the N-terminus and a ubiquitin-binding domain (UBD) at the C-terminus that allows it to interact with ubiquitin chains associated with receptor signalling complexes. αH, α-helical domain; CC, coiled-coil domain, LZ, leucine zipper; Z, zinc finger domain (adapted from 112).

phosphorylate IκBα, IκBβ, IκBε, and p105 molecules that are acting as IκB proteins. IKKβ is the primary subunit involved in phosphorylating IκB, and this event has been most extensively studied in the context of IκBα, which is phosphorylated on serines 32 and 36 (47). The serines in IκBα make up a conserved motif (DSGXXS) that, when phosphorylated, allows for recognition of IκB by proteins that target it for degradation, which is discussed in more detail below. IκBα is a preferred substrate to IκBβ and IκBε, which could explain why they are degraded at slower rate than IκBα (302). Interestingly, IκB bound to NFκB is the preferred a substrate for the IKK complex compared to free IκB. This prevents degradation of newly synthesized IκB, contributing to a negative feedback loop (316). Activation of the non-canonical IKK complex is less elaborate, IKKα is directly phosphorylated and activated by NIK and then phosphorylates p100 molecules that are acting as IκB proteins (112). Interestingly, canonical IKK complexes can enhance the processing of p105 to p50, while the non-canonical IKK complex can enhance the processing of p100 to p52. As described in section 1.2.2, whether or not p105 and p100 become processed depends on the amount of free NFκB dimers that exist in the cytoplasm at the time that they are newly synthesized. IKKα and IKKβ also mediate crosstalk with other signalling cascades including the interferon regulatory transcription factor (IRF), mitogen-activated protein (MAP) kinase, and p53 pathways, amplifying the inflammatory response (210).

1.2.4 Activation of the classical NFκB signalling pathway

The classical NFκB pathway is induced by stimulation of the tumor necrosis factor receptor (TNFR) and the toll-like receptor/interleukin-1 receptor (TLR/IL-1R) family of receptors (212). Though the signalling cascades that take place following TNFα and IL-1β stimulation differ, both activate the IKK complex, which results in degradation of IκBα and translocation of the NFκB transcription factor into the nucleus.

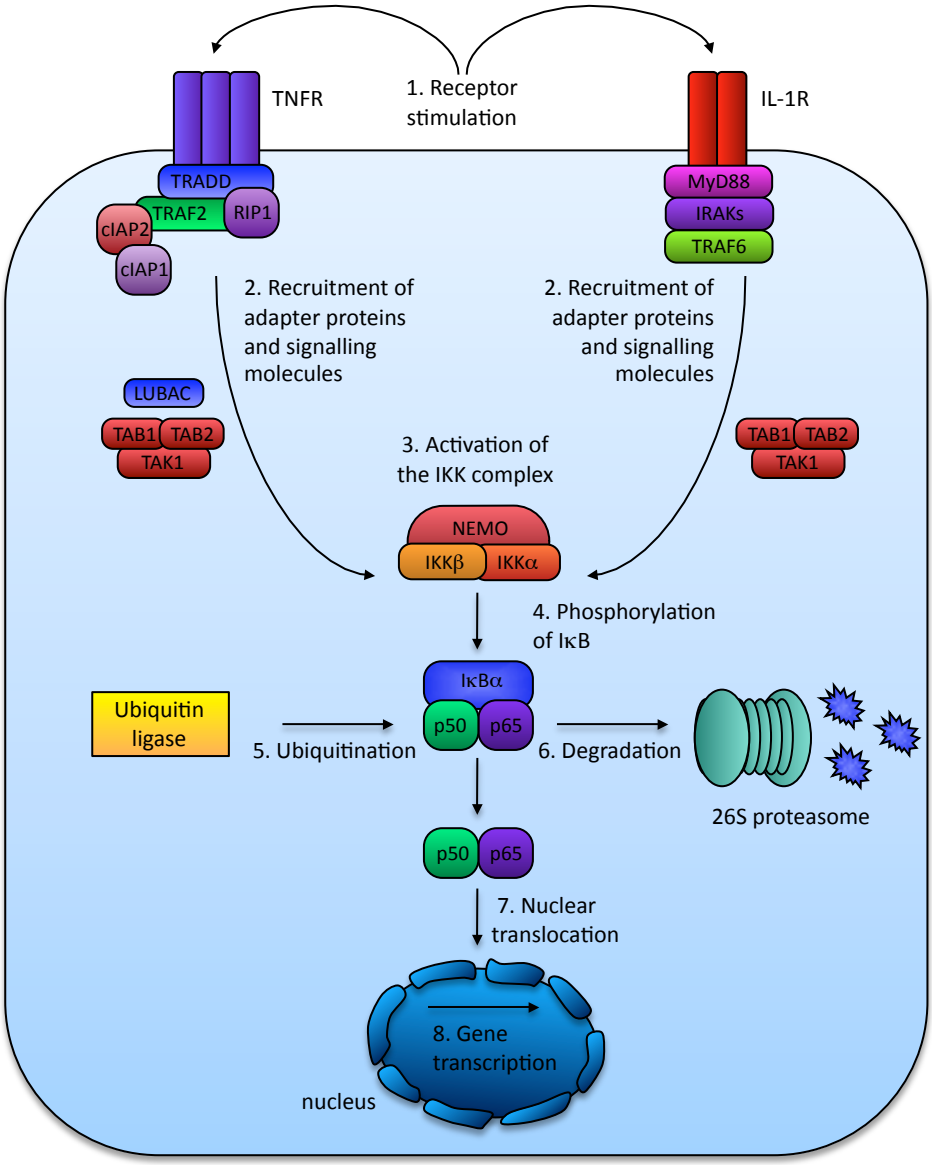

Figure 1-7. Classical activation of the NFκB pathway. Ligation of TNFα to the TNFR **(1)** induces its trimerization, resulting in the recruitment of TRADD, RIP1, TRAF2, cIAP1 and cIAP2, leading to the recruitment of LUBAC and the kinase TAK1 **(2)**. The IKK complex is also recruited to the receptor signalling complex. In the MyD88-dependent TLR/IL-1R pathway, MyD88 is recruited to the receptor following ligation of IL-1β to the receptor **(1)**. IRAK1/4 bind MyD88, and recruit TRAF6, which subsequently recruits TAK1 and the IKK complex **(2)**. In both the TNFα and TLR/IL-1R pathways, the IKK complex is phosphorylated by TAK1, resulting in its activation **(3)**. The IKK complex subsequently phosphorylates IκBα **(4)**, which is ubiquitinated **(5)**, and subsequently degraded by the 26S proteosome **(6)**. Free from its inhibitor, the NFκB dimer translocates into the nucleus **(7)** where it activates gene transcription **(8)**.

TNFα-mediated NFκB activation is induced following engagement of TNFα with the TNFR1 (212) (Figure 1-7). Ligand binding leads to receptor trimerization, resulting the recruitment of the death domain-containing adapter proteins TNFR1-associated death domain protein (TRADD) and receptor-interacting protein 1 (RIP1) to the TNFR. The receptor-interacting proteins are a family of serine/threonine kinases that are involved in both TNFR and IL-1/TLR pathways (112). The kinase activity of RIP1 is dispensable for NFκB activation (163, 182); however, RIP1 acts as an adapter in conjunction with TRADD, to recruit TNF receptor-associated factor 2 (TRAF2) to the TNFR signalling complex (125, 319). TRAF proteins are important for both TNFR- and IL-1/TLR-induced NFκB pathways. They are characterized by a TRAF domain at the C-terminus that mediates binding to adapter proteins to the cytoplasmic tail of TNFR family members (214). TRAF2 recruits the cellular inhibitor of apoptosis proteins cIAP1 and cIAP2 (320). Following this event, the IKK complex and kinase TGFβ-activated kinase-1 (TAK1) are recruited to the ubiquitinated TNFR complex via their ubiquitin binding domain-containing regulatory subunits, NEMO and TAB2/TAB3 respectively (144). The regulatory subunits NEMO and TAB2/TAB3 are important adapters that mediate recruitment of their respective kinases. As such, NEMO and TAB2/TAB3 are required for kinase recruitment following activation of the NFκB pathway.

The classical NFκB pathway is also activated following ligand engagement with the TLR/Il-1R (Figure 1-7). A number of ligands can activate the TLR/IL-1R pathway, including the cytokine IL-1β, flagellin, lipopolysaccharides, lipopeptides, double-stranded RNA, viral single-stranded RNA, and microbial DNA (5, 51, 70, 113, 132, 212). Members of the TLR/IL-1R family are defined by a Toll IL-1R (TIR) domain in their cytoplasmic tails (148). Upon ligand binding, TIR-containing adapters, myeloid differentiation primary response gene 88 (MyD88) or TIR domain-containing adapter-inducing IFN-β (TRIF), are recruited to the

TLR/IL-1 receptors (148). Interestingly, MyD88 and TRIF can be recruited directly to the receptor, or recruited through the intermediary adapters TIRAP (Toll/interleukin-1 receptor adapter protein) or TRAM, respectively (311). The folding patterns and electrostatic properties of the TIR domains in the IL-1R and the different TLRs determine whether MyD88 and TRIF can be recruited directly or if they require intermediary adapters. MyD88 is used in all TLR pathways; however, TLR2 and TLR4 recruit MyD88 through TIRAP (143).

TRIF and MyD88 activate NFκB in slightly different ways. Following recruitment to the receptor, MyD88 recruits the IL-1R-associated kinase (IRAK) 1 and IRAK4 by interaction with their death domains (268). Like RIP1, the kinase activity of the IRAKs is dispensable for NFκB activation (152). Instead, these proteins act as adapters to recruit TRAF6, which in turn leads to the recruitment of the IKK complex and TAK1 (195). On the other hand, TRIF can directly interact with TRAF6 and RIP1, leading to the activation of the NFκB pathway (60).

There are many mechanisms that contribute to activation of the IKK complex once it has been recruited to a receptor-signalling complex. Since evidence linking a single mechanism to IKK activation is inconclusive, it is likely that these mechanisms work in cooperation with each other to achieve IKK activation. Assembly of the large adapter protein signalling complex that brings many IKKs into close proximity can itself facilitate IKK activation, since the recruitment of the IKK causes a conformational change in NEMO that allows it to oligomerize (303). NEMO oligomerization results in autophosphorylation and subsequent activation of the IKK complex, as described in section 1.2.3. However, other proteins that are recruited to the signalling complex also play a role in activating the IKK complex. Upon recruitment to the receptor signalling complexes, TAK1 is activated, allowing it to directly phosphorylate IKKα and IKKβ, leading IκB degradation (87). Alternatively, MEKK3, a MAP kinase that interacts with RIP1

and TRAF2, has also been implicated in IKK phosphorylation (312). Interestingly, in addition to phosphorylating IKKα and IKKβ, MEKK3 also stimulates TAK1 (312). Furthermore, MEKK3 forms a complex with the IKK complex and IκBα, which could make NFκB signalling more efficient (239). MEKK2 acts in a similar manner to MEKK3; however, it forms a delayed complex with IκBβ and the IKK complex (239). The interplay between NEMO, TAK1, MEKK3, and MEKK2 is not well understood, but it is clear that they act to amplify activation of the IKK complex and subsequent NFκB signalling.

1.2.5. Activation of the alternative NFκB pathway

In contrast to the classical pathway, the alternative NFκB signalling pathways are defined by activating the alternative IKK complex, which is composed of two IKKα subunits and is activated independently of NEMO. In resting cells, NIK (NFκB-inducing kinase) is constitutively active, and it directly phosphorylates IKKα (245, 308). To prevent constitutive activation of this pathway in resting cells, TRAF3 ubiquitinates NIK, resulting in its degradation (Figure 1-8). Ubiquitination is discussed in detail in section 1.3. The alternative NFκB pathway is induced by certain TNF family cytokines, including lymphotoxin-β (245). Following receptor engagement, TRAF2 is recruited to the cytoplasmic domain, in conjunction with cIAP1 and cIAP2, and together these proteins target TRAF3 for proteasomal degradation (171). This promotes stabilization of NIK, and activation of IKKα. IKKα phosphorylates p100 associated with RelB leading to partial processing of p100, resulting in the generation of transcriptionally active p52/RelB complexes (308). NIK may also phosphorylate p100 directly (308). In contrast to the classical NFκB pathway that relies heavily on RIP1, alternative NFκB activation is independent of RIP1 (293).

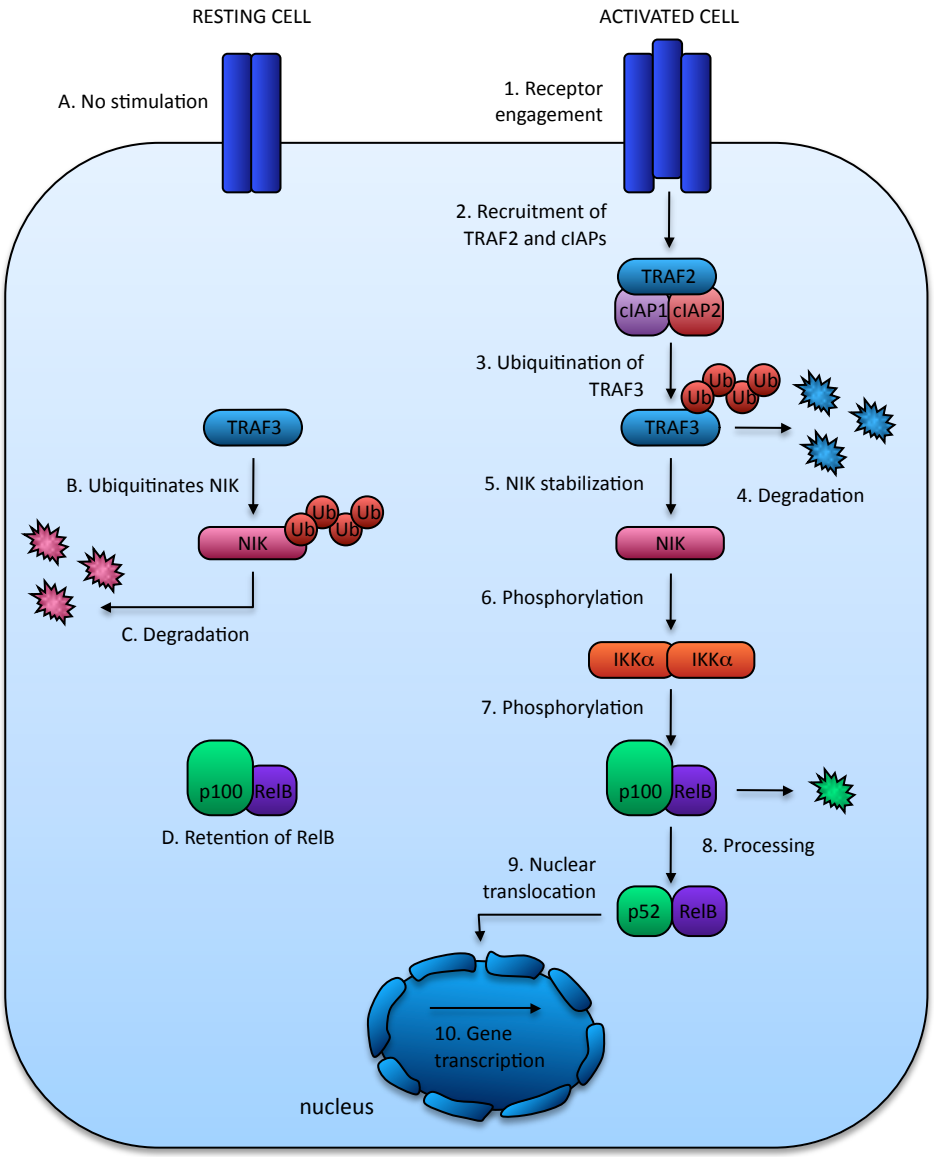

Figure 1-8. Non-classical activation of the pathway. In resting cells, there is no engagement of the receptor **(A)**, and TRAF3 ubiquitinates NIK **(B)**, resulting in its degradation **(C)**. The p100-RelB dimer remains intact **(D)**. Following receptor engagement **(1)**, TRAF2 is recruited to the cytoplasmic domain of the receptor in conjunction with cIAPs **(2)**, and together these proteins ubiquitinate TRAF3 **(3)** resulting in its degradation **(4)**. This promotes stabilization of NIK **(5)**, which phosphorylates IKKα **(6)**. IKKα phosphorylates p100 associated with RelB **(7)**, leading to partial processing of p100, resulting in the generation of the p52-RelB dimer **(8)**. The dimer translocates into the nucleus **(9)**, and upregulates gene transcription **(10)**.

1.3 UBIQUITIN IS AN IMPORTANT REGULATOR OF THE NFκB PATHWAY

Ubiquitin is a post-translational modification that plays an essential role in many cellular processes, including regulation of transcription, modulation of protein interactions, alteration of subcellular distribution, regulation of signalling pathways, internalization and lysosomal targeting, and DNA repair (296). Recently, it has become apparent that the NFκB pathway is also regulated at multiple steps by ubiquitination (18, 46, 48, 275, 305). Ubiquitin is a small 76 amino acid globular protein that is highly conserved in eukaryotes. In fact, only three amino acids differ between yeast, plant, and mammalian ubiquitin sequences (291). The importance of ubiquitin in the cell is evident; mutated, dysfunctional, or deregulated enzymes in the ubiquitination pathway have been linked to breast, uterine, prostate, and colorectal cancers, as well as inherited diseases such as Angleman's syndrome, Liddle's syndrome, and early-onset Parkinson's disease (297).

Ubiquitin is conjugated onto target proteins through covalent attachment to lysine residues within the target. A single ubiquitin molecule can be added to proteins at one (mono-ubiquitination) or more (multi-ubiquitination) sites. Alternatively, chains of ubiquitin (poly-ubiquitination) can be added to target proteins. Interestingly, proteins possessing various ubiquitin-binding domains can distinguish the type of ubiquitin modification on a protein and bind to distinct ubiquitin structures (130). Proteins with a particular ubiquitin-binding domain are involved in different cellular processes, so consequently the way in which a protein is ubiquitinated can alter its fate in different ways. For instance, mono-ubiquitination is important for regulating DNA repair, histone modification, and receptor endocytosis (116); multi-ubiquitination is important for receptor endocytosis (105); and poly-ubiquitination is crucial for signal transduction and protein degradation (215, 273). Poly-ubiquitin chains form

through isopeptide linkages between one of seven lysines on the ubiquitin molecule itself and the carboxy-terminal glycine on the subsequent ubiquitin molecule. All seven lysine residues in the ubiquitin molecule, K6, K11, K27, K29, K33, K48, and K63, can mediate the formation of ubiquitin chains (216); however, chains formed through K48 and K63 linkages are the most well-studied. K48-linked chains that are formed between four or more ubiquitin molecules are important for targeting proteins for degradation by the 26S proteasome (273). K63-linked chains on the other hand, act as scaffolds to mediate signal transduction (215). Recently, a number of other types of ubiquitin chains have also been identified, including branched chains and chains with mixed linkages; however, the importance of these chains remains unclear (130). In certain circumstances, linear ubiquitin chains formed through the N-terminal methionine residue can also be generated (274, 276), and these are important for NFκB signalling which is discussed in more detail in section 1.3.3.

1.3.1 Process of ubiquitination

Ubiquitination is a three-step process involving three classes of enzymes (Figure 1-9). It begins when the catalytic cysteine in one of two (135) ubiquitin activating enzymes (also known as E1) forms a thiol-ester bond with the carboxy-terminal glycine of the ubiquitin molecule (296). Activation of ubiquitin by the two E1 proteins requires ATP. Next, the catalytic cysteine of one of approximately 50 (135) ubiquitin conjugating enzymes (also known as E2) accepts the ubiquitin molecule via a *trans*-thiolation reaction. Although the E2 can sometimes directly transfer ubiquitin to the target protein, it usually works cooperatively with an ubiquitin ligase (also known as E3) (296). Interestingly, each E2 protein interacts with a distinct set of E3 ubiquitin ligases, which are critical for recruiting the target protein. To date, hundreds of putative E3 enzymes have been identified (107).

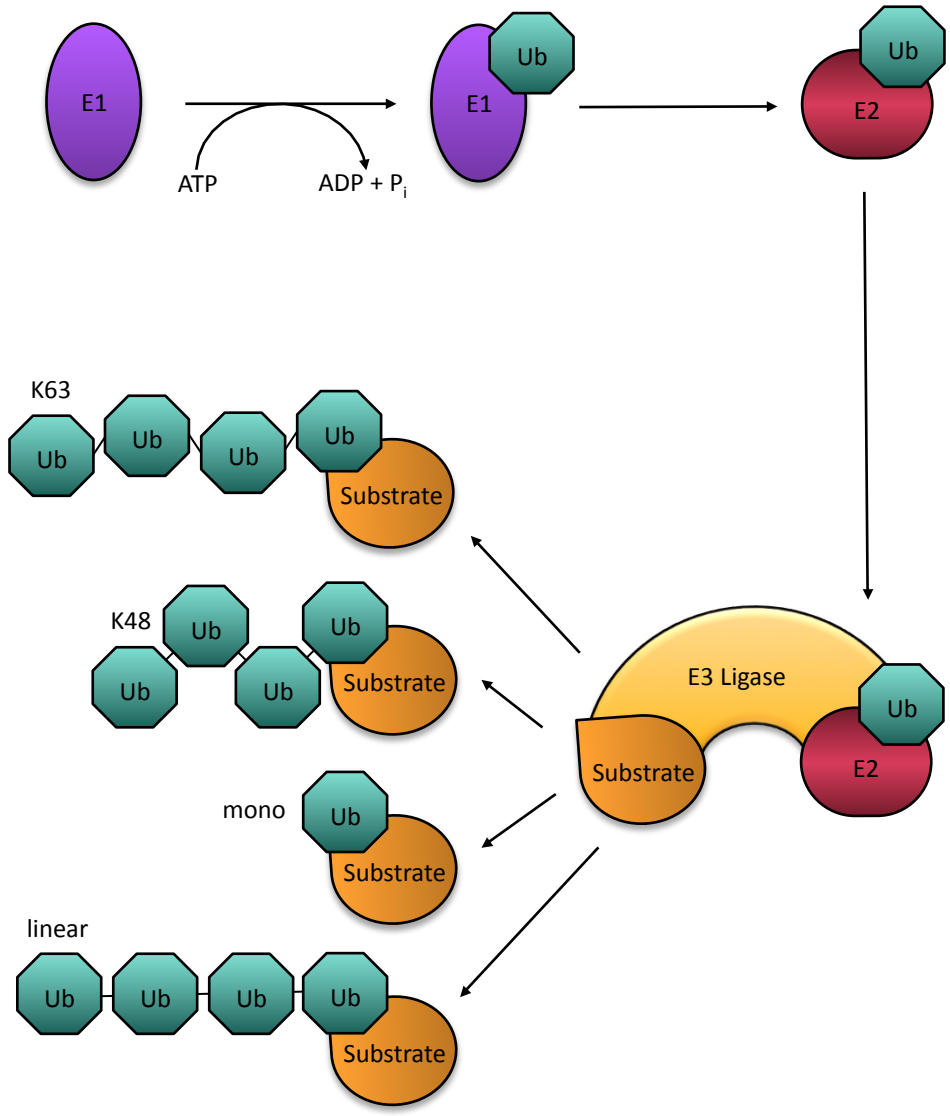

Figure 1-9. The process of ubiquitination. Conjugation of ubiquitin onto target proteins is a three step process. It begins when one of two E1 ubiquitin-activating-enzymes covalently binds the ubiquitin molecule in an ATP-dependent manner. Next, ubiquitin is transferred to one of approximately 50 E2 conjugating enzymes. The conjugating enzyme then binds one of hundreds of E3 ubiquitin ligases, which covalently attach ubiquitin to the ε-amino terminus of a lysine residue on the substrate. Mono-ubiquitination alters protein function, while multi-ubiquitin chains target proteins for degradation or act as scaffold proteins. The NFκB pathway is regulated by ubiquitin chains linked in a linear conformation through the terminal methionine residue on each ubiquitin molecule, and by chains generated through lysine (K) 48 linkages and lysine 63 linkages.

1.3.2 Ubiquitin ligases

Mammalian E3 ubiquitin ligases are divided into three classes based on sequence motifs, those that contain homologous to E6AP C-terminus (HECT) domains, those that contain really interesting new gene (RING) domains, and those that contain U-box domains (111, 187). Approximately 30 HECT domain-containing E3s have been identified (232), and these ligases possess a catalytic cysteine residue that accepts the ubiquitin molecule from the E2 before transferring it to the target protein (187). There are approximately 600 potential RING domain E3s (168). Unlike HECT domain E3s, RING domain E3s do not accept the ubiquitin molecule from the E2 (187). Instead, they mediate direct transfer of ubiquitin to the target by acting as a scaffold that simultaneously binds the E2 and target protein. Like RING domain-containing ubiquitin ligases, U-box domain E3s also act as a scaffold to mediate substrate ubiquitination (111).

RING domain-containing E3 ubiquitin ligases can be either single-subunit or multi-subunit ligases (136). Single-subunit ligases have a substrate-binding domain and a RING-finger domain that binds an E2. Multi-subunit ligases, on the other hand, require several proteins to make up the scaffold that aids in protein ubiquitination. Multi-subunit ubiquitin ligases are based around a family of six closely related cullin proteins, cullin-1, -2, -3, -4A, -4B, and -5 (217). Each cullin protein uses a unique family of substrate adapter proteins. For instance, BTB/Kelch proteins act as adapters for the cullin-3 based ubiquitin ligase (93, 310). The best-characterized multi-subunit ubiquitinligase is the SCF complex (Figure 1-10). It is involved in the regulation of the cell cycle, and mutations in this complex have been linked to cancer (11, 202). Components of the SCF complex include ROC1, cullin-1, Skp1, and an F-box protein (217). ROC1 is a RING-finger protein that possesses ubiquitin ligase activity (211). Cullin-1 acts as a molecular scaffold, interacting with the adapter protein Skp1 (188). Substrate adapter proteins containing F-box domains are recruited to the SCF complex by

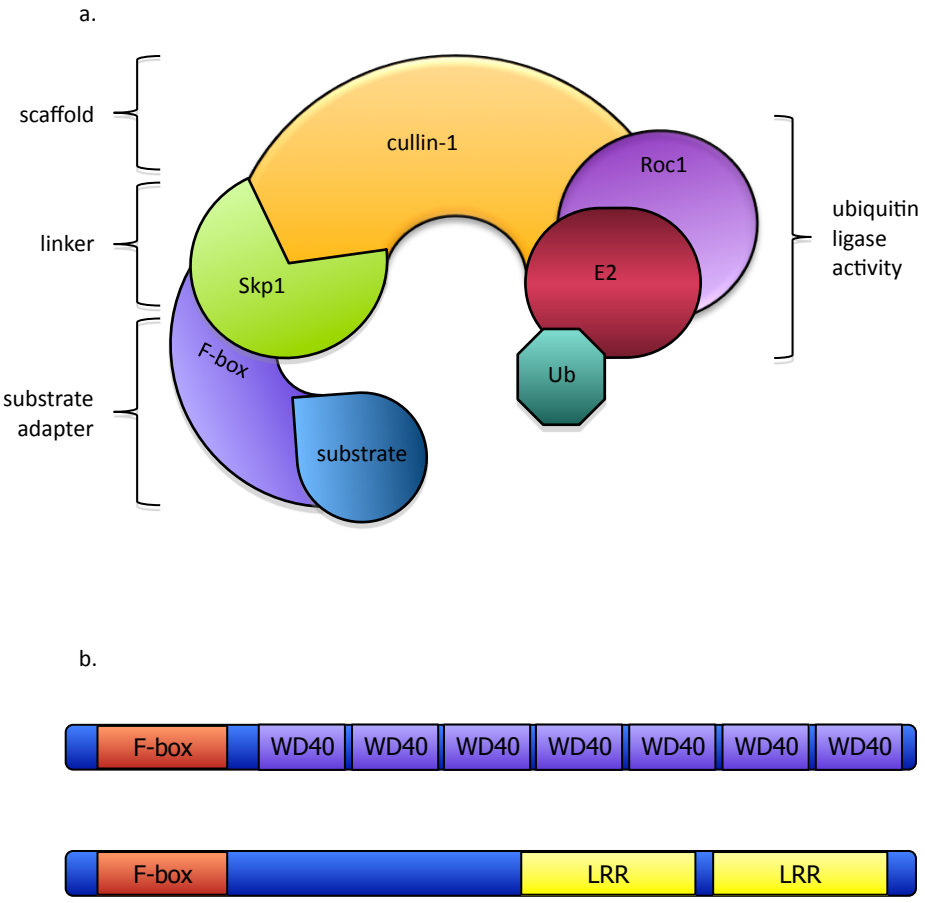

Figure 1-10. The SCF ubiquitin ligase. (a.) The SCF is a multi-subunit E3 ubiquitin ligase. Roc1 supplies the ubiquitin ligase activity and recruits the E2 bound to activated ubiquitin. Cullin-1, the scaffold protein, interacts through its C-terminus with Roc1, and through its N-terminus with the linker protein Skp1. Skp1 recruits the substrate adapter protein, and the interaction with Skp1 is dependent on the F-box domain contained in the substrate adapter protein. **(b.)** Cellular proteins that contain F-box domains exist in conjunction with tryptophan-aspartic 40 amino acid (WD40) domains or leucine-rich repeats (LRR) at the C-terminus. For instance βTrCP, the F-box protein associated with the SCF ubiquitin ligase, contains seven WD40 domains at the C-terminus.

interacting with Skp1 (33, 321). Interaction between Skp1 and the substrate adapter protein is mediated by the F-box domain (37). Cellular F-box proteins possess additional protein-protein interaction domains such as leucine rich repeats (LRR) or tryptophan-aspartic 40 amino acid (WD40) repeats at the C-terminus that are responsible for recruiting the substrate (37) (Figure 1-10).

1.3.3 Regulation of the NFκB pathway by ubiquitin

The NFκB pathway is regulated at multiple steps by ubiquitination (46, 48, 275, 305) (Figure 1-11). As described in section 1.2.4, the adapter protein TRADD is recruited to the TNFR following stimulation, and TRADD further recruits TRAF2, cIAP1, cIAP2, and RIP1. Following its recruitment, RIP1 is subjected to K63-linked polyubiquitination. Interestingly, cIAP1, cIAP2, and TRAF2 all contain RING finger domains at their N-termini that mediate K63-linked polyubiquitination (230, 269). Though evidence has suggested that TRAF2 ubiquitinates RIP1, it is more likely that TRAF2 is important for recruitment of cIAP1 and cIAP2, which then ubiquitinate RIP1 (80, 109, 166). Ubiquitination also plays a role in signalling in the IL-1R/TLR pathway. TRAF6 is recruited to the IL-1R/TLR as it catalyzes the formation of K63-linked polyubiquitin chains onto the IRAKs (57).

Recruitment of TAK1 and the IKK complex to receptor signalling complexes is also dependant on ubiquitination, since the regulatory proteins of TAK1 (TAB2 and TAB3) and the IKK complex (NEMO) contain ubiquitin-binding domains (153). Recruitment of the IKK complex to receptor signalling complexes is mediated by linear ubiquitin chains, which are generated by the linear ubiquitin chain assembly complex (LUBAC) ubiquitin ligase complex (274, 276). Interestingly, association of LUBAC with the receptor signalling complexes is dependant on the formation of K63-linked ubiquitin chains; however, the details of LUBAC recruitment require additional investigation (275). TAK1 recruitment is much less

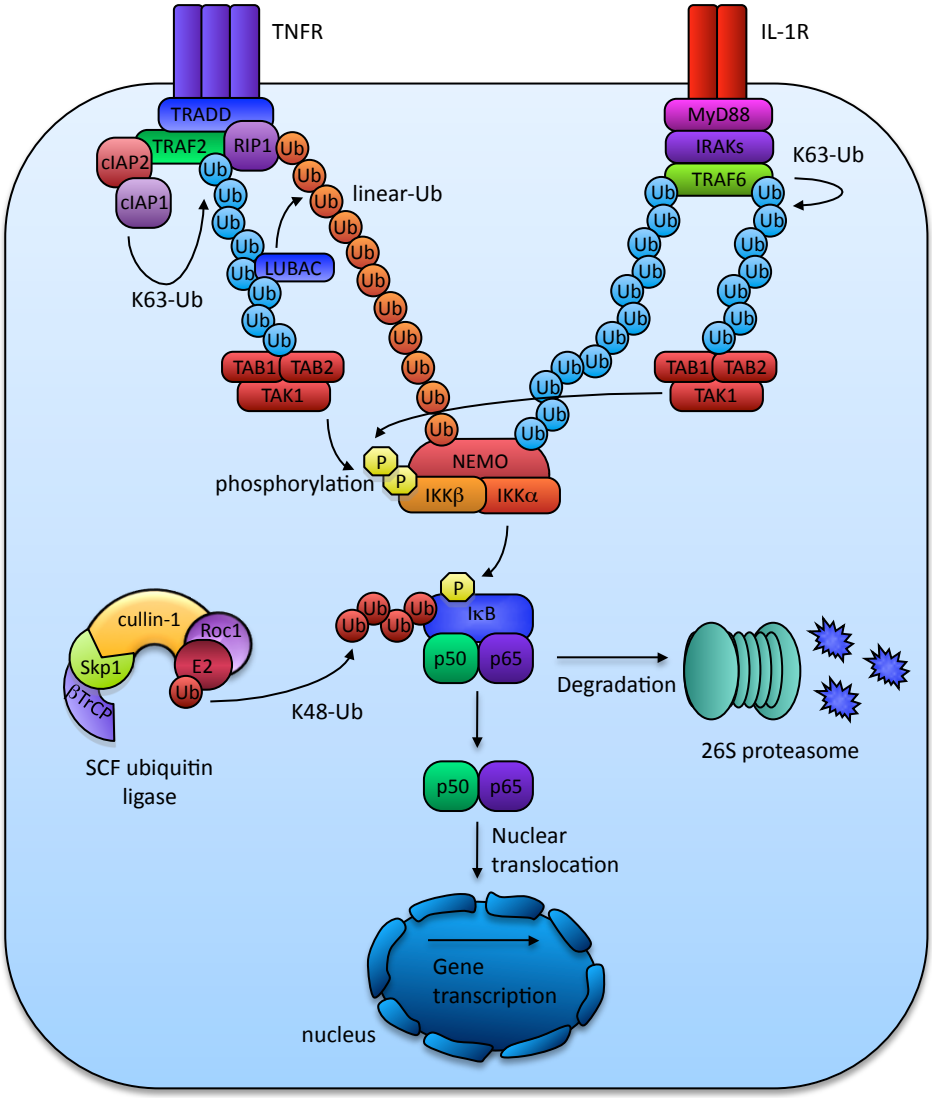

Figure 1-11. Ubiquitin mediates signalling in the classical NFκB pathway. Ligation of TNFα to the TNFR induces its trimerization, resulting in the recruitment of TRADD, RIP1, TRAF2, and cIAP1 and cIAP2. cIAP1 and cIAP2 subsequently K63-ubiquitinate RIP1 , which recruits the kinase TAK1 and LUBAC. LUBAC catalyzes the formation of linear ubiquitin chains, which recruit the IKK complex. In the MyD88-dependent TLR/IL-1R pathway, MyD88 is recruited to the receptor following ligation of IL-1β to the receptor. IRAK1/4 bind MyD88, and recruit TRAF6, which K63-ubiquitinates itself and IRAK1/4. TAK1 and NEMO are recruited to the ubiquitinated receptor signalling complex. The IKK complex is phosphorylated by TAK1, resulting in activation of the IKK complex, which subsequently phosphorylates IκBα. IκBα is K48-ubiquitinated by the SCF ubiquitin ligase, and subsequently degraded by the 26S proteosome. Free from its inhibitor, the NFκB dimer translocates into the nucleus and activates gene transcription.

complex; formation of K63-linked ubiquitin chains recruit and activate TAK1, allowing it to directly phosphorylate IKKα and IKKβ, leading IκB degradation (87).

The $SCF^{\beta TrCP}$ ubiquitin ligase also serves several important roles in the NFκB pathway; however, it is most well known for its regulation of IκB (47, 110, 157, 260). During NFκB activation, IκB proteins become rapidly phosphorylated (47). Phosphorylated IκB is recruited to the SCF ubiquitin ligase by the F-box-containing protein transducin repeat-containing protein (βTrCP), and it is subjected to K48 poly-ubiquitination, targeting it for degradation by the 26S proteasome (110, 157, 260). Degradation of IκB proteins is crucial for translocation of NFκB dimers into the nucleus. However, the $SCF^{\beta TrCP}$ ubiquitin ligase also ubiquitinates the precursor proteins p105 and p100 (21, 245), allowing them to undergo processing by the proteasome to generate the NFκB family members, p50 and p52, respectively (213, 218).

1.4 VIRAL MANIPULATION OF THE NFκB PATHWAY

Since NFκB plays a vital role in apoptosis, inflammation, and the immune response, it is not surprising that many viruses have developed mechanisms to regulate the NFκB signalling pathway (18, 220). As discussed below, some viruses promote NFκB activation in order to facilitate virus gene expression. On the other hand, many viruses require inhibition of the NFκB pathway in order to prevent the antiviral response. Interestingly, some viruses exhibit dual regulation of the NFκB pathway during their lifecycle, where they activate it at one step and inhibit it at other steps (220). Though the strategies used to modulate NFκB vary between viruses, the multitude of NFκB-modulating proteins encoded by viruses emphasizes important the control of this pathway is to the viral life cycle.

Table 1-4. Viral proteins that activate the NFκB pathway

Virus	Viral Factor	Mechanism	References
Cell surface receptor stimulation			
EBV	gp350	Stimulates CD21 and TLR2	(94)
EBV	LMP1	Has two domains that mimic a constitutively active classical or alternative TNF receptor; recruits adapter proteins to induce NFκB signalling	(176, 304)
HCV	Core and NS3	Stimulates TLR2	(40)
Herpes simplex virus	gpD	Binds HVEA; leads to NFκB activation through an unknown mechanism	(243)
RSV	F protein	Stimulates TLR4 and CD14	(158)
Manipulation of adapter proteins			
African swine fever virus	A224L	cIAP homologue; associates with TRAF2; K63 ubiquitinates RIP1	(227)
Herpesvirus ateles	Tio	Activates TRAF6	(65)
Herpesvirus saimiri	StpA11	Activates TRAF2	(49)
Herpesvirus saimiri	StpC	Activates TRAF6	(52)
Herpes simplex virus	UL37	Activates TRAF6	(173)
KSHV	K15	Activates TRAF2	(28)
Activation of the IKK complex			
Bovine foamy virus	BTas	Binds IKKα and IKKβ; activates them through an unknown mechanism	(294)
HIV-1	Vpr (exogenous)	Binds non-specifically to cell surface and enters target cells; may phosphorylate IKKβ	(289)
HTLV-1	Tax1	Binds NEMO and recruits MEKK to activate IKKβ; also activates IKKα potentially by inducing oligermization	(117, 307)
HTLV-2	Tax2	Binds NEMO and recruits MEKK to activate IKKβ	(117)
KSHV	K13 (vFlip)	Binds NEMO; constitutively activates it	(9)
Murine gammaherpesvirus 68	ORF50 (RTA)	Activates IKKβ	(78)
Activation of the NFκB transcription factor			
HBV	HBx	Binds RelA; enhances transcriptional activity of NFκB	(31)
HIV-1	Tat	Increases DNA binding by NFκB; interacts with CREBBP-p300 transcriptional activators to promote NFκB acetylation	(92)
RSV	M2-1	Associates with p65; induces persistent nuclear localization of p65	(225)

Table 1-4. Continued…

Modification of the cellular environment resulting in NFκB activation			
Herpes simplex virus	ICP4 and ICP27	Activates JNK pathway	(106)
HIV-1	Tat	Stimulates PKR	(68)
RSV	Unknown	Activates classical and alternative NFκB pathways; related to redox modification by the virus	(314)
Activation through unknown mechanisms			
HIV-1	Nef (exogenous)	Binds non-specifically to cell surface and enters target cells; NFκB activation mechanism unknown	(290)

Many viruses encode proteins that activate the NFκB pathway. EBV, Epstein-Barr virus; gp, glycoprotein; CD21, cluster of differentiation 21; TLR2, Toll-like receptor 2; LMP1, latent membrane protein 1; TNF, tumour necrosis factor; NS3, non-structural protein 3; HVEA, herpesvirus entry mediator A; NFκB, nuclear factor kappa B; RSV, respiratory syncitial virus; TLR4, Toll-like receptor 4; CD14, cluster of differentiation 14; cIAP, cellular inhibitor of apoptosis; TRAF2, TNF receptor-associated factor 2; RIP1, receptor-interacting protein 1; stp, *Saimiri* transformation associated protein; TRAF6, TNF receptor-associated factor 6; KSHV, Karposi's sarcoma-associated virus; IKK, IκB kinase; HIV-1, human immunodeficiency virus 1; HTLV, Human T-lymphotrophic virus; NEMO, NFκB essential modulator; MEKK, MAP/ERK kinase-kinase; RTA, replication and transcription activator; Tat, trans-activator of transcription; CREBBP, CREB-binding protein; ICP, infected cell protein; JNK, c-Jun NH(2)-terminal protein Kinases; PKR, protein kinase R; Nef, negative factor.

Table 1-5. Viral proteins that inhibit the NFκB pathway

Virus	Viral Factor	Mechanism	References
Manipulation of adapter proteins			
Borna disease virus	protein P	Decoy; gets phosphorylated by TBK1, preventing phosphorylation of cellular targets	(280)
Hepatitis C virus	NS3-NS4A	Cleaves TRIF adapter protein	(167)
Hepatitis C virus	NS5A	Binds MyD88; prevents recruitment to TLR/IL-1R	(1)
Herpes simplex virus	ICP0	E3 ubiquitin ligase; degrades MyD88	(288)
Human cytomegalovirus	M45	Binds RIP1; prevents its ubiquitination	(178)
Inhibition of the IKK complex			
Adenoviruses	E3 14.5 and 10.4 kDa protein	Inhibits activation of IKK complex; mechanism unknown	(91)
Bovine viral diarrhoea virus	NS5A	Binds NIBP; prevents phosphorylation of IKKβ and NIK	(315)
Epstein-Barr virus	EBNA1	Prevents phosphorylation of IKKα and IKKβ	(285)
Hepatitis C virus	Core	Binds IKKβ; prevents IKK complex activity	(142)
Hepatitis C virus	NS5B	Binds IKKα; prevents its phosphorylation	(50)
HIV-1	Tat (extracellular)	Mechanism unknown; may inhibit IKKβ activation	(313)
Human cytomegalovirus	Late gene product	Prevents activation of the IKK complex; mechanism unknown	(133, 194)
Human papillomavirus	E7	Binds IKKα and IKKβ; prevents IKK complex activation	(261)
Infectious spleen and kidney necrosis virus	ORF124L	Mechanism unknown; binds IKKβ	(104)
Murine Cytomegalovirus	M45	Targets NEMO to lysosomes; induces proteasome-independent degradation	(90)
SARS-coronavirus	M protein	Binds IKKβ; prevents IKK complex activity	(88)
Inhibition of IκB proteins			
African swine fever virus	A238L	Homologue of IκBα; interacts with p65-containing dimers, preventing nuclear translocation	(267)
Classical swine fever virus	Npro	Binds IκBα; mechanism of inhibition unknown	(77)
Coxsackievirus	3C protease	Cleaves IκBα; yields N-terminal fragment bound to NFκB dimer; translocates to nucleus but remains inactive	(318)
Herpes simplex virus	ICP27	Binds IκBα; prevents its phosphorylation	(151)

Table 1-5. Continued…

Kaposi's sarcoma-associated virus	MicroRNAs	Represses IκBα expression	(165)
Inhibition of βTrCP			
HIV-1	Vpu	Binds βTrCP; prevents IκBα degradation	(26)
Rotavirus	NSP1	Degrades βTrCP; prevents IκBα degradation	(98)
Inhibition of the NFκB transcription factor			
Human adenovirus 12	E1A	Binds NFκB; prevents phosphorylation by PKA	(101, 134)
Poliovirus	3C protease	Cleaves p65; inactivates its transcription-activation activity	(206)
Inhibition of NFκB nuclear translocation			
Hantaan virus	protein N	Binds importin-α; prevents nuclear translocation of NFκB	(271)
Inhibition of NFκB activity in the nucleus			
Human cytomegalovirus	IE86	Prevents NFκB binding to κB sites through unknown mechanism; may target cellular proteins required for NFκB binding	(270)
Inhibition through unknown mechanisms			
Varicella-zoster virus	unknown	Mechanism unknown	(141)
West Nile virus	NS1	Inhibits TLR3-induced NFκB activation; mechanism unknown	(300)

Many viruses encode proteins that inhibit the NFκB pathway. TBK1, TANK-binding kinase 1; NS3, non-structural protein 3; NS4A, non-structural protein 4A; TRIF, TIR domain-containing adapter-inducing IFN-β; NS5A, non-structural protein 5A; MyD88, myeloid differentiation primary response gene 88; TLR, Toll-like receptor; IL-1R, interleukin-1 receptor; ICP, infected cell protein; RIP1, receptor-interacting protein 1; IKK, IκB kinase; NIBP, NIK and IKKbeta binding protein; EBNA1, Epstein-Barr nuclear protein 1; NS5B, non-structural protein 5B; Tat, trans-activator of transcription; NEMO, NFκB essential modulator; Npro, amino-terminal protease; Vpu, viral protein u; βTrCP, beta transducin repeat-containing protein; NSP1, PKA, protein kinase A.

1.4.1 NFκB activation by viruses

For some viruses, it is beneficial to promote activation of the NFκB pathway in order to upregulate viral transcription, prevent apoptosis, and manipulate the host immune reponse (120, 220). Hepatitis B virus (HBV) has κB sites in certain promoters in its genome, while viruses such as human immunodeficiency virus 1 (HIV-1) and human T-lymphotrophic virus 1 (HTLV-1) integrate into regions in the cellular genome which are located downstream of kB sites (119, 120, 220). As such, promoting activation of the NFκB pathway induces viral gene expression. Viruses such as HTLV, Epstein-Barr virus (EBV), Kaposi's sarcoma-associated herpesvirus (KSHV), Herpesvirus saimiri, and Herpesvirus ateles promote NFκB activation in order to promote viral transcription and prevent apoptosis (119, 220). Interestingly, persistent activation of NFκB (119, 220) induces transformation of infected cells, resulting in multiple types of cancer (220). Viruses that promote NFκB activation are listed in Table 1-4.

1.4.2 NFκB inhibition by viruses

For most viruses, it is necessary to inhibit activation of the NFκB pathway (119, 120, 220). Some viruses, such as HCV, encode multiple inhibitors of the NFκB signalling cascade (1, 50, 142, 167), while other viruses encode only a single inhibitor that seems to be sufficient for inhibiting NFκB (Table 1-5). Interestingly, different viruses target different steps in the NFκB signalling cascade, and there is no single target that is preferred by all viruses. Viruses that prevent NFκB activation are listed in Table 1-5.

1.4.3 NFκB inhibition by poxviruses

The *Poxviridae* interfere with NFκB activation at several steps in the signalling cascade, including ligand-receptor engagement, receptor signalling, activation of the IKK complex, nuclear translocation of NFκB, and activity of NFκB in the nucleus (Figure 1-12). Certain poxviruses also prevent processing of IL-1β,

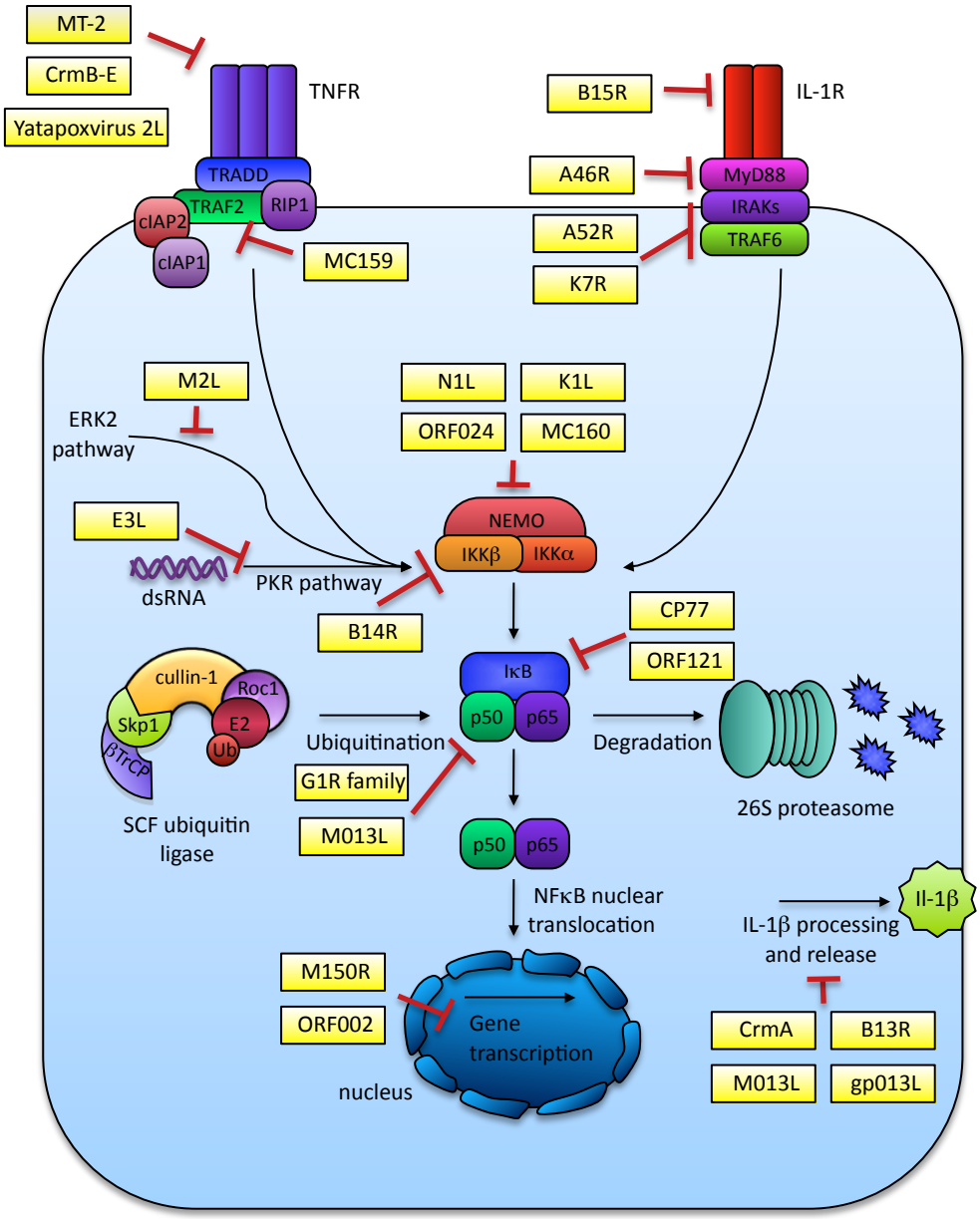
MT-2
CrmB-E
Yatapoxvirus 2L
TNFR
TRADD
TRAF2
RIP1
cIAP2
cIAP1
MC159
B15R
IL-1R
A46R
MyD88
IRAKs
A52R
TRAF6
K7R
M2L
ERK2
pathway
N1L
K1L
ORF024
MC160
NEMO
IKKβ
IKKα
E3L
dsRNA
PKR pathway
B14R
CP77
ORF121
IκB
p50
p65
cullin-1
Roc1
Skp1
E2
Ub
βTrCP
Ubiquitination
Degradation
26S proteasome
SCF ubiquitin
ligase
G1R family
M013L
p50
p65
NFκB nuclear
translocation
Il-1β
IL-1β processing
and release
M150R
ORF002
Gene
transcription
nucleus
CrmA
B13R
M013L
gp013L

Figure 1-12. Poxviral inhibitors of the NFκB pathway. Poxvirus encode many inhibitors of the NFκB pathway. Multiple poxviruses encode TNFα and IL-1β cytokine-binding proteins or TNFR or IL-1R decoys that prevent ligand-receptor engagement. VACV encodes three proteins that prevent receptor signalling from the IL-1R; A46R interacts TIR domain-containing adapters including MyD88, and A52R and K7R bind IRAKs and TRAF6. Molluscum contagiosum virus MC159 binds TRAF2 and prevents IκBβ degradation. VACV N1L and K1L, Orf virus ORF024, and Molluscum contagiosum virus MC160 inhibit activation of the IKK complex through unknown mechanisms. VACV B14R binds IKKβ specifically and inhibits its phosphorylation. CPXV CP77 and Orf virus ORF121 bind NFκB in the cytoplasm and prevent nuclear translocation, while ORF002 and MYXV M150R bind NFκB in the nucleus and prevent gene transcription. Members of the *Orthopoxvirus* genus encodes the G1R family, and MYXV encodes M013L, and these proteins interfere with the processing of the precursor protein p105 to the NFκB subunit p50. CPXV CrmA, VACV B13R, MYXV M013L, and Shope fibroma virus gp013L also prevent the processing and release of IL-1β, thus preventing NFκB activation in surrounding cells. Finally, the VACV proteins E3L prevents activation of NFκB by the PKR pathway, and M2L prevents activation by ERK2.

consequently preventing a positive feedback loop that amplifies NFκB signalling (Figure 1-12). Several inhibitors of the NFκB pathway have been identified in the prototypic poxvirus, VACV, including A46R, A52R, B13R, B14R, B15R, E3L, M2L, N1L, K1L, and K7L (3, 27, 44, 45, 74, 95, 100, 108, 118, 200, 242, 248, 262). The ORF B15R encodes a soluble secreted IL-1R, which interferes with IL-1/TLR signalling by preventing IL-1β from engaging its receptor at the plasma membrane (3, 262). Within the cell, proteins encoded by some VACV ORFs, including A52R and A46R, contain TIR-homology domains that allow them to disrupt formation of receptor signalling complexes. A46R binds the TIR-domain containing adapter proteins MyD88, TRIF, TIRAP, and TRAM, and prevents them from associating with the IL-1R and TLRs (27, 263). On the other hand, A52R and K7L bind TRAF6 and IRAK2 to disrupt signalling complexes containing these proteins (27, 100, 108). Rather than inhibiting only IL-1β-mediated NFκB activation like B15R, A52R, A46R, and K7L, proteins encoded by certain ORFs in VACV also prevent TNFα-mediated NFκB activation by targeting the IKK complex. For instance, the protein encoded by K1L prevents activation of the IKK complex, potentially by inhibiting the kinases that phosphorylate the IKK subunits (248). Additionally, the gene product of B14R inhibits IKK complex activation directly by binding IKKβ and preventing its phosphorylation (44, 45). Interestingly, though it shares no sequence similarity to cellular or viral Bcl-2 proteins, B14R adopts a Bcl-2-like fold (100). Typically, Bcl-2 proteins modulate apoptosis; however, B14R does not have the binding pocket necessary to bind and inhibit pro-apoptotic proteins. As such, this protein has evolved to inhibit NFκB (100). A52R also has a Bcl-2-like fold, but like B14R, it also lacks a binding groove (100).

The VACV protein encoded by N1L has also been reported to inhibit the NFκB pathway, although its mechanism of inhibition is controversial. Initially, it was thought that N1L inhibited a variety of NFκB stimulation pathways by binding the IKK complex (74). However, later reports were unable to demonstrate that N1L

could inhibit these same pathways, nor could they demonstrate interactions with components of the IKK complex (45, 58, 100). It is possible that N1L inhibits adapter proteins that act upstream of the IKK complex in the NFκB pathway, but whether N1L actually even inhibits any of the NFκB pathways still needs to be resolved. Like A52R and B14R, N1L adopts a Bcl-2-like fold; however, N1L is unique among poxviral Bcl-2-like proteins because it inhibits apoptosis by binding to pro-apoptotic proteins (6, 58). However, even the anti-apoptotic ability of N1L is refuted by contradictory data (16). Recently, an attempt was made to resolve the controversy surrounding the function of N1L (180). However, these investigations looked at what residues of N1L were necessary for it to inhibit NFκB and apoptosis, rather than looking at how it specifically inhibits cellular pathways.

Two VACV proteins, encoded by E3L and M2L, inhibit NFκB by targeting pathways leading to activation of NFκB, rather than components of the classical NFκB signalling pathway (95, 118, 200). As described in section 1.2, recognition of double-stranded RNA can also activate the NFκB pathway (292). Upon recognition of double-stranded RNA by the pattern recognition receptor protein kinase R (PKR), PKR is activated by autophosphorylation. Activated PKR can directly activate the IKK complex, leading to NFκB activation. The gene product of E3L binds double stranded RNA and prevents its recognition by PKR (200). ERK2 can also activate the NFκB pathway (69); however, how this pathway is initiated to specifically activate NFκB is not known (95). The gene product of M2L localizes to the endoplasmic reticulum and prevents ERK2 phosphorylation (95). Interestingly, M2L only inhibits NFκB activation when it is localized to the ER (118).

Some poxviruses encode gene products that are unique from the NFκB inhibitors found in VACV. At the receptor level, the leporipoxviruses Shope fibroma virus

and MYXV virus encode a soluble TNFR called M-T2 (251, 281). MT-2 is released into the extracellular space and interferes with the TNF pathway by binding TNFα and preventing it from engaging the TNFR. Many orthopoxviruses also express secreted versions of innate immune receptors that prevent the ligands from engaging the appropriate receptors. CPXV encodes four secreted proteins, the cytokine response modifiers CrmB, CrmC, CrmD, and CrmE, which bind TNFα, and all but CrmC can also bind lymphotoxin-β (126, 175, 235, 252). VARV and MXPV also encode an orthologue of CrmB, which inhibits NFκB activation to varying degrees (97), while ECTV encodes an orthologue of CrmD (43). Furthermore, members of the *Yatapoxvirus* genus encode the protein 2L that binds TNFα, though it does not resemble the TNFR (30, 162). CPXV also encode B15R, a soluble secreted IL-1R, which consequently interferes with IL-1/TLR signalling (262).

Like VACV, many members of the *Poxviridae* also interfere with activation of the IKK complex. A member of the *Molluscipoxvirus* genus*,* molluscum contagiosum virus (MOCV), encodes two death-domain containing proteins, MC159 and MC160, which prevent activation of the IKK complex (199, 208). MC159 binds TRAF2 and prevents further signalling that normally results in IKK activation and subsequent IκBβ degradation (199). In contrast, MC160 directly targets the IKK complex through a mechanism that has not been completely elucidated. MC160 reduces IKK subunit phosphorylation, yet it does not interact with any components of the IKK complex (208). Interestingly, the interaction between IKKα and IKKβ is not detected in cells that express MC160, suggesting that it disrupts proper IKK complex formation (208). MC160 also induces degradation of IKKα by competing for binding with the cellular heat shock protein 90, which is required to stabilize IKKα (209). A member of the *Parapoxvirus* genus, Orf virus, also encodes an inhibitor that prevents IKK complex activation. ORFV024 inhibits phosphorylation of IKKα and IKKβ, but it does not bind any members of the IKK

complex, suggesting that it modulates a protein that leads to activation of the IKK complex (71).

Unlike VACV, other members of the *Poxviridae* inhibit NFκB downstream of the IKK complex. The CPXV protein CP77 binds to p65-containing NFκB dimers in the cytoplasm after IκBα is degraded; it binds p65 through its N-terminal domain while it interacts with the SCF ubiquitin ligase through its C-terminus, thus preventing nuclear translocation of the NFκB dimer (41). Orf virus encodes the protein ORFV121, which interacts with p65-containing NFκB dimers in the cytoplasm, preventing phosphorylation and subsequent nuclear translocation of the dimers (73). Orf virus also encodes a nuclear inhibitor of the NFκB pathway. ORFV002 binds p65-containing NFκB dimers in the nucleus and prevents them from associating with p300, thereby preventing acetylation of NFκB (72). The MYXV protein M150, or MNF (MYXV nuclear factor), also colocalizes with NFκB in the nucleus and inhibits the inflammatory response through an unknown mechanism (32).

Rather than directly inhibiting the NFκB pathway, some poxviruses interfere with the processing of p105 to p50. VARV encodes the protein G1R, which is conserved among CPXV (CPXV006), MPXV (MPXV003), and ECTV (ECTV002). These proteins interact with p105 and prevent its degradation during TNFα stimulation (192). Further study of CPXV006 suggests it inhibits NFκB activation by an additional undetermined mechanism as well, since increased levels of phosphorylated IKKα and IKKβ are observed in cells infected with CPXV devoid of CPXV006 (193). The MYXV protein, M013L, also interacts with p105 and functions in a manner similar to the G1R family (221). Another indirect mechanism of NFκB inhibition used by some poxviruses is prevention of processing of pro-IL-1β to IL-1β, which consequently prevents the positive feedback loop that amplifies NFκB signalling. The CPXV protein CrmA, and B13R,

which is encoded by VACV, inhibit caspase-1 and prevent it from processing pro-IL-1β (150, 223). MYXV M013L and the Shope fibroma virus protein, gp013L, also prevent pro-IL-1β processing, except they inhibit processing of pro-caspase-1 to its active form, caspase-1 (79, 221).

Since poxviruses encode so many inhibitors of the NFκB pathway, it is obvious that activation of the NFκB signalling cascade can be detrimental to the poxvirus lifecycle. Many of the poxviral inhibitors described above have been assessed for their contribution to virulence *in vivo*. Often, the absence of a single inhibitor does not decrease the ability of the virus to inhibit the NFκB pathway, indicating that the effects of these inhibitors are additive.

1.5 THESIS RATIONALE

Our lab studies many proteins in ECTV that modulate the ubiquitin-proteasome system, including the E3 ubiquitin ligase p28 (205), and the BTB/Kelch family of substrate adapter proteins that associate with cullin-3 based ubiquitin ligases (301). Recently, we identified four proteins in ECTV, ECTV002, ECTV005, ECTV154, and ECTV165, which contain a F-box domain that allows them to associate with the SCF ubiquitin ligase (258, 287). Interestingly, the SCF ubiquitin ligase is an important regulator of the NFκB pathway. F-box proteins are expressed by many poxviruses; however, in contrast to cellular F-box proteins, the F-box domain is located at the C-terminus in poxviral proteins, and multiple Ank domains are located at the N-terminus (184, 259). Many poxviral Ank-containing proteins inhibit the NFκB pathway (32, 41, 248). For example, the VACV gene product of K1L contains nine Ank repeats, and blocks degradation of IκBα (169, 248). The MYXV protein M150 (MNF) contains nine Ank domains in combination with an F-box domain and co-localizes with NFκB in the nucleus following stimulation with TNFα, suggesting that M150 might mimic IκBα and

prevent association of NFκB with DNA (32). CPXV also encodes an F-box domain-containing protein called CP77 that contains nine predicted Ank domains (41). As already described, CP77 anchors p65-containing NFκB dimers to the SCF ubiquitin ligase following degradation of IκBα, thus preventing nuclear translocation of NFκB (41).

Recently, our lab set out to identify additional inhibitors of the NFκB pathway encoded by VACV (86). By comparing the genomes of large deletion viruses, eighteen ORFs were identified that might contribute to the ability of VACV to inhibit TNFα-induced NFκB activation (86). One of the potential ORFs that might inhibit the NFκB pathway was a gene called VACVB4R. Interestingly, the orthologue of VACVB4R in ECTV is one of the four Ank/F-box proteins that we identified, suggesting that the Ank/F-box proteins in ECTV might inhibit activation of the NFκB pathway. The suggestion that the ECTV Ank/F-box proteins might prevent NFκB activation, combined with the observations that the ECTV Ank/F-box proteins associate with the SCF ubiquitin ligase (287), and that Ank domain-containing poxviral proteins play an important role in inhibiting NFκB during viral infection (32, 41, 248), led to the hypothesis that ECTV002, ECTV005, ECTV154 and ECTV165 inhibit the NFκB pathway. The purpose of this thesis was to further explore how poxviruses manipulate the NFκB signalling pathway.

OBJECTIVES

1. To determine if ECTV002, ECTV005, ECTV154, and ECTV165 inhibit NFκB activation.
2. To generate a large deletion VACV that is missing all of the currently identified inhibitors of TNFα-induced NFκB activation, including the orthologues of ECTV002, ECTV005, ECTV154, and ECTV165, and assess its ability to inhibit the NFκB pathway.

1.6 REFERENCES

1. **Abe, T., Y. Kaname, I. Hamamoto, Y. Tsuda, X. Wen, S. Taguwa, K. Moriishi, O. Takeuchi, T. Kawai, T. Kanto, N. Hayashi, S. Akira, and Y. Matsuura.** 2007. Hepatitis C virus nonstructural protein 5A modulates the toll-like receptor-MyD88-dependent signaling pathway in macrophage cell lines. J Virol **81:**8953-66.
2. **Ahn, B. Y., P. D. Gershon, E. V. Jones, and B. Moss.** 1990. Identification of rpo30, a vaccinia virus RNA polymerase gene with structural similarity to a eucaryotic transcription elongation factor. Mol Cell Biol **10:**5433-41.
3. **Alcami, A., and G. L. Smith.** 1992. A soluble receptor for interleukin-1 beta encoded by vaccinia virus: a novel mechanism of virus modulation of the host response to infection. Cell **71:**153-67.
4. **Alcami, A., and G. L. Smith.** 1995. Vaccinia, cowpox, and camelpox viruses encode soluble gamma interferon receptors with novel broad species specificity. J Virol **69:**4633-9.
5. **Alexopoulou, L., A. C. Holt, R. Medzhitov, and R. A. Flavell.** 2001. Recognition of double-stranded RNA and activation of NF-kappaB by Toll-like receptor 3. Nature **413:**732-8.
6. **Aoyagi, M., D. Zhai, C. Jin, A. E. Aleshin, B. Stec, J. C. Reed, and R. C. Liddington.** 2007. Vaccinia virus N1L protein resembles a B cell lymphoma-2 (Bcl-2) family protein. Protein Sci **16:**118-24.
7. **Assarsson, E., J. A. Greenbaum, M. Sundstrom, L. Schaffer, J. A. Hammond, V. Pasquetto, C. Oseroff, R. C. Hendrickson, E. J. Lefkowitz, D. C. Tscharke, J. Sidney, H. M. Grey, S. R. Head, B. Peters, and A. Sette.** 2008. Kinetic analysis of a complete poxvirus transcriptome reveals an immediate-early class of genes. Proc Natl Acad Sci U S A **105:**2140-5.
8. **Baeuerle, P. A., and D. Baltimore.** 1988. I kappa B: a specific inhibitor of the NF-kappa B transcription factor. Science **242:**540-6.
9. **Bagneris, C., A. V. Ageichik, N. Cronin, B. Wallace, M. Collins, C. Boshoff, G. Waksman, and T. Barrett.** 2008. Crystal structure of a vFlip-IKKgamma complex: insights into viral activation of the IKK signalosome. Mol Cell **30:**620-31.
10. **Bahar, M. W., J. C. Kenyon, M. M. Putz, N. G. Abrescia, J. E. Pease, E. L. Wise, D. I. Stuart, G. L. Smith, and J. M. Grimes.** 2008. Structure and function of A41, a vaccinia virus chemokine binding protein. PLoS Pathog **4:**e5.
11. **Bai, C., P. Sen, K. Hofmann, L. Ma, M. Goebl, J. W. Harper, and S. J. Elledge.** 1996. SKP1 connects cell cycle regulators to the ubiquitin proteolysis machinery through a novel motif, the F-box. Cell **86:**263-74.
12. **Baldick, C. J., Jr., and B. Moss.** 1993. Characterization and temporal regulation of mRNAs encoded by vaccinia virus intermediate-stage genes. J Virol **67:**3515-27.

13. **Ballard, D. W., E. P. Dixon, N. J. Peffer, H. Bogerd, S. Doerre, B. Stein, and W. C. Greene.** 1992. The 65-kDa subunit of human NF-kappa B functions as a potent transcriptional activator and a target for v-Rel-mediated repression. Proc Natl Acad Sci U S A **89:**1875-9.
14. **Banadyga, L., J. Gerig, T. Stewart, and M. Barry.** 2007. Fowlpox virus encodes a Bcl-2 homologue that protects cells from apoptotic death through interaction with the proapoptotic protein Bak. J Virol **81:**11032-45.
15. **Banadyga, L., S. C. Lam, T. Okamoto, M. Kvansakul, D. C. Huang, and M. Barry.** 2011. Deerpox virus encodes an inhibitor of apoptosis that regulates Bak and Bax. J Virol **85:**1922-34.
16. **Banadyga, L., K. Veugelers, S. Campbell, and M. Barry.** 2009. The fowlpox virus BCL-2 homologue, FPV039, interacts with activated Bax and a discrete subset of BH3-only proteins to inhibit apoptosis. J Virol **83:**7085-98.
17. **Baroudy, B. M., S. Venkatesan, and B. Moss.** 1982. Incompletely base-paired flip-flop terminal loops link the two DNA strands of the vaccinia virus genome into one uninterrupted polynucleotide chain. Cell **28:**315-24.
18. **Barry, M., N. van Buuren, K. Burles, K. Mottet, Q. Wang, and A. Teale.** 2010. Poxvirus exploitation of the ubiquitin-proteasome system. Viruses **2:**2356-80.
19. **Bartee, E., M. Mansouri, B. T. Hovey Nerenberg, K. Gouveia, and K. Fruh.** 2004. Downregulation of major histocompatibility complex class I by human ubiquitin ligases related to viral immune evasion proteins. J Virol **78:**1109-20.
20. **Basak, S., H. Kim, J. D. Kearns, V. Tergaonkar, E. O'Dea, S. L. Werner, C. A. Benedict, C. F. Ware, G. Ghosh, I. M. Verma, and A. Hoffmann.** 2007. A fourth IkappaB protein within the NF-kappaB signaling module. Cell **128:**369-81.
21. **Beinke, S., M. P. Belich, and S. C. Ley.** 2002. The death domain of NF-kappa B1 p105 is essential for signal-induced p105 proteolysis. J Biol Chem **277:**24162-8.
22. **Bengali, Z., A. C. Townsley, and B. Moss.** 2009. Vaccinia virus strain differences in cell attachment and entry. Virology **389:**132-40.
23. **Betts, J. C., and G. J. Nabel.** 1996. Differential regulation of NF-kappaB2(p100) processing and control by amino-terminal sequences. Mol Cell Biol **16:**6363-71.
24. **Blasco, R., and B. Moss.** 1992. Role of cell-associated enveloped vaccinia virus in cell-to-cell spread. J Virol **66:**4170-9.
25. **Born, T. L., L. A. Morrison, D. J. Esteban, T. VandenBos, L. G. Thebeau, N. Chen, M. K. Spriggs, J. E. Sims, and R. M. Buller.** 2000. A poxvirus protein that binds to and inactivates IL-18, and inhibits NK cell response. J Immunol **164:**3246-54.

26. **Bour, S., C. Perrin, H. Akari, and K. Strebel.** 2001. The human immunodeficiency virus type 1 Vpu protein inhibits NF-kappa B activation by interfering with beta TrCP-mediated degradation of Ikappa B. J Biol Chem **276:**15920-8.
27. **Bowie, A., E. Kiss-Toth, J. A. Symons, G. L. Smith, S. K. Dower, and L. A. O'Neill.** 2000. A46R and A52R from vaccinia virus are antagonists of host IL-1 and toll-like receptor signaling. Proc Natl Acad Sci U S A **97:**10162-7.
28. **Brinkmann, M. M., M. Glenn, L. Rainbow, A. Kieser, C. Henke-Gendo, and T. F. Schulz.** 2003. Activation of mitogen-activated protein kinase and NF-kappaB pathways by a Kaposi's sarcoma-associated herpesvirus K15 membrane protein. J Virol **77:**9346-58.
29. **Broyles, S. S.** 2003. Vaccinia virus transcription. J Gen Virol **84:**2293-303.
30. **Brunetti, C. R., M. Paulose-Murphy, R. Singh, J. Qin, J. W. Barrett, A. Tardivel, P. Schneider, K. Essani, and G. McFadden.** 2003. A secreted high-affinity inhibitor of human TNF from Tanapox virus. Proc Natl Acad Sci U S A **100:**4831-6.
31. **Bui-Nguyen, T. M., S. B. Pakala, R. D. Sirigiri, W. Xia, M. C. Hung, S. K. Sarin, V. Kumar, B. L. Slagle, and R. Kumar.** 2010. NF-kappaB signaling mediates the induction of MTA1 by hepatitis B virus transactivator protein HBx. Oncogene **29:**1179-89.
32. **Camus-Bouclainville, C., L. Fiette, S. Bouchiha, B. Pignolet, D. Counor, C. Filipe, J. Gelfi, and F. Messud-Petit.** 2004. A virulence factor of myxoma virus colocalizes with NF-kappaB in the nucleus and interferes with inflammation. J Virol **78:**2510-6.
33. **Cardozo, T., and M. Pagano.** 2004. The SCF ubiquitin ligase: insights into a molecular machine. Nat Rev Mol Cell Biol **5:**739-51.
34. **Carlotti, F., S. K. Dower, and E. E. Qwarnstrom.** 2000. Dynamic shuttling of nuclear factor kappa B between the nucleus and cytoplasm as a consequence of inhibitor dissociation. J Biol Chem **275:**41028-34.
35. **Carmen E Gomez, J. L. N., Magdalena Krupa and Mariano Estaban.** 2008. Poxvirus Vectors and Their Use as Vaccines. European Infectous Diseas.
36. **Carter, G. C., G. Rodger, B. J. Murphy, M. Law, O. Krauss, M. Hollinshead, and G. L. Smith.** 2003. Vaccinia virus cores are transported on microtubules. J Gen Virol **84:**2443-58.
37. **Cenciarelli, C., D. S. Chiaur, D. Guardavaccaro, W. Parks, M. Vidal, and M. Pagano.** 1999. Identification of a family of human F-box proteins. Curr Biol **9:**1177-9.
38. **Chang, H. W., and B. L. Jacobs.** 1993. Identification of a conserved motif that is necessary for binding of the vaccinia virus E3L gene products to double-stranded RNA. Virology **194:**537-47.
39. **Chang, H. W., J. C. Watson, and B. L. Jacobs.** 1992. The E3L gene of vaccinia virus encodes an inhibitor of the interferon-induced, double-stranded RNA-dependent protein kinase. Proc Natl Acad Sci U S A **89:**4825-9.

40. **Chang, S., A. Dolganiuc, and G. Szabo.** 2007. Toll-like receptors 1 and 6 are involved in TLR2-mediated macrophage activation by hepatitis C virus core and NS3 proteins. J Leukoc Biol **82:**479-87.
41. **Chang, S. J., J. C. Hsiao, S. Sonnberg, C. T. Chiang, M. H. Yang, D. L. Tzou, A. A. Mercer, and W. Chang.** 2009. Poxvirus host range protein CP77 contains an F-box-like domain that is necessary to suppress NF-kappaB activation by tumor necrosis factor alpha but is independent of its host range function. J Virol **83:**4140-52.
42. **Chen, L. F., and W. C. Greene.** 2004. Shaping the nuclear action of NF-kappaB. Nat Rev Mol Cell Biol **5:**392-401.
43. **Chen, N., R. M. Buller, E. M. Wall, and C. Upton.** 2000. Analysis of host response modifier ORFs of ectromelia virus, the causative agent of mousepox. Virus Res **66:**155-73.
44. **Chen, R. A., N. Jacobs, and G. L. Smith.** 2006. Vaccinia virus strain Western Reserve protein B14 is an intracellular virulence factor. J Gen Virol **87:**1451-8.
45. **Chen, R. A., G. Ryzhakov, S. Cooray, F. Randow, and G. L. Smith.** 2008. Inhibition of IkappaB kinase by vaccinia virus virulence factor B14. PLoS Pathog **4:**e22.
46. **Chen, Z. J.** 2005. Ubiquitin signalling in the NF-kappaB pathway. Nat Cell Biol **7:**758-65.
47. **Chen, Z. J., L. Parent, and T. Maniatis.** 1996. Site-specific phosphorylation of IkappaBalpha by a novel ubiquitination-dependent protein kinase activity. Cell **84:**853-62.
48. **Chiu, Y. H., M. Zhao, and Z. J. Chen.** 2009. Ubiquitin in NF-kappaB signaling. Chem Rev **109:**1549-60.
49. **Cho, I. R., S. Jeong, B. H. Jhun, W. G. An, B. Lee, Y. T. Kwak, S. H. Lee, J. U. Jung, and Y. H. Chung.** 2007. Activation of non-canonical NF-kappaB pathway mediated by STP-A11, an oncoprotein of Herpesvirus saimiri. Virology **359:**37-45.
50. **Choi, S. H., K. J. Park, B. Y. Ahn, G. Jung, M. M. Lai, and S. B. Hwang.** 2006. Hepatitis C virus nonstructural 5B protein regulates tumor necrosis factor alpha signaling through effects on cellular IkappaB kinase. Mol Cell Biol **26:**3048-59.
51. **Chow, J. C., D. W. Young, D. T. Golenbock, W. J. Christ, and F. Gusovsky.** 1999. Toll-like receptor-4 mediates lipopolysaccharide-induced signal transduction. J Biol Chem **274:**10689-92.
52. **Chung, Y. H., B. H. Jhun, S. C. Ryu, H. S. Kim, C. M. Kim, B. S. Kim, Y. O. Kim, and S. J. Lee.** 2007. STP-C, an oncoprotein of herpesvirus saimiri augments the activation of NF-kappaB through ubiquitination of TRAF6. J Biochem Mol Biol **40:**341-8.

53. **Cohen, S., H. Achbert-Weiner, and A. Ciechanover.** 2004. Dual effects of IkappaB kinase beta-mediated phosphorylation on p105 Fate: SCF(beta-TrCP)-dependent degradation and SCF(beta-TrCP)-independent processing. Mol Cell Biol **24:**475-86.
54. **Cohen, S., A. Orian, and A. Ciechanover.** 2001. Processing of p105 is inhibited by docking of p50 active subunits to the ankyrin repeat domain, and inhibition is alleviated by signaling via the carboxyl-terminal phosphorylation/ ubiquitin-ligase binding domain. J Biol Chem **276:**26769-76.
55. **Colamonici, O. R., P. Domanski, S. M. Sweitzer, A. Larner, and R. M. Buller.** 1995. Vaccinia virus B18R gene encodes a type I interferon-binding protein that blocks interferon alpha transmembrane signaling. J Biol Chem **270:**15974-8.
56. **Condit, R. C., N. Moussatche, and P. Traktman.** 2006. In a nutshell: structure and assembly of the vaccinia virion. Adv Virus Res **66:**31-124.
57. **Conze, D. B., C. J. Wu, J. A. Thomas, A. Landstrom, and J. D. Ashwell.** 2008. Lys63-linked polyubiquitination of IRAK-1 is required for interleukin-1 receptor- and toll-like receptor-mediated NF-kappaB activation. Mol Cell Biol **28:**3538-47.
58. **Cooray, S., M. W. Bahar, N. G. Abrescia, C. E. McVey, N. W. Bartlett, R. A. Chen, D. I. Stuart, J. M. Grimes, and G. L. Smith.** 2007. Functional and structural studies of the vaccinia virus virulence factor N1 reveal a Bcl-2-like anti-apoptotic protein. J Gen Virol **88:**1656-66.
59. **Cudmore, S., P. Cossart, G. Griffiths, and M. Way.** 1995. Actin-based motility of vaccinia virus. Nature **378:**636-8.
60. **Cusson-Hermance, N., S. Khurana, T. H. Lee, K. A. Fitzgerald, and M. A. Kelliher.** 2005. Rip1 mediates the Trif-dependent toll-like receptor 3- and 4-induced NF-{kappa}B activation but does not contribute to interferon regulatory factor 3 activation. J Biol Chem **280:**36560-6.
61. **Dales, S., and E. H. Mosbach.** 1968. Vaccinia as a model for membrane biogenesis. Virology **35:**564-83.
62. **Dales, S., and L. Siminovitch.** 1961. The development of vaccinia virus in Earle's L strain cells as examined by electron microscopy. J Biophys Biochem Cytol **10:**475-503.
63. **Damon, I. K.** 2007. Poxviruses, Fields Virology.
64. **Davies, M. V., O. Elroy-Stein, R. Jagus, B. Moss, and R. J. Kaufman.** 1992. The vaccinia virus K3L gene product potentiates translation by inhibiting double-stranded-RNA-activated protein kinase and phosphorylation of the alpha subunit of eukaryotic initiation factor 2. J Virol **66:**1943-50.
65. **de Jong, S. J., J. C. Albrecht, M. Schmidt, I. Muller-Fleckenstein, and B. Biesinger.** 2010. Activation of noncanonical NF-kappaB signaling by the oncoprotein Tio. J Biol Chem **285:**16495-503.
66. **DeFilippes, F. M.** 1982. Restriction enzyme mapping of vaccinia virus DNA. J Virol **43:**136-49.

67. **Delhase, M., M. Hayakawa, Y. Chen, and M. Karin.** 1999. Positive and negative regulation of IkappaB kinase activity through IKKbeta subunit phosphorylation. Science **284:**309-13.
68. **Demarchi, F., M. I. Gutierrez, and M. Giacca.** 1999. Human immunodeficiency virus type 1 tat protein activates transcription factor NF-kappaB through the cellular interferon-inducible, double-stranded RNA-dependent protein kinase, PKR. J Virol **73:**7080-6.
69. **Dhawan, P., and A. Richmond.** 2002. A novel NF-kappa B-inducing kinase-MAPK signaling pathway up-regulates NF-kappa B activity in melanoma cells. J Biol Chem **277:**7920-8.
70. **Diebold, S. S., T. Kaisho, H. Hemmi, S. Akira, and C. Reis e Sousa.** 2004. Innate antiviral responses by means of TLR7-mediated recognition of single-stranded RNA. Science **303:**1529-31.
71. **Diel, D. G., G. Delhon, S. Luo, E. F. Flores, and D. L. Rock.** 2010. A novel inhibitor of the NF-{kappa}B signaling pathway encoded by the parapoxvirus orf virus. J Virol **84:**3962-73.
72. **Diel, D. G., S. Luo, G. Delhon, Y. Peng, E. F. Flores, and D. L. Rock.** 2011. A nuclear inhibitor of NF-kappaB encoded by a poxvirus. J Virol **85:**264-75.
73. **Diel, D. G., S. Luo, G. Delhon, Y. Peng, E. F. Flores, and D. L. Rock.** 2011. Orf virus ORFV121 encodes a novel inhibitor of NF-kappaB that contributes to virus virulence. J Virol **85:**2037-49.
74. **DiPerna, G., J. Stack, A. G. Bowie, A. Boyd, G. Kotwal, Z. Zhang, S. Arvikar, E. Latz, K. A. Fitzgerald, and W. L. Marshall.** 2004. Poxvirus protein N1L targets the I-kappaB kinase complex, inhibits signaling to NF-kappaB by the tumor necrosis factor superfamily of receptors, and inhibits NF-kappaB and IRF3 signaling by toll-like receptors. J Biol Chem **279:**36570-8.
75. **Dobbelstein, M., and T. Shenk.** 1996. Protection against apoptosis by the vaccinia virus SPI-2 (B13R) gene product. J Virol **70:**6479-85.
76. **Dobrzanski, P., R. P. Ryseck, and R. Bravo.** 1995. Specific inhibition of RelB/p52 transcriptional activity by the C-terminal domain of p100. Oncogene **10:**1003-7.
77. **Doceul, V., B. Charleston, H. Crooke, E. Reid, P. P. Powell, and J. Seago.** 2008. The Npro product of classical swine fever virus interacts with IkappaBalpha, the NF-kappaB inhibitor. J Gen Virol **89:**1881-9.
78. **Dong, X., H. Feng, Q. Sun, H. Li, T. T. Wu, R. Sun, S. A. Tibbetts, Z. J. Chen, and P. Feng.** 2010. Murine gamma-herpesvirus 68 hijacks MAVS and IKKbeta to initiate lytic replication. PLoS Pathog **6:**e1001001.
79. **Dorfleutner, A., S. J. Talbott, N. B. Bryan, K. N. Funya, S. L. Rellick, J. C. Reed, X. Shi, Y. Rojanasakul, D. C. Flynn, and C. Stehlik.** 2007. A Shope Fibroma virus PYRIN-only protein modulates the host immune response. Virus Genes **35:**685-94.

80. **Ea, C. K., L. Deng, Z. P. Xia, G. Pineda, and Z. J. Chen.** 2006. Activation of IKK by TNFalpha requires site-specific ubiquitination of RIP1 and polyubiquitin binding by NEMO. Mol Cell **22:**245-57.
81. **Earp, L. J., S. E. Delos, H. E. Park, and J. M. White.** 2005. The many mechanisms of viral membrane fusion proteins. Curr Top Microbiol Immunol **285:**25-66.
82. **Enari, M., H. Hug, and S. Nagata.** 1995. Involvement of an ICE-like protease in Fas-mediated apoptosis. Nature **375:**78-81.
83. **Esteban, D., S. Parker, J. Schriewer, H. Hartzler, and R. M. Buller.** 2012. Mousepox, a small animal model of smallpox. Methods Mol Biol **890:**177-98.
84. **Esteban, D. J., and R. M. Buller.** 2005. Ectromelia virus: the causative agent of mousepox. J Gen Virol **86:**2645-59.
85. **Everett, H., M. Barry, S. F. Lee, X. Sun, K. Graham, J. Stone, R. C. Bleackley, and G. McFadden.** 2000. M11L: a novel mitochondria-localized protein of myxoma virus that blocks apoptosis of infected leukocytes. J Exp Med **191:**1487-98.
86. **Fagan-Garcia, K., and M. Barry.** 2011. A vaccinia virus deletion mutant reveals the presence of additional inhibitors of NF-kappaB. J Virol **85:**883-94.
87. **Fan, Y., Y. Yu, Y. Shi, W. Sun, M. Xie, N. Ge, R. Mao, A. Chang, G. Xu, M. D. Schneider, H. Zhang, S. Fu, J. Qin, and J. Yang.** 2010. Lysine 63-linked polyubiquitination of TAK1 at lysine 158 is required for tumor necrosis factor alpha- and interleukin-1beta-induced IKK/NF-kappaB and JNK/AP-1 activation. J Biol Chem **285:**5347-60.
88. **Fang, X., J. Gao, H. Zheng, B. Li, L. Kong, Y. Zhang, W. Wang, Y. Zeng, and L. Ye.** 2007. The membrane protein of SARS-CoV suppresses NF-kappaB activation. J Med Virol **79:**1431-9.
89. **Fenner, F., DA Henderson, I Arita, Z Jezek, and ID Ladnyi.** 1988. Smallpox and its Eradication. World Health Organization.
90. **Fliss, P. M., T. P. Jowers, M. M. Brinkmann, B. Holstermann, C. Mack, P. Dickinson, H. Hohenberg, P. Ghazal, and W. Brune.** 2012. Viral mediated redirection of NEMO/IKKgamma to autophagosomes curtails the inflammatory cascade. PLoS Pathog **8:**e1002517.
91. **Friedman, J. M., and M. S. Horwitz.** 2002. Inhibition of tumor necrosis factor alpha-induced NF-kappa B activation by the adenovirus E3-10.4/14.5K complex. J Virol **76:**5515-21.
92. **Furia, B., L. Deng, K. Wu, S. Baylor, K. Kehn, H. Li, R. Donnelly, T. Coleman, and F. Kashanchi.** 2002. Enhancement of nuclear factor-kappa B acetylation by coactivator p300 and HIV-1 Tat proteins. J Biol Chem **277:**4973-80.
93. **Furukawa, M., Y. J. He, C. Borchers, and Y. Xiong.** 2003. Targeting of protein ubiquitination by BTB-Cullin 3-Roc1 ubiquitin ligases. Nat Cell Biol **5:**1001-7.

94. **Gaudreault, E., S. Fiola, M. Olivier, and J. Gosselin.** 2007. Epstein-Barr virus induces MCP-1 secretion by human monocytes via TLR2. J Virol **81:**8016-24.
95. **Gedey, R., X. L. Jin, O. Hinthong, and J. L. Shisler.** 2006. Poxviral regulation of the host NF-kappaB response: the vaccinia virus M2L protein inhibits induction of NF-kappaB activation via an ERK2 pathway in virus-infected human embryonic kidney cells. J Virol **80:**8676-85.
96. **Gil, J., J. Rullas, J. Alcami, and M. Esteban.** 2001. MC159L protein from the poxvirus molluscum contagiosum virus inhibits NF-kappaB activation and apoptosis induced by PKR. J Gen Virol **82:**3027-34.
97. **Gileva, I. P., T. S. Nepomnyashchikh, D. V. Antonets, L. R. Lebedev, G. V. Kochneva, A. V. Grazhdantseva, and S. N. Shchelkunov.** 2006. Properties of the recombinant TNF-binding proteins from variola, monkeypox, and cowpox viruses are different. Biochim Biophys Acta **1764:**1710-8.
98. **Graff, J. W., K. Ettayebi, and M. E. Hardy.** 2009. Rotavirus NSP1 inhibits NFkappaB activation by inducing proteasome-dependent degradation of beta-TrCP: a novel mechanism of IFN antagonism. PLoS Pathog **5:**e1000280.
99. **Graham, K. A., A. S. Lalani, J. L. Macen, T. L. Ness, M. Barry, L. Y. Liu, A. Lucas, I. Clark-Lewis, R. W. Moyer, and G. McFadden.** 1997. The T1/35kDa family of poxvirus-secreted proteins bind chemokines and modulate leukocyte influx into virus-infected tissues. Virology **229:**12-24.
100. **Graham, S. C., M. W. Bahar, S. Cooray, R. A. Chen, D. M. Whalen, N. G. Abrescia, D. Alderton, R. J. Owens, D. I. Stuart, G. L. Smith, and J. M. Grimes.** 2008. Vaccinia virus proteins A52 and B14 Share a Bcl-2-like fold but have evolved to inhibit NF-kappaB rather than apoptosis. PLoS Pathog **4:**e1000128.
101. **Guan, H., J. Jiao, and R. P. Ricciardi.** 2008. Tumorigenic adenovirus type 12 E1A inhibits phosphorylation of NF-kappaB by PKAc, causing loss of DNA binding and transactivation. J Virol **82:**40-8.
102. **Gubser, C., S. Hue, P. Kellam, and G. L. Smith.** 2004. Poxvirus genomes: a phylogenetic analysis. J Gen Virol **85:**105-17.
103. **Guerin, J. L., J. Gelfi, S. Boullier, M. Delverdier, F. A. Bellanger, S. Bertagnoli, I. Drexler, G. Sutter, and F. Messud-Petit.** 2002. Myxoma virus leukemia-associated protein is responsible for major histocompatibility complex class I and Fas-CD95 down-regulation and defines scrapins, a new group of surface cellular receptor abductor proteins. J Virol **76:**2912-23.
104. **Guo, C. J., W. J. Chen, L. Q. Yuan, L. S. Yang, S. P. Weng, X. Q. Yu, and J. G. He.** 2011. The viral ankyrin repeat protein (ORF124L) from infectious spleen and kidney necrosis virus attenuates nuclear factor-kappaB activation and interacts with IkappaB kinase beta. J Gen Virol **92:**1561-70.
105. **Haglund, K., P. P. Di Fiore, and I. Dikic.** 2003. Distinct monoubiquitin signals in receptor endocytosis. Trends Biochem Sci **28:**598-603.

106. **Hargett, D., S. Rice, and S. L. Bachenheimer.** 2006. Herpes simplex virus type 1 ICP27-dependent activation of NF-kappaB. J Virol **80:**10565-78.
107. **Harper, J. W., and M. K. Tan.** 2012. Ubiquitin Pathway Proteomics. Mol Cell Proteomics.
108. **Harte, M. T., I. R. Haga, G. Maloney, P. Gray, P. C. Reading, N. W. Bartlett, G. L. Smith, A. Bowie, and L. A. O'Neill.** 2003. The poxvirus protein A52R targets Toll-like receptor signaling complexes to suppress host defense. J Exp Med **197:**343-51.
109. **Hasegawa, M., Y. Fujimoto, P. C. Lucas, H. Nakano, K. Fukase, G. Nunez, and N. Inohara.** 2008. A critical role of RICK/RIP2 polyubiquitination in Nod-induced NF-kappaB activation. EMBO J **27:**373-83.
110. **Hatakeyama, S., M. Kitagawa, K. Nakayama, M. Shirane, M. Matsumoto, K. Hattori, H. Higashi, H. Nakano, K. Okumura, K. Onoe, and R. A. Good.** 1999. Ubiquitin-dependent degradation of IkappaBalpha is mediated by a ubiquitin ligase Skp1/Cul 1/F-box protein FWD1. Proc Natl Acad Sci U S A **96:**3859-63.
111. **Hatakeyama, S., and K. I. Nakayama.** 2003. U-box proteins as a new family of ubiquitin ligases. Biochem Biophys Res Commun **302:**635-45.
112. **Hayden, M. S., and S. Ghosh.** 2012. NF-kappaB, the first quarter-century: remarkable progress and outstanding questions. Genes Dev **26:**203-34.
113. **Hemmi, H., O. Takeuchi, T. Kawai, T. Kaisho, S. Sato, H. Sanjo, M. Matsumoto, K. Hoshino, H. Wagner, K. Takeda, and S. Akira.** 2000. A Toll-like receptor recognizes bacterial DNA. Nature **408:**740-5.
114. **Heusch, M., L. Lin, R. Geleziunas, and W. C. Greene.** 1999. The generation of nfkb2 p52: mechanism and efficiency. Oncogene **18:**6201-8.
115. **Heuser, J.** 2005. Deep-etch EM reveals that the early poxvirus envelope is a single membrane bilayer stabilized by a geodetic "honeycomb" surface coat. J Cell Biol **169:**269-83.
116. **Hicke, L.** 2001. Protein regulation by monoubiquitin. Nat Rev Mol Cell Biol **2:**195-201.
117. **Higuchi, M., and M. Fujii.** 2009. Distinct functions of HTLV-1 Tax1 from HTLV-2 Tax2 contribute key roles to viral pathogenesis. Retrovirology **6:**117.
118. **Hinthong, O., X. L. Jin, and J. L. Shisler.** 2008. Characterization of wild-type and mutant vaccinia virus M2L proteins' abilities to localize to the endoplasmic reticulum and to inhibit NF-kappaB activation during infection. Virology **373:**248-62.
119. **Hiscott, J., H. Kwon, and P. Genin.** 2001. Hostile takeovers: viral appropriation of the NF-kappaB pathway. J Clin Invest **107:**143-51.
120. **Hiscott, J., T. L. Nguyen, M. Arguello, P. Nakhaei, and S. Paz.** 2006. Manipulation of the nuclear factor-kappaB pathway and the innate immune response by viruses. Oncogene **25:**6844-67.

121. **Hoffmann, A., T. H. Leung, and D. Baltimore.** 2003. Genetic analysis of NF-kappaB/Rel transcription factors defines functional specificities. EMBO J **22:**5530-9.
122. **Hoffmann, A., A. Levchenko, M. L. Scott, and D. Baltimore.** 2002. The IkappaB-NF-kappaB signaling module: temporal control and selective gene activation. Science **298:**1241-5.
123. **Hollinshead, M., A. Vanderplasschen, G. L. Smith, and D. J. Vaux.** 1999. Vaccinia virus intracellular mature virions contain only one lipid membrane. J Virol **73:**1503-17.
124. **Hruby, D. E., and L. A. Ball.** 1982. Mapping and identification of the vaccinia virus thymidine kinase gene. J Virol **43:**403-9.
125. **Hsu, H., H. B. Shu, M. G. Pan, and D. V. Goeddel.** 1996. TRADD-TRAF2 and TRADD-FADD interactions define two distinct TNF receptor 1 signal transduction pathways. Cell **84:**299-308.
126. **Hu, F. Q., C. A. Smith, and D. J. Pickup.** 1994. Cowpox virus contains two copies of an early gene encoding a soluble secreted form of the type II TNF receptor. Virology **204:**343-56.
127. **Hughes, A. L., S. Irausquin, and R. Friedman.** 2010. The evolutionary biology of poxviruses. Infect Genet Evol **10:**50-9.
128. **Husain, M., A. S. Weisberg, and B. Moss.** 2006. Existence of an operative pathway from the endoplasmic reticulum to the immature poxvirus membrane. Proc Natl Acad Sci U S A **103:**19506-11.
129. **Husain, M., A. S. Weisberg, and B. Moss.** 2007. Sequence-independent targeting of transmembrane proteins synthesized within vaccinia virus factories to nascent viral membranes. J Virol **81:**2646-55.
130. **Ikeda, F., N. Crosetto, and I. Dikic.** 2010. What determines the specificity and outcomes of ubiquitin signaling? Cell **143:**677-81.
131. **Isaacs, S. N., G. J. Kotwal, and B. Moss.** 1992. Vaccinia virus complement-control protein prevents antibody-dependent complement-enhanced neutralization of infectivity and contributes to virulence. Proc Natl Acad Sci U S A **89:**628-32.
132. **Janssens, S., and R. Beyaert.** 2003. Role of Toll-like receptors in pathogen recognition. Clin Microbiol Rev **16:**637-46.
133. **Jarvis, M. A., J. A. Borton, A. M. Keech, J. Wong, W. J. Britt, B. E. Magun, and J. A. Nelson.** 2006. Human cytomegalovirus attenuates interleukin-1beta and tumor necrosis factor alpha proinflammatory signaling by inhibition of NF-kappaB activation. J Virol **80:**5588-98.
134. **Jiao, J., H. Guan, A. M. Lippa, and R. P. Ricciardi.** 2010. The N terminus of adenovirus type 12 E1A inhibits major histocompatibility complex class I expression by preventing phosphorylation of NF-kappaB p65 Ser276 through direct binding. J Virol **84:**7668-74.
135. **Jin, J., X. Li, S. P. Gygi, and J. W. Harper.** 2007. Dual E1 activation systems for ubiquitin differentially regulate E2 enzyme charging. Nature **447:**1135-8.

136. **Joazeiro, C. A., and A. M. Weissman.** 2000. RING finger proteins: mediators of ubiquitin ligase activity. Cell **102:**549-52.
137. **Johnston, J. B., J. W. Barrett, S. H. Nazarian, M. Goodwin, D. Ricciuto, G. Wang, and G. McFadden.** 2005. A poxvirus-encoded pyrin domain protein interacts with ASC-1 to inhibit host inflammatory and apoptotic responses to infection. Immunity **23:**587-98.
138. **Johnston, J. B., and G. McFadden.** 2003. Poxvirus immunomodulatory strategies: current perspectives. J Virol **77:**6093-100.
139. **Jones, E. V., and B. Moss.** 1984. Mapping of the vaccinia virus DNA polymerase gene by marker rescue and cell-free translation of selected RNA. J Virol **49:**72-7.
140. **Jones, E. V., C. Puckett, and B. Moss.** 1987. DNA-dependent RNA polymerase subunits encoded within the vaccinia virus genome. J Virol **61:**1765-71.
141. **Jones, J. O., and A. M. Arvin.** 2006. Inhibition of the NF-kappaB pathway by varicella-zoster virus in vitro and in human epidermal cells in vivo. J Virol **80:**5113-24.
142. **Joo, M., Y. S. Hahn, M. Kwon, R. T. Sadikot, T. S. Blackwell, and J. W. Christman.** 2005. Hepatitis C virus core protein suppresses NF-kappaB activation and cyclooxygenase-2 expression by direct interaction with IkappaB kinase beta. J Virol **79:**7648-57.
143. **Kagan, J. C., and R. Medzhitov.** 2006. Phosphoinositide-mediated adaptor recruitment controls Toll-like receptor signaling. Cell **125:**943-55.
144. **Kanayama, A., R. B. Seth, L. Sun, C. K. Ea, M. Hong, A. Shaito, Y. H. Chiu, L. Deng, and Z. J. Chen.** 2004. TAB2 and TAB3 activate the NF-kappaB pathway through binding to polyubiquitin chains. Mol Cell **15:**535-48.
145. **Karin, M., and Y. Ben-Neriah.** 2000. Phosphorylation meets ubiquitination: the control of NF-[kappa]B activity. Annu Rev Immunol **18:**621-63.
146. **Katsafanas, G. C., and B. Moss.** 2007. Colocalization of transcription and translation within cytoplasmic poxvirus factories coordinates viral expression and subjugates host functions. Cell Host Microbe **2:**221-8.
147. **Katz, E., E. Wolffe, and B. Moss.** 2002. Identification of second-site mutations that enhance release and spread of vaccinia virus. J Virol **76:**11637-44.
148. **Kawai, T., and S. Akira.** 2007. Signaling to NF-kappaB by Toll-like receptors. Trends Mol Med **13:**460-9.
149. **Keck, J. G., C. J. Baldick, Jr., and B. Moss.** 1990. Role of DNA replication in vaccinia virus gene expression: a naked template is required for transcription of three late trans-activator genes. Cell **61:**801-9.

150. **Kettle, S., A. Alcami, A. Khanna, R. Ehret, C. Jassoy, and G. L. Smith.** 1997. Vaccinia virus serpin B13R (SPI-2) inhibits interleukin-1beta-converting enzyme and protects virus-infected cells from TNF- and Fas-mediated apoptosis, but does not prevent IL-1beta-induced fever. J Gen Virol **78 (Pt 3):**677-85.
151. **Kim, J. C., S. Y. Lee, S. Y. Kim, J. K. Kim, H. J. Kim, H. M. Lee, M. S. Choi, J. S. Min, M. J. Kim, H. S. Choi, and J. K. Ahn.** 2008. HSV-1 ICP27 suppresses NF-kappaB activity by stabilizing IkappaBalpha. FEBS Lett **582:**2371-6.
152. **Knop, J., and M. U. Martin.** 1999. Effects of IL-1 receptor-associated kinase (IRAK) expression on IL-1 signaling are independent of its kinase activity. FEBS Lett **448:**81-5.
153. **Komander, D., F. Reyes-Turcu, J. D. Licchesi, P. Odenwaelder, K. D. Wilkinson, and D. Barford.** 2009. Molecular discrimination of structurally equivalent Lys 63-linked and linear polyubiquitin chains. EMBO Rep **10:**466-73.
154. **Kotwal, G. J., S. N. Isaacs, R. McKenzie, M. M. Frank, and B. Moss.** 1990. Inhibition of the complement cascade by the major secretory protein of vaccinia virus. Science **250:**827-30.
155. **Kotwal, G. J., C. G. Miller, and D. E. Justus.** 1998. The inflammation modulatory protein (IMP) of cowpox virus drastically diminishes the tissue damage by down-regulating cellular infiltration resulting from complement activation. Mol Cell Biochem **185:**39-46.
156. **Kotwal, G. J., and B. Moss.** 1988. Vaccinia virus encodes a secretory polypeptide structurally related to complement control proteins. Nature **335:**176-8.
157. **Kroll, M., F. Margottin, A. Kohl, P. Renard, H. Durand, J. P. Concordet, F. Bachelerie, F. Arenzana-Seisdedos, and R. Benarous.** 1999. Inducible degradation of IkappaBalpha by the proteasome requires interaction with the F-box protein h-betaTrCP. J Biol Chem **274:**7941-5.
158. **Kurt-Jones, E. A., L. Popova, L. Kwinn, L. M. Haynes, L. P. Jones, R. A. Tripp, E. E. Walsh, M. W. Freeman, D. T. Golenbock, L. J. Anderson, and R. W. Finberg.** 2000. Pattern recognition receptors TLR4 and CD14 mediate response to respiratory syncytial virus. Nat Immunol **1:**398-401.
159. **Lalani, A. S., K. Graham, K. Mossman, K. Rajarathnam, I. Clark-Lewis, D. Kelvin, and G. McFadden.** 1997. The purified myxoma virus gamma interferon receptor homolog M-T7 interacts with the heparin-binding domains of chemokines. J Virol **71:**4356-63.
160. **Lalani, A. S., J. Masters, K. Graham, L. Liu, A. Lucas, and G. McFadden.** 1999. Role of the myxoma virus soluble CC-chemokine inhibitor glycoprotein, M-T1, during myxoma virus pathogenesis. Virology **256:**233-45.
161. **Law, M., G. C. Carter, K. L. Roberts, M. Hollinshead, and G. L. Smith.** 2006. Ligand-induced and nonfusogenic dissolution of a viral membrane. Proc Natl Acad Sci U S A **103:**5989-94.

162. **Lee, H. J., K. Essani, and G. L. Smith.** 2001. The genome sequence of Yaba-like disease virus, a yatapoxvirus. Virology **281:**170-92.
163. **Lee, T. H., J. Shank, N. Cusson, and M. A. Kelliher.** 2004. The kinase activity of Rip1 is not required for tumor necrosis factor-alpha-induced IkappaB kinase or p38 MAP kinase activation or for the ubiquitination of Rip1 by Traf2. J Biol Chem **279:**33185-91.
164. **Lee-Chen, G. J., and E. G. Niles.** 1988. Transcription and translation mapping of the 13 genes in the vaccinia virus HindIII D fragment. Virology **163:**52-63.
165. **Lei, X., Z. Bai, F. Ye, J. Xie, C. G. Kim, Y. Huang, and S. J. Gao.** 2010. Regulation of NF-kappaB inhibitor IkappaBalpha and viral replication by a KSHV microRNA. Nat Cell Biol **12:**193-9.
166. **Li, H., M. Kobayashi, M. Blonska, Y. You, and X. Lin.** 2006. Ubiquitination of RIP is required for tumor necrosis factor alpha-induced NF-kappaB activation. J Biol Chem **281:**13636-43.
167. **Li, K., E. Foy, J. C. Ferreon, M. Nakamura, A. C. Ferreon, M. Ikeda, S. C. Ray, M. Gale, Jr., and S. M. Lemon.** 2005. Immune evasion by hepatitis C virus NS3/4A protease-mediated cleavage of the Toll-like receptor 3 adaptor protein TRIF. Proc Natl Acad Sci U S A **102:**2992-7.
168. **Li, W., M. H. Bengtson, A. Ulbrich, A. Matsuda, V. A. Reddy, A. Orth, S. K. Chanda, S. Batalov, and C. A. Joazeiro.** 2008. Genome-wide and functional annotation of human E3 ubiquitin ligases identifies MULAN, a mitochondrial E3 that regulates the organelle's dynamics and signaling. PLoS One **3:**e1487.
169. **Li, Y., X. Meng, Y. Xiang, and J. Deng.** 2010. Structure function studies of vaccinia virus host range protein k1 reveal a novel functional surface for ankyrin repeat proteins. J Virol **84:**3331-8.
170. **Li, Z., and G. J. Nabel.** 1997. A new member of the I kappaB protein family, I kappaB epsilon, inhibits RelA (p65)-mediated NF-kappaB transcription. Mol Cell Biol **17:**6184-90.
171. **Liao, G., M. Zhang, E. W. Harhaj, and S. C. Sun.** 2004. Regulation of the NF-kappaB-inducing kinase by tumor necrosis factor receptor-associated factor 3-induced degradation. J Biol Chem **279:**26243-50.
172. **Liou, H. C., G. P. Nolan, S. Ghosh, T. Fujita, and D. Baltimore.** 1992. The NF-kappa B p50 precursor, p105, contains an internal I kappa B-like inhibitor that preferentially inhibits p50. EMBO J **11:**3003-9.
173. **Liu, X., K. Fitzgerald, E. Kurt-Jones, R. Finberg, and D. M. Knipe.** 2008. Herpesvirus tegument protein activates NF-kappaB signaling through the TRAF6 adaptor protein. Proc Natl Acad Sci U S A **105:**11335-9.
174. **Lomas, D. A., D. L. Evans, C. Upton, G. McFadden, and R. W. Carrell.** 1993. Inhibition of plasmin, urokinase, tissue plasminogen activator, and C1S by a myxoma virus serine proteinase inhibitor. J Biol Chem **268:**516-21.

175. **Loparev, V. N., J. M. Parsons, J. C. Knight, J. F. Panus, C. A. Ray, R. M. Buller, D. J. Pickup, and J. J. Esposito.** 1998. A third distinct tumor necrosis factor receptor of orthopoxviruses. Proc Natl Acad Sci U S A **95:**3786-91.
176. **Luftig, M., T. Yasui, V. Soni, M. S. Kang, N. Jacobson, E. Cahir-McFarland, B. Seed, and E. Kieff.** 2004. Epstein-Barr virus latent infection membrane protein 1 TRAF-binding site induces NIK/IKK alpha-dependent noncanonical NF-kappaB activation. Proc Natl Acad Sci U S A **101:**141-6.
177. **Macen, J. L., C. Upton, N. Nation, and G. McFadden.** 1993. SERP1, a serine proteinase inhibitor encoded by myxoma virus, is a secreted glycoprotein that interferes with inflammation. Virology **195:**348-63.
178. **Mack, C., A. Sickmann, D. Lembo, and W. Brune.** 2008. Inhibition of proinflammatory and innate immune signaling pathways by a cytomegalovirus RIP1-interacting protein. Proc Natl Acad Sci U S A **105:**3094-9.
179. **Makris, C., J. L. Roberts, and M. Karin.** 2002. The carboxyl-terminal region of IkappaB kinase gamma (IKKgamma) is required for full IKK activation. Mol Cell Biol **22:**6573-81.
180. **Maluquer de Motes, C., S. Cooray, H. Ren, G. M. Almeida, K. McGourty, M. W. Bahar, D. I. Stuart, J. M. Grimes, S. C. Graham, and G. L. Smith.** 2011. Inhibition of apoptosis and NF-kappaB activation by vaccinia protein N1 occur via distinct binding surfaces and make different contributions to virulence. PLoS Pathog **7:**e1002430.
181. **Mansouri, M., E. Bartee, K. Gouveia, B. T. Hovey Nerenberg, J. Barrett, L. Thomas, G. Thomas, G. McFadden, and K. Fruh.** 2003. The PHD/LAP-domain protein M153R of myxomavirus is a ubiquitin ligase that induces the rapid internalization and lysosomal destruction of CD4. J Virol **77:**1427-40.
182. **McCarthy, J. V., J. Ni, and V. M. Dixit.** 1998. RIP2 is a novel NF-kappaB-activating and cell death-inducing kinase. J Biol Chem **273:**16968-75.
183. **McFadden, G.** 2005. Poxvirus tropism. Nat Rev Microbiol **3:**201-13.
184. **Mercer, A. A., S. B. Fleming, and N. Ueda.** 2005. F-box-like domains are present in most poxvirus ankyrin repeat proteins. Virus Genes **31:**127-33.
185. **Mercer, J., S. Knebel, F. I. Schmidt, J. Crouse, C. Burkard, and A. Helenius.** 2010. Vaccinia virus strains use distinct forms of macropinocytosis for host-cell entry. Proc Natl Acad Sci U S A **107:**9346-51.
186. **Messud-Petit, F., J. Gelfi, M. Delverdier, M. F. Amardeilh, R. Py, G. Sutter, and S. Bertagnoli.** 1998. Serp2, an inhibitor of the interleukin-1beta-converting enzyme, is critical in the pathobiology of myxoma virus. J Virol **72:**7830-9.
187. **Metzger, M. B., V. A. Hristova, and A. M. Weissman.** 2012. HECT and RING finger families of E3 ubiquitin ligases at a glance. J Cell Sci **125:**531-7.

188. **Michel, J. J., and Y. Xiong.** 1998. Human CUL-1, but not other cullin family members, selectively interacts with SKP1 to form a complex with SKP2 and cyclin A. Cell Growth Differ **9:**435-49.
189. **Miller, B. S., and E. Zandi.** 2001. Complete reconstitution of human IkappaB kinase (IKK) complex in yeast. Assessment of its stoichiometry and the role of IKKgamma on the complex activity in the absence of stimulation. J Biol Chem **276:**36320-6.
190. **Miller, C. G., S. N. Shchelkunov, and G. J. Kotwal.** 1997. The cowpox virus-encoded homolog of the vaccinia virus complement control protein is an inflammation modulatory protein. Virology **229:**126-33.
191. **Mohamed, M. R., and G. McFadden.** 2009. NFkB inhibitors: strategies from poxviruses. Cell Cycle **8:**3125-32.
192. **Mohamed, M. R., M. M. Rahman, J. S. Lanchbury, D. Shattuck, C. Neff, M. Dufford, N. van Buuren, K. Fagan, M. Barry, S. Smith, I. Damon, and G. McFadden.** 2009. Proteomic screening of variola virus reveals a unique NF-kappaB inhibitor that is highly conserved among pathogenic orthopoxviruses. Proc Natl Acad Sci U S A **106:**9045-50.
193. **Mohamed, M. R., M. M. Rahman, A. Rice, R. W. Moyer, S. J. Werden, and G. McFadden.** 2009. Cowpox virus expresses a novel ankyrin repeat NF-kappaB inhibitor that controls inflammatory cell influx into virus-infected tissues and is critical for virus pathogenesis. J Virol **83:**9223-36.
194. **Montag, C., J. Wagner, I. Gruska, and C. Hagemeier.** 2006. Human cytomegalovirus blocks tumor necrosis factor alpha- and interleukin-1beta-mediated NF-kappaB signaling. J Virol **80:**11686-98.
195. **Morlon, A., A. Munnich, and A. Smahi.** 2005. TAB2, TRAF6 and TAK1 are involved in NF-kappaB activation induced by the TNF-receptor, Edar and its adaptator Edaradd. Hum Mol Genet **14:**3751-7.
196. **Mosavi, L. K., T. J. Cammett, D. C. Desrosiers, and Z. Y. Peng.** 2004. The ankyrin repeat as molecular architecture for protein recognition. Protein Sci **13:**1435-48.
197. **Moss, B.** 2007. *Poxviridae:* The Viruses and Their Replication. *In* D. M. K. a. P. M. Howley (ed.), Fields Virology 5ed.
198. **Moss, B., and J. L. Shisler.** 2001. Immunology 101 at poxvirus U: immune evasion genes. Semin Immunol **13:**59-66.
199. **Murao, L. E., and J. L. Shisler.** 2005. The MCV MC159 protein inhibits late, but not early, events of TNF-alpha-induced NF-kappaB activation. Virology **340:**255-64.
200. **Myskiw, C., J. Arsenio, R. van Bruggen, Y. Deschambault, and J. Cao.** 2009. Vaccinia virus E3 suppresses expression of diverse cytokines through inhibition of the PKR, NF-kappaB, and IRF3 pathways. J Virol **83:**6757-68.
201. **Najarro, P., P. Traktman, and J. A. Lewis.** 2001. Vaccinia virus blocks gamma interferon signal transduction: viral VH1 phosphatase reverses Stat1 activation. J Virol **75:**3185-96.

202. **Nakayama, K. I., and K. Nakayama.** 2006. Ubiquitin ligases: cell-cycle control and cancer. Nat Rev Cancer **6:**369-81.
203. **Nash, P., A. Whitty, J. Handwerker, J. Macen, and G. McFadden.** 1998. Inhibitory specificity of the anti-inflammatory myxoma virus serpin, SERP-1. J Biol Chem **273:**20982-91.
204. **Natoli, G., S. Saccani, D. Bosisio, and I. Marazzi.** 2005. Interactions of NF-kappaB with chromatin: the art of being at the right place at the right time. Nat Immunol **6:**439-45.
205. **Nerenberg, B. T., J. Taylor, E. Bartee, K. Gouveia, M. Barry, and K. Fruh.** 2005. The poxviral RING protein p28 is a ubiquitin ligase that targets ubiquitin to viral replication factories. J Virol **79:**597-601.
206. **Neznanov, N., K. M. Chumakov, L. Neznanova, A. Almasan, A. K. Banerjee, and A. V. Gudkov.** 2005. Proteolytic cleavage of the p65-RelA subunit of NF-kappaB during poliovirus infection. J Biol Chem **280:**24153-8.
207. **Ng, A., D. C. Tscharke, P. C. Reading, and G. L. Smith.** 2001. The vaccinia virus A41L protein is a soluble 30 kDa glycoprotein that affects virus virulence. J Gen Virol **82:**2095-105.
208. **Nichols, D. B., and J. L. Shisler.** 2006. The MC160 protein expressed by the dermatotropic poxvirus molluscum contagiosum virus prevents tumor necrosis factor alpha-induced NF-kappaB activation via inhibition of I kappa kinase complex formation. J Virol **80:**578-86.
209. **Nichols, D. B., and J. L. Shisler.** 2009. Poxvirus MC160 protein utilizes multiple mechanisms to inhibit NF-kappaB activation mediated via components of the tumor necrosis factor receptor 1 signal transduction pathway. J Virol **83:**3162-74.
210. **Oeckinghaus, A., M. S. Hayden, and S. Ghosh.** 2011. Crosstalk in NF-kappaB signaling pathways. Nat Immunol **12:**695-708.
211. **Ohta, T., J. J. Michel, A. J. Schottelius, and Y. Xiong.** 1999. ROC1, a homolog of APC11, represents a family of cullin partners with an associated ubiquitin ligase activity. Mol Cell **3:**535-41.
212. **Osborn, L., S. Kunkel, and G. J. Nabel.** 1989. Tumor necrosis factor alpha and interleukin 1 stimulate the human immunodeficiency virus enhancer by activation of the nuclear factor kappa B. Proc Natl Acad Sci U S A **86:**2336-40.
213. **Palombella, V. J., O. J. Rando, A. L. Goldberg, and T. Maniatis.** 1994. The ubiquitin-proteasome pathway is required for processing the NF-kappa B1 precursor protein and the activation of NF-kappa B. Cell **78:**773-85.
214. **Park, Y. C., H. Ye, C. Hsia, D. Segal, R. L. Rich, H. C. Liou, D. G. Myszka, and H. Wu.** 2000. A novel mechanism of TRAF signaling revealed by structural and functional analyses of the TRADD-TRAF2 interaction. Cell **101:**777-87.
215. **Passmore, L. A., and D. Barford.** 2004. Getting into position: the catalytic mechanisms of protein ubiquitylation. Biochem J **379:**513-25.

216. **Peng, J., D. Schwartz, J. E. Elias, C. C. Thoreen, D. Cheng, G. Marsischky, J. Roelofs, D. Finley, and S. P. Gygi.** 2003. A proteomics approach to understanding protein ubiquitination. Nat Biotechnol **21:**921-6.
217. **Petroski, M. D., and R. J. Deshaies.** 2005. Function and regulation of cullin-RING ubiquitin ligases. Nat Rev Mol Cell Biol **6:**9-20.
218. **Pomerantz, J. L., and D. Baltimore.** 2002. Two pathways to NF-kappaB. Mol Cell **10:**693-5.
219. **Quan, L. T., A. Caputo, R. C. Bleackley, D. J. Pickup, and G. S. Salvesen.** 1995. Granzyme B is inhibited by the cowpox virus serpin cytokine response modifier A. J Biol Chem **270:**10377-9.
220. **Rahman, M. M., and G. McFadden.** 2011. Modulation of NF-kappaB signalling by microbial pathogens. Nat Rev Microbiol **9:**291-306.
221. **Rahman, M. M., M. R. Mohamed, M. Kim, S. Smallwood, and G. McFadden.** 2009. Co-regulation of NF-kappaB and inflammasome-mediated inflammatory responses by myxoma virus pyrin domain-containing protein M013. PLoS Pathog **5:**e1000635.
222. **Rao, P., M. S. Hayden, M. Long, M. L. Scott, A. P. West, D. Zhang, A. Oeckinghaus, C. Lynch, A. Hoffmann, D. Baltimore, and S. Ghosh.** 2010. IkappaBbeta acts to inhibit and activate gene expression during the inflammatory response. Nature **466:**1115-9.
223. **Ray, C. A., R. A. Black, S. R. Kronheim, T. A. Greenstreet, P. R. Sleath, G. S. Salvesen, and D. J. Pickup.** 1992. Viral inhibition of inflammation: cowpox virus encodes an inhibitor of the interleukin-1 beta converting enzyme. Cell **69:**597-604.
224. **Reed, K. D., J. W. Melski, M. B. Graham, R. L. Regnery, M. J. Sotir, M. V. Wegner, J. J. Kazmierczak, E. J. Stratman, Y. Li, J. A. Fairley, G. R. Swain, V. A. Olson, E. K. Sargent, S. C. Kehl, M. A. Frace, R. Kline, S. L. Foldy, J. P. Davis, and I. K. Damon.** 2004. The detection of monkeypox in humans in the Western Hemisphere. N Engl J Med **350:**342-50.
225. **Reimers, K., K. Buchholz, and H. Werchau.** 2005. Respiratory syncytial virus M2-1 protein induces the activation of nuclear factor kappa B. Virology **331:**260-8.
226. **Roberts, K. L., and G. L. Smith.** 2008. Vaccinia virus morphogenesis and dissemination. Trends Microbiol **16:**472-9.
227. **Rodriguez, C. I., M. L. Nogal, A. L. Carrascosa, M. L. Salas, M. Fresno, and Y. Revilla.** 2002. African swine fever virus IAP-like protein induces the activation of nuclear factor kappa B. J Virol **76:**3936-42.
228. **Rosel, J., and B. Moss.** 1985. Transcriptional and translational mapping and nucleotide sequence analysis of a vaccinia virus gene encoding the precursor of the major core polypeptide 4b. J Virol **56:**830-8.
229. **Rosengard, A. M., Y. Liu, Z. Nie, and R. Jimenez.** 2002. Variola virus immune evasion design: expression of a highly efficient inhibitor of human complement. Proc Natl Acad Sci U S A **99:**8808-13.

230. **Rothe, M., V. Sarma, V. M. Dixit, and D. V. Goeddel.** 1995. TRAF2-mediated activation of NF-kappa B by TNF receptor 2 and CD40. Science **269:**1424-7.
231. **Rothwarf, D. M., E. Zandi, G. Natoli, and M. Karin.** 1998. IKK-gamma is an essential regulatory subunit of the IkappaB kinase complex. Nature **395:**297-300.
232. **Rotin, D., and S. Kumar.** 2009. Physiological functions of the HECT family of ubiquitin ligases. Nat Rev Mol Cell Biol **10:**398-409.
233. **Sandgren, K. J., J. Wilkinson, M. Miranda-Saksena, G. M. McInerney, K. Byth-Wilson, P. J. Robinson, and A. L. Cunningham.** 2010. A differential role for macropinocytosis in mediating entry of the two forms of vaccinia virus into dendritic cells. PLoS Pathog **6:**e1000866.
234. **Sanz, P., and B. Moss.** 1999. Identification of a transcription factor, encoded by two vaccinia virus early genes, that regulates the intermediate stage of viral gene expression. Proc Natl Acad Sci U S A **96:**2692-7.
235. **Saraiva, M., and A. Alcami.** 2001. CrmE, a novel soluble tumor necrosis factor receptor encoded by poxviruses. J Virol **75:**226-33.
236. **Scheibel, M., B. Klein, H. Merkle, M. Schulz, R. Fritsch, F. R. Greten, M. C. Arkan, G. Schneider, and R. M. Schmid.** 2010. IkappaBbeta is an essential co-activator for LPS-induced IL-1beta transcription in vivo. J Exp Med **207:**2621-30.
237. **Scheidereit, C.** 2006. IkappaB kinase complexes: gateways to NF-kappaB activation and transcription. Oncogene **25:**6685-705.
238. **Schmelz, M., B. Sodeik, M. Ericsson, E. J. Wolffe, H. Shida, G. Hiller, and G. Griffiths.** 1994. Assembly of vaccinia virus: the second wrapping cisterna is derived from the trans Golgi network. J Virol **68:**130-47.
239. **Schmidt, C., B. Peng, Z. Li, G. M. Sclabas, S. Fujioka, J. Niu, M. Schmidt-Supprian, D. B. Evans, J. L. Abbruzzese, and P. J. Chiao.** 2003. Mechanisms of proinflammatory cytokine-induced biphasic NF-kappaB activation. Mol Cell **12:**1287-300.
240. **Schmidt, F. I., C. K. Bleck, A. Helenius, and J. Mercer.** 2011. Vaccinia extracellular virions enter cells by macropinocytosis and acid-activated membrane rupture. EMBO J **30:**3647-61.
241. **Schmidt, F. I., C. K. Bleck, and J. Mercer.** 2012. Poxvirus host cell entry. Curr Opin Virol **2:**20-7.
242. **Schroder, M., M. Baran, and A. G. Bowie.** 2008. Viral targeting of DEAD box protein 3 reveals its role in TBK1/IKKepsilon-mediated IRF activation. EMBO J **27:**2147-57.
243. **Sciortino, M. T., M. A. Medici, F. Marino-Merlo, D. Zaccaria, M. Giuffre-Cuculletto, A. Venuti, S. Grelli, and A. Mastino.** 2008. Involvement of HVEM receptor in activation of nuclear factor kappaB by herpes simplex virus 1 glycoprotein D. Cell Microbiol **10:**2297-311.

244. **Seet, B. T., J. B. Johnston, C. R. Brunetti, J. W. Barrett, H. Everett, C. Cameron, J. Sypula, S. H. Nazarian, A. Lucas, and G. McFadden.** 2003. Poxviruses and immune evasion. Annu Rev Immunol **21:**377-423.
245. **Senftleben, U., Y. Cao, G. Xiao, F. R. Greten, G. Krahn, G. Bonizzi, Y. Chen, Y. Hu, A. Fong, S. C. Sun, and M. Karin.** 2001. Activation by IKKalpha of a second, evolutionary conserved, NF-kappa B signaling pathway. Science **293:**1495-9.
246. **Senkevich, T. G., S. Ojeda, A. Townsley, G. E. Nelson, and B. Moss.** 2005. Poxvirus multiprotein entry-fusion complex. Proc Natl Acad Sci U S A **102:**18572-7.
247. **Shih, V. F., J. D. Kearns, S. Basak, O. V. Savinova, G. Ghosh, and A. Hoffmann.** 2009. Kinetic control of negative feedback regulators of NF-kappaB/RelA determines their pathogen- and cytokine-receptor signaling specificity. Proc Natl Acad Sci U S A **106:**9619-24.
248. **Shisler, J. L., and X. L. Jin.** 2004. The vaccinia virus K1L gene product inhibits host NF-kappaB activation by preventing IkappaBalpha degradation. J Virol **78:**3553-60.
249. **Shisler, J. L., and B. Moss.** 2001. Molluscum contagiosum virus inhibitors of apoptosis: The MC159 v-FLIP protein blocks Fas-induced activation of procaspases and degradation of the related MC160 protein. Virology **282:**14-25.
250. **Sieczkarski, S. B., and G. R. Whittaker.** 2005. Viral entry. Curr Top Microbiol Immunol **285:**1-23.
251. **Smith, C. A., T. Davis, J. M. Wignall, W. S. Din, T. Farrah, C. Upton, G. McFadden, and R. G. Goodwin.** 1991. T2 open reading frame from the Shope fibroma virus encodes a soluble form of the TNF receptor. Biochem Biophys Res Commun **176:**335-42.
252. **Smith, C. A., F. Q. Hu, T. D. Smith, C. L. Richards, P. Smolak, R. G. Goodwin, and D. J. Pickup.** 1996. Cowpox virus genome encodes a second soluble homologue of cellular TNF receptors, distinct from CrmB, that binds TNF but not LT alpha. Virology **223:**132-47.
253. **Smith, G. L., Y. S. Chan, and S. M. Kerr.** 1989. Transcriptional mapping and nucleotide sequence of a vaccinia virus gene encoding a polypeptide with extensive homology to DNA ligases. Nucleic Acids Res **17:**9051-62.
254. **Smith, G. L., A. de Carlos, and Y. S. Chan.** 1989. Vaccinia virus encodes a thymidylate kinase gene: sequence and transcriptional mapping. Nucleic Acids Res **17:**7581-90.
255. **Smith, G. L., B. J. Murphy, and M. Law.** 2003. Vaccinia virus motility. Annu Rev Microbiol **57:**323-42.
256. **Smith, V. P., N. A. Bryant, and A. Alcami.** 2000. Ectromelia, vaccinia and cowpox viruses encode secreted interleukin-18-binding proteins. J Gen Virol **81:**1223-30.

257. **Solan, N. J., H. Miyoshi, E. M. Carmona, G. D. Bren, and C. V. Paya.** 2002. RelB cellular regulation and transcriptional activity are regulated by p100. J Biol Chem **277:**1405-18.
258. **Sonnberg, S., S. B. Fleming, and A. A. Mercer.** 2009. A truncated two-alpha-helix F-box present in poxvirus ankyrin-repeat proteins is sufficient for binding the SCF1 ubiquitin ligase complex. J Gen Virol **90:**1224-8.
259. **Sonnberg, S., B. T. Seet, T. Pawson, S. B. Fleming, and A. A. Mercer.** 2008. Poxvirus ankyrin repeat proteins are a unique class of F-box proteins that associate with cellular SCF1 ubiquitin ligase complexes. Proc Natl Acad Sci U S A **105:**10955-60.
260. **Spencer, E., J. Jiang, and Z. J. Chen.** 1999. Signal-induced ubiquitination of IkappaBalpha by the F-box protein Slimb/beta-TrCP. Genes Dev **13:**284-94.
261. **Spitkovsky, D., S. P. Hehner, T. G. Hofmann, A. Moller, and M. L. Schmitz.** 2002. The human papillomavirus oncoprotein E7 attenuates NF-kappa B activation by targeting the Ikappa B kinase complex. J Biol Chem **277:**25576-82.
262. **Spriggs, M. K., D. E. Hruby, C. R. Maliszewski, D. J. Pickup, J. E. Sims, R. M. Buller, and J. VanSlyke.** 1992. Vaccinia and cowpox viruses encode a novel secreted interleukin-1-binding protein. Cell **71:**145-52.
263. **Stack, J., I. R. Haga, M. Schroder, N. W. Bartlett, G. Maloney, P. C. Reading, K. A. Fitzgerald, G. L. Smith, and A. G. Bowie.** 2005. Vaccinia virus protein A46R targets multiple Toll-like-interleukin-1 receptor adaptors and contributes to virulence. J Exp Med **201:**1007-18.
264. **Su, J., G. Wang, J. W. Barrett, T. S. Irvine, X. Gao, and G. McFadden.** 2006. Myxoma virus M11L blocks apoptosis through inhibition of conformational activation of Bax at the mitochondria. J Virol **80:**1140-51.
265. **Symons, J. A., A. Alcami, and G. L. Smith.** 1995. Vaccinia virus encodes a soluble type I interferon receptor of novel structure and broad species specificity. Cell **81:**551-60.
266. **Szajner, P., A. S. Weisberg, J. Lebowitz, J. Heuser, and B. Moss.** 2005. External scaffold of spherical immature poxvirus particles is made of protein trimers, forming a honeycomb lattice. J Cell Biol **170:**971-81.
267. **Tait, S. W., E. B. Reid, D. R. Greaves, T. E. Wileman, and P. P. Powell.** 2000. Mechanism of inactivation of NF-kappa B by a viral homologue of I kappa b alpha. Signal-induced release of i kappa b alpha results in binding of the viral homologue to NF-kappa B. J Biol Chem **275:**34656-64.
268. **Takatsuna, H., H. Kato, J. Gohda, T. Akiyama, A. Moriya, Y. Okamoto, Y. Yamagata, M. Otsuka, K. Umezawa, K. Semba, and J. Inoue.** 2003. Identification of TIFA as an adapter protein that links tumor necrosis factor receptor-associated factor 6 (TRAF6) to interleukin-1 (IL-1) receptor-associated kinase-1 (IRAK-1) in IL-1 receptor signaling. J Biol Chem **278:**12144-50.

269. **Takeuchi, M., M. Rothe, and D. V. Goeddel.** 1996. Anatomy of TRAF2. Distinct domains for nuclear factor-kappaB activation and association with tumor necrosis factor signaling proteins. J Biol Chem **271:**19935-42.
270. **Taylor, R. T., and W. A. Bresnahan.** 2006. Human cytomegalovirus IE86 attenuates virus- and tumor necrosis factor alpha-induced NFkappaB-dependent gene expression. J Virol **80:**10763-71.
271. **Taylor, S. L., N. Frias-Staheli, A. Garcia-Sastre, and C. S. Schmaljohn.** 2009. Hantaan virus nucleocapsid protein binds to importin alpha proteins and inhibits tumor necrosis factor alpha-induced activation of nuclear factor kappa B. J Virol **83:**1271-9.
272. **Thorne, S. H.** 2011. Immunotherapeutic potential of oncolytic vaccinia virus. Immunol Res **50:**286-93.
273. **Thrower, J. S., L. Hoffman, M. Rechsteiner, and C. M. Pickart.** 2000. Recognition of the polyubiquitin proteolytic signal. EMBO J **19:**94-102.
274. **Tokunaga, F., and K. Iwai.** 2009. [Involvement of LUBAC-mediated linear polyubiquitination of NEMO in NF-kappaB activation]. Tanpakushitsu Kakusan Koso **54:**635-42.
275. **Tokunaga, F., and K. Iwai.** 2012. Linear ubiquitination: A novel NF-kappaB regulatory mechanism for inflammatory and immune responses by the LUBAC ubiquitin ligase complex [Review]. Endocr J.
276. **Tokunaga, F., S. Sakata, Y. Saeki, Y. Satomi, T. Kirisako, K. Kamei, T. Nakagawa, M. Kato, S. Murata, S. Yamaoka, M. Yamamoto, S. Akira, T. Takao, K. Tanaka, and K. Iwai.** 2009. Involvement of linear polyubiquitylation of NEMO in NF-kappaB activation. Nat Cell Biol **11:**123-32.
277. **Townsley, A. C., A. S. Weisberg, T. R. Wagenaar, and B. Moss.** 2006. Vaccinia virus entry into cells via a low-pH-dependent endosomal pathway. J Virol **80:**8899-908.
278. **Turner, P. C., M. T. Baquero, S. Yuan, S. R. Thoennes, and R. W. Moyer.** 2000. The cowpox virus serpin SPI-3 complexes with and inhibits urokinase-type and tissue-type plasminogen activators and plasmin. Virology **272:**267-80.
279. **Turner, P. C., and R. W. Moyer.** 1995. Orthopoxvirus fusion inhibitor glycoprotein SPI-3 (open reading frame K2L) contains motifs characteristic of serine proteinase inhibitors that are not required for control of cell fusion. J Virol **69:**5978-87.
280. **Unterstab, G., S. Ludwig, A. Anton, O. Planz, B. Dauber, D. Krappmann, G. Heins, C. Ehrhardt, and T. Wolff.** 2005. Viral targeting of the interferon-{beta}-inducing Traf family member-associated NF-{kappa}B activator (TANK)-binding kinase-1. Proc Natl Acad Sci U S A **102:**13640-5.
281. **Upton, C., J. L. Macen, M. Schreiber, and G. McFadden.** 1991. Myxoma virus expresses a secreted protein with homology to the tumor necrosis factor receptor gene family that contributes to viral virulence. Virology **184:**370-82.

282. **Upton, C., J. L. Macen, D. S. Wishart, and G. McFadden.** 1990. Myxoma virus and malignant rabbit fibroma virus encode a serpin-like protein important for virus virulence. Virology **179:**618-31.
283. **Upton, C., K. Mossman, and G. McFadden.** 1992. Encoding of a homolog of the IFN-gamma receptor by myxoma virus. Science **258:**1369-72.
284. **Upton, C., S. Slack, A. L. Hunter, A. Ehlers, and R. L. Roper.** 2003. Poxvirus orthologous clusters: toward defining the minimum essential poxvirus genome. J Virol **77:**7590-600.
285. **Valentine, R., C. W. Dawson, C. Hu, K. M. Shah, T. J. Owen, K. L. Date, S. P. Maia, J. Shao, J. R. Arrand, L. S. Young, and J. D. O'Neil.** 2010. Epstein-Barr virus-encoded EBNA1 inhibits the canonical NF-kappaB pathway in carcinoma cells by inhibiting IKK phosphorylation. Mol Cancer **9:**1.
286. **Vallabhapurapu, S., and M. Karin.** 2009. Regulation and function of NF-kappaB transcription factors in the immune system. Annu Rev Immunol **27:**693-733.
287. **van Buuren, N., B. Couturier, Y. Xiong, and M. Barry.** 2008. Ectromelia virus encodes a novel family of F-box proteins that interact with the SCF complex. J Virol **82:**9917-27.
288. **van Lint, A. L., M. R. Murawski, R. E. Goodbody, M. Severa, K. A. Fitzgerald, R. W. Finberg, D. M. Knipe, and E. A. Kurt-Jones.** 2010. Herpes simplex virus immediate-early ICP0 protein inhibits Toll-like receptor 2-dependent inflammatory responses and NF-kappaB signaling. J Virol **84:**10802-11.
289. **Varin, A., A. Z. Decrion, E. Sabbah, V. Quivy, J. Sire, C. Van Lint, B. P. Roques, B. B. Aggarwal, and G. Herbein.** 2005. Synthetic Vpr protein activates activator protein-1, c-Jun N-terminal kinase, and NF-kappaB and stimulates HIV-1 transcription in promonocytic cells and primary macrophages. J Biol Chem **280:**42557-67.
290. **Varin, A., S. K. Manna, V. Quivy, A. Z. Decrion, C. Van Lint, G. Herbein, and B. B. Aggarwal.** 2003. Exogenous Nef protein activates NF-kappa B, AP-1, and c-Jun N-terminal kinase and stimulates HIV transcription in promonocytic cells. Role in AIDS pathogenesis. J Biol Chem **278:**2219-27.
291. **Vijay-Kumar, S., C. E. Bugg, K. D. Wilkinson, R. D. Vierstra, P. M. Hatfield, and W. J. Cook.** 1987. Comparison of the three-dimensional structures of human, yeast, and oat ubiquitin. J Biol Chem **262:**6396-9.
292. **Visvanathan, K. V., and S. Goodbourn.** 1989. Double-stranded RNA activates binding of NF-kappa B to an inducible element in the human beta-interferon promoter. EMBO J **8:**1129-38.
293. **Vivarelli, M. S., D. McDonald, M. Miller, N. Cusson, M. Kelliher, and R. S. Geha.** 2004. RIP links TLR4 to Akt and is essential for cell survival in response to LPS stimulation. J Exp Med **200:**399-404.
294. **Wang, J., J. Tan, X. Zhang, H. Guo, Q. Zhang, T. Guo, Y. Geng, and W. Qiao.** 2010. BFV activates the NF-kappaB pathway through its transactivator (BTas) to enhance viral transcription. Virology **400:**215-23.

295. **Wasilenko, S. T., A. F. Meyers, K. Vander Helm, and M. Barry.** 2001. Vaccinia virus infection disarms the mitochondrion-mediated pathway of the apoptotic cascade by modulating the permeability transition pore. J Virol **75:**11437-48.
296. **Weissman, A. M.** 2001. Themes and variations on ubiquitylation. Nat Rev Mol Cell Biol **2:**169-78.
297. **Wertz, I. E., and V. M. Dixit.** 2008. Ubiquitin-mediated regulation of TNFR1 signaling. Cytokine Growth Factor Rev **19:**313-24.
298. **Whitbeck, J. C., C. H. Foo, M. Ponce de Leon, R. J. Eisenberg, and G. H. Cohen.** 2009. Vaccinia virus exhibits cell-type-dependent entry characteristics. Virology **385:**383-91.
299. **Whiteside, S. T., and A. Israel.** 1997. I kappa B proteins: structure, function and regulation. Semin Cancer Biol **8:**75-82.
300. **Wilson, J. R., P. F. de Sessions, M. A. Leon, and F. Scholle.** 2008. West Nile virus nonstructural protein 1 inhibits TLR3 signal transduction. J Virol **82:**8262-71.
301. **Wilton, B. A., S. Campbell, N. Van Buuren, R. Garneau, M. Furukawa, Y. Xiong, and M. Barry.** 2008. Ectromelia virus BTB/kelch proteins, EVM150 and EVM167, interact with cullin-3-based ubiquitin ligases. Virology **374:**82-99.
302. **Wu, C., and S. Ghosh.** 2003. Differential phosphorylation of the signal-responsive domain of I kappa B alpha and I kappa B beta by I kappa B kinases. J Biol Chem **278:**31980-7.
303. **Wu, C. J., D. B. Conze, T. Li, S. M. Srinivasula, and J. D. Ashwell.** 2006. Sensing of Lys 63-linked polyubiquitination by NEMO is a key event in NF-kappaB activation [corrected]. Nat Cell Biol **8:**398-406.
304. **Wu, L., H. Nakano, and Z. Wu.** 2006. The C-terminal activating region 2 of the Epstein-Barr virus-encoded latent membrane protein 1 activates NF-kappaB through TRAF6 and TAK1. J Biol Chem **281:**2162-9.
305. **Wullaert, A., K. Heyninck, S. Janssens, and R. Beyaert.** 2006. Ubiquitin: tool and target for intracellular NF-kappaB inhibitors. Trends Immunol **27:**533-40.
306. **Xiang, Y., and B. Moss.** 1999. IL-18 binding and inhibition of interferon gamma induction by human poxvirus-encoded proteins. Proc Natl Acad Sci U S A **96:**11537-42.
307. **Xiao, G., M. E. Cvijic, A. Fong, E. W. Harhaj, M. T. Uhlik, M. Waterfield, and S. C. Sun.** 2001. Retroviral oncoprotein Tax induces processing of NF-kappaB2/p100 in T cells: evidence for the involvement of IKKalpha. EMBO J **20:**6805-15.
308. **Xiao, G., A. Fong, and S. C. Sun.** 2004. Induction of p100 processing by NF-kappaB-inducing kinase involves docking IkappaB kinase alpha (IKKalpha) to p100 and IKKalpha-mediated phosphorylation. J Biol Chem **279:**30099-105.

309. **Xu, G., Y. C. Lo, Q. Li, G. Napolitano, X. Wu, X. Jiang, M. Dreano, M. Karin, and H. Wu.** 2011. Crystal structure of inhibitor of kappaB kinase beta. Nature **472:**325-30.
310. **Xu, L., Y. Wei, J. Reboul, P. Vaglio, T. H. Shin, M. Vidal, S. J. Elledge, and J. W. Harper.** 2003. BTB proteins are substrate-specific adaptors in an SCF-like modular ubiquitin ligase containing CUL-3. Nature **425:**316-21.
311. **Yamamoto, M., K. Takeda, and S. Akira.** 2004. TIR domain-containing adaptors define the specificity of TLR signaling. Mol Immunol **40:**861-8.
312. **Yang, J., Y. Lin, Z. Guo, J. Cheng, J. Huang, L. Deng, W. Liao, Z. Chen, Z. Liu, and B. Su.** 2001. The essential role of MEKK3 in TNF-induced NF-kappaB activation. Nat Immunol **2:**620-4.
313. **Yim, H. C., J. C. Li, J. S. Lau, and A. S. Lau.** 2009. HIV-1 Tat dysregulation of lipopolysaccharide-induced cytokine responses: microbial interactions in HIV infection. AIDS **23:**1473-84.
314. **Yoboua, F., A. Martel, A. Duval, E. Mukawera, and N. Grandvaux.** 2010. Respiratory syncytial virus-mediated NF-kappa B p65 phosphorylation at serine 536 is dependent on RIG-I, TRAF6, and IKK beta. J Virol **84:**7267-77.
315. **Zahoor, M. A., D. Yamane, Y. M. Mohamed, Y. Suda, K. Kobayashi, K. Kato, Y. Tohya, and H. Akashi.** 2010. Bovine viral diarrhea virus non-structural protein 5A interacts with NIK- and IKKbeta-binding protein. J Gen Virol **91:**1939-48.
316. **Zandi, E., Y. Chen, and M. Karin.** 1998. Direct phosphorylation of IkappaB by IKKalpha and IKKbeta: discrimination between free and NF-kappaB-bound substrate. Science **281:**1360-3.
317. **Zandi, E., D. M. Rothwarf, M. Delhase, M. Hayakawa, and M. Karin.** 1997. The IkappaB kinase complex (IKK) contains two kinase subunits, IKKalpha and IKKbeta, necessary for IkappaB phosphorylation and NF-kappaB activation. Cell **91:**243-52.
318. **Zaragoza, C., M. Saura, E. Y. Padalko, E. Lopez-Rivera, T. R. Lizarbe, S. Lamas, and C. J. Lowenstein.** 2006. Viral protease cleavage of inhibitor of kappaBalpha triggers host cell apoptosis. Proc Natl Acad Sci U S A **103:**19051-6.
319. **Zhang, S. Q., A. Kovalenko, G. Cantarella, and D. Wallach.** 2000. Recruitment of the IKK signalosome to the p55 TNF receptor: RIP and A20 bind to NEMO (IKKgamma) upon receptor stimulation. Immunity **12:**301-11.
320. **Zheng, C., V. Kabaleeswaran, Y. Wang, G. Cheng, and H. Wu.** 2010. Crystal structures of the TRAF2: cIAP2 and the TRAF1: TRAF2: cIAP2 complexes: affinity, specificity, and regulation. Mol Cell **38:**101-13.
321. **Zheng, N., B. A. Schulman, L. Song, J. J. Miller, P. D. Jeffrey, P. Wang, C. Chu, D. M. Koepp, S. J. Elledge, M. Pagano, R. C. Conaway, J. W. Conaway, J. W. Harper, and N. P. Pavletich.** 2002. Structure of the Cul1-Rbx1-Skp1-F boxSkp2 SCF ubiquitin ligase complex. Nature **416:**703-9.

322. **Zhong, H., R. E. Voll, and S. Ghosh.** 1998. Phosphorylation of NF-kappa B p65 by PKA stimulates transcriptional activity by promoting a novel bivalent interaction with the coactivator CBP/p300. Mol Cell **1:**661-71.

Chapter 2: Materials and Methods

2.1 CELL LINES

CV-1, HEK293T, and HeLa cells were obtained from the American Type Culture Collection (ATCC) and grown at 37°C in 5% CO_2 in Dulbecco's Modified Eagle medium (DMEM) supplemented with 10% heat inactivated fetal bovine serum (HI-FBS) (Invitrogen), 50 U/mL of penicillin (Invitrogen), 50 U/mL of streptomycin (Invitrogen), and 200 μM of L-glutamine (Invitrogen). RK13 cells were obtained from Dr. D. Evans (University of Alberta, Canada) and U20S-Cre cells were obtained from Dr. J. Bell (University of Ottawa, Canada). RK13 and U20S-Cre cells were grown in the same conditions as described above. BGMK cells were obtained from ATCC and grown at 37°C in 5% CO_2 in DMEM supplemented with 10% newborn calf serum (NCS) (Invitrogen), 50 U/mL of penicillin, 50 U/mL of streptomycin, and 200 μM of L-glutamine.

2.2 VIRUSES

Table 2-1 summarizes the viruses used in this study. Ectromelia virus strain Moscow (ECTV) was provided by Dr. M. Buller (University of St. Louis, USA). Vaccinia virus (VACV) strain Copenhagen (Cop), and VACV expressing β-glactosidase (VACV65) were provided by Dr. G McFadden (University of Florida, USA). Vaccinia virus strain 811 (VACV811), which is missing 55 ORFs from the variable regions of the VACVCop genome, was provided by E. Paoletti (3). ECTVΔ002-YFP, ECTVΔ005-YFP, ECTVΔ154-YFP, ECTVΔ165-YFP, and VACV811ΔB4R-YFP were generated by inserting a *YFP/gpt* cassette into the respective ORF. ECTVΔ002-Cre, ECTVΔ005-Cre, ECTVΔ154-Cre, and ECTVΔ165-Cre were generated by passaging the *YFP/gpt*-containing viruses though U20S-Cre cells. VACV811ΔB4R-Cre was not generated sine VACV811 could not be passaged through U20S-Cre cells. ECTVΔ005-rev, ECTVΔ154-rev, and ECTVΔ165-rev and were generated by re-inserting the respective ORF into the *YFP/gpt*-

Table 2-1. Viruses used in this study

Virus	Description	Source
ECTV	Wild type ectromelia virus strain Moscow; causative agent of mousepox	M. Buller
ECTVΔ002-Cre	Devoid of ECTV002 and *YFP/gpt*; marker free	N. van Buuren
ECTVΔ005-Cre	Devoid of ECTV005 and *YFP/gpt*; marker free	N. van Buuren
ECTVΔ154-YFP	Devoid of ECTV154; contains *YFP/gpt*	This study
ECTVΔ154-Cre	Devoid of ECTV154 and *YFP/gpt*; marker free	This study
ECTVΔ154-Rev	Revertant containing ECTV154; generated from ECTVΔ154-YFP	This study
ECTVΔ165-YFP	Devoid of ECTV165; contains *YFP/gpt*	M. Edwards
ECTVΔ165-Cre	Devoid of ECTV165 and *YFP/gpt*; marker free	M. Edwards
ECTVΔ165-Rev	Revertant containing ECTV165; generated from ECTVΔ165-YFP	This study
VACVCop	vaccinia virus strain Copenhagen	G. McFadden
VACV65	vaccinia virus strain Copenhagen, expresses β-galactosidase	G. McFadden
VACV-Flag-ECTV002	Recombinant virus; expresses Flag-ECTV002	N. van Buuren
VACV-Flag-ECTV005	Recombinant virus; expresses Flag-ECTV005	N. van Buuren
VACV-Flag-ECTV154	Recombinant virus; expresses Flag-ECTV154	N. van Buuren
VACV-Flag-ECTV165	Recombinant virus; expresses Flag-ECTV165	N. van Buuren
VACV811	Vaccinia virus strain 811; missing 55 open reading frames	E. Paoletti
VACV811ΔB4R-YFP	Devoid of VACVB4R; contains *YFP/gpt*	This study
VACV811ΔB4R-Rev	Revertant containing VACVB4R; generated from ECTVΔ154-YFP	This study

containing viruses by homologous recombination. ECTVΔ002-rev was not generated. The generation of the *YFP/gpt*-containing viruses, the viruses generated by Cre recombination, and the revertant viruses are described in more detail in section 2.8.1. Recombinant vaccinia viruses: VACV-Flag-ECTV004, VACV-Flag-ECTV002, VACV-Flag-ECTV005, VACV-Flag-ECTV154, and VACV-FlagECTV165 were generated by inserting the Flag-tagged ORF from ECTV into TK locus in VACVCop (6, 7). All viruses were stored at -80°C. Prior to use, viruses were sonicated on ice for 20 seconds with 0.5 second on/off pulses using a Sonic Dismembranator (Misonix Inc.).

2.3 DNA METHODOLOGY

2.3.1 Polymerase chain reaction

Polymerase Chain Reactions (PCR) were made up in a total volume of 50 μL and contained 250 mM KCl, 100 mM Tris-HCl, 50 mM $(NH_4)_2SO_4$, 20 mM $MgSO_4$, 10 mM deoxyribonucleotide triphosphate (dNTPs) (Invitrogen), 1 pmole of each primer, and 2.5 U of *Pwo* DNA polymerase (Roche Diagnostics), *Pfu* DNA polymerase (Stratagene) or *Taq* DNA polymerase (Invitrogen). Primers used in this study were obtained from Integrated DNA Technologies and are listed in Table 2-2. Reactions also contained 10 ng of plasmid DNA or 100 ng of viral DNA. Reactions were performed in a Techgene thermal cycler (Techne) with a program that involved an initial denaturation step (95°C for 2 minutes), followed by a 30 cycles that involved a melting step (95°C for 30 seconds), a primer annealing step (55°C for 30 seconds), and a primer extension step (72°C for 1 minute/kb), followed by a final extension step (72°C for 10 minutes). Alternatively, PCR reactions were made up in a total volume of 50 μL and contained 60 mM Tris-SO_4 (pH 9.0 at 25°C), 20 mM $(NH_4)_2SO_4$, 2 mM $MgSO_4$, 3% glycerol, 0.06% Nonident P-40 (NP-40), 0.05% Tween-20, 10 mM dNTPs, 1 pmole of each primer, and 2.5 U of LongAmp *Taq* DNA polymerase (New England Biolabs). Reactions

Table 2-2. Primers used in this study

Primer name	Primer Sequence (5' to 3')	Restriction Site	Description
COECTV002 Flag Forward	AAG CTT ATG GAC TAC AAA GAC GAT GAC GAC AAG GGC GAG ATG GAC GAG ATC	*HindIII*	Used to generate pcDNA-Flag-CO-ECTV002(1-542)
COECTV002(1-554) Reverse	GGA TCC TCA GCT GTA GTA CTT GTA	*BamHI*	Used to generate pcDNA-Flag-CO-ECTV002(1-554)
COECTV005 Flag Forward	GGA TCC ATG GAC TAC AAA GAC GAT GAC GAC AAG GAG CGG TAC AGC CTG CAC	*BamHI*	Used to generate pcDNA-Flag-CO-ECTV005(1-593)
COECTV005(1-593) Reverse	GC GGC CGC TCA CAC GTA GGT GGG CTG GTC	*NotI*	Used to generate pcDNA-Flag-CO-ECTV005(1-593)
COECTV154 Flag Forward-HindIII	AAG CTT ATG GAC TAC AAA GAC GAT GAC GAC AAG GAC TTC TTC AAG AAA GAG	*HindIII*	Used to generate pcDNA-Flag-CO-ECTV154(1-532)
COECTV154(1-532) Reverse-BamHI	GGA TCC TCA CCA CTT GTC GCC GGC GTC	*BamHI*	Used to generate pcDNA-Flag-CO-ECTV154(1-532)
COECTV165 Flag Forward	GGA TCC ATG GAC TAC AAA GAC GAT GAC GAC AAG AAC ATC AAG CAG CTG AAC	*BamHI*	Used to generate pcDNA-Flag-CO-ECTV165(1-566)
COECTV165 (1-566) Reverse	GAA TCC TCA TCA CAG GGT CAG CAG ACA GTT	*EcoRI*	Used to generate pcDNA-Flag-CO-ECTV165(1-566)
COECTV154(F534A/P535A)-Forward	GAC AAG TGG AGC TGC ***GCC GCC*** AAC GAG ATC AAG	N/A	Used for site directed mutagenesis
COECTV154(F534A/P535A)-Reverse	CTT GAT CTC GTT ***GGC GGC*** GCA GCT CCA CTT GTC	N/A	Used for site directed mutagenesis
ECTV002(150)-5'-Forward	AAG CTT CTC ATA ATG ATT TAC TTT TTC	*HindIII*	Used to clone pDGloxP-ECTV002-KO
ECTV002(150)-5'-Reverse	CTC GAG CGA TTC CGT CCA AGA TGA TAA	*XhoI*	Used to clone pDGloxP-ECTV002-KO
ECTV002(150)-3'-Forward	GC GGC CGC GGT GCT ATA TCT TTT CCG TTT	*NotI*	Used to clone pDGloxP-ECTV002-KO
ECTV002(150)-3'-Reverse	GGA TCC TAG AAA GAA AAT ATT TAA AAA	*BamHI*	Used to clone pDGloxP-ECTV002-KO
ECTV005(150)-5'-Forward	AAG CTT CTC TAC AAA GTA TAA TAT ATT	*HindIII*	Used to clone pDGloxP-ECTV005-KO
ECTV005(150)-5'-Reverse	CTC GAG ATA TTA TAC ATA TTA GAT GTG	*XhoI*	Used to clone pDGloxP-ECTV005-KO
ECTV005(150)-3'-Forward	GC GGC CGC TCG TAC CCG CGA ACA AAA TAG	*NotI*	Used to clone pDGloxP-ECTV005-KO
ECTV005(150)-3'-Reverse	GGA TCC TTT TTT ATA AAC GAT ATT GTT	*BamHI*	Used to clone pDGloxP-ECTV005-KO
WT ECTV154(200)-5'-Forward-XhoI	CTC GAG ATC ATA TAG ACA ATA ACT	*XhoI*	Used to clone pDGloxP-ECTV154-KO

Table 2-2. Continued…

WT ECTV154(200)-5'-Reverse-SalI	GTC GAC ATA TAA TTT ATA TTC TGT	*SalI*	Used to clone pDGloxP-ECTV154-KO
WT ECTV154(200)-3'-Forward-BamHI	GGA TCC AAT CTA AGT AGG ATA AAA	*BamHI*	Used to clone pDGloxP-ECTV154-KO
WT ECTV154(200)-3'-Reverse-NotI	GC GGC CGC AAA CGA TGT TTC GGT AGA	*NotI*	Used to clone pDGloxP-ECTV154-KO
WT ECTV154(200)-5'-Reverse-HindIII	AAG CTT GAC ATA TAA TTT ATA TTC TGT	*HindIII*	Used to clone pDGloxP-ECTV154-KO
ECTV165(200)-5'-Forward	CTG GAG ACT ATA GTA TTC TGG ACT	*XhoI*	Used to clone pDGloxP-ECTV165-KO
ECTV165(200)-5'-Reverse	AAG CTT TAT TAT AAA CGA GTC CCA	*HindIII*	Used to clone pDGloxP-ECTV165-KO
ECTV165(200)-3'-Forward	GGA TCC TTG TAT TTT TAT CAT GTG	*BamHI*	Used to clone pDGloxP-ECTV165-KO
ECTV165(200)-3'-Reverse	GC GGC CGC GTA TCT CTC ATT TTA TTG	*NotI*	Used to clone pDGloxP-ECTV165-KO
WT ECTV154(400)-5'-Forward-XhoI	CTG GAG AAG GTA TAT AAA CCT GGG	*XhoI*	Used to generate revertant virus ECTVΔ154-rev
WT ECTV154(400)-5'-Reverse-NotI	GC GGC CGC GTT TCG CTG TTG CAA CGT	*NotI*	Used to generate revertant virus ECTVΔ154-rev
WT ECTV165(400)-5'-Forward-XhoI	CTG GAG GAA TCA CCT ACC TTA GAT	*XhoI*	Used to generate revertant virus ECTVΔ165-rev
WT ECTV165(400)-5'-Reverse-NotI	GC GGC CGC GTC TAT TAA GAG GTC GTC	*NotI*	Used to generate revertant virus ECTVΔ165-rev
WT VACV-B4R(400)-L-For-SpeI	ACT AGT CAA GGT ATA TAA ACC TGG	*SpeI*	Used to clone pDGloxP-VACVB4R-KO
WT VACV-B4R(400)-L-Rev-HindIII	AAG CTT ATA TAA TTT ATA TTC TGT AAC ATG TTA	*HindIII*	Used to clone pDGloxP-VACVB4R-KO
WT VACV-B4R(400)-R-For-NotI	GC GGC CGC ACA CTA TTA AAA TAT AAA	*HindIII*	Used to clone pDGloxP-VACVB4R-KO
WT VACV-B4R(400)-R-Rev-BglII	AGA TCT TAG TGT CAT GGT GGA AAT	*BglII*	Used to clone pDGloxP-VACVB4R-KO

Restriction enzyme digestion sites are underlined, and nucleotides introducing amino acid mutations are italicized in bold.

also contained 10 ng of plasmid DNA or 100 ng of viral DNA. Reactions were performed as described above, except that extensions were carried out at 65°C. PCR products were purified by agarose gel electrophoresis and gel extraction, as described in sections 2.3.4, and 2.3.5, respectively.

2.3.2 Site directed mutagenesis

Mutations were introduced into DNA using QuickChange II site directed mutagenesis, as per manufacturer's instructions (Stratagene). PCR were made up in a total volume of 50 μL and contained 10x reaction buffer, 10 mM dNTPs, 1 pmole of each primer, and 2.5 U of *PfuUltra* high fidelity DNA polymerase (Stratagene). Reactions also contained 10 ng of plasmid DNA. Reactions were performed in a Techgene thermal cycler with a program involving an initial denaturation step (95°C for 30 seconds), followed by a 18 cycles that involved a melting step (95°C for 30 seconds), a primer annealing step (55°C for 1 minute), and a primer extension step (68°C for 8.5 minutes for of pcDNA-Flag-CO-ECTV154 and for 7.5 minutes for pEGFP-CO-ECTV154). Subsequently, PCR products were treated with 10 U/μL *DpnI* at 37°C for 1 hour to digest parental DNA. The mutant plasmids were transformed into *Escherichia coli* (*E. coli*) XL1-Blue supercompetent cells (Stratagene) by heat shocking the transformation reactions at 42°C for 45 seconds followed by 2 minutes on ice. Reactions were incubated at 37°C for 1 hour in NZY^+ broth (pH 7.5) containing 10 mg/mL NZ amine (casein hydrosylate), 5 mg/mL yeast extract, 5 mg/mL NaCl, 20 mM glucose, 12.5 mM $MgCl_2$, and 12.5 mM $MgSO_4$. The pcDNA-Flag-ECTV154 mutant was grown overnight on Luria Burtani (LB) agarose plates supplemented with 100 μg/mL ampicillin (Sigma-Aldrich) while the pEGFP-ECTV154 mutant was grown on LB agarose supplemented with 30 μg/mL kanamycin (Sigma-Aldrich).

2.3.3 Restriction enzyme digestions

Restriction enzymes were purchased from Invitrogen. Digestion reactions were made up as per manufacturer's instructions, in a total volume of 20 μL. Reactions

were supplemented 10 ug of RNase A (Sigma-Aldrich) and were carried out at 37°C for 1 hour. Digested products were purified by agarose gel electrophoresis and gel extracted, as described in sections 2.3.4, and 2.3.5, respectively.

2.3.4 Agarose gel electrophoresis

PCR products and restriction enzyme digestion products were prepared in a loading dye containing 5% glycerol (Fischer Scientific), 0.04% w/v bromophenol blue (BioRad), 0.04% w/v xylene cyanol (Sigma-Aldrich), and 10 mM EDTA (pH 7.5). One percent w/v agarose gels were made up of UltraPure Agarose (Invitrogen) in 1x Tris-acetate-EDTA (TAE) buffer containing 40 mM Tris-acetate and 1 mM ethylenediaminetetraacetic acid (EDTA) (EMD). Agarose gels were run in 1x TAE buffer in a Mini-Sub Cell GT (Bio-Rad) at 100 V, stained with 10 μg/μL ethidium bromide (Sigma-Aldrich) for 10 minutes, and de-stained by running the gels for an additional 5 minutes at 100 V. Gels were visualized using an ImageQuant 300 imager (GE Healthcare). Alternatively, agarose gels were prepared with 0.0001% v/v SYBR Safe DNA gel stain (Invitrogen) and visualized using a Gel Doc EZ imager (Bio-Rad). DNA bands were excised with a scalpel and the DNA was purified by gel extraction, as described in section 2.3.5.

2.3.5 Gel extraction

Gel extractions were performed using a QIAquick Gel Extraction Kit (Qiagen) as per manufacturer's instructions, with slight modifications. The agarose slice containing DNA was solubilized at 50°C in 1 mL buffer QG, which provides the appropriate conditions for DNA binding to the silica membrane in the QIAquick column. The solubilized DNA solution was transferred to a QIAquick column where DNA was bound and washed with 0.5 mL of buffer QG, followed by 0.75 mL of buffer PE, which washes away residual salts. DNA was eluted in 30 μL of buffer EB.

2.3.6 DNA ligation

Ligation of PCR products and restriction enzyme digestion products into pGEM-T were performed using the pGEM-T Easy Vector Kit (Promega), as per manufacturer's instructions. Ligation reactions were made up in a total volume of 10 μL, containing 3 μL of the insert DNA, and were carried out at 4°C overnight. PCR products that were generated using *Pwo* DNA polymerase or *Pfu* DNA polymerase were subjected to A-addition prior to ligation, using an A-addition kit (Qiagen), while PCR products that were generated using *Taq* DNA polymerase or LongAmp *Taq* DNA polymerase could be ligated directly into pGEM-T. Ligations into other plasmid backbones were carried out using T4 DNA Ligase (New England Biolabs), as per manufacturer's instructions. Ligation reactions were made up in a total volume of 20 μL and contained ratios of insert DNA to backbone plasmid DNA of 0:1, 4:1, or 8:1, and were carried out at 16°C overnight. Small-scale isolation of plamsid DNA (minipreps) was utilized to screen plasmids for proper ligation of the DNA insert, as described in section 2.3.8.

2.3.7 Bacterial transformation

Five μL of a ligation reaction were transformed into 50 μL *E. coli* DH5α competent cells (Invitrogen), 50 μL *E. coli* Mach1 competent cells (Invitrogen), or 50 μL *E. coli* TOP10 cells (Invitrogen) by heat shocking the transformation reactions at 42°C for 1 minute followed by 2 minutes on ice. Reactions were incubated at 37°C for 1 hour in 250 μL of super optimal broth with catabolite repression (SOC) containing 20 mg/mL tryptone, 5 mg/mL yeast extract, 0.5 mg/mL NaCl, 20 mM glucose, and 2.5mM KCl (pH 7.0). Plasmids possessing the pGEM-T backbone were grown overnight on LB agarose plates supplemented with 100 μg/mL ampicillin, 80 μg/mL 5-bromo-4-chloro-3-indoyl-β-galactopyranoside (X-gal) (Rose Scientific), and 0.5 mM isopropyl β-D-1-thiogalactopyranoside (IPTG) (Rose Scientific). Plasmids possessing the pcDNA3

backbone were grown overnight on LB agarose plates supplemented with 100 μg/mL ampicillin, plasmids possessing the pEGFP backbone were grown on LB agarose supplemented with 30 μg/mL kanamycin, and plasmids possessing the pDGloxP backbone were grown on LB agarose plates supplemented with 30 μg/mL spectinomycin (Sigma-Aldrich).

2.3.8 Plasmid preparation

Minipreps were performed by inoculating a single bacterial colony into 5 mL of LB broth, supplemented with either 100 μg/mL ampicillin, 30 μg/mL kanamycin, or 30 μg/mL spectinomycin. The following day, a 1.5 mL aliquot of the overnight cultures was centrifuged at 2305 x *g* for 1 minute and the pellet was resuspended in 100 μL of a solution containing 50 mM glucose, 25 mM Tris (pH 8.0), and 10 mM EDTA. After a 5-minute incubation, 200 μL of a cold lysis buffer containing 1% SDS, and 0.2 N NaOH was added, and the suspension was incubated on ice for 5 minutes. Finally, 150 μL of a solution containing 3 M potassium acetate, and 11.5% glacial acetic acid was added and the suspension was incubated on ice for an additional 5 minutes, allowing proteins and chromosomal DNA to precipitate. The suspensions were centrifuged at 9223 x *g* at 4°C for 15 minutes and the supernatant was transferred to a new tube, mixed with 400 μL phenol/chloroform (1:1 v/v), and centrifuged at 9223 x *g* for 10 minutes. The aqueous phase was transferred to a new tube, mixed with 400 μL of chloroform, and centrifuged at 9223 x *g* for 10 minutes. Finally, the aqueous phase was again transferred to a new tube, and mixed with 1 mL of 95% v/v cold ethanol and incubated at –20°C for 20 minutes before being centrifuged at 9223 x *g* for 15 minutes. The DNA pellet was allowed to air dry before being resuspended in 30 μL of Tris-EDTA (TE) buffer.

For large-scale isolation of plasmid DNA, 1 mL of a 5 mL overnight LB broth culture was inoculated into 250 mL of LB broth supplemented with either of 100

μg/mL ampicillin, 30 μg/mL kanamycin, or 30 μg/mL spectinomycin. The following day, the overnight cultures were subjected to plasmid DNA isolation using a commercially available Plasmid Maxi kit (Qiagen), as per manufacturer's instructions.

2.3.9 DNA sequencing and computer analysis

DNA sequencing was performed by the Molecular Biology Sequencing Unit in the Department of Biological Sciences at the University of Alberta. Sequences were analyzed using the Basic Local Alignment Search Tool (BLAST) provided by the National Centre for Biotechnology Information (NCBI) (1).

2.4 CLONING

2.4.1 Plasmids

Table 2-3 summarizes the plasmids used in this study. pGEM-T (Promega) was used as a subcloning vector for sequencing PCR and restriction enzyme digestion products. Sequencing was performed prior to cloning the products into the final vector, using the T7 and SP6 primer sites that flank the multiple cloning site in pGEM-T. DNA sequences preceded by a Flag sequence were cloned into pcDNA3 (Invitrogen). pEGFP-C2 (Clontech) was used for generating proteins with an N-terminal GFP fusion. pDGloxP was described previously (4) (Figure 2-1). pDGloxP contains a yellow fluorescent protein (*YFP*)/guanine phosphoribosyltransferase (*gpt*) fusion open reading frame under the control of a poxvirus early/late promoter. The promoter and open reading frame are flanked by loxP sites. All plasmids were maintained as 15% glycerol stocks and were stored at -80°C.

2.4.2 Plasmid generation

2.4.2.1 Codon-optimization of ECTV002, ECTV005, ECTV154, and ECTV165. Since poxviruses replicate in the cytoplasm, ORFs are not subjected to the RNA

Table 2-3. Plasmids used in this study

Plasmid	Description	Source
pMK-RQ-CO-ECTV002	Codon optimized ECTV002; N-terminal Flag sequence; *HindIII* at extreme N-terminus, *EcoRI* between Flag and ECTV002; *BamHI* at C-terminus	GENEART
pGA15-CO-ECTV005	Codon optimized ECTV005; N-terminal Flag sequence; *HindIII* at extreme N-terminus, *EcoRI* between Flag and ECTV005; *BamHI* at C-terminus	GENEART
pMK-RQ-CO-ECTV154	Codon optimized ECTV154; N-terminal Flag sequence; *HindIII* at extreme N-terminus, *EcoRI* between Flag and ECTV154; *BamHI* at C-terminus	GENEART
pMA-RQ-CO-ECTV165	Codon optimized ECTV165; N-terminal Flag sequence; *HindIII* at extreme N-terminus, *EcoRI* between Flag and ECTV165; *BamHI* at C-terminus	GENEART
pcDNA3.1	T7 and CMV promotor	Invitrogen
pcDNA3-Flag-CO-ECTV002	Codon optimized; N-terminal Flag sequence	N. van Buuren
pcDNA3-Flag-CO-ECTV002(1-554)	Codon optimized; N-terminal Flag sequence; deletion of F-box domain from 555 to 587	N. van Buuren
pcDNA3-Flag-CO-ECTV005	Codon optimized; N-terminal Flag sequence	N. van Buuren
pcDNA3-Flag-CO-ECTV005(1-593)	Codon optimized; N-terminal Flag sequence; deletion of PRANC domain from 594 to 650	N. van Buuren
pcDNA3-Flag-CO-ECTV154	Codon optimized; N-terminal Flag sequence	This study
pcDNA3-Flag-CO-ECTV154(1-532)	Codon optimized; N-terminal Flag sequence; deletion of PRANC domain from 533 to 564	This study
pcDNA3-Flag-CO-ECTV154(F534A/P535A)	Codon optimized; N-terminal Flag sequence; residues phenylalanine 534 and proline 535 mutated to alanine	This study
pcDNA3-Flag-CO-ECTV165	Codon optimized; N-terminal Flag sequence	N. van Buuren
pcDNA3-Flag-CO-ECTV165(1-566)	Codon optimized; N-terminal Flag sequence deletion of PRANC domain from 567 to 594	M. Edwards
pEGFP-C2	GFP sequence upstream of the multiple cloning site	Clontech
pEGFP-CO-ECTV154	Codon optimized; N-terminal GFP sequence	This study
pEGFP-CO-ECTV154(F534A/P535A)	Codon optimized; N-terminal GFP- sequence residues F534 and P535 mutated to A	This study
pGEM-T	Subcloning vector; CMV promoter	Promega
pGEM-T-ECTV002-5'150	Wildtype sequence; 150 base pair nucleotide sequence directly upstream of ECTV002; flanked by *HindIII* and *XhoI*	N. van Buuren
pGEM-T-ECTV002-3'150	Wildtype sequence; 150 base pair nucleotide sequence directly downstream of ECTV002; flanked by *NotI* and *BamHI*	N. van Buuren
pGEM-T-ECTV005-5'150	Wildtype sequence; 150 base pair nucleotide sequence directly upstream of ECTV005; flanked by *HindIII* and *XhoI*	N. van Buuren

Table 2-3. Continued…

pGEM-T-ECTV005-3'150	Wildtype sequence; 150 base pair nucleotide sequence directly downstream of ECTV005; flanked by *NotI* and *BamHI*	N. van Buuren
pGEM-T-ECTV154-5'200	Wildtype sequence; 200 base pair nucleotide sequence directly upstream of ECTV154; flanked by *XhoI* and *HindIII*	This study
pGEM-T-ECTV154-3'200	Wildtype sequence; 200 base pair nucleotide sequence directly downstream of ECTV154; flanked by *BamHI* and *NotI*	This study
pGEM-T-ECTV165-5'200	Wildtype sequence; 200 base pair nucleotide sequence directly upstream of ECTV165; flanked by *XhoI* and *HindIII*	N. van Buuren
pGEM-T-ECTV165-3'200	Wildtype sequence; 200 base pair nucleotide sequence directly downstream of ECTV165; flanked by *BamHI* and *NotI*	N. van Buuren
pGEM-T-VACVB4R-400L	Wildtype sequence; 400 base pair nucleotide sequence directly upstream of VACVB4R; flanked by *SpeI* and *HindIII*	This study
pGEM-T-VACVB4R-400R	Wildtype sequence; 400 base pair nucleotide sequence directly downstream of VACVB4R; flanked by *BglII* and *NotI*	This study
pDGloxP	Poxvirus early/late promoter upstream of a *YFP/gpt* fusion open reading frame; flanked by loxP sites	(4)
pDGloxP-ECTV002-5'150	Wildtype sequence; 150 base pair nucleotide sequence directly upstream of ECTV002; inserted upstream of *YFP/gpt* fusion open reading frame and loxP site	N. van Buuren
pDGloxP-ECTV002-KO	Wildtype sequence; 150 base pair nucleotide sequences directly upstream and downstream of ECTV002 inserted upstream and downstream of *YFP/gpt* fusion open reading frame and loxP sites	N. van Buuren
pDGloxP-ECTV005-5'150	Wildtype sequence; 150 base pair nucleotide sequence directly upstream of ECTV005; inserted upstream of *YFP/gpt* fusion open reading frame and loxP site	N. van Buuren
pDGloxP-ECTV005-KO	Wildtype sequence; 150 base pair nucleotide sequences directly upstream and downstream of ECTV005 inserted upstream and downstream of *YFP/gpt* fusion open reading frame and loxP sites	N. van Buuren
pDGloxP-ECTV154-5'200	Wildtype sequence; 200 base pair nucleotide sequence directly upstream of ECTV154; inserted upstream of *YFP/gpt* fusion open reading frame and loxP site	This study
pDGloxP-ECTV154-KO	Wildtype sequence; 200 base pair nucleotide sequences directly upstream and downstream of ECTV154 inserted upstream and downstream of *YFP/gpt* fusion open reading frame and loxP sites	This study

Table 2-3. Continued…

pDGloxP-ECTV165-5'200	Wildtype sequence; 200 base pair nucleotide sequence directly upstream of ECTV165; inserted upstream of *YFP/gpt* fusion open reading frame and loxP site	M. Edwards
pDGloxP-ECTV165-KO	Wildtype sequence; 200 base pair nucleotide sequences directly upstream and downstream of ECTV165 inserted upstream and downstream of *YFP/gpt* fusion open reading frame and loxP sites	M. Edwards
pDGloxP-VACVB4R-400L	Wildtype sequence; 400 base pair nucleotide sequence directly upstream of VACVB4R; inserted upstream of *YFP/gpt* fusion open reading frame and loxP site	Q. Wang
pDGloxP-VACVB4R-KO	Wildtype sequence; 400 base pair nucleotide sequences directly upstream and downstream of VACVB4R inserted upstream and downstream of *YFP/gpt* fusion open reading frame and loxP sites	This study

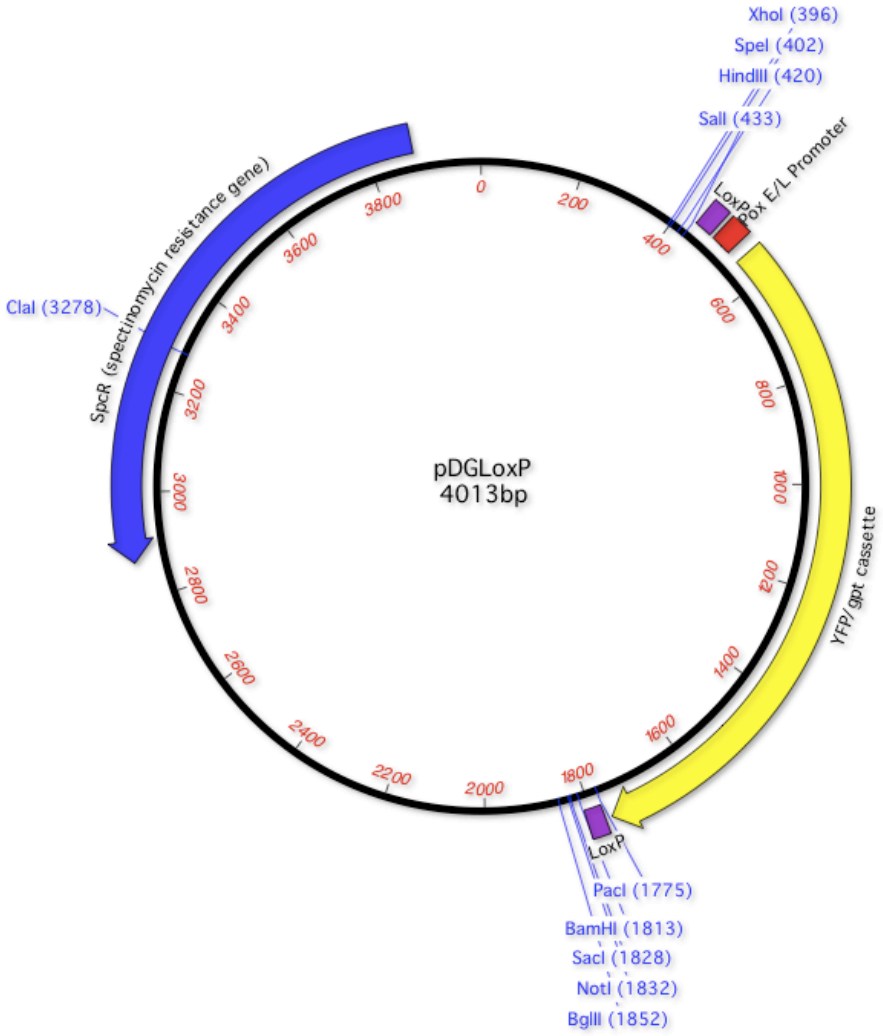

Figure 2-1. The pDGloxP vector. The pDGloxP vector is utilized to construct marker-free knockout viruses (4). The plasmid contains a YFP/gpt cassette under the control of a synthetic early/late poxvirus promoter p7.5. The cassette is flanked by two loxP sites oriented in the same direction, which are flanked by multiple cloning sites containing various restriction enzyme digestion sites. Regions of homology corresponding to the sequences directly up and downstream of the gene of interest are cloned into the multiple cloning sites.

processing machinery that exists in the nucleus. As such, many poxvirus ORFs contain cryptic splice sites that are recognized in the nucleus during transient expression, resulting in degradation of the ORF in the nucleus (2). In order to increase the efficiency of transient expression of ECTV002, ECTV005, ECTV154, and ECTV165, we utilized codon optimization (2). Vectors containing codon-optimized (CO) ECTV002, ECTV005, ECTV154, and ECTV165 were designed to remove cryptic splice sites, and optimize the expression of the ORFs in *Homo sapiens* by increasing the guanine and cytosine content in the sequence of the ORFs. In addition, vectors were designed for easy cloning into pcDNA3.1 and pEGFP, in order to generate Flag-tagged and GFP-tagged versions of the ORFs. Vectors were purchased from GENEART (Table 2-3). pMK-RQ-CO-ECTV002 contains from 5' to 3': a *HindIII* cut site, a Flag sequence, an *EcoRI* cut site, the CO-ECTV002 sequence, and a *BamHI* cut site. pMK-RQ-COECTV002 also carries kanamycin resistance. pGA15-CO-ECTV005 contains from 5' to 3': a *HindIII* cut site, a Flag sequence, an *EcoRI* cut site, the CO-ECTV005 sequence, and a *BamHI* cut site. pGA15-CO-ECTV005 also carries kanamycin resistance. pMK-RQ-CO-ECTV154 contains from 5' to 3': a *HindIII* cut site, a Flag sequence, an *EcoRI* cut site, CO-ECTV154 sequence, and a *BamHI* cut site. pMK-RQ-CO-ECTV154 also carries kanamycin resistance. pMA-RQ-CO-ECTV165 contains from 5' to 3': a *HindIII* cut site, a Flag sequence, an *EcoRI* cut site, the CO-ECTV165 sequence, and a *BamHI* cut site. pMA-RQ-CO-ECTV165 also carries ampicillin resistance.

2.4.2.2 Generation of pcDNA-Flag-CO-ECTV002, pcDNA-Flag-CO-ECTV005, pcDNA-Flag-CO-ECTV154, and pcDNA-Flag-CO-ECTV65. Flag-tagged CO versions of ECTV002, ECTV005, ECTV154, and ECTV165 were generated by digesting pMK-RQ-Flag-CO-ECTV002, pGA15-CO-ECTV005, pMK-RQ-Flag-CO-ECTV154, and pMA-RQ-Flag-CO-ECTV165 with *HindIII* and *BamHI*. The digestion products wwre ligated into pcDNA3.1 (Table 2-3) using the *HindIII* and *BamHI* restriction sites.

2.4.2.3 Generation of pcDNA-Flag-CO-ECTV002(1-554), pcDNA-Flag-CO-ECTV005(1-593), pcDNA-Flag-CO-ECTV154(1-532), and pcDNA-Flag-CO-ECTV165(1-566). The F-box domain was deleted from Flag-tagged CO versions of ECTV002, ECTV005, ECTV154, and ECTV165. pMK-RQ-Flag-CO-ECTV002, pGA15-CO-ECTV005, pMK-RQ-Flag-CO-ECTV154, and pMA-RQ-Flag-CO-ECTV165 were used as PCR templates with the following primers (Table 2-2): CO-ECTV002 Flag Forward and CO-ECTV002(1-554) Reverse, CO-ECTV005 Flag Forward and CO-ECTV005(1-593) Reverse, CO-ECTV154 Flag Forward-*HindIII* and CO-ECTV154(1-532) Reverse-*BamHI*, and COE-CTV165 Flag Forward and CO-ECTV165(1-566) Reverse. The PCR products were subcloned into pGEM-T (Table 2-3) prior to ligation into pcDNA3.1 using the *HindIII* and *BamHI* restriction sites.

2.4.2.4 Generation of pcDNA-Flag-CO-ECTV154(F534A/P535A). Since we could not express pcDNA-Flag-CO-ECTV154(1-532), we mutated phenyalanine 534 and proline 535 in the F-box domain to alanine residues, using site directed mutagenesis as described in section 2.3.2. The mutations were introduced using pcDNA-Flag-CO-ECTV154 as a PCR template with the following primers: CO-ECTV154(F534A/P535A)-Forward (Table 2-2) and CO-ECTV154(F534A/P535A)-Reverse (Table 2-2).

2.4.2.5 Generation of pEGFP-CO-ECTV154. GFP-CO-ECTV154 was constructed by digesting pMK-RQ-Flag-COECTV154 with *EcoRI* and *BamHI* and ligating the fragment into pEGFP-C2 (Table 2-3) using the *EcoRI* and *BamHI* restriction sites.

2.4.2.6 Generation of pEGFP-CO-ECTV154(F534A/P535A). An F-box mutated GFP-CO-ECTV154 was generated by mutating phenyalanine 534 and proline 535 to alanine residues using site directed mutagenesis as described in section 2.3.2. The mutations were introduced using pEGFP-CO-ECTV154 as a PCR template with the following primers: CO-ECTV154(F534A/P535A)-Forward (Table 2-2) and CO-ECTV154(F534A/P535A)-Reverse (Table 2-2).

2.4.2.7 Generation of pDGloxP knockout vector for ECTV002

In order to knock out the ECTV002 ORF from ECTV, we generated pDGloxP-ECTV002-KO. This was done by first cloning the 150 base pair sequences corresponding to the regions located directly 5' and 3' of the ECTV002 ORF in the ECTV genome separately into pGEM-T (Table 2-3) so they could be sequenced. Next, the sequences were digested and subcloned into the pDGloxP vector (Table 2-3), one at a time so that they flanked the *YFP/gpt* cassette. Each of these steps is described in detail below.

pGEM-T-ECTV002-5'150. A plasmid containing the 150 nucleotide sequence located directly upstream (5') of the ECTV002 ORF in the ECTV genome was generated by ECTV DNA as a PCR template, with the following primers: ECTV002(150)-5'-Forward (Table 2-2) and ECTV002(150)-5'-Reverse (Table 2-2). The resulting 150-nucleotide fragment contained a *HindIII* restriction digest site at the 5' end and an *XhoI* restriction digest site at the 3' end. The fragment was ligated into pGEM-T.

pGEM-T-ECTV002-3'150. A plasmid containing the 150 nucleotide sequence located directly downstream (3') of the ECTV002 ORF in the ECTV genome was generated by using ECTV DNA as a PCR template, with the following primers: ECTV002(150)-3'-Forward (Table 2-2) and ECTV002(150)-3'-Reverse (Table 2-2). The resulting 150-nucleotide fragment contained a *NotI* restriction digest site at the 5' end and a *BamHI* restriction digest site at the 3' end. The fragment was ligated into pGEM-T.

pDGloxP-ECTV002-5'150. To generate a plasmid containing *YFP/gpt* cassette preceded by the 200-nucleotide sequence located directly upstream (5') of the ECTV002 ORF, the 150-nucleotide sequence was digested from pGEM-T-ECTV002-5'150 using *HindIII* and *XhoI* restriction

enzymes. The resulting fragment was ligated into pDGloxP using the *HindIII* and *XhoI* restriction sites.

pDGloxP-ECTV002-KO. To generate a plasmid containing the *YFP/gpt* cassette preceded by the 150-nucleotide sequence located directly upstream (5') of the ECTV002 ORF, and followed by the 150 nucleotide sequence located directly downstream (3') of the ECTV002 ORF, the 150 nucleotide sequence was digested from pGEM-T-ECTV002-3'150 using *NotI* and *BamHI* restriction enzymes. The resulting fragment was ligated into pDGloxP-ECTV002-5'150 using the *NotI* and *BamHI* restriction sites.

2.4.2.8 Generation of pDGloxP knockout vector for ECTV005

In order to knock out the ECTV005 ORF from ECTV, we generated pDGloxP-ECTV005-KO. This was done by first cloning the 150 base pair sequences corresponding to the regions located directly 5' and 3' of the ECTV005 ORF in the ECTV genome separately into pGEM-T (Table 2-3) so they could be sequenced. Next, the sequences were digested and subcloned into the pDGloxP vector (Table 2-3), one at a time so that they flanked the *YFP/gpt* cassette. Each of these steps is described in detail below.

pGEM-T-ECTV005-5'150. A plasmid containing the 150 nucleotide sequence located directly upstream (5') of the ECTV005 ORF in the ECTV genome was generated by ECTV DNA as a PCR template, with the following primers: ECTV005(150)-5'-Forward (Table 2-2) and ECTV005(150)-5'-Reverse (Table 2-2). The resulting 150-nucleotide fragment contained a *HindIII* restriction digest site at the 5' end and an *XhoI* restriction digest site at the 3' end. The fragment was ligated into pGEM-T.

pGEM-T-ECTV005-3'150. A plasmid containing the 150 nucleotide sequence located directly downstream (3') of the ECTV005 ORF in the ECTV genome was generated by using ECTV DNA as a PCR template, with the following primers: ECTV005(150)-3'-Forward (Table 2-2) and

ECTV005(150)-3'-Reverse (Table 2-2). The resulting 150-nucleotide fragment contained a *NotI* restriction digest site at the 5' end and a *BamHI* restriction digest site at the 3' end. The fragment was ligated into pGEM-T.

pDGloxP-ECTV005-5'150. To generate a plasmid containing *YFP/gpt* cassette preceded by the 150-nucleotide sequence located directly upstream (5') of the ECTV005 ORF, the 150 nucleotide sequence was digested from pGEM-T-ECTV005-5'150 using *HindIII* and *XhoI* restriction enzymes. The resulting fragment was ligated into pDGloxP using the *HindIII* and *XhoI* restriction sites.

pDGloxP-ECTV005-KO. To generate a plasmid containing the *YFP/gpt* cassette preceded by the 150-nucleotide sequence located directly upstream (5') of the ECTV005 ORF, and followed by the 150 nucleotide sequence located directly downstream (3') of the ECTV005 ORF, the 150 nucleotide sequence was digested from pGEM-T-ECTV005-3'200 using *NotI* and *BamHI* restriction enzymes. The resulting fragment was ligated into pDGloxP-ECTV005-5'150 using the *NotI* and *BamHI* restriction sites.

2.4.2.9 Generation of pDGloxP knockout vector for ECTV154

In order to knock out the ECTV154 ORF from ECTV, we generated pDGloxP-ECTV154-KO. This was done by first cloning the 200 base pair sequences corresponding to the regions located directly 5' and 3' of the ECTV154 ORF in the ECTV genome separately into pGEM-T (Table 2-3) so they could be sequenced. Next, the sequences were digested and subcloned into the pDGloxP vector (Table 2-3), one at a time so that they flanked the *YFP/gpt* cassette. Each of these steps is described in detail below.

pGEM-T-ECTV154-5'200. A plasmid containing the 200-nucleotide sequence located directly upstream (5') of the ECTV154 ORF in the ECTV genome was generated by ECTV DNA as a PCR template, with the following primers: WT ECTV154(200)-5'-Forward-*XhoI* (Table 2-2) and WT

ECTV154(200)-5'-Reverse-*HindIII* (Table 2-2). The resulting 200-nucleotide fragment contained an *XhoI* restriction digest site at the 5' end and a *HindIII* restriction digest site at the 3' end. The fragment was ligated into pGEM-T.

pGEM-T-ECTV154-3'200. A plasmid containing the 200-nucleotide sequence located directly downstream (3') of the ECTV154 ORF in the ECTV genome was generated by using ECTV DNA as a PCR template, with the following primers: WT ECTV154(200)-3'-Forward-*BamHI* (Table 2-2) and WT ECTV154(200)-3'-Reverse-*NotI* (Table 2-2). The resulting 200-nucleotide fragment contained a *BamHI* restriction digest site at the 5' end and a *NotI* restriction digest site at the 3' end. The fragment was ligated into pGEM-T.

***pDGloxP-ECTV154-5'200*.** To generate a plasmid containing *YFP/gpt* cassette preceded by the 200-nucleotide sequence located directly upstream (5') of the ECTV154 ORF, the 200 nucleotide sequence was digested from pGEM-T-ECTV154-5'200 using *XhoI* and *HindIII* restriction enzymes. The resulting fragment was ligated into pDGloxP using the *XhoI* and *HindIII* restriction sites.

pDGloxP-ECTV154-KO. To generate a plasmid containing the *YFP/gpt* cassette preceded by the 200-nucleotide sequence located directly upstream (5') of the ECTV154 ORF, and followed by the 200 nucleotide sequence located directly downstream (3') of the ECTV154 ORF, the 200 nucleotide sequence was digested from pGEM-T-ECTV154-3'200 using *BamHI* and *NotI* restriction enzymes. The resulting fragment was ligated into pDGloxP-ECTV154-5'200 using the *BamHI* and *NotI* restriction sites.

2.4.2.10 Generation of pDGloxP knockout vector for ECTV165

In order to knock out the ECTV165 ORF from ECTV, we generated pDGloxP-ECTV165-KO. This was done by first cloning the 200 base pair sequences corresponding to the regions located directly 5' and 3' of the ECTV165 ORF in the

ECTV genome separately into pGEM-T (Table 2-3) so they could be sequenced. Next, the sequences were digested and subcloned into the pDGloxP vector (Table 2-3), one at a time so that they flanked the *YFP/gpt* cassette. Each of these steps is described in detail below.

pGEM-T-ECTV165-5'200. A plasmid containing the 200-nucleotide sequence located directly upstream (5') of the ECTV165 ORF in the ECTV genome was generated by ECTV DNA as a PCR template, with the following primers: ECTV165(200)-5'-Forward (Table 2-2) and ECTV165(200)-5'-Reverse (Table 2-2). The resulting 200-nucleotide fragment contained an *XhoI* restriction digest site at the 5' end and a *HindIII* restriction digest site at the 3' end. The fragment was ligated into pGEM-T.

pGEM-T-ECTV165-3'200. A plasmid containing the 200-nucleotide sequence located directly downstream (3') of the ECTV165 ORF in the ECTV genome was generated by using ECTV DNA as a PCR template, with the following primers: ECTV165 (200)-3'-Forward (Table 2-2) and ECTV165(200)-3'-Reverse (Table 2-2). The resulting 200-nucleotide fragment contained a *BamHI* restriction digest site at the 5' end and a *NotI* restriction digest site at the 3' end. The fragment was ligated into pGEM-T.

***pDGloxP-ECTV165-5'200*.** To generate a plasmid containing *YFP/gpt* cassette preceded by the 200-nucleotide sequence located directly upstream (5') of the ECTV165 ORF, the 200 nucleotide sequence was digested from pGEM-T-ECTV165-5'200 using *XhoI* and *HindIII* restriction enzymes. The resulting fragment was ligated into pDGloxP using the *XhoI* and *HindIII* restriction sites.

pDGloxP-ECTV165-KO. To generate a plasmid containing the *YFP/gpt* cassette preceded by the 200-nucleotide sequence located directly upstream (5') of the ECTV165 ORF, and followed by the 200 nucleotide

sequence located directly downstream (3') of the ECTV165 ORF, the 200 nucleotide sequence was digested from pGEM-T-ECTV165-3'200 using *BamHI* and *NotI* restriction enzymes. The resulting fragment was ligated into pDGloxP-ECTV165-5'200 using the *BamHI* and *NotI* restriction sites.

2.4.2.11 Generation of pDGloxP knockout vector for VACVB4R

In order to knock out the VACVB4R ORF from VACV, we generated pDGloxP-VACVB4R-KO. This was done by first cloning the 400 base pair sequences corresponding to the regions located directly 5' and 3' of the VACVB4R ORF in the VACV genome separately into pGEM-T (Table 2-3) so they could be sequenced. Next, the sequences were digested and subcloned into the pDGloxP vector (Table 2-3), one at a time so that they flanked the *YFP/gpt* cassette. Each of these steps is described in detail below.

pGEM-T-VACVB4R-400L. A plasmid containing the 400-nucleotide sequence located directly upstream (L) of the VACVB4R ORF in the VACV genome was generated by using VACVCop as a PCR template, with the following primers: WT VACV-B4R(400)-L-For-*SpeI* (Table 2-2) and WT VACV-B4R(400)-L-Rev-*HindIII* (Tablw 2-2). The resulting 400-nucleotide fragment contained a *SpeI* restriction digest site at the 5' end and a *HindIII* restriction digest site at the 3' end. The fragment was ligated into pGEM-T.

pGEM-T-VACVB4R-400R. A plasmid containing the 400-nucleotide sequence located directly downstream (R) of the VACVB4R ORF in the VACV genome was generated by using VACVCop as a PCR template, with the following primers: WT VACV-B4R(400)-R-For-*NotI* (Table 2-2) and WT VACV-B4R(400)-R-Rev-*BglII* (Table 2-2). The resulting 400-nucleotide fragment contained a *NotI* restriction digest site at the 5' end and a *BglII* restriction digest site at the 3' end. The fragment was ligated into pGEM-T.

pDGloxPKO-VACVB4R-400L. To generate a plasmid containing the *YFP/gpt* cassette preceded by the 400-nucleotide sequence located directly upstream (L) of the VACVB4R ORF, the 400-nucleotide sequence was digested from pGEM-T-VACVB4R-400L using *SpeI* and *HindIII* restriction enzymes. The resulting fragment was ligated into pDGloxP using the *SpeI* and *HindIII* restriction sites.

pDGloxPKO-VACVB4R-KO. To generate a plasmid containing the *YFP/gpt* cassette preceded by the 400-nucleotide sequence located directly upstream (L) of the VACVB4R ORF, and followed by the 400-nucleotide sequence located directly downstream (L) of the VACVB4R ORF, the 400 nucleotide sequence was digested from pGEM-T-VACVB4R-400R using *NotI* and *BglII* restriction enzymes. The resulting fragment was ligated into pDGloxP-VACVB4R-400L using the *BamHI* and *NotI* restriction sites.

2.5 TRANSFECTIONS

Transfections were performed using Lipofectamine 2000 as per manufacturer's instructions (Invitrogen). For each transfection, 2 μL of Lipofectamine 2000 was added to 50 μL of Opti-MEM (Invitrogen) and incubated at room temperature for 5 minutes. Meanwhile, the appropriate amount of DNA was added to a second tube containing 50 μL of Opti-MEM and this mixture was added to the Lipofectamine 2000 mixture after the 5-minute incubation. The mixture was mixed gently and incubated for an additional 15 minutes at room temperature. During the incubation, cells were washed with Opti-MEM, and 400 μL was added to each well in the 12-well plates containing coverslips, while 900 μL was added to each well in the 6-well plates. After 15 minutes, 100 μL of the DNA-Lipofectamine mixture was added to each well. One hour post-transfection, 500 μL of DMEM supplemented with 20% HI-FBS and 400 μg/mL L-glutamine was

added to each well in the 12-well plates, and 1 mL was added to each well in the 6-well plates.

2.6 INFECTIONS

Cells were infected with virus at the indicated multiplicity of infection (MOI). Media was removed from 12-well plates containing coverslips or 6-well plates and replaced with 400 μL of warm DMEM supplemented with 10% NCS, 50 U/mL of penicillin, 50 U/mL of streptomycin, and 200 μM of L-glutamine. Alternatively, media was removed from 10 cm dishes and replaced with 5 mL of supplemented DMEM. Cells were infected and incubated for 1 hour at 37°C in 5% CO_2, with gentle rocking of the plates every 10 minutes. One hour post-infection, 1 mL of supplemented DMEM was added back to each well of the 6-well plates and the 12-well plates containing coverslips, while 5 mL of supplemented DMEM was added back to each 10 cm dish.

2.7 INFECTION-TRANSFECTIONS

Infection-transfections were used during initial generation of the *YFP/gpt*-containing knockout viruses and the revertant viruses. BGMK cells (1 x 10^6/well) were washed with Opti-MEM, and 900 μL of Opti-MEM was added back to 2 wells of a 6-well plate. Cells were infected with ECTV or VACV811 at an MOI of 0.01. Meanwhile, 10 μL of Lipofectamine 2000 was added to 100 μL of Opti-MEM. The mixture was incubated at room temperature for 5 minutes. Ten μg of DNA was added to a second tube containing 100 μL of Opti-MEM, and this mixture was added to the Lipofectamine 2000 mixture after the 5-minute incubation. The mixture was mixed gently and incubated for an additional 15 minutes at room temperature. After 15 minutes, which corresponded to 1 hour post-infection, 100 μL of the DNA-Lipofectamine mixture was added to each

well. One hour post-transfection, 1 mL of DMEM supplemented with 20% NCS and 400 μg/mL glutamine was added to each well. The following day, the media was replaced with fresh supplemented DMEM.

2.8 VIRUS METHODOLOGY

2.8.1 Generation of recombinant viruses

2.8.1.1 Generation of *YFP/gpt*-containing knockout viruses. Recombinant viruses lacking the ORF of interest were generated by first cloning a pDGloxP vector containing the upstream and downstream flanking regions of the ORF as described in section 2.4. Ten μg of vector were linearized using restriction enzyme digestion, at cut sites at the 5' end of the upstream flanking region and the 3' end of the downstream flanking region (Figure 2-2). Linearized DNA was subject to DNA cleanup, by adding 5 volumes of buffer PB (Qiagen), followed by washing with 0.75 mL of buffer PE in a QIAquick column. DNA was eluted in 20 μL of distilled water. Infection-transfections were performed as described in section 2.7. Forty-eight hours post-infection and transfection, cells were harvested with standard saline citrate (SSC) containing 150 mM NaCl and 15 mM tris-sodium citrate, washed with PBS, and resuspended in 200 μL of swelling buffer, containing 10 mM Tris (pH 8.0) and 2 mM $MgCl_2$. The cell suspension was resuspended in 1 mL of mycophenolic acid (MPA) selection media containing 250 μg/mL xanthine (Sigma-Aldrich), 25 μg/mL MPA (Sigma-Aldrich), and 15 μg/μL hypoxanthine (Sigma-Aldrich) and titred on BGMK cells. ECTV foci or VACV811 plaques were screened visually using the FITC filter on a fluorescent microscope (Leica). YFP fluorescence was used as an indicator that homologous recombination had occurred between the virus and the pDGloxP vector, and these foci and plaques were marked with a permanent marker. Viruses were purified as described in section 2.8.3.

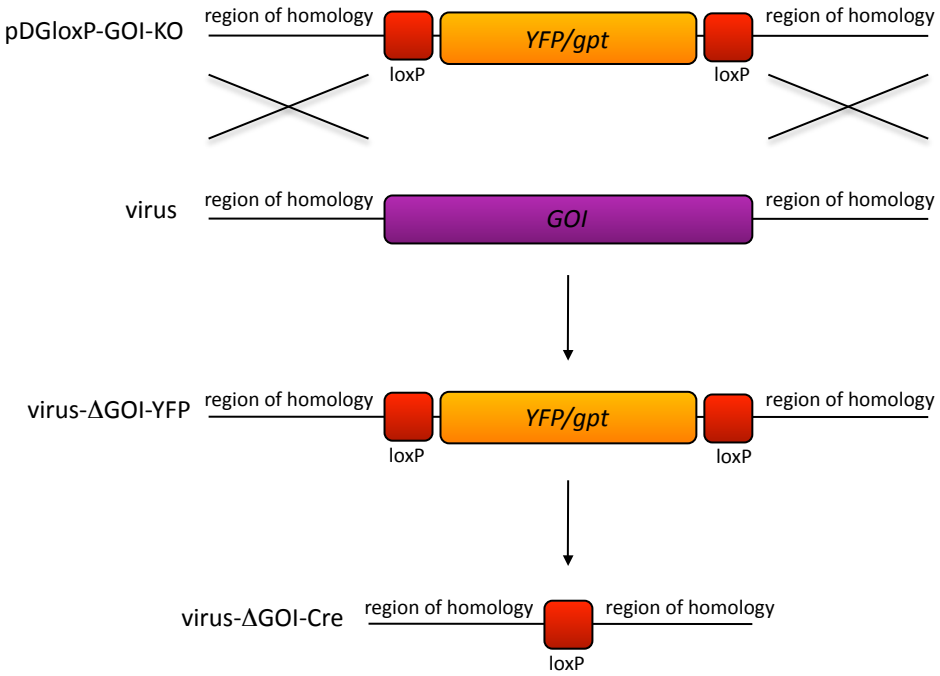

Figure 2-2. Schematic representation for generation of a marker-free poxvirus. Marker-free poxviruses are generated by transfecting the pDGloxP plasmid containing flanking regions of homology to the gene of interest (GOI), into cells infected with the virus. Homologous recombination occurs between the virus and the pDGloxP plasmid, resulting in a knockout virus containing a *YFPgpt* cassette in the place of the GOI (virus-ΔGOI-YFP). By passaging the the *YFP/gpt*-containing plasmid through U2OS cells expressing a cytoplasmic Cre recombinase, the a *YFP/gpt* cassette was excised, resulting in a marker-free deletion virus containing a single loxP site (virus-ΔGOI-Cre).

2.8.1.2 Generation of marker-free knockout viruses. To generate marker-free viruses lacking drug resistant and fluorescent markers, *YFP/gpt*-containing viruses were passaged through U20S-Cre cells (4). One well of a 6 well plate was infected with the *YFP/gpt*-containing virus at an MOI of 5. Twenty-four hours post-infection, cells were harvested with SSC, washed with PBS, and resuspended in 200 μL of swelling buffer. The cell suspension was resuspended in 1000 μL of DMEM, and titred out over U2OS-Cre cells. ECTV foci were screened visually, using the absence of YFP as an indicator that excision by the Cre recombinase had occurred.

2.8.1.3 Generation of revertant viruses. *YFP/gpt*-containing viruses were used to generate revertant viruses that had the original knocked out gene sequence reinserted. Primers to the the 5' end of the upstream flanking region and the 3' end of the downstream flanking region of the gene were used to generate a PCR product using ECTV or VACV811 as a template, as described in section 2.3.1. The PCR product was subjected to DNA cleanup by adding 5 volumes of buffer PB (Qiagen), followed by washing with 0.75 mL of buffer PE in a QIAquick column. DNA was eluted in 20 μL of distilled water. Infection-transfections were performed as described in section 2.7. Forty-eight hours post-infection-transfection, cells were harvested with SSC, washed with PBS, and resuspended in 200 μL of swelling buffer. The cell suspension was resuspended in 1000 μL of DMEM and titred out over BGMK cells. ECTV foci or VACV811 plaques were screened visually; using the absence of YFP as an indicator that homologous recombination had occurred between the virus and the PCR product.

2.8.2 Virus purification

Infected cell monolayers were overlaid with 2 mL of a low melting point (LMP) agarose containing 2.5 mL of LMP agarose (Sigma-Aldrich), 2.5 mL of 2x DMEM (2.7% w/v DMEM, 88 mM $NaHCO_3$), and 1 mL of NCS. The agarose was allowed to solidify at room temperature before marked foci or plaques were picked using

a Pasteur pipette and resuspended in 50 μL of swelling buffer. Foci and plaque suspensions were freeze thawed three times at -80°C and 37°C, and 50 μL of 2x DMEM was added and the plaques were sonicated as described in section 2.2. Recombinant viruses were subjected to 3 to 5 rounds of purification, and were tested for purity by isolating viral genomic DNA as described in section 2.8.3 and performing PCR analysis as described in section 2.3.1, using primers specific to the gene of interest.

2.8.3 Preparation of viral genomic DNA

Viral genomic DNA was isolated to check for insertion or deletion of the *YFP/gpt* cassette. During the purification step of virus generation, foci or plaques were titred in Cre cells or BGMK cells and the infection proceeded for 48 hours. Wells suspected to contain the virus of interest were washed with warm PBS and subjected to lysis overnight at 37°C with 1 mL of a lysis buffer containing 50 mM Tris (pH 8.0), 4 mM EDTA, 4 mM $CaCl_2$, and 1.2% v/v SDS, supplemented with 0.2 mg/mL Proteinase K (Roche-Diagnostics). The following day, 0.5 mL of phenol/chloroform (1:1 v/v) was added to the cell lysates, and the suspensions was centrifuged at 9223 x *g* for 10 minutes. Three hundred μL of the aqueous layer was removed and transferred to a new tube, and the DNA was precipitated by adding 1 mL of 95% cold ethanol and 50 μL of 3 M sodium acetate and incubating at -80°C for 15 minutes. DNA was pelleted by centrifugation at 18000 x *g* for 15 minutes. Pelleted DNA was dried briefly and resuspended in 100 μL of distilled water. Alternatively, amplified viruses were checked for purity by infecting BGMK cells at an MOI of 5. Twenty-four hours post infection, cells were subject to lysis and viral DNA was isolated by phenol-chloroform extraction.

2.8.4 Preparation of virus stocks

2.8.4.1 Preparation of ECTV and VACV811 virus stocks. All ECTV and VACV811 viruses were amplified by infecting BGMK cells (3.75×10^7) in one T150 flask

(Corning). Three to 4 days post infection, media and cells were harvested using SSC and centrifuged at 300 x *g* for 10 minutes. The pellet was resuspended in 10 mL of swelling buffer and freeze thawed 3 times. Cell membranes were disrupted to release virus particles by dounce homogenization on ice approximately 100 times with a B pestle (Bellco Biotechnology). Homogenates were centrifuged at 300 x *g* for 10 minutes and the supernatant was set aside. The pellet was resuspended in 10 mL of swelling buffer and subject to dounce homogenization on ice for an additional 50 times, before being centrifuged at 300 x *g* for 10 minutes. The supernatants were combined and centrifuged at 10 000 x *g* at 4°C for 60 minutes. The virus pellet was resuspended in 500 μL DMEM and used to infect 3 T150 flasks containing BGMK cells. The process of harvesting and homogenization was repeated. One hundred μL of resuspended virus was set aside as a stock to reinfect 1 T150 at a later date, while 400 μL was used to infect 6 T150 flasks containing BGMK cells. For ECTV, virus was isolated as described above and resuspended in a final volume of 500 μL of DMEM. For VACV811, it was necessary to purify the virus using a sucrose cushion. Virus was harvested from 6 T150 flasks and prepped as described above, and homogenate resuspended in a total of 32 mL of swelling buffer. The homogenate was divided into 16 mL fractions and layered onto 16 mL of 36% w/v sucrose in 1 mM Tris (pH 9.0) in 35 mL (25 x 89 mm) polyallomer centrifuge tubes (Beckman). The virus was pelleted by centrifugation at 35 000 x *g* at 4°C for 80 minutes. The virus pellet was resuspended in 500 μL DMEM. Virus titers were determined as described in section 2.8.5.

2.8.4.2 Preparation of VACV stocks. All VACV viruses were amplified by infecting BGMK cells (3 x 10^8) in three roller bottles. Twenty-four to 48 hours post-infection, media and cells were harvested using SSC and centrifuged at 300 x *g* for 10 minutes. The pellet was resuspended in 20 mL of swelling buffer and freeze thawed three times, before dounce homogenization on ice approximately 100 times. Homogenates were centrifuged at 300 x *g* for 10 minutes and the

supernatant was set aside. The pellet was resuspended in 10 mL of swelling buffer and subject to dounce homogenization on for an additional 50 times before being centrifuged at 300 x *g* for 10 minutes. The supernatants were combined and centrifuged at 10 000 x *g* at 4°C for 60 minutes. The virus pellet was resuspended in 1500 μL DMEM and divided equally into three tubes.

2.8.5 Determination of viral titers

2.8.5.1 Determination of ECTV viral titers. To determine the number of foci or plaque forming units (PFU) per mL of virus, serial dilutions were performed in BGMK or CV-1 cells. Ten μL of virus stock was diluted by a factor of 100 in 990 μL of PBS. Six serial dilutions (10^{-3} to 10^{-8}) were performed by diluting 100 μL of the initial dilution in 900 μL of PBS, and BGMK cells (1 x 10^{6}) were infected in duplicate with these dilutions. One hour post-infection, 2 mL of DMEM supplemented with 5% HI-FBS, 1% w/v carboxymethylcellulose (CMC) (Sigma-Aldrich), 50 μg/mL of penicillin, 50 μg/mL of streptomycin and 200 μM of glutamine was added to each well. Four days post-infection, after plaque formation had occurred, cell monolayers were stained by adding 2 mL of crystal violet containing 11.1% formaldehyde (Sigma-Aldrich), 4.75% ethanol, and 0.13% crystal violet (Sigma-Aldrich) directly to the CMC media. Plates were rocked at room temperature overnight to fix and stain the monolayer and washed and dried at room temperature the following day. Plaques were visible as clearings in the cell monolayers. Wells containing 30 to 200 plaques were counted and PFU/mL was determined by multiplying the number of plaques by the reciprocal of the dilution of that well, and dividing by the volume of media used to infect that well [(number of plaques) x (1/dilution) / (volume of infection)].

2.8.5.2 Determination of VACV and VACV811 viral titers. Viruses were serial diluted as described above in section 2.8.5.1. One hour post-infection, 1 mL of DMEM was added to each well, and monolayers were incubated for 2 days. Monolayers were fixed with 1 mL of neutral buffered formalin containing 4% v/v

formaldehyde (pH 7.4) (Sigma-Aldrich), 1.45 M NaCl, 550 mM Na_2HPO_4, and 350 mM NaH_2PO_4. After 10 minutes at room temperature, the fixing agent was removed and cell monolayers were stained with a crystal violet solution containing 20% v/v ethanol and 0.1% w/v crystal violet.

2.9 PROTEIN METHODOLOGY

2.9.1 Antibodies

All antibodies used in this study are summarized Table 2-4. The amount of antibody used and the source of each antibody is also provided.

2.9.2 SDS poly-acrylamide gel electrophoresis

Protein samples were prepared in sodium dodecyl sulphate (SDS) loading buffer, containing 62.5 mM Tris (pH 6.8), 12.5% v/v glycerol, 2% w/v SDS, 90 mM β-mercaptoethanol (BioShop), and 74.5 nM bromophenol blue (Biorad), and boiled at 100°C for 15 minutes. Samples were loaded into 10-15% acrylamide gels and separated using SDS polyacrylamide gel electrophoresis (SDS-PAGE) in a Mini-PROTEAN3 Cell system (Biorad). Gels were run at 150 V to 200 V in 1x SDS buffer containing 190 mM glycine, 25 mM Tris, and 3.5 mM SDS.

2.9.3 Semi-dry transfer

Proteins resolved by SDS-PAGE were transferred to a nitrocellulose membrane (Fischer Scientific) for 2 hours at 420 mA using a semi-dry transfer apparatus (TYLER Research Instruments) and transfer buffer containing 192 mM glycine, 25 mM Tris, and 20% v/v methanol. Membranes were blocked for 3 hours at room temperature in 5% w/v skimmed milk containing Tris-buffered saline with Tween 20 (TBS-T), containing 200 mM Tris (pH 7.5), 15 mM NaCl, and 0.1% v/v Tween-20 (Fischer Scientific).

Table 2-4. Antibodies used in this study

Antibody	Immunoblot	Source
Immunoblot		
Rabbit anti-A34	1:10 000	D. Evans
Mouse anti-B5	1:10 000	J. Shisler
Mouse anti-β-tubulin	1:5000	ECM Biosciences
Mouse anti-E3L	1:1000	J. Cao
Mouse anti-FlagM2	1:5000	Sigma-Aldrich
Rabbit anti-histone H3	1:5000	Cell Signalling Technology
Rabbit anti-I5L	1:5000	M. Barry
Mouse anti-IκBα	1:1000	Cell Signalling Technology
Mouse anti-NFκB p-50	1:5000	Biolegend
Rabbit anti-NFκB p-65	1:5000	Santa Cruz Biotechnology
Mouse anti-PARP	1:2000	BD Biosciences
Peroxidase-conjugated AffiniPure goat anti-rabbit	1:25000	Jackson Laboratories
Peroxidase-conjugated AffiniPure goat anti-mouse	1:25000	Jackson Laboratories
Immunofluorescence		
Mouse anti-FlagM2	1:200	Sigma-Aldrich
Rabbit anti-NFκB p65	1:200	Santa Cruz Biotechnology
Rabbit anti-Flag	1:200	Sigma-Aldrich
Mouse anti-IκBα	1:125	Cell Signalling Technology
Goat anti-mouse Alexaflour 488	1:400	Invitrogen
Goat anti-rabbit Alexaflour 546	1:400	Invitrogen
Flow Cytometry		
Mouse anti-I3L	1:100	D. Evans
Mouse anti-IκBα	1:400	Cell Signalling Technology
Phycoerythrin-conjugated goat anti-mouse	1:1000	Jackson ImmunoResearch Laboratories Ltd.
Goat anti-mouse Alexaflour 488	1:400	Invitrogen Corporation

2.9.4 Immunoblotting

Membranes were incubated with primary antibody (Table 2-4) diluted in TBS-T overnight at 4°C. Membranes were subjected to four 15-minute washes with TBS-T and probed with the appropriate horse-radish peroxidase (HRP)-conjugated secondary antibody (Table 2-4) diluted in TBS-T for 1 hour at room temperature. Membranes were subjected to four 15-minute washes with TBS-T and proteins were visualized using enhanced chemiluminescence (ECL) (GE Healthcare) and Amersham Hyerfilm ECL (GE Healthcare).

2.10 ASSAYS

2.10.1 Reverse transcription PCR to detect viral gene expression

RNA transcripts for ECTV002, ECTV005, ECTV154 and ECTV165 were analyzed by reverse transcription PCR (RT-PCR). CV-1 cells (1×10^6) were mock infected or infected with ECTV at an MOI of 5. One hour post-infection, media was removed and cells were washed with DMEM, and 1 mL of DMEM or DMEM containing 80 μg/mL of cytosine β-D-arabinofuransoside hydrochloride (AraC) (Sigma-Aldrich) was added back. Samples were collected 4, 12, and 24 hours post-infection by washing the cells with warm PBS and harvesting with 1 mL of TRIZOL (Invitrogen). A mock sample was also collected at the 12-hour time point. Samples were stored at -80°C. RNA was extracted using a TRIZOL extraction protocol (Invitrogen). Two hundred μL of chloroform was added to the TRIZOL suspension and samples were shaken for 15 seconds and incubated for 3 minutes at room temperature. The aqueous and organic phases were separated by centrifugation at 12,000 *x* g at 4°C for 10 minutes. The aqueous phase containing the RNA was harvested to a new tube, and 0.5 mL of isopropanol was added, followed by incubation at room temperature for 10 minutes. Precipitated RNA was isolated by centrifugation at 12,000 *x* g at 4°C for 10 minutes. The RNA pellet was washed with 75% v/v ethanol made in

Table 2-5. Primers used for RT-PCR

Primer name	Primer Sequence (5’ to 3’)
I-WT ECTV004-RTPCR-Forward	GTT TAA TAT CAT GAA CTG CGA CTA TCT
WT ECTV004-RTPCR-Reverse	TTA ATA ATA CCT AGA AAA TAT TCC ACG AGC
I-WT ECTV002-RTPCR-Forward	AGT CAT ACA TTC GGA CAA ACA
WT ECTV002-RTPCR-Reverse	TTA TGA ATA ATA TTT GTA ATG GTT CTT TCC
I-WT ECTV005-RTPCR-Forward	TAG TGG TAT TAG AGA GAA ATG CAA TCT
WT ECTV005-RTPCR-Reverse	TCA TTC ATG TGT CTG TGT TTG
I-WT ECTV154-RTPCR-Forward	TAA TGA GAT ACG GTA GAC ATC CTT CTT
WT ECTV154-RTPCR-Reverse	TTA TAT TTT AAT AGT GTT TAT AAG ATT TTT TAG
I-WT ECTV165-RTPCR-Forward	CCT CAA TGA ATT AAA AAA ATA TAT TAA TGA TAC GTC
WT ECTV165-RTPCR-Reverse	CTA TAC TTT GGT AGA TGG ATA CGA TAT
2-WT VACVI5L-RTPCR-Forward	ATG GCG GAT GCT ATA ACC GTT
WT VACVI5L-RTPCR-Reverse	TTA ACT TTT CAT TAA TAG GGA

diethylpyrocarbonate (DEPC)-treated water (Invitrogen), and centrifuged 7500 *x* g at 4°C for 5 minutes. Pellets were air-dryed and re-suspended in 50 μL DEPC-treated water, followed by a 10 minute incubation on ice and a 10 minute incubation at 55°C. RNA concentrations were determined using a NanoVue *Plus* spectrophotometer (GE Healthcare).

Contaminating single and double stranded DNA was removed from the samples by treating 2 μg of RNA with 1 U/μL of RQ1 RNase-free DNase (Promega). After 1 hour at 37°C, 2 μL of a stop-solution was added and the DNase was inactivated at 65°C for 10 minutes. cDNA was generated using first-strand synthesis. Twenty μL of the DNase-treated RNA mixture was combined with 2 μL of Oligo$(dT)_{12-18}$ primer (Invitrogen) and 2 μL of 10 mM RNA-free dNTPs. Following a primer annealing step at 65°C for 5 minutes, 8 μL of 5x First-Strand Buffer, 4 μL of 0.1 M DTT, and 2 μL of DEPC-treated water was added and the reaction mixture. The mixture was incubated at 42°C for 2 minutes and 400 U of SuperScript II RT (Invitrogen) was added, followed by incubation at 42°C for 50 minutes and 70°C for 15 minutes. After, the reactions were treated with 2 μL of RNase H (Invitrogen) at 37°C for 20 minutes to degrade parental RNA. PCR reactions to assess RNA transcript levels were performed using *Taq* polymerase as described in section 2.3.1. Five μL of the cDNA was used as a template and gene-specific primers (Table 2-5) were used to amplify the last 250 nucleotides (at the 3' end) of each ORF.

2.10.2 Immunofluorescence microscopy

2.10.2.1 Detection of NFκB p65 nuclear translocation. HeLa cells (2 X 10^5) were seeded on coverslips and mock transfected or transfected with 2 μg of the indicated plasmid expressing a Flag-tagged protein. Alternatively, cells were mock infected or infected with the indicated virus at an MOI of 5. Fourteen hours post-transfection or 12 hours post-infection, cells were stimulated with 10 ng/mL

of TNFα (Roche) or IL-1β (Peprotech, Inc) for 20 minutes. Following stimulation, cells were fixed with 2% w/v paraformaldehyde (Sigma-Aldrich) in PBS for 10 minutes, permeabilized with 1% v/v NP-40 (Sigma-Aldrich) in PBS for 5 minutes, and blocked with 30% v/v goat serum (Invitrogen) in PBS for 15 minutes. Cells were incubated overnight with mouse anti-FlagM2 (Table 2-4) and rabbit anti-NFκB p65 (Table 2-4). The cells were stained with goat anti-mouse Alexaflour 488 (Table 2-4) and goat anti-rabbit Alexaflour 546 (Table 2-4). The cover slips were mounted in 50% v/v glycerol containing 4 mg/mL N-propyl-gallate (Sigma-Aldrich) and 250 μg/mL 4,6-diamino-2-phenylindole (DAPI) (Invitrogen) to visualize nuclei. Cells were visualized using the 40x oil immersion objective of a Ziess Axiovert 200M fluorescent microscope outfitted with an ApoTome 10 optical sectioning device (Carl Zeiss, Inc). NFκB p65 nuclear translocation was quantified by counting 150 Flag-positive cells over three independent trials.

2.10.2.2 Detection of IκBα degradation. HeLa cells (2 X 10^5) were seeded on coverslips and mock transfected or transfected with 2 μg of pcDNA-Flag-CO-ECTV002, pcDNA-Flag-CO-ECTV005, pcDNA-Flag-CO-ECTV154, or pcDNA-Flag-CO-ECTV165. Fourteen hours post-transfection, cells were stimulated with 10 ng/mL of TNFα. Cells were fixed and permeabilized as described in section 2.9.2.1, and incubated with rabbit anti-Flag (Table 2-4) and mouse anti-IκBα (Table 2-4) for 2 hours. Cells were stained with goat anti-mouse Alexaflour 488 (Table 2-4) and goat anti-rabbit Alexaflour 546 (Table 2-4), and visualized as described in section 2.10.2.1.

2.10.3 Whole cell lysates

2.10.3.1 Detection of p50, p65 and IκBα degradation. HeLa cells (1 x 10^6) were infected with the indicated viruses at an MOI of 5. Whole cell lysates were harvested 0, 4, 8, 12 and 25 hours post-infection in 125 μL of SDS loading buffer. Samples were immunoblotted with mouse anti-FlagM2 (Table 2-4), rabbit anti-

NFκB p65 (Table 2-4), mouse anti-IκBα (Table 2-4), mouse anti-NFκB p50 (Table 2-4), and mouse anti-β-tubulin (Table 2-4).

2.10.3.2 Detection of IκBα accumulation during ankyrin/F-box protein expression. HeLa cells (1 x 10^6) were mock transfected, or transfected with 0.25 μg, 0.75 μg, 1.5 μg, or 3 μg of pcDNA-Flag-CO-ECTV002, pcDNA-Flag-CO-ECTV005, pcDNA-Flag-CO-ECTV154, or pcDNA-Flag-CO-ECTV165. Twenty-four hours post-transfection, cells were stimulated with 10 ng/mL of TNFα for 20 minutes. Whole cell lysates were harvested in 150 μL of SDS loading buffer. Samples were immunoblotted with mouse anti-FlagM2 (Table 2-4), mouse anti-IκBα (Table 2-4), and mouse anti-β-tubulin (Table 2-4).

2.10.3.3 Detection of VACV late gene expression. RK13 cells (1 x 10^6) were mock infected or infected with the indicated virus at an MOI of 5. Whole cell lysates were collected 3, 6, 9, 12 and 24 hours post-infection in 150 μL of SDS loading buffer. Samples were immunoblotted with mouse anti-E3L (Table 2-4), mouse anti-B5R (Table 2-4), rabbit anti-A34R (Table 2-4), and rabbit anti-I5L (Table 2-4).

2.10.4 Growth curves

Single-step growth curves were performed by infecting BGMK or CV-1 cells (1 x 10^6) with the indicated viruses at an MOI of 10. One hour post-infection, cells were washed with warm PBS and 2 mL of supplemented DMEM was added back to each well. Zero, 4, 8, 12, 24 and 48 hours post-infection, media and cells were harvested using SSC and centrifuged at 300 x *g* for 5 minutes. The pellet was washed with PBS, centrifuged at 300 x *g* for 5 minutes, and resuspended in 100 μL of swelling buffer. Titers were determined as described in section 2.8.5 and the data was plotted on a logarithmic scale. The experiment was performed in triplicate. Alternatively, multi-step growth curves were performed by infecting BGMK or CV-1 cells at an MOI of 0.01 and harvesting samples at 0, 12, 24, 48, and 72 hours post-infection. For multi-step growth curves, no wash step was performed 1 hour post-infection.

2.10.5 Plaque assays

Viruses were serial diluted and titred on BGMK or CV-1 cells (1 x 10^6) as described in section 2.8.5. ECTV foci were allowed to form over a period of 3 to 5 days, while VACV plaques were allowed to form over 2 to 5 days. Thirty isolated foci or plaques were photographed for each sample using an Axioscope 2 *plus* microscope (Zeiss) at a magnification of 2.5x. Foci and plaques were measured using the measure function in ImageJ (NIH). Foci and Plaque sizes were compared using GraphPad Prism version 5 and statistical significance was determined using a one-way anova with a Tukey post-test (GraphPad Software, La Jolla California USA, www.graphpad.com).

2.10.6 Nuclear and cytoplasmic extracts

HeLa cells (1 x 10^6) were mock infected or infected with the indicated viruses at an MOI of 5. Twelve hours post-infection, cells were stimulated with 10 ng/mL of TNFα or IL-1β at 37°C for 20 minutes. Following stimulation, cells were washed with PBS and collected by trypsinization. Cells were resuspended in 150 μL of cold cytoplasmic extract buffer containing 10 mM HEPES, 10 mM KCl, 0.1 mM EDTA (pH 8.0), 0.1 mM EGTA (pH 8.0), 1 mM dithiothreitol (DTT), 0.05% v/v NP-40, and EDTA-free protease inhibitor cocktail (Roche Diagnostics), and incubated at 4°C for 30 minutes on a rotator. Lysed cells were centrifuged at 1000 *x g* at 4°C for 5 minutes and the supernatant was collected and resuspended in 50 μL of 4x SDS loading buffer containing 50% v/v glycerol, 20% v/v BME, 1% v/v SDS, 312.5 mM Tris (pH 8.0), and 5 mg/mL bromophenol blue. The pellet was washed with 150 μL cold cytoplasmic extract buffer and centrifuged at 1000 *x g* at 4°C for 5 minutes before being resuspended in 50 μL of cold nuclear extract buffer containing 20 mM HEPES, 25% v/v glycerol, 0.4 M NaCl, 1 mM EDTA (pH 8.0), 1 mM EGTA (pH 8.0), 1 mM DTT, and EDTA-free protease inhibitor cocktail. The pellet was briefly vortexed, incubated on ice for 20 minutes, and centrifuged at 18000 *x g* at 4°C for 10 minutes. The supernatant was collected and resuspended

in 20 μL of 4x SDS loading buffer. Samples were immunoblotted with rabbit anti NFκB p65 (Table 2-4), mouse anti-β-tubulin (Table 2-4), mouse anti-PARP (Table 2-4), and rabbit anti-I5L (Table 2-4).

2.10.7 Flow cytometry

HeLa cells (1 x 10^6) were mock infected or infected with the indicated viruses at an MOI of 5. Twelve hours post-infection, cells were stimulated with 10 ng/mL of TNFα at 37°C for 20 minutes. Alternatively, mock-infected cells were treated with 10 μM of the proteasome inhibitor MG132 (Sigma-Aldrich) for 1 hour prior to stimulation with TNFα (5). Following stimulation, cells were washed with PBS, then fixed at 37°C for 10 minutes in 0.5% w/v paraformaldehyde in PBS and permeabilized with cold 90% methanol on ice for 30 minutes. Cells were washed twice with PBS containing 1% v/v HI-FBS, and stained for 1 hour at room temperature with mouse anti-IκBα (Table 2-4) and mouse anti-I3L (Table 2-4) diluted in 1% v/v FBS. Cells were washed twice with PBS containing 1% v/v HI-FBS and stained with phycoerythrin-conjugated goat anti-rabbit (Table 2-4) and goat anti-mouse Alexaflour488 diluted (Table 2-4) in 1% v/v HI-FBS. Data were collected using a FACSan flow cytometer (Bectin Dickinson).

2.11 REFERENCES

1. **Altschul, S. F., W. Gish, W. Miller, E. W. Myers, and D. J. Lipman.** 1990. Basic local alignment search tool. J Mol Biol **215:**403-10.
2. **Barrett, J. W., Y. Sun, S. H. Nazarian, T. A. Belsito, C. R. Brunetti, and G. McFadden.** 2006. Optimization of codon usage of poxvirus genes allows for improved transient expression in mammalian cells. Virus Genes **33:**15-26.
3. **Perkus, M. E., S. J. Goebel, S. W. Davis, G. P. Johnson, E. K. Norton, and E. Paoletti.** 1991. Deletion of 55 open reading frames from the termini of vaccinia virus. Virology **180:**406-10.
4. **Rintoul, J. L., J. Wang, D. B. Gammon, N. J. van Buuren, K. Garson, K. Jardine, M. Barry, D. H. Evans, and J. C. Bell.** 2011. A selectable and excisable marker system for the rapid creation of recombinant poxviruses. PLoS One **6:**e24643.
5. **Traenckner, E. B., S. Wilk, and P. A. Baeuerle.** 1994. A proteasome inhibitor prevents activation of NF-kappa B and stabilizes a newly phosphorylated form of I kappa B-alpha that is still bound to NF-kappa B. EMBO J **13:**5433-41.
6. **van Buuren, N., B. Couturier, Y. Xiong, and M. Barry.** 2008. Ectromelia virus encodes a novel family of F-box proteins that interact with the SCF complex. J Virol **82:**9917-27.
7. **Wilton, B. A., S. Campbell, N. Van Buuren, R. Garneau, M. Furukawa, Y. Xiong, and M. Barry.** 2008. Ectromelia virus BTB/kelch proteins, EVM150 and EVM167, interact with cullin-3-based ubiquitin ligases. Virology **374:**82-99.

Chapter 3: The Ectromelia Virus Ankyrin/F-box Proteins Inhibit the Classical NFκB Pathway

The results contained within this chapter consist of unpublished material. Experiments in this chapter were performed by K. Burles. The document was written by K. Burles with a major editorial contribution made by Dr. M. Barry.

pcDNA3-Flag-CO-ECTV002, pcDNA3-Flag-CO-ECTV002 (1-532), pcDNA3-Flag-CO-ECTV005, and pcDNA3-Flag-CO-ECTV005 (1-593), and pcDNA3-Flag-CO-ECTV165 were cloned by N. van Buuren. pcDNA3-Flag-CO-ECTV165(1-566) was cloned by M. Edwards. VACV-Flag-ECTV002, VACV-Flag-ECTV005, VACV-Flag-ECTV154, VACV-Flag-ECTV165, ECTVΔ002, and ECTVΔ005 were generated by N. van Buuren and ECTVΔ165 was generated by M. Edwards. Significant contributions to experiments presented in Figures 3-2 to 3-7 were made by N. van Buuren and M. Edwards. The final figures were constructed by K. Burles.

3.1 INTRODUCTION

During poxvirus infection, an inflammatory response is initiated by the cell, which includes activation of potent antiviral mechanisms that eliminates virus infection. There are a number of important components of antiviral defense, including the NFκB signalling pathway (12, 13, 44). Initiation of the NFκB signalling pathway can occur in response to a variety of stimuli, however, the best studied activation pathways occur through the TNFR and IL-1R (29). Both pathways are activated when pro-inflammatory cytokines, TNFα and IL-1β, respectively, engage their receptors at the cell surface, resulting in the recruitment of adapter proteins and signalling molecules to the receptors. Though the signalling cascades vary between the TNFα and IL-1β pathways, both culminate in activating the IKK complex by phosphorylation (37). Following activation, the IKK complex phosphorylates IκBα, which normally sequesters the p65-p50 NFκB transcription factor in the cytoplasm (17). Following phosphorylation, IκBα is recruited to the SCF ubiquitin ligase by the F-box protein βTrCP, where it is poly-ubiquitinated and targeted for degradation by the 26S proteasome (11, 20, 40). Left unsequestered by its inhibitor IκBα, the p65-p50 NFκB transcription factor translocates into the nucleus, where it stimulates transcription of genes involved in the antiviral response (13).

Significantly, many viruses have evolved strategies to modulate the NFκB pathway to ensure their own survival (25, 30). The *Poxviridae* are a family of large dsDNA viruses that are notorious for inhibiting the immune response and regulating cellular signalling pathways (16, 27, 34). Interestingly, a number of inhibitors of the NFκB pathway have been identified in poxviruses, especially in VACV, which is considered the prototypic poxvirus (25, 30). Activation of the NFκB pathway through the IL-1R is prevented by A52R, A46R, and K7L (2, 33). A46R binds the TIR-domain containing adapter proteins MyD88, TRIF, TIRAP, and TRAM, and prevents them from associating with the IL-1R (2, 41). A52R and K7 bind TRAF6 and IRAK2 to disrupt signalling complexes containing these

proteins (2, 8, 10, 33). The IKK complex is targeted by N1L, B14R, and K1L (3, 4, 6, 35). N1L interacts with multiple subunits of the IKK complex (6), while B14R binds specifically to IKKβ (3, 4). Phosphorylation and subsequent activation of the IKK complex is prevented by both N1L and B14R (4, 6). In contrast to N1L and B14R, K1L does not interact with components of the IKK complex, instead it is thought to inhibit unidentified kinases responsible for phosphorylating the IKK complex (35). VACV also encodes two additional proteins that inhibit NFκB activation; M2L prevents ERK2 phosphorylation and subsequent signalling to the IKK complex (7, 14), while E3L prevents NFκB activation induced by the PKR pathway, following recognition of viral double stranded RNA (28). Due to the number of inhibitors of the NFκB pathway encoded by VACV, it is obvious that preventing the antiviral response induced by NFκB is important for poxviruses.

Using a bioinformatics screen, our lab identified four Ank/F-box proteins, ECTV002, ECTV005, ECTV154, and ECTV165, in ECTV (45). The combination of multiple Ank domains in conjunction with a C-terminal F-box was unique to poxviruses (24, 38), until recently when Ank/F-box proteins were identified in the parasitoid wasp, *Nasonia* (46). Ank repeats are present in a number of cellular proteins, and mediate distinctive protein-protein interactions (22). The F-box domain is necessary for interaction with Skp1 in the SCF ubiquitin ligase, and cellular F-box proteins recruit substrates to the SCF to be ubiquitinated (19). Interestingly, each protein has variation in the number and location of the Ank repeats that it possesses, suggesting that these unique combinations may allow the four proteins to interact with different substrates (Figure 3-1). Previously, our laboratory demonstrated that ECTV002, ECTV005, ECTV154, and ECTV165 associate with the SCF ubiquitin ligase in an F-box dependent manner (45). Since degradation of IκBα is catalyzed by the $SCF^{\beta TrCP}$ ubiquitin ligase, we investigated whether the ECTV Ank/F-box proteins inhibited NFκB activation. Here, we report that ectopic expression of ECTV002, ECTV005, ECTV154, and ECTV165 inhibited TNFα and IL-1β induced NFκB activation by preventing degradation of IκBα. However, deletion of the F-box domain abrogated the ability of ECTV002, ECTV005, ECTV154, and ECTV165 to inhibit NFκB

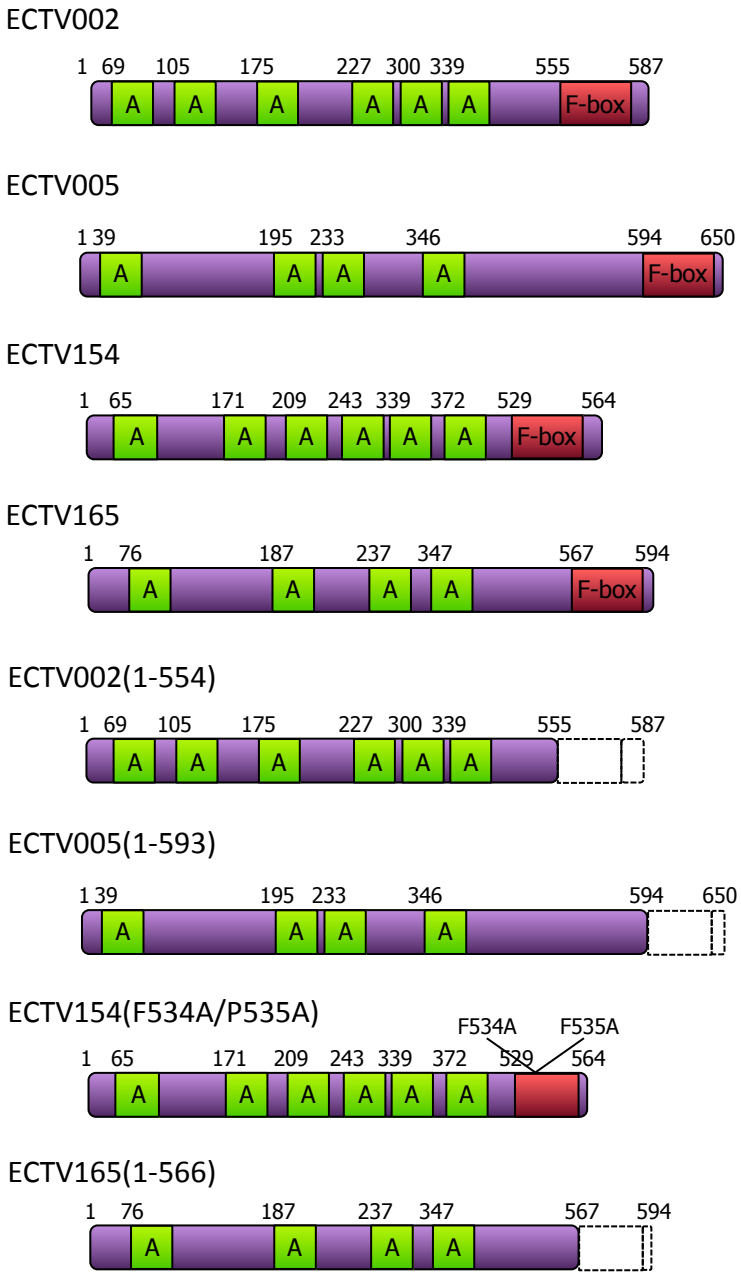

Figure 3-1. Schematic representation of the ECTV002, ECTV005, ECTV154, and ECTV165 constructs used in this study. Ectromelia virus encodes four proteins that contain an F-box domain at the C-terminus and multiple ankyrin domains throughout the C-terminus. In this study, we used codon-optimized sequences of ECTV002, ECTV005, ECTV154, and ECTV165, that were tagged with a Flag sequence at the N-terminus. The F-box deletion mutants for ECTV002, ECTV005, and ECTV165 are displayed. Since the truncation mutant for ECTV154 did not express, we used site-directed mutagenesis to mutate F534 and F535, to alanine.

activation. Additionally, our studies revealed that IκBα degradation and NFκB activation were still inhibited by ECTV, even after deletion of any of the Ank/F-box. Our results suggest that ECTV encodes four additional inhibitors of the NFκB pathway that modulate the $SCF^{\beta TrCP}$ ubiquitin ligase to prevent degradation of IκBα.

3.2 RESULTS

3.2.1 ECTV002, ECTV005, ECTV154 and ECTV165 are transcribed during virus infection

Since ECTV encodes four Ank/F-box proteins, ECTV002, ECTV005, ECTV154, and ECTV165, we wanted to verify when these genes were transcribed during infection. To do this, we used reverse transcription PCR to examine mRNA levels during infection. CV-1 cells were infected with ECTV and RNA was harvested at the indicated 4, 12, and 24 hours post-infection, and gene expression was assessed using primers specific for ECTV002, ECTV004, ECTV154, and ECTV165. As controls, we monitored transcript levels of ECTV004 and ECTV058. ECTV004 is a gene that is transcribed early during ECTV infection, while ECTV058 is transcribed late during ECTV infection (47). ECTV004 transcripts were detected at 4, 12, and 24 hours post-infection (Figure 3-2). In the presence of AraC, an inhibitor of late gene expression, ECTV004 transcripts were still detected, indicating that ECTV004 was transcribed early during infection (1, 5) (Figure 3-2). In contrast to ECTV004, ECTV058 transcripts were detected at only 12 and 24 hours post-infection, and detection was decreased in the presence of AraC, indicating that ECTV058 was transcribed late during infection (Figure 3-2). Transcripts for ECTV002, ECTV005, and ECTV165 were detected at 4, 12, and 24 hours post infection, while ECTV154 was not detected until 12 hours post-infection (Figure 3-2). Upon AraC treatment, transcripts for ECTV002, ECTV005, and ECTV165 were still detected, while transcripts for ECTV154 were no longer detected, indicating that ECTV154 was a late gene. Overall, the data indicated that ECTV002, ECTV005, and ECTV165 are transcribed early during infection, while ECTV154 is transcribed late during infection.

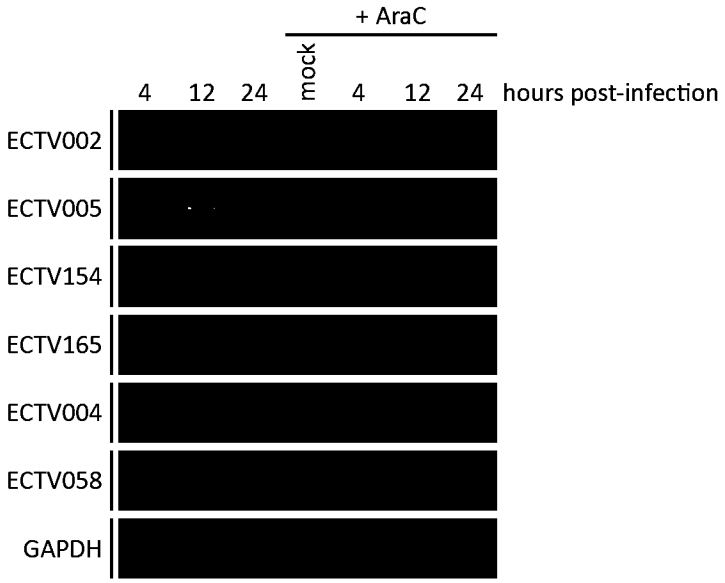

Figure 3-2. ECTV002, ECTV005, and ECTV165 are transcribed early during infection and ECTV154 is transcribed late. CV-1 cells were infected with ECTV at an MOI of 5 in the absence or presence of 80 μg/mL cytosine arabinoside (AraC). RNA was harvested at 4, 12, and 24 hours post-infection and gene transcription was assessed using gene-specific primers for ECTV002, ECTV005, ECTV154 and ECTV165. ECTV004 was used as a control for early gene transcription, ECTV058 was used as a control for late gene transcription, and GAPDH was used as a loading control.

3.2.2 ECTV002, ECTV005, ECTV154 and ECTV165 inhibit NFκB p65 nuclear translocation

Upon NFκB activation, phosphorylated IκBα is ubiquitinated by the $SCF^{\beta TrCP}$ ubiquitin ligase, resulting in the degradation of IκBα (11, 20, 40). Degradation of IκBα is crucial for translocation of NFκB into the nucleus. Since we have previously demonstrated that the four ECTV Ank/F-box proteins associate with the SCF ubiquitin ligase that regulates the NFκB pathway (45), we wanted to determine if ECTV002, ECTV005, ECTV154, or ECTV165 could inhibit activation of the NFκB pathway. To do this, we used immunofluorescence microscopy to visualize the localization of the NFκB subunit p65 (Figure 3-3). HeLa cells were mock transfected or transfected with pcDNA3-Flag-CO-ECTV002, pcDNA3-Flag-CO-ECTV005, pcDNA3-Flag-CO-ECTV154, or pcDNA3-Flag-CO-ECTV165. Twelve hours post-transfection, cells were stimulated with TNFα. Nuclei were detected with DAPI, and transfected cells were detected using an antibody for Flag. Staining with an antibody to NFκB p65 revealed that p65 was dispersed throughout the cytoplasm in mock-transfected cells (Figure 3-3, panels a-d), whereas mock-transfected cells treated with TNFα displayed dramatic accumulation of p65 in the nucleus (32, 33) (Figure 3-3, panels e-h). In contrast, cells expressing ECTV002, ECTV005, ECTV154, or ECTV165 stimulated with TNFα showed retention of p65 in cytoplasm (Figure 3-3, panels i-x). The experiment was repeated using IL-1β to stimulate the cells. Mock-transfected cells that were stimulated with IL-1β displayed nuclear localization of p65 (Figure 3-4, panels e-h), while p65 remained in the cytoplasm of cells transfected with the Ank/F-box proteins (Figure 3-4, panels i-x). To quantify the percentage of cells displaying p65 nuclear translocation, experiments were performed in triplicate, and p65 nuclear translocation was quantified by counting greater than 150 cells (Figure 3-5). Approximately 90% of cells stimulated with TNFα or IL-1β displayed nuclear accumulation of p65 (Figure 3-5). In cells transfected with the ECTV Ank/F-box proteins, p65 accumulated in the nuclei of between 5% and 35% of cells treated with TNFα or IL-1β. Overall, the data indicated that ECTV002, ECTV005, ECTV154, and ECTV165 inhibit NFκB activation stimulated by TNFα or IL-1β.

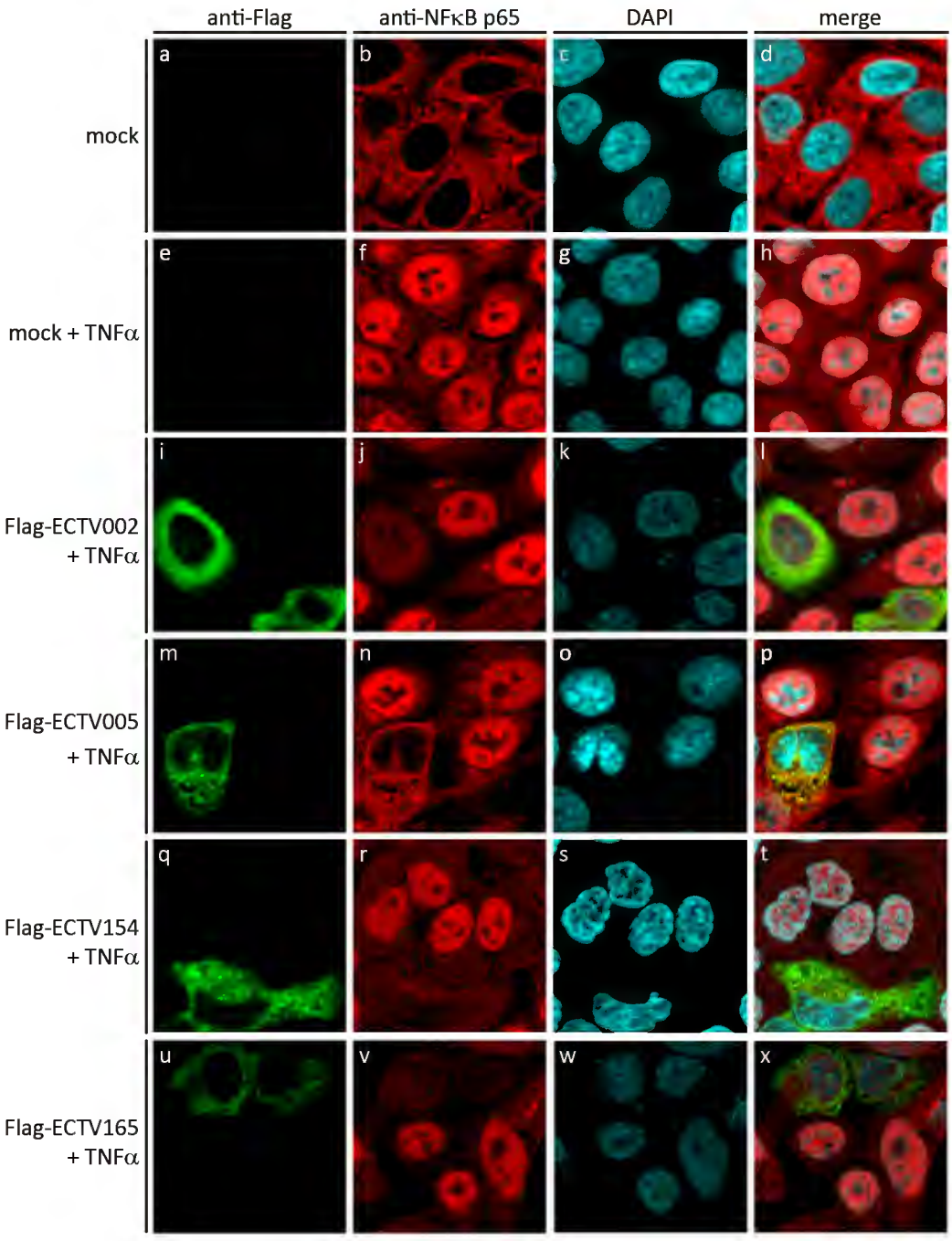

Figure 3-3. Expression of ECTV002, ECTV005, ECTV154, and ECTV165 prevent TNFα-induced NFκB p65 nuclear translocation. HeLa cells were mock transfected (a-h) or transfected with pcDNA3-Flag-CO-ECTV002 (i-l), pcDNA3-Flag-CO-ECTV005 (m-p), pcDNA3-Flag-CO-ECTV154 (q-t), or pcDNA3-Flag-CO-ECTV165 (u-x). Twelve hours post-transfection, cells were mock stimulated (a-d) or stimulated with 10 ng/mL of TNFα for 20 minutes (e-x). Endogenous p65 was detected with an antibody specific for p65, and nuclei were

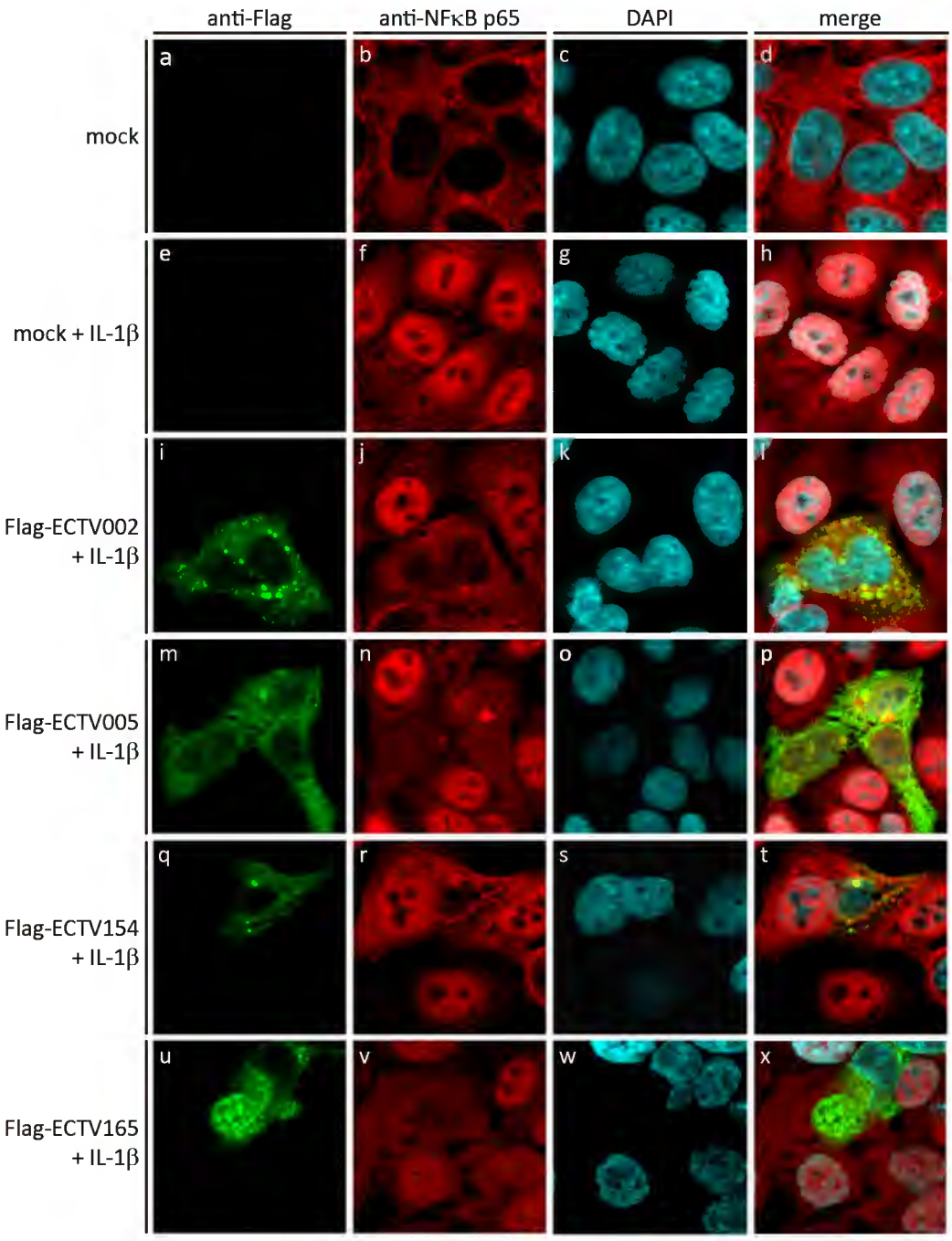

Figure 3-4. Expression of EVM002, EVM005, EVM154, and EVM165 prevent IL-1β-induced NFκB p65 nuclear translocation. HeLa cells were mock transfected (a-h) or transfected with pcDNA3-Flag-CO-ECTV002 (i-l), pcDNA3-Flag-CO-ECTV005 (m-p), pcDNA3-Flag-CO-ECTV154 (q-t), or pcDNA3-Flag-CO-ECTV165 (u-x). Twelve hours post-transfection, cells were mock stimulated (a-d) or stimulated with 10 ng/uL of IL-1β for 20 minutes (e-x). Endogenous p65 was detected with an antibody specific for p65, and nuclei were

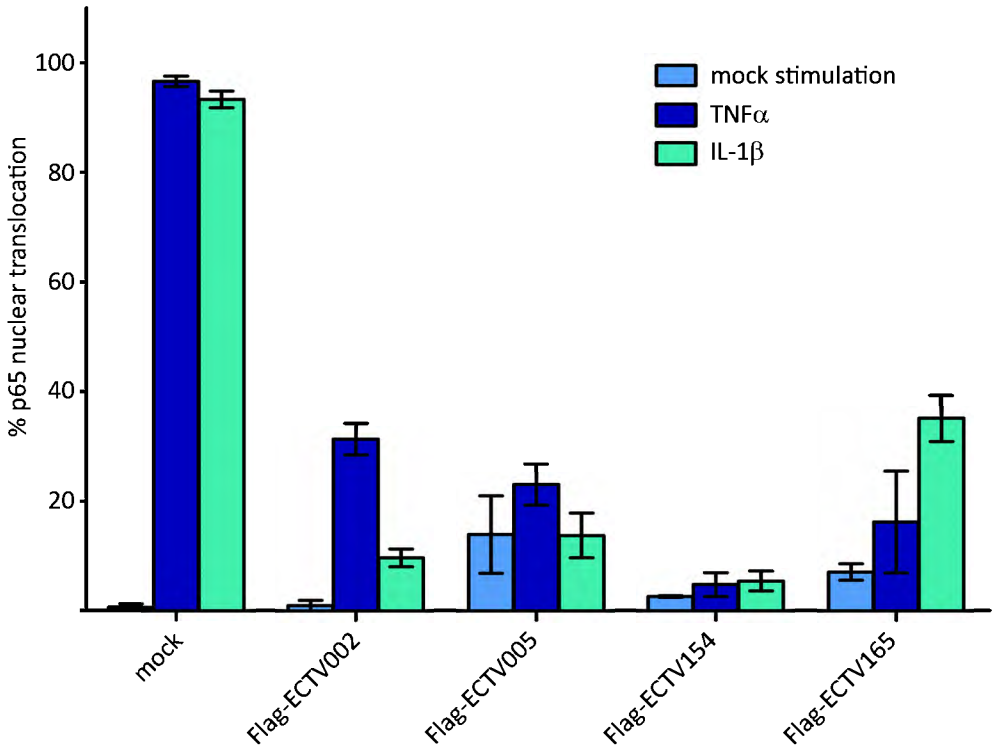

Figure 3-5. ECTV Ank/F-box proteins inhibit NFκB p65 nuclear translocation. To quantify NFκB p65 nuclear translocation, a total of 150 transfected cells were counted from three independent experiments and the percentage of cells exhibiting NFκB p65 in the nucleus was calculated.

3.2.3 Inhibition of NFκB activation is dependent on the F-box domain

Since association of the ECTV Ank/F-box proteins is dependent on the F-box domain (45), we wanted to determine if inhibition of NFκB by the ECTV Ank/F-box proteins is dependant on the F-box domain. To do this, we used mutants of ECTV002, ECTV005, and ECTV165 that are missing the F-box domain, or in the case of ECTV154, are mutated in the F-box domain (Figure 3-1), and are unable to interact with the SCF ubiquitin ligase (45). We repeated the immunofluorescence assay, and transfected HeLa cells with pcDNA3-Flag-CO-ECTV002(1-554), pcDNA3-Flag-CO-ECTV005(1-593), pcDNA3-Flag-CO-ECTV154(F534A/P535A), or pcDNA3-Flag-CO-ECTV165(1-566). Twelve hours post-transfection, cells were stimulated with TNFα or IL-1β. Nuclei were detected with DAPI, and transfected cells were detected using an antibody for Flag. Staining with an antibody to NFκB p65 revealed that, in contrast to cells expressing full-length ECTV002, ECTV005, ECTV154, or ECTV165, cells expressing ECTV002(1-554), ECTV005(1-593), ECTV154(F534A/P535A), or ECTV165(1-566) displayed p65 nuclear translocation following stimulation with TNFα and IL-1β (Figure 3-6, Figure 3-7). These data were quantified by performing the experiments in triplicate and counting cells that contained p65 in the nucleus. (Figure 3-8). The percentage of cells transfected with ECTV002(1-532), ECTV005(1-593), or ECTV165(1-566) that contained p65 in the nucleus was similar to that of stimulated mock-transfected cells, while the percentage of cells transfected with ECTV154(F534A/P535A) containing p65 in the nucleus was slightly less (Figure 3-8). Taken together, these data indicated that the F-box is important for the ability of the ECTV Ank/F-box proteins to inhibit the classical NFκB pathway.

3.2.4 The ECTV Ank/F-box proteins do not target p50 or p65 for degradation

Since we hypothesized that the ECTV Ank/F-box proteins act as substrate adapters, we wanted to determine if ECTV002, ECTV005, ECTV154, or ECTV165 target important components of the NFκB signalling cascade for degradation. We focused on components downstream of the IKK complex, since the ECTV Ank/F-box proteins inhibited NFκB activation when cells were stimulated with either TNFα or IL1β (Figure 3-

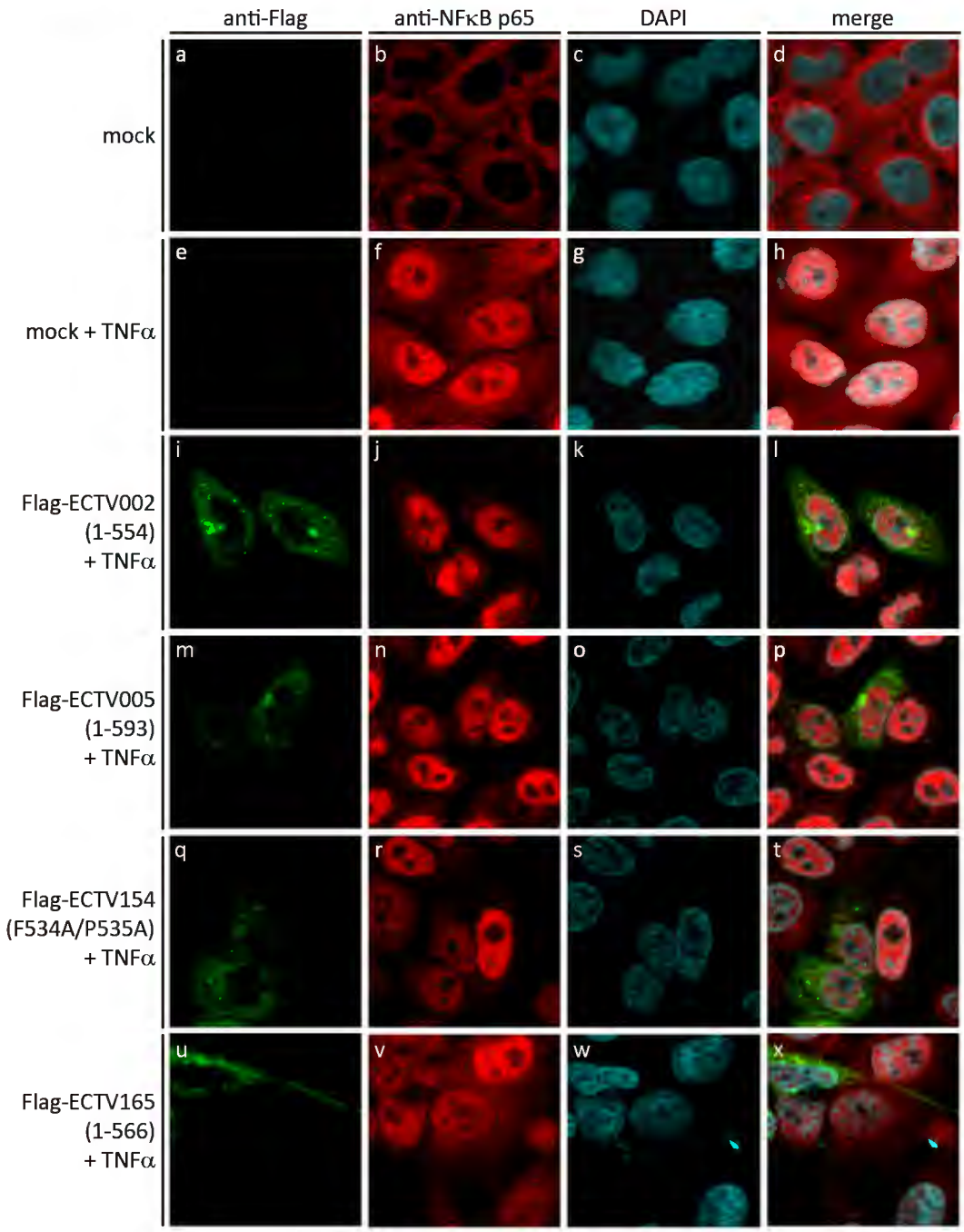

Figure 3-6. ECTV002, ECTV005, ECTV154, and ECTV165 devoid of the F-box do not prevent TNfα-induced NFκB p65 nuclear translocation. HeLa cells were mock transfected (a-h) or transfected with pcDNA3-Flag-CO-ECTV002(1-554) (i-l), pcDNA3-Flag-CO-ECTV005(1-593 (m-p), pcDNA3-Flag-CO-ECTV154(F534A/P535A) (q-t), or pcDNA3-Flag-CO-ECTV165(1-566) (u-x). Twelve hours post-transfection, cells were mock stimulated (a-d) or stimulated with 10 ng/mL of TNFα for 20 minutes (e-x). Endogenous p65 was detected with an antibody specific for p65, and nuclei were detected with DAPI.

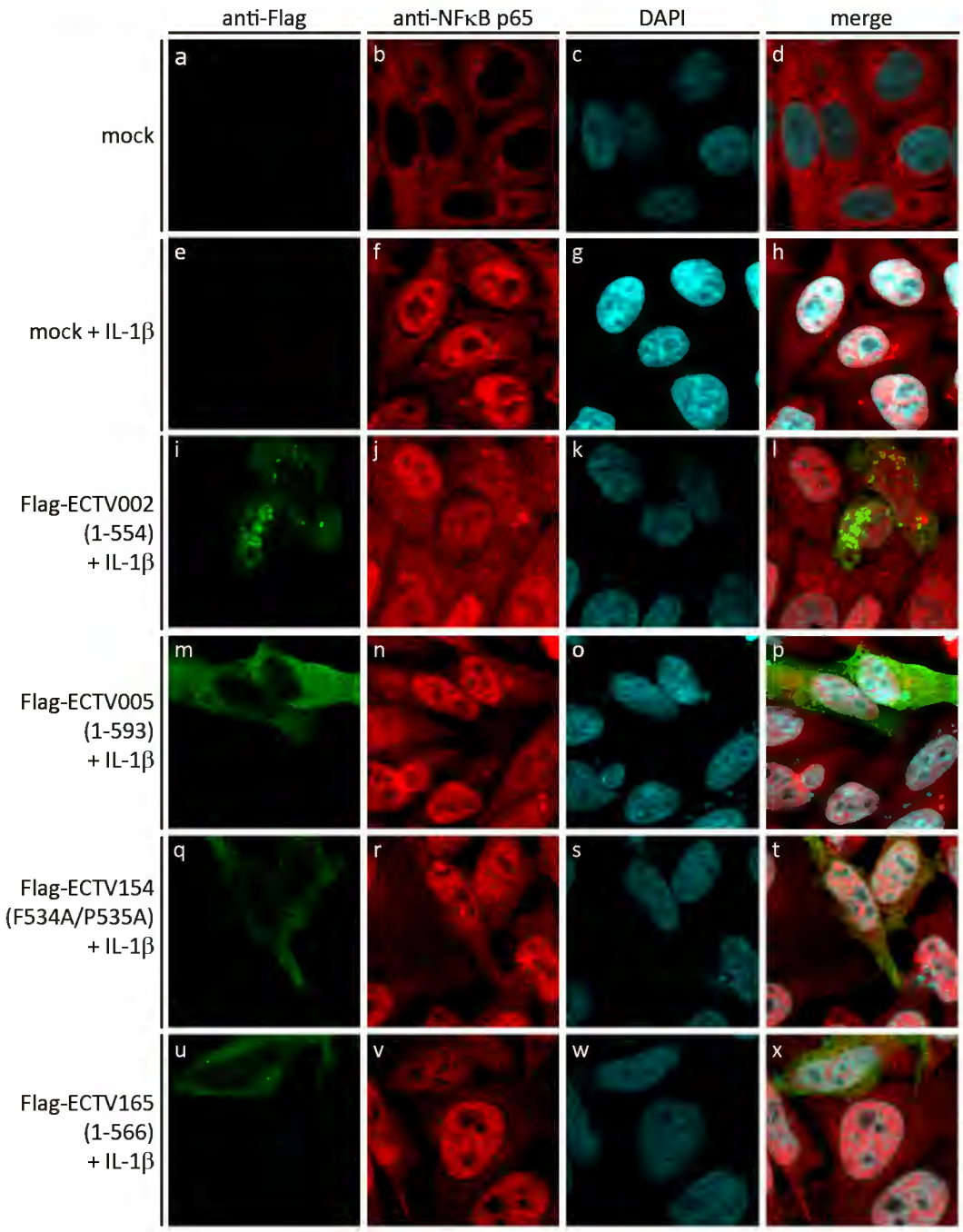

Figure 3-7. ECTV002, ECTV005, ECTV154, and ECTV165 devoid of the F-box do not prevent IL-1β-induced NFκB p65 nuclear translocation. HeLa cells were mock transfected (a-h) or transfected with pcDNA3-Flag-CO-ECTV002(1-554) (i-l), pcDNA3-Flag-CO-ECTV005(1-593 (m-p), pcDNA3-Flag-CO-ECTV154(F534A/P535A) (q-t), or pcDNA3-Flag-CO-ECTV165(1-566) (u-x). Twelve hours post-transfection, cells were mock stimulated (a-d) or stimulated with 10 ng/mL of IL-1β for 20 minutes (e-x). Endogenous p65 was detected with an antibody specific for p65, and nuclei were detected with DAPI.

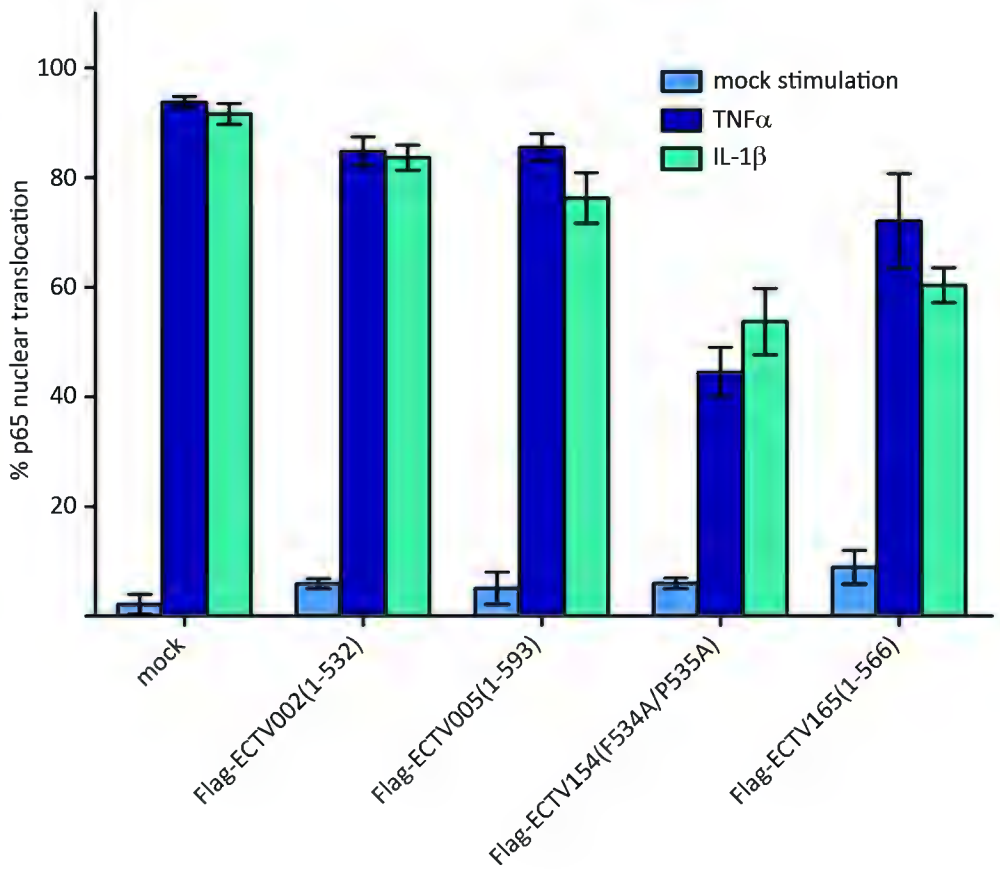

Figure 3-8. Inhibition of NFκB p65 nuclear translocation by ECTV Ank/F-box proteins is dependent on the F-box domain. To quantify NFκB p65 nuclear translocation, a total of 150 transfected cells were counted from three independent experiments and the percentage of cells exhibiting NFκB p65 in the nucleus was calculated.

3 and 3-4). Since phosphorylated IκBα accumulated in cells infected with ECTV, we focused on components of the NFκB dimer, p50 and p65. In order to determine if ECTV002, ECTV005, ECTV154, or ECTV165 facilitate degradation of p50 or p65, we used immunoblotting to monitor levels of these proteins following infection (Figure 3-9). HeLa cells were infected with VACV65 or the recombinant viruses, VACV-Flag-ECTV002, VACV-Flag-ECTV005, VACV-Flag-ECTV154, or VACV-Flag-ECTV165, and whole cell lysates were harvested at 0, 4, 8, 12, 16, and 24 hours post-infection. Changes in levels of p50 and p65 were detected by immunoblotting with antibodies specific for NFκB p50 and NFκB p65. We also immunoblotted for Flag to detect expression of the ECTV Ank/F-box proteins, and β-tubulin and IκBα as loading controls. Not surprisingly, no Flag-accumulation was observed in cells infected with VACV65, since no Flag-tagged proteins were expressed (Figure 3-9). Additionally, levels of p50, p65, and IκBα remained constant in cells infected with VACV65 (Figure 3-9). In contrast, increasing levels of Flag expression were observed over time in cells that were infected with VACV-Flag-ECTV002, VACV-Flag-ECTV005, VACV-Flag-ECTV154, or VACV-Flag-ECTV165, indicating that the proteins were expressed during infection (Figure 3-9). However levels of p50, p65, and IκBα remained constant, indicating that expression of ECTV002, ECTV005, ECTV154, or ECTV165 did not result in degradation of these proteins. The data demonstrated that the ECTV Ank/F-box proteins do not target p50, p65, or IκBα for degradation.

3.2.5 The ECTV Ank/F-box proteins prevent degradation of IκBα

Since ECTV002, ECTV005, ECTV154, and ECTV165 interact with the SCF ubiquitin ligase, we wanted to determine if the ECTV Ank/F-box proteins inhibit IκBα degradation. To do this, we used immunofluorescence microscopy to visualize levels of IκBα in the cell (Figure 3-10). HeLa cells were mock transfected or transfected with pcDNA3-Flag-CO-ECTV002, pcDNA3-Flag-CO-ECTV005, pcDNA3-Flag-CO-ECTV154, or pcDNA3-Flag-CO-ECTV165. Twelve hours post-transfection, cells were stimulated with TNFα. Nuclei were detected with DAPI, and transfected cells were detected using an antibody for Flag.

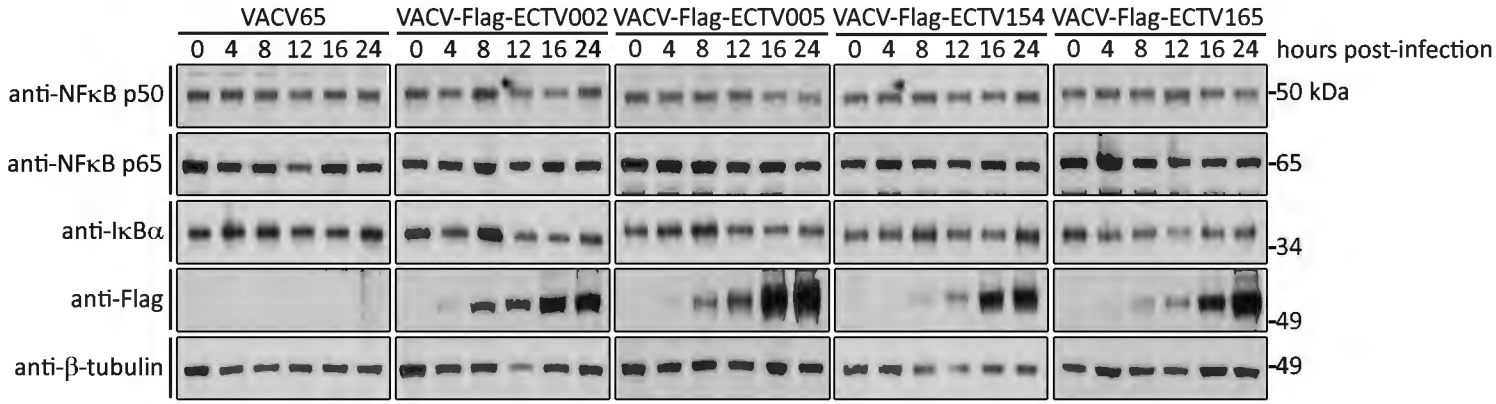

Figure 3-9. ECTV002, ECTV005, ECTV154, and ECTV165 do not degrade NFκB p50, NFκB p65, or IκBα. HeLa cells were infected at an MOI of 5 with VACV65, VACV-Flag-EVM002, VACV-Flag-EVM005, VACV-Flag-EVM154, or VACV-Flag-EVM165. Infected cell lysates were harvested at 0, 4, 8, 12, 16, and 24 hours post-infection and immunoblotted with antibodies specific for NFκB p50, NFκB p65, and IκBα. Infected cell lysates were also immunoblotted with an antibody specific for Flag as a control for expression of the Flag-tagged proteins, and an antibody specific for β-tubulin as a loading control.

Staining with an antibody to IκBα revealed that IκBα was expressed at high levels in the cytoplasm of mock-transfected cells (Figure 3-10, panels a-d), whereas mock-transfected cells treated with TNFα displayed dramatic loss of IκBα (Figure 3-10, panels e-h). In contrast, cells expressing Flag-ECTV002, Flag-ECTV005, Flag-ECTV154, or Flag-ECTV165 stimulated with TNFα showed retention of IκBα (Figure 3-10, panels i-x). Overall, these data indicated that ECTV002, ECTV005, ECTV154, and ECTV165 inhibit IκBα degradation when cells are stimulated with TNFα.

To further demonstrate that the ECTV Ank/F-box proteins stabilize IκBα during activation of the NFκB pathway, we used immunoblotting to monitor levels of IκBα following transfection with increasing amounts of ECTV002, ECTV005, ECTV154, or ECTV165 (Figure 3-11). HeLa cells were mock transfected or transfected with 0.25 μg, 0.75 μg, 1.5 μg, or 3 μg of pcDNA3-Flag-CO-ECTV002, pcDNA3-Flag-CO-ECTV005, pcDNA3-Flag-CO-ECTV154, or pcDNA3-Flag-CO-ECTV165. Twelve hours post-transfection, cells were stimulated with TNFα. Whole cells lysates were collected and immunobloted to detect changes in levels of IκBα. In mock-transfected cells, high levels of IκBα were observed (Figure 3-11). However, levels of IκBα were significantly reduced following stimulation with TNFα, indicating that IκBα was being degraded as a result of NFκB activation (Figure 3-11). In transfected cells, increased levels of Flag expression were observed, corresponding to the increasing amounts of pcDNA3-Flag-ECTV002, pcDNA3-Flag-ECTV005, pcDNA3-Flag-ECTV154, or pcDNA3-Flag-ECTV165 that were transfected. Interestingly, when cells were transfected with higher amounts of plasmid (3 μg), increased levels of IκBα were observed following TNFα stimulation, demonstrating that expression of the Ank/F-box proteins could prevent degradation of IκBα (Figure 3-11). Together, these data indicate that ECTV002, ECTV005, ECTV154, and ECTV165 inhibited degradation of IκBα during activation of the NFκB pathway.

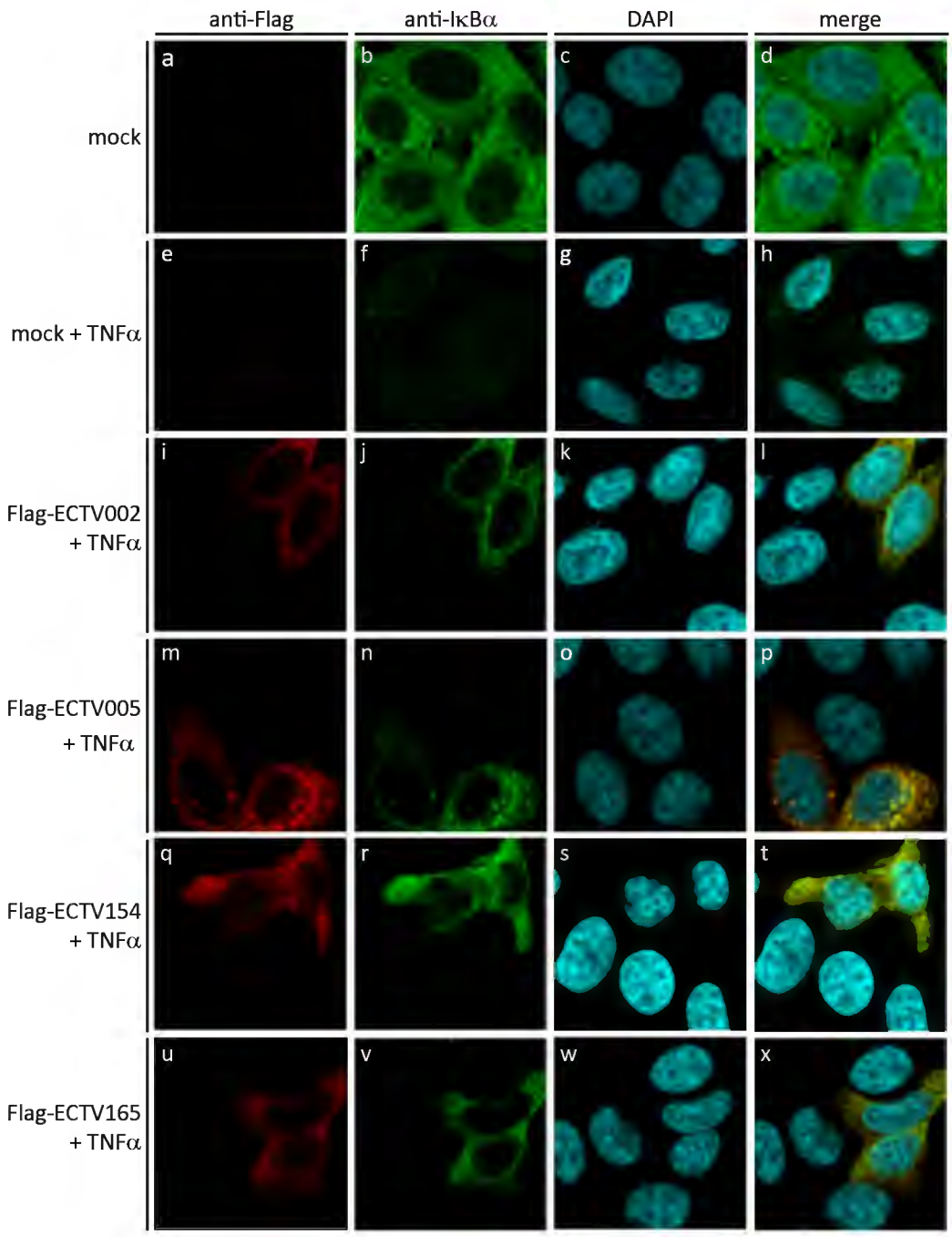

Figure 3-10. Expression of ECTV002, ECTV005, ECTV154, and ECTV165 prevent TNFα-induced IκBα degradation. HeLa cells were mock transfected (a-h) or transfected with pcDNA3-Flag-CO-ECTV002 (i-l), pcDNA3-Flag-CO-ECTV005 (m-p), pcDNA3-Flag-CO-ECTV154 (q-t), or pcDNA3-Flag-CO-ECTV165 (u-x). Twelve hours post-transfection, cells were mock stimulated (a-d) or stimulated with 10 ng/mL of TNFα for 20 minutes (e-x). Endogenous IκBα was detected with an antibody specific for IκBα, and nuclei were detected with DAPI.

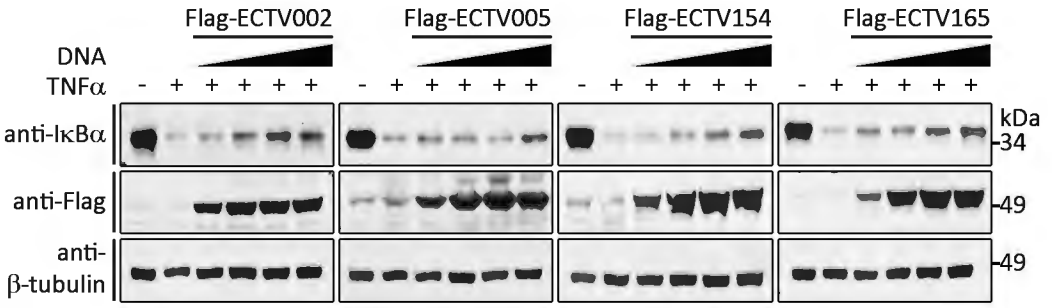

Figure 3-11. Expression of ECTV002, ECTV005, ECTV154, and ECTV165 prevent TNFα-induced IκBα degradation. HeLa cells were mock transfected or transfected with pcDNA3-Flag-CO-ECTV002, pcDNA3-Flag-CO-ECTV005, pcDNA3-Flag-CO-ECTV154, or pcDNA3-Flag-CO-ECTV165. Twelve hours post-transfection, cells were mock stimulated or stimulated with 10 ng/mL of TNFα for 20 minutes. Whole cell lysates were collected and immunoblotted for endogenous IκBα, Flag as a control for expression of the Flag-tagged proteins, and β-tubulin as a loading control.

3.2.6 Characterization of knockout virus growth properties

In order to understand the function of the Ank/F-box proteins in the context of virus infection, we generated four deletion viruses, ECTVΔ002, ECTVΔ005, ECTVΔ154, and ECTVΔ165, each devoid of a single ECTV Ank/F-box protein. We used a novel selectable and excisable marker system that relies on the Cre recombinase to delete ORFs of interest (31) (Figure 2-2). Since we suspected that the ECTV Ank/F-box proteins might contribute to virulence, we sought to determine if knocking out a single gene affected growth of ECTV in tissue culture, by performing a single-step growth curve. The knockout viruses replicated at levels comparable to wildtype ECTV in BGMK cells (Figure 3-12). Interestingly, when determining viral titers, we noticed a slight variation in the sizes of plaque produced by the different viruses. To determine if any of these differences were significant, we used a plaque assay to compare foci (Figure 3-13). BGMK cells were infected with the viruses and foci were photographed at the indicated times post-infection. There were no distinguishable differences in foci size at 3 days post-infection, however plaques formed by viruses devoid of ECTV002 or ECTV154 were smaller following 4 days of infection (Figure 3-13). Using computer analysis we measured the foci, and statistical testing revealed that the differences in foci size between ECTV and ECTVΔ002, and ECTV and ECTVΔ154 were significant 4 days post-infection, with a p-value of < 0.001 (Figure 3-14). Interestingly, the differences in foci size were not significant 5 days post-infection, with the exception of differences between ECTV and ECTVΔ154, though the p-value, < 0.01, was less significant in that case (Figure 3-14).

There are a few different cell lines that are used to propagate ECTV, including BGMK, VERO, BSC-1, and CV-1 cells. Interestingly, virus yields are lower when ECTV is propagated in BSC-1 or CV-1 cells (J. Schriewer and M. Buller, personal communication). To determine if the knockout viruses were defective for replication in a cell line that yields lower titers of ECTV, we used CV-1 cells and repeated the single-step growth curve described above (Figure 3-15). CV-1 cells were used instead of BSC-1 cells,

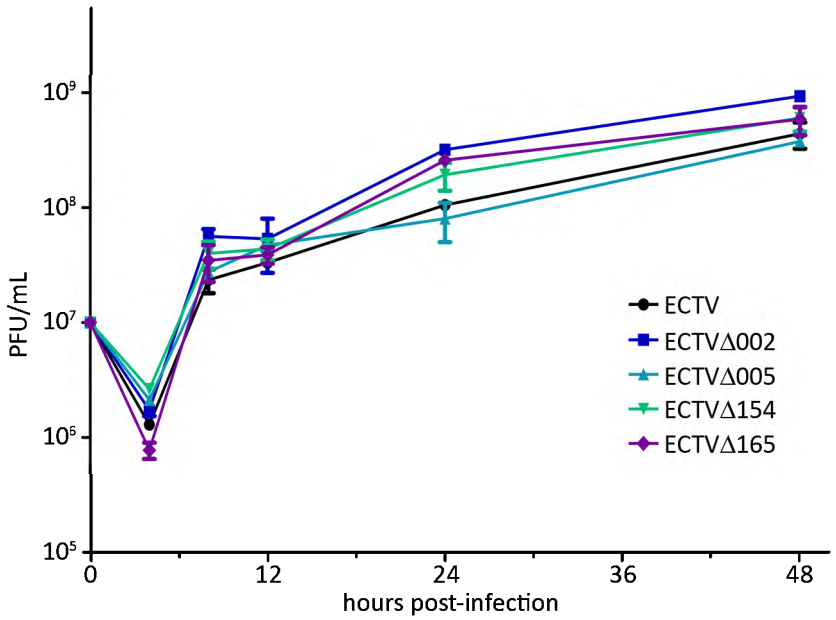

Figure 3-12. Single-step analysis of virus growth in BGMK cells indicates that ECTV devoid of ECTV002, ECTV005, ECTV154, or ECTV165 grow as well as wildtype ECTV. BGMK cells were infected at an MOI of 10 with ECTV, ECTVΔ002, ECTVΔ005, ECTVΔ154, or ECTVΔ165 for single-step growth analysis. Infected cells were harvested up to 48 hours post-infection and lysed to release infectious virus. Serial dilutions of infectious virus were plated on BGMK cells. Infected monolayers were fixed and stained with crystal violet and plaques were counted to generate a single-step growth curve. Representative of three independent experiments with double titrations.

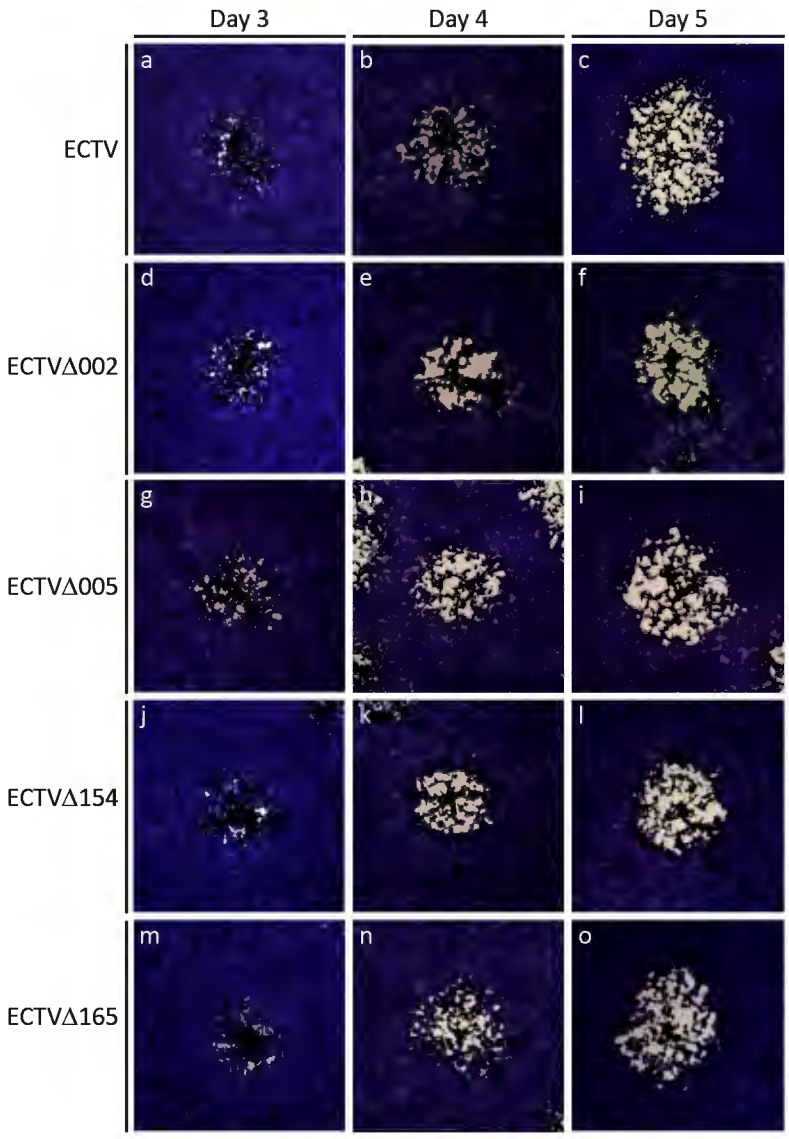

Figure 3-13. ECTV, ECTVΔ002, ECTVΔ005, ECTVΔ154, and ECTVΔ165 produce foci in BGMK cells. BGMK cells were infected with ECTV (a-c), ECTVΔ002 (d-f), ECTVΔ005 (g-i), ECTVΔ154 (j-l), or ECTVΔ165 (q-o). Cells were stained with crystal violet at 3 days (a, d, g, j, q), 4 days (b, e, h, k, n), or 5 days post-infection (c, f, i, l, o).

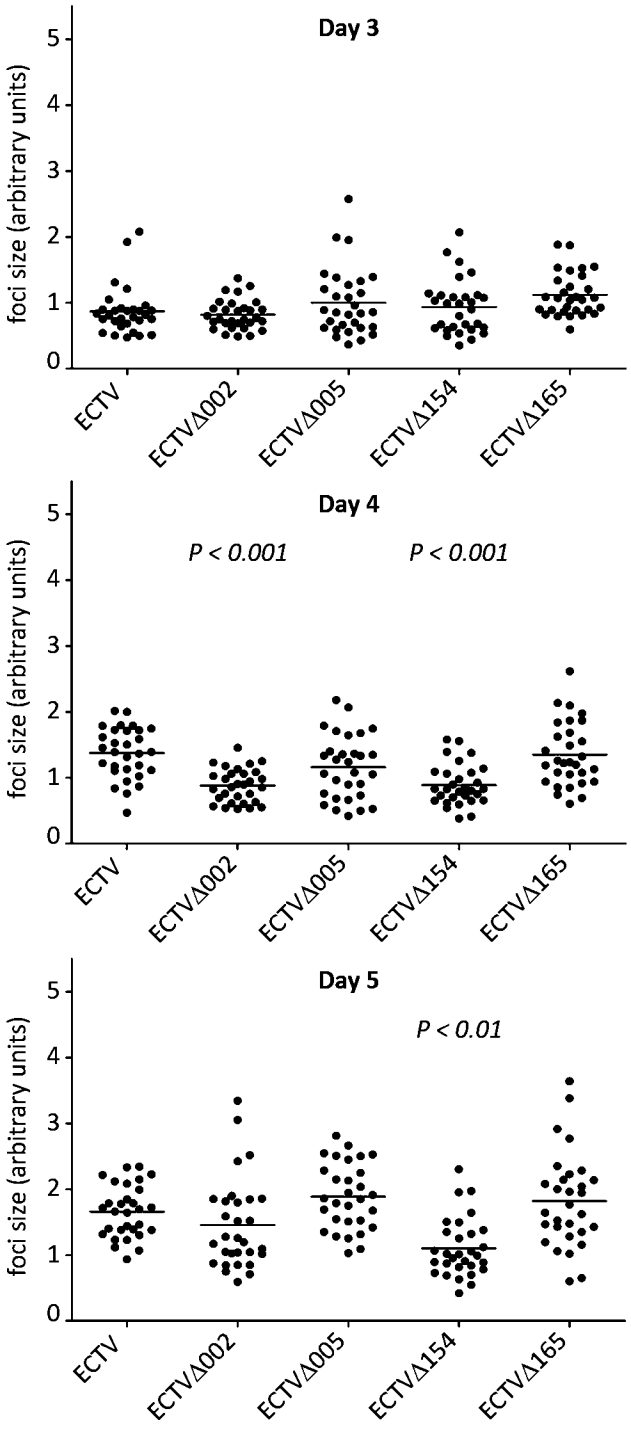

Figure 3-14. Comparison of ECTV, ECTVΔ002, ECTVΔ005, ECTVΔ154, and ECTVΔ165 foci in BGMK cells. BGMK cells were infected and stained with crystal violet 3, 4, or 5 days post-infection. Photographed foci were measured using ImageJ and analyzed using GraphPad to determine significant differences in foci size between ECTV and the knockout viruses. Any significant differences between ECTV and the knockout viruses are listed above the knockout virus.

because BSC-1 cells were not available to us. Similarly to BGMK cells, the knockout viruses replicated to comparable levels to wildtype ECTV in CV-1 (Figure 3-15). Strikingly, when determining viral titers, we noticed a visible difference in the sizes of foci produced by the different viruses. We repeated the plaque assay described above, and CV-1 cells were infected with ECTVΔ002, ECTVΔ005, ECTVΔ154, or ECTVΔ165, and foci were photographed at the indicated times post-infection. Again, we observed visible differences in foci size between ECTV and ECVTΔ002, and ECTV and ECVTΔ154, and no differences between ECTV and the ECTV devoid of ECTV005 or ECTV165 (Figure 3-16). Statistical analyses revealed that the differences in foci size between ECTV and ECVTΔ002, and ECTV and ECVTΔ154 were significant at all days post-infection, with p-values of *<0.001* at all times, indicating that ECVTΔ002 and ECVTΔ154 exhibited defects in virion release or spread in CV-1 cells (Figure 3-17). To confirm the defect in release or spread, we performed a multiple-step growth curve. Surprisingly, the knockout viruses replicated at comparable levels to wildtype ECTV (Figure 3-18). Together, these data indicated that loss of a single ECTV Ank/F-box protein does not affect growth kinetics of ECTV in tissue culture. Though, loss of ECTV002 or ECTV154 could limit foci size.

3.2.7 Knockout viruses inhibit NFκB p65 nuclear translocation

Poxviruses encode many inhibitors of the NFκB pathway (25, 30), however ECTV is missing a few of these inhibitors, including A52R, K7L, B14R, and M2L (2, 7, 14, 33). Since we demonstrated that ECTV002, ECTV005, ECTV154, and ECTV165 inhibited classical activation of the NFκB pathway (Figures 3-3 and 3-4), we wanted to determine if loss of ECTV002, ECTV005, ECTV154, or ECTV165 decreased the ability of ECTV to inhibit the NFκB pathway. To do this, we used immunofluorescence microscopy to visualize the localization of the NFκB subunit p65 (Figure 3-19). HeLa cells were mock infected or infected with ECTV, ECTVΔ002, ECTVΔ005, ECTVΔ154, or ECTVΔ165. Twelve hours post-infection, cells were stimulated with TNFα. Cells were stained with DAPI to visualize nuclei and the DNA-rich virus factories surrounding the nucleus, indicating infected cells. Staining with an antibody to NFκB p65 revealed that p65 was dispersed

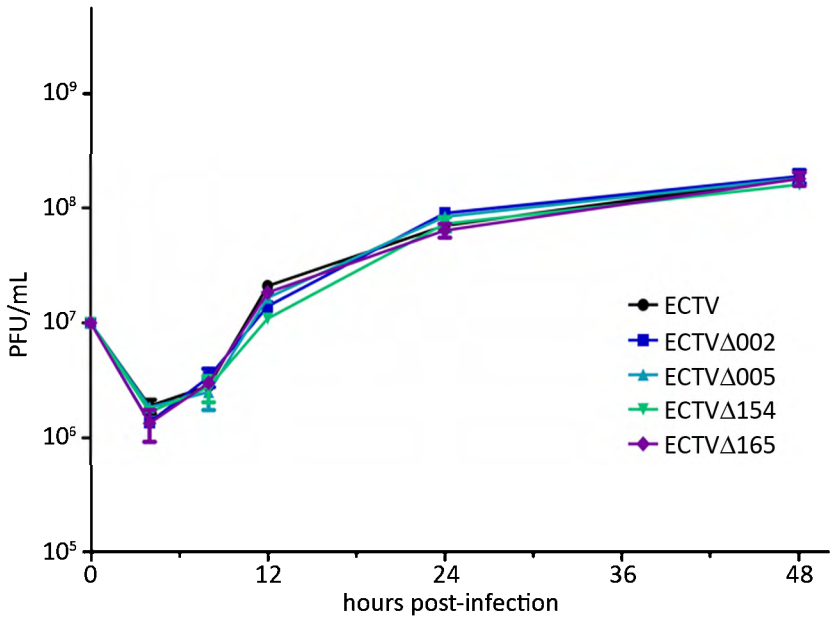

Figure 3-15. Single-step analysis of virus growth in CV-1 cells indicates that ECTV devoid of ECTV002, ECTV005, ECTV154, or ECTV165 grow as well as wildtype ECTV. CV-1 cells were infected at an MOI of 10 with ECTV, ECTVΔ002, ECTVΔ005, ECTVΔ154, or ECTVΔ165 for single-step growth analysis. Infected cells were harvested up to 48 hours post-infection and lysed to release infectious virus. Serial dilutions of infectious virus were plated on CV-1 cells. Infected monolayers were fixed and stained with crystal violet and plaques were counted to generate a single-step growth curve. Representative of three independent experiments with double titrations.

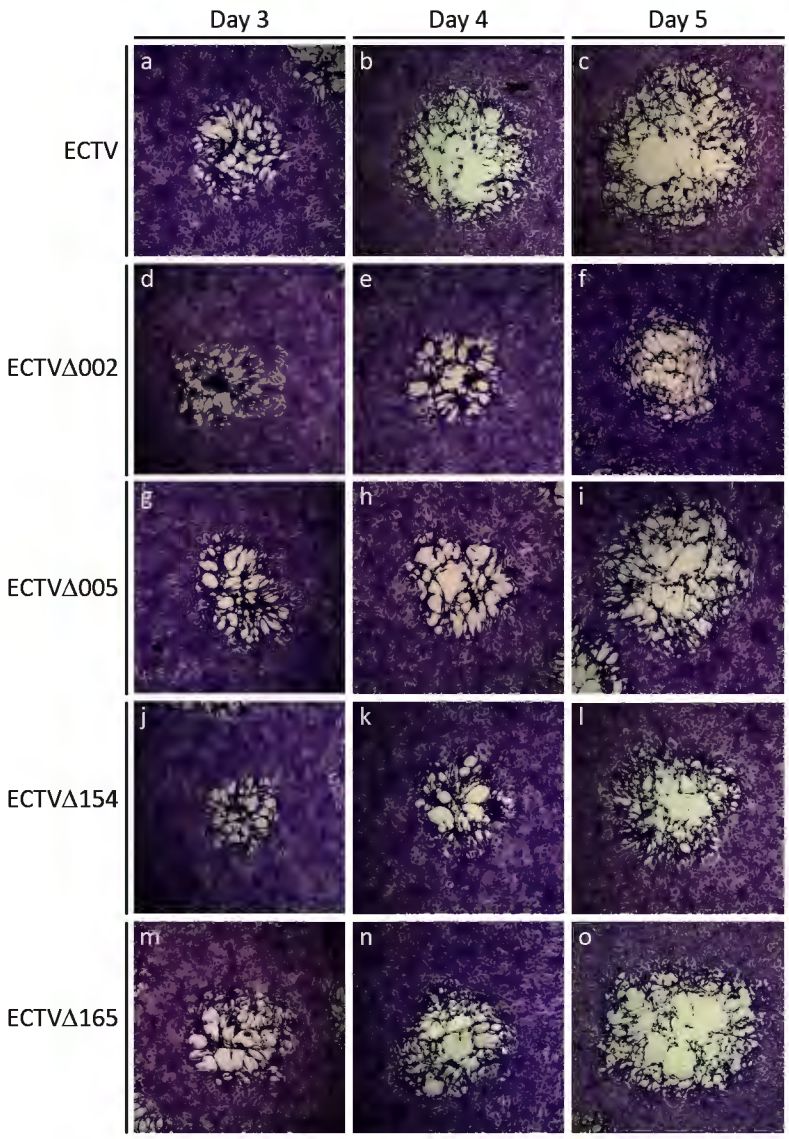

Figure 3-16. ECTV, ECTVΔ002, ECTVΔ005, ECTVΔ154, and ECTVΔ165 produce foci in CV-1 cells. CV-1 cells were infected with ECTV (a-c), ECTVΔ002 (d-f), ECTVΔ005 (g-i), ECTVΔ154 (j-l), or ECTVΔ165 (q-o). Cells were stained with crystal violet at 3 days (a, d, g, j, q), 4 days (b, e, h, k, n), or 5 days post-infection (c, f, i, l, o).

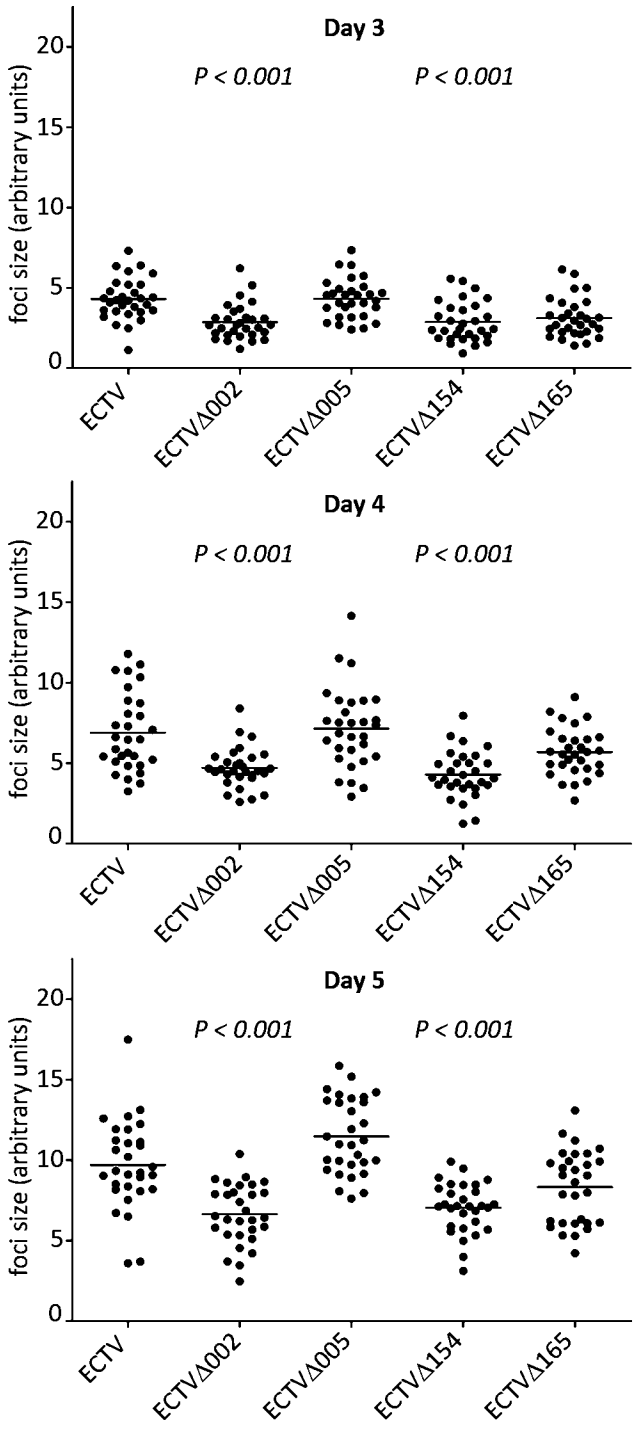

Figure 3-17. Comparison of ECTV, ECTVΔ002, ECTVΔ005, ECTVΔ154, and ECTVΔ165 foci in CV-1 cells. CV-1 cells were infected and stained with crystal violet 3, 4, or 5 days post-infection. Photographed foci were measured using ImageJ and analyzed uaing GraphPad to determine significant differences in foci size between ECTV and the knockout viruses. Any significant differences between ECTV and the knockout viruses are listed above the knockout virus.

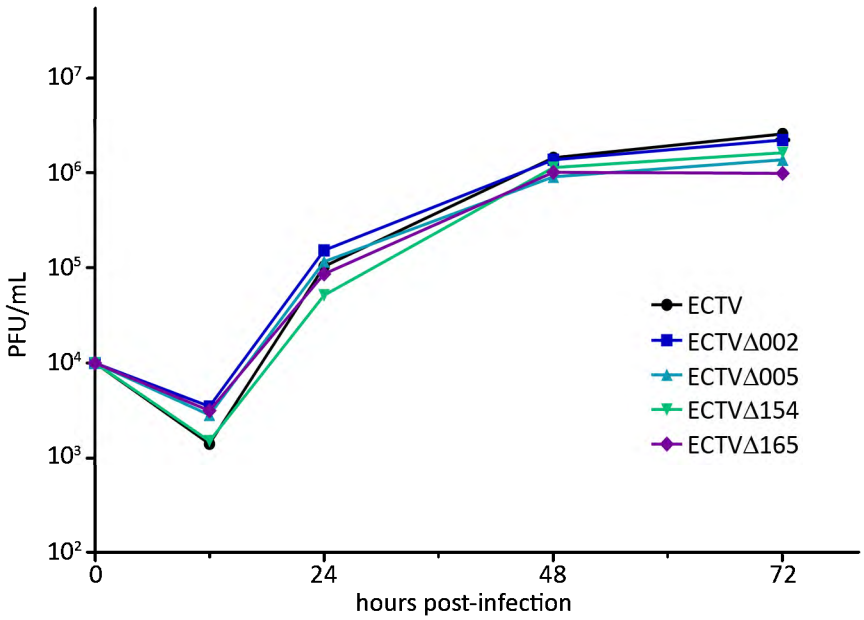

Figure 3-18. Multiple-step analysis of virus growth in CV-1 cells indicates that ECTV devoid of the Ank/F-box proteins grow as well as wildtype ECTV. CV-1 cells were infected at an MOI of 0.01 with ECTV, ECTVΔ002, ECTVΔ005, ECTVΔ154, or ECTVΔ165 for multiple-step growth analysis. Infected cells were harvested up to 72 hours post-infection and lysed to release infectious virus. Serial dilutions of infectious virus were plated on CV-1 cells. Infected monolayers were fixed and stained with crystal violet and plaques were counted to generate a multiple-step growth curve. Representative of three independent experiments with double titrations.

throughout the cytoplasm in mock-infected cells (Figure 3-1, panels a-c), whereas mock-infected cells treated with TNFα displayed dramatic accumulation of p65 in the nucleus (Figure 3-19, panels d-f) (32, 33). In contrast, cells infected with ECTV displayed cytoplasmic retention of p65 following stimulation (Figure 3-19, panels g-i). Cells infected with ECTVΔ002, ECTVΔ005, ECTVΔ154, or ECTVΔ165 also displayed localization of p65 in the cytoplasm following stimulation, indicating that deletion of a single Ank/F-box gene was not enough to abrogate the ability of ECTV to inhibit NFκB activation (Figure 3-19, panels j-u). The experiment was repeated using IL-1β to stimulate the cells. Mock-infected cells that were stimulated with IL-1β displayed nuclear localization of p65 (Figure 3-20, panels d-f), while p65 remained in the cytoplasm of cells infected with ECTV, ECTVΔ002, ECTVΔ005, ECTVΔ154, or ECTVΔ165 (Figure 3-20, panels g-u).

To confirm that ECTV devoid of ECTV002, ECTV005, ECTV154, or ECTV165 inhibited NFκB, we generated nuclear and cytoplasmic extracts to monitor NFκB p65 nuclear translocation. HeLa cells were mock infected, or infected with ECTV or the knockout viruses. Twelve hours post-infection, cells were stimulated with TNFα. Nuclear and cytoplasmic extracts were immunoblotted for NFκB p65, I5L, as a control to indicate virus infection (39), and PARP and β-tubulin, as controls to indicate the purity of the nuclear and cytoplasmic fractions, respectively (23, 36). In mock-infected cells, a large amount of p65 was detected in the cytoplasm, but very low levels were detected in the nucleus (Figure 3-21). Following stimulation with TNFα, high levels of p65 were observed in the nuclear fraction, indicating that the NFκB pathway had been activated. Strikingly, infected cells subjected to stimulation with TNFα displayed minimal levels of p65 in the nuclear fraction, indicating that NFκB activation was inhibited. The experiment was repeated using IL-1β, and similar results were observed (Figure 3-22). Overall, these data indicated that ECTV devoid of ECTV002, ECTV005, ECTV154, or ECTV165 inhibit TNFα and IL-1β p65 nuclear translocation.

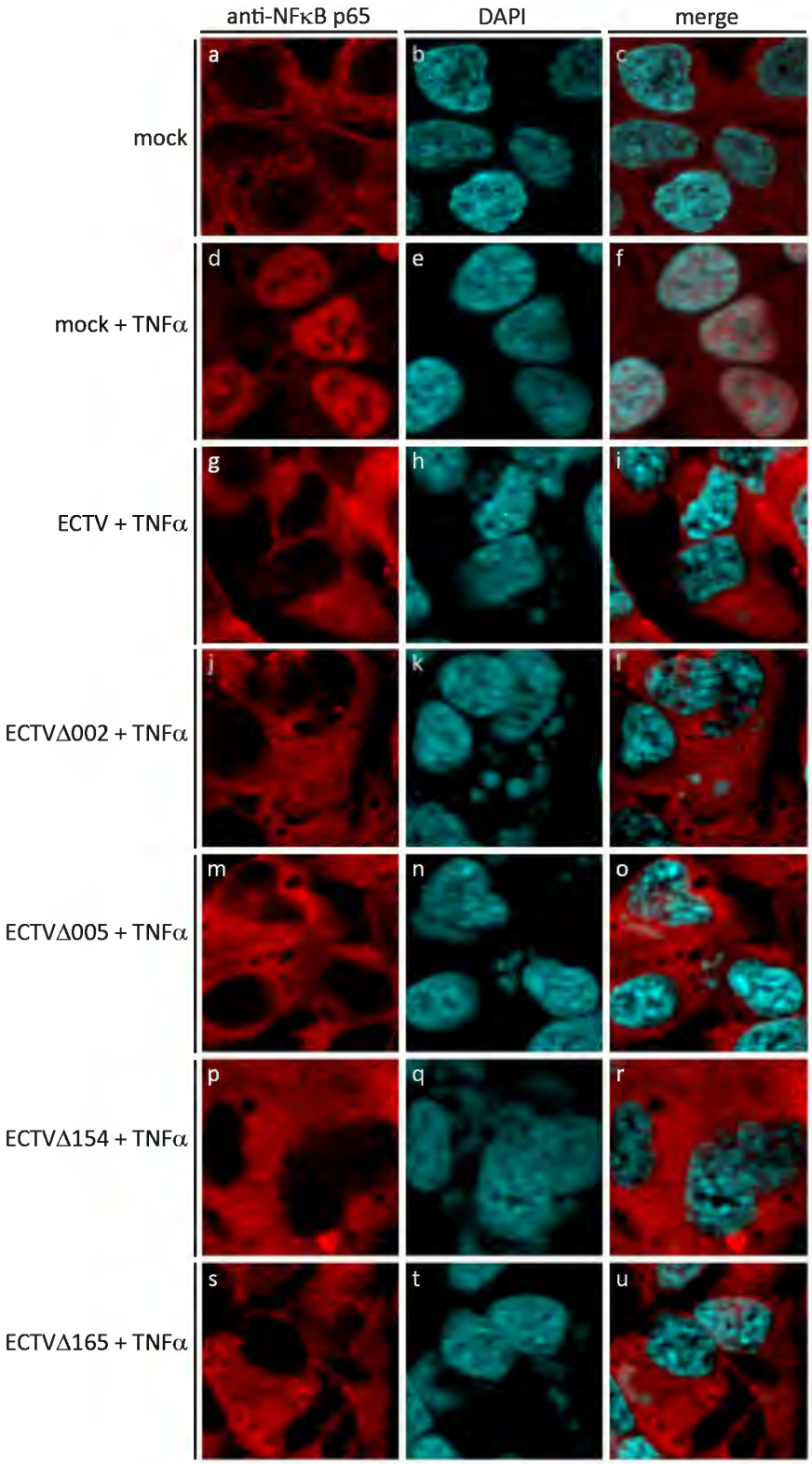
anti-NFκB p65
DAPI
merge
mock
mock + TNFα
ECTV + TNFα
ECTVΔ002 + TNFα
ECTVΔ005 + TNFα
ECTVΔ154 + TNFα
ECTVΔ165 + TNFα
a
b
c
d
e
f
g
h
i
j
k
l
m
n
o
p
q
r
s
t
u

Figure 3-19. ECTV, ECTVΔ002, ECTVΔ005, ECTVΔ154, or ECTVΔ165 inhibit TNFα-induced NFκB p65 nuclear translocation. HeLa cells were mock infected (a-f), or infected at an MOI of 5 with ECTV (g-i), ECTVΔ002 (j-l), ECTVΔ005 (m-o), ECTVΔ154 (p-r), or ECTVΔ165 (s-u). Twelve hours post-infection, cells were mock stimulated (a-c) or stimulated with 10 ng/mL of TNFα for 20 minutes (d-u). Endogenous NFκB p65 was detected with an antibody specific for p65, and nuclei were detected with DAPI.

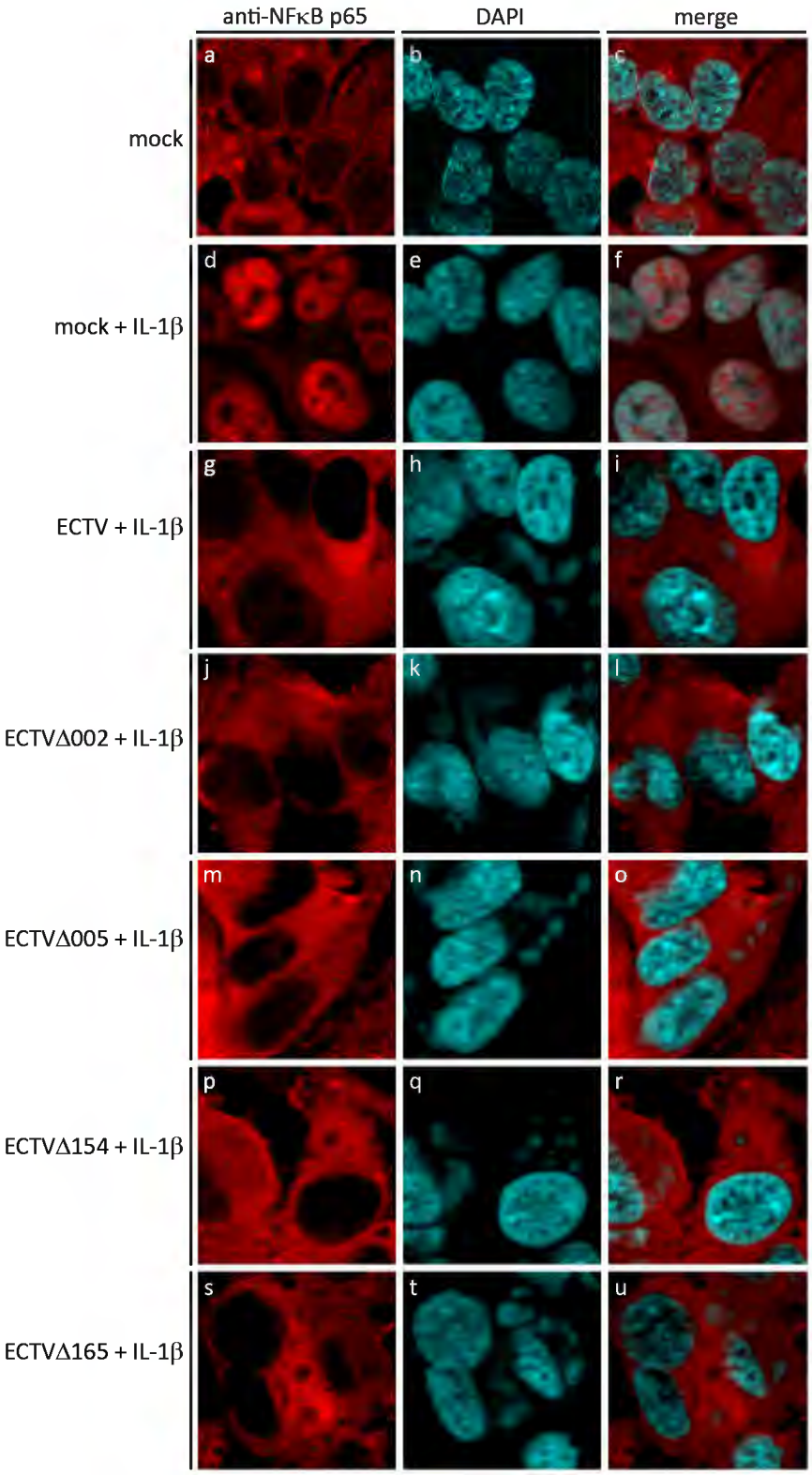
anti-NFκB p65
DAPI
merge
mock
mock + IL-1β
ECTV + IL-1β
ECTVΔ002 + IL-1β
ECTVΔ005 + IL-1β
ECTVΔ154 + IL-1β
ECTVΔ165 + IL-1β
a
b
c
d
e
f
g
h
i
j
k
l
m
n
o
p
q
r
s
t
u

Figure 3-20. ECTV, ECTVΔ002, ECTVΔ005, ECTVΔ154, or ECTVΔ165 inhibit IL-1β-induced NFκB p65 nuclear translocation. HeLa cells were mock infected (a-f), or infected at an MOI of 5 with ECTV (g-i), ECTVΔ002 (j-l), ECTVΔ005 (m-o), ECTVΔ154 (p-r), or ECTVΔ165 (s-u). Twelve hours post-infection, cells were mock stimulated (a-c) or stimulated with 10 ng/mL IL-1β for 20 minutes (d-u). Endogenous NFκB p65 was detected with an antibody specific for p65, and nuclei were detected with DAPI.

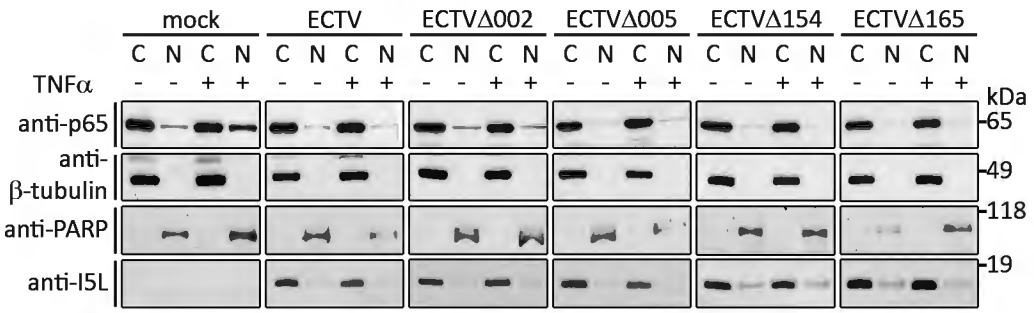

Figure 3-21. ECTV devoid of ECTV002, ECTV005, ECTV154, or ECTV165 inhibit TNFα-induced NFκB p65 nuclear translocation. HeLa cells were mock infected, or infected at an MOI of 5 with ECTV, ECTVΔ002, ECTVΔ005, ECTVΔ154, or ECTVΔ165. Twelve hours post-infection, cells were mock stimulated or stimulated with 10 ng/mL of TNFα for 20 minutes. Cytoplasmic and nuclear extracts were immunoblotted for endogenous NFκB p65, β-tubulin as a control for cytoplasmic extracts, PARP as a control for nuclear extracts, and I5L as a control to indicate that infection had occured.

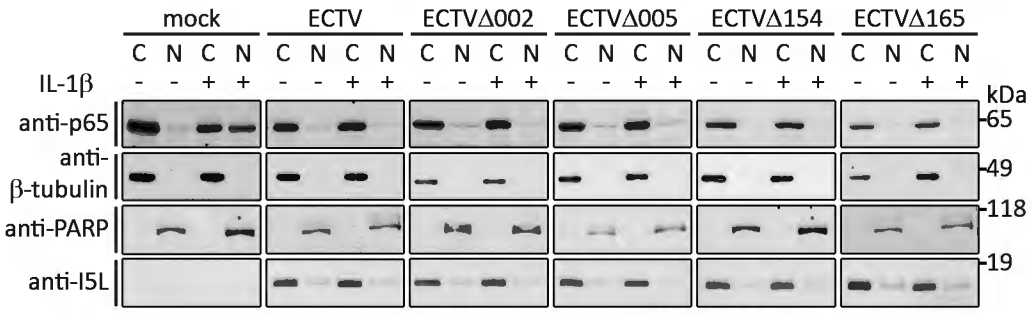

Figure 3-22. ECTV devoid of ECTV002, ECTV005, ECTV154, or ECTV165 inhibit IL-1β-induced NFκB p65 nuclear translocation. HeLa cells were mock infected, or infected at an MOI of 5 with ECTV, ECTVΔ002, ECTVΔ005, ECTVΔ154, or ECTVΔ165. Twelve hours post-infection, cells were mock stimulated or stimulated with 10 ng/mL of IL-1β for 20 minutes. Cytoplasmic and nuclear extracts were immunoblotted for endogenous NFκB p65, β-tubulin as a control for cytoplasmic extracts, PARP as a control for nuclear extracts, and I5L as a control to indicate that infection had occured.

3.2.8 Viruses devoid of ECTV002, ECTV005, ECTV154, or ECTV165 inhibit IκBα degradation

Next, we sought to determine if the lack of any of the ECTV Ank/F-box proteins prevented ECTVΔ002, ECTVΔ005, ECTVΔ154, or ECTVΔ165 from inhibiting degradation of IκBα. To do this, we used flow cytometry to monitor levels of IκBα in infected cells, following simulation with TNFα (Figure 3-23). HeLa cells were mock infected, or infected with ECTV or the knockout viruses. Twelve hours post-infection, cells were stimulated with TNFα, and fixed and stained with antibodies to IκBα, and I3L, which was a control for virus infection. Alternatively, mock-infected cells were pretreated with the proteasome inhibitor MG132 prior to stimulation. Cells treated with MG132 were a control since MG132 prevents degradation of IκBα induced by TNFα (43). Mock-infected cells exhibited high levels of IκBα, while cells stimulated with TNFα displayed lower levels of IκBα, indicating degradation (Figure 3-23). Degradation of IκBα following TNFα stimulation was prevented in cells that were pretreated with MG132, since proteasomal activity was blocked (43). Significantly, cells infected with wildtype ECTV displayed no loss in IκBα, indicating that degradation was prevented. Similar results were also observed in cells infected with ECTVΔ002, ECTVΔ005, ECTVΔ154, or ECTVΔ165. These data indicated that ECTV devoid of ECTV002, ECTV005, ECTV154, or ECTV165 still prevent degradation of IκBα.

3.3 DISCUSSION

The NFκB signalling pathway is an important regulator of the antiviral response (12, 13, 44). Importantly, a number of inhibitors of the NFκB pathway have been identified in poxviruses (25, 30). Translocation of NFκB into the nucleus is dependent on the ubiquitination and degradation of IκBα, an event that is tightly regulated by the $SCF^{\beta TrCP}$ ubiquitin ligase (11, 20, 40). Recently, we identified four Ank/F-box proteins in ECTV that interact with the SCF ubiquitin ligase (45). Using transient transfection and immunofluorescence experiments, we monitored the localization of the NFκB subunit

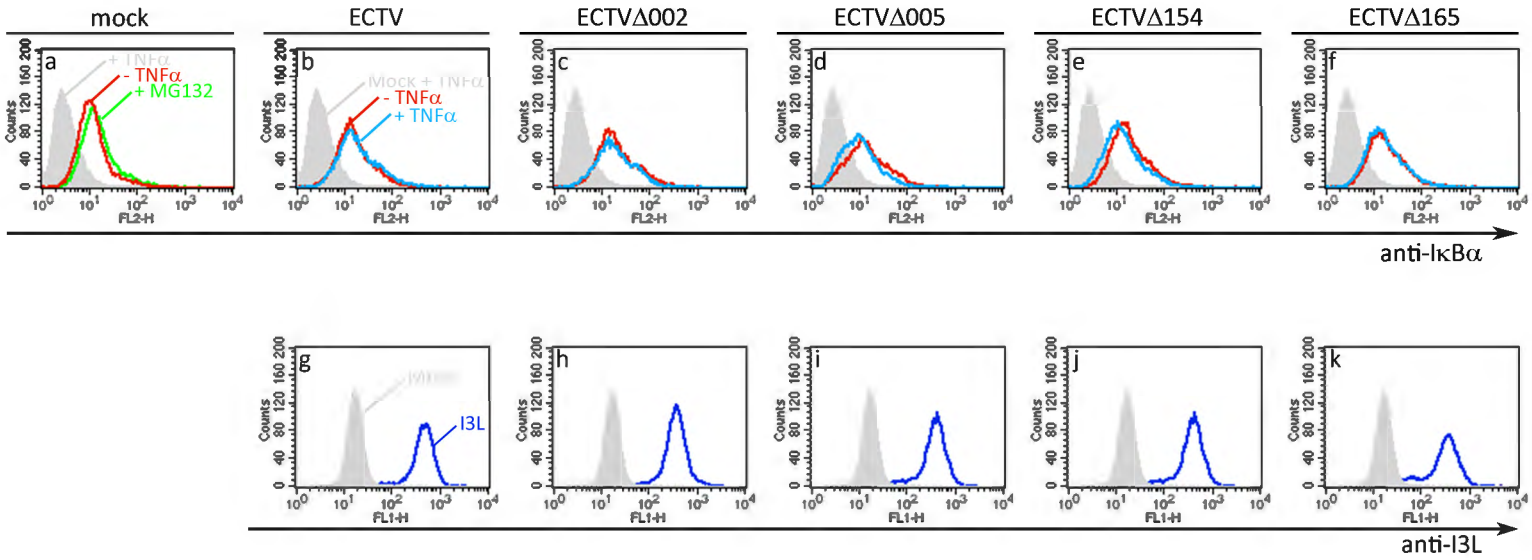

Figure 3-23. ECTV devoid of the ankyrin/F-box proteins inhibit TNFα-induced IκBα degradation. HeLa cells were mock infected (a), or infected at an MOI of 5 with ECTV (b and g), ECTVΔ002 (c and h), ECTVΔ005 (d and i), ECTVΔ154 (e and j), or ECTVΔ165 (f and k). Twelve hours post-infection, cells were mock stimulated or stimulated with 10 ng/mL TNFα for 20 minutes. Alternatively, mock-infected cells were treated with 10 μM of MG132 for one hour prior to stimulation with TNFα. Cells were stained with an antibody specific for endogenous IκBα (a-f), and an antibody specific for I3L (g-k), which was a control to indicate that infection had occured.

p65 following activation of the NFκB pathway. We found that expression of the ECTV Ank/F-box proteins inhibited TNFα and IL-1β-induced p65 nuclear translocation (Figures 3-2, 3-3, and 3-4). Significantly, inhibition of this pathway was dependent on the F-box domain, since deletion or mutation of this domain prevented the ECTV Ank/F-box proteins from inhibiting TNFα and IL-1β-induced p65 nuclear translocation (Figures 3-5, 3-6, and 3-7). Interestingly, although the loss of the F-box domain decreased the ability ECTV154 and ECTV165 to inhibit NFκB activation, these proteins still inhibited this pathway to a greater extent than ECTV002 or ECTV005 did, suggesting that ECTV154 and ECTV165 may not rely exclusively on the F-box domain to inhibit NFκB (Figure 3-7).

Additionally, we demonstrated that expression of the ECTV Ank/F-box proteins prevented TNFα-induced IκBα degradation (Figure 3-9 and 3-10). Degradation of IκBα occurs after the convergence point of many NFκB signalling pathways. Thus it is an attractive target for many viruses that inhibit NFκB (18, 21, 42). For instance, the 3C protease encoded by Coxsackie virus cleaves IκBα to yield an N-terminal fragment bound to NFκB dimer (48). Although the fragmented IκB-NFκB complex translocates into nucleus, it remains inactive and is unable to activate gene transcription. HSV also encodes a protein that targets IκBα. ICP27 binds to IκBα and prevents its phosphorylation, thereby resulting in stabilization of IκBα (18). African swine fever virus, on the other hand, induces degradation of IκBα, which then allows the virus-encoded protein A238L to interact with p65-containing NFκB dimers, preventing their nuclear translocation (42). Additionally, KSHV encodes microRNAs that repress expression of IκBα (21).

In order to understand the function of the Ank/F-box proteins in the context of virus infection, we created four knockout viruses, each devoid of a single ECTV Ank/F-box protein. The ECTV viruses still inhibited IκBα degradation (Figure 3-22) and p65 nuclear translocation induced by TNFα (Figures 3-18 and 3-20) and IL-1β (Figures 3-19 and 3-21). This was not surprising, since ECTV002, ECTV005, ECTV154, and ECTV165 were

transcribed at overlapping times during the course of infection (Figure 3-1), we expected that these four proteins might exhibit some redundancy. Interestingly, when we used single-step growth analysis to assess production of infectious virions, there was no attenuation of any of these viruses in BGMK or CV-1 cells (Figure 3-11 and 3-14). This was not surprising; often deletion of only a single immune modulator does not affect growth in tissue culture (9, 26). Interestingly, we did observe a small foci phenotype for ECTVΔ002 and ECTVΔ154 in BGMK cells, which indicated reduced virion release or spread (Figure 3-12 and 3-13), and this phenotype was more striking in CV-1 cells (Figure 3-15 and 3-16). As described in section 3.2.6, ECTV does not grow as efficiently in CV-1 cells compared to BGMK cells, (J. Schriewer and M. Buller, personal communication). It is possible that the pronounced small foci phenotype that we observed in CV-1 cells is due CV-1 cells being more restrictive to virus growth than BGMK cells, however this would be difficult to determine, since there has been no characterization of the differences between CV-1 and BGMK cells. Since the small-foci phenotype was more prominent in CV-1 cells, we performed multiple-step growth analysis to further confirm the observed defect in virion release or spread. However, no striking differences between the ECTV Ank/F-box knockout viruses and ECTV were observed (Figure 3-17). The fact that ECTV deletion viruses devoid of ECTV002 or ECTV154 grew as well as ECTV, even though they had a small foci phenotype was surprising, though not unheard of; myxoma virus devoid of M125R grows as well as wildtype myxoma virus, even though it has a small plaque phenotype (15). In conclusion, we demonstrated that ECTV encodes four additional inhibitors of the NFκB pathway. Evidence suggests that ECTV002, ECTV005, ECTV154, and ECTV165 inhibit IκBα degradation through modulation of the SCF ubiquitin ligase. In VACV, the orthologues of of ECTV154 and ECTV165, B4R and B18R, respectively, can be added to the growing list of NFκB inhibitors.

3.4 REFERENCES

1. **Babiuk, L. A., B. Meldrum, V. S. Gupta, and B. T. Rouse.** 1975. Comparison of the antiviral effects of 5-methoxymethyl-deoxyuridine with 5-iododeoxyuridine, cytosine arabinoside, and adenine arabinoside. Antimicrob Agents Chemother **8:**643-50.
2. **Bowie, A., E. Kiss-Toth, J. A. Symons, G. L. Smith, S. K. Dower, and L. A. O'Neill.** 2000. A46R and A52R from vaccinia virus are antagonists of host IL-1 and toll-like receptor signaling. Proc Natl Acad Sci U S A **97:**10162-7.
3. **Chen, R. A., N. Jacobs, and G. L. Smith.** 2006. Vaccinia virus strain Western Reserve protein B14 is an intracellular virulence factor. J Gen Virol **87:**1451-8.
4. **Chen, R. A., G. Ryzhakov, S. Cooray, F. Randow, and G. L. Smith.** 2008. Inhibition of IkappaB kinase by vaccinia virus virulence factor B14. PLoS Pathog **4:**e22.
5. **De Clercq, E., E. Darzynkiewicz, and D. Shugar.** 1975. Antiviral activity of O'-alkylated derivatives of cytosine arabinoside. Biochem Pharmacol **24:**523-7.
6. **DiPerna, G., J. Stack, A. G. Bowie, A. Boyd, G. Kotwal, Z. Zhang, S. Arvikar, E. Latz, K. A. Fitzgerald, and W. L. Marshall.** 2004. Poxvirus protein N1L targets the I-kappaB kinase complex, inhibits signaling to NF-kappaB by the tumor necrosis factor superfamily of receptors, and inhibits NF-kappaB and IRF3 signaling by toll-like receptors. J Biol Chem **279:**36570-8.
7. **Gedey, R., X. L. Jin, O. Hinthong, and J. L. Shisler.** 2006. Poxviral regulation of the host NF-kappaB response: the vaccinia virus M2L protein inhibits induction of NF-kappaB activation via an ERK2 pathway in virus-infected human embryonic kidney cells. J Virol **80:**8676-85.
8. **Graham, S. C., M. W. Bahar, S. Cooray, R. A. Chen, D. M. Whalen, N. G. Abrescia, D. Alderton, R. J. Owens, D. I. Stuart, G. L. Smith, and J. M. Grimes.** 2008. Vaccinia virus proteins A52 and B14 Share a Bcl-2-like fold but have evolved to inhibit NF-kappaB rather than apoptosis. PLoS Pathog **4:**e1000128.
9. **Gubser, C., S. Hue, P. Kellam, and G. L. Smith.** 2004. Poxvirus genomes: a phylogenetic analysis. J Gen Virol **85:**105-17.
10. **Harte, M. T., I. R. Haga, G. Maloney, P. Gray, P. C. Reading, N. W. Bartlett, G. L. Smith, A. Bowie, and L. A. O'Neill.** 2003. The poxvirus protein A52R targets Toll-like receptor signaling complexes to suppress host defense. J Exp Med **197:**343-51.
11. **Hatakeyama, S., M. Kitagawa, K. Nakayama, M. Shirane, M. Matsumoto, K. Hattori, H. Higashi, H. Nakano, K. Okumura, K. Onoe, and R. A. Good.** 1999. Ubiquitin-dependent degradation of IkappaBalpha is mediated by a ubiquitin ligase Skp1/Cul 1/F-box protein FWD1. Proc Natl Acad Sci U S A **96:**3859-63.
12. **Hayden, M. S., and S. Ghosh.** 2012. NF-kappaB, the first quarter-century: remarkable progress and outstanding questions. Genes Dev **26:**203-34.
13. **Hayden, M. S., and S. Ghosh.** 2008. Shared principles in NF-kappaB signaling. Cell **132:**344-62.

14. **Hinthong, O., X. L. Jin, and J. L. Shisler.** 2008. Characterization of wild-type and mutant vaccinia virus M2L proteins' abilities to localize to the endoplasmic reticulum and to inhibit NF-kappaB activation during infection. Virology **373:**248-62.
15. **Irwin, C. R., and D. H. Evans.** 2012. Modulation of the myxoma virus plaque phenotype by vaccinia virus protein f11. J Virol **86:**7167-79.
16. **Johnston, J. B., and G. McFadden.** 2003. Poxvirus immunomodulatory strategies: current perspectives. J Virol **77:**6093-100.
17. **Karin, M., and Y. Ben-Neriah.** 2000. Phosphorylation meets ubiquitination: the control of NF-[kappa]B activity. Annu Rev Immunol **18:**621-63.
18. **Kim, J. C., S. Y. Lee, S. Y. Kim, J. K. Kim, H. J. Kim, H. M. Lee, M. S. Choi, J. S. Min, M. J. Kim, H. S. Choi, and J. K. Ahn.** 2008. HSV-1 ICP27 suppresses NF-kappaB activity by stabilizing IkappaBalpha. FEBS Lett **582:**2371-6.
19. **Kipreos, E. T., and M. Pagano.** 2000. The F-box protein family. Genome Biol **1:**REVIEWS3002.
20. **Kroll, M., F. Margottin, A. Kohl, P. Renard, H. Durand, J. P. Concordet, F. Bachelerie, F. Arenzana-Seisdedos, and R. Benarous.** 1999. Inducible degradation of IkappaBalpha by the proteasome requires interaction with the F-box protein h-betaTrCP. J Biol Chem **274:**7941-5.
21. **Lei, X., Z. Bai, F. Ye, J. Xie, C. G. Kim, Y. Huang, and S. J. Gao.** 2010. Regulation of NF-kappaB inhibitor IkappaBalpha and viral replication by a KSHV microRNA. Nat Cell Biol **12:**193-9.
22. **Li, J., A. Mahajan, and M. D. Tsai.** 2006. Ankyrin repeat: a unique motif mediating protein-protein interactions. Biochemistry **45:**15168-78.
23. **Machesky, L. M., N. B. Cole, B. Moss, and T. D. Pollard.** 1994. Vaccinia virus expresses a novel profilin with a higher affinity for polyphosphoinositides than actin. Biochemistry **33:**10815-24.
24. **Mercer, A. A., S. B. Fleming, and N. Ueda.** 2005. F-box-like domains are present in most poxvirus ankyrin repeat proteins. Virus Genes **31:**127-33.
25. **Mohamed, M. R., and G. McFadden.** 2009. NFkB inhibitors: strategies from poxviruses. Cell Cycle **8:**3125-32.
26. **Moss, B.** 2007. *Poxviridae:* The Viruses and Their Replication. *In* D. M. K. a. P. M. Howley (ed.), Fields Virology 5ed.
27. **Moss, B., and J. L. Shisler.** 2001. Immunology 101 at poxvirus U: immune evasion genes. Semin Immunol **13:**59-66.
28. **Myskiw, C., J. Arsenio, R. van Bruggen, Y. Deschambault, and J. Cao.** 2009. Vaccinia virus E3 suppresses expression of diverse cytokines through inhibition of the PKR, NF-kappaB, and IRF3 pathways. J Virol **83:**6757-68.
29. **Osborn, L., S. Kunkel, and G. J. Nabel.** 1989. Tumor necrosis factor alpha and interleukin 1 stimulate the human immunodeficiency virus enhancer by activation of the nuclear factor kappa B. Proc Natl Acad Sci U S A **86:**2336-40.
30. **Rahman, M. M., and G. McFadden.** 2011. Modulation of NF-kappaB signalling by microbial pathogens. Nat Rev Microbiol **9:**291-306.

31. **Rintoul, J. L., J. Wang, D. B. Gammon, N. J. van Buuren, K. Garson, K. Jardine, M. Barry, D. H. Evans, and J. C. Bell.** 2011. A selectable and excisable marker system for the rapid creation of recombinant poxviruses. PLoS One **6:**e24643.
32. **Salminen, A., T. Paimela, T. Suuronen, and K. Kaarniranta.** 2008. Innate immunity meets with cellular stress at the IKK complex: regulation of the IKK complex by HSP70 and HSP90. Immunol Lett **117:**9-15.
33. **Schroder, M., M. Baran, and A. G. Bowie.** 2008. Viral targeting of DEAD box protein 3 reveals its role in TBK1/IKKepsilon-mediated IRF activation. EMBO J **27:**2147-57.
34. **Seet, B. T., J. B. Johnston, C. R. Brunetti, J. W. Barrett, H. Everett, C. Cameron, J. Sypula, S. H. Nazarian, A. Lucas, and G. McFadden.** 2003. Poxviruses and immune evasion. Annu Rev Immunol **21:**377-423.
35. **Shisler, J. L., and X. L. Jin.** 2004. The vaccinia virus K1L gene product inhibits host NF-kappaB activation by preventing IkappaBalpha degradation. J Virol **78:**3553-60.
36. **Smith, G. L., Y. S. Chan, and S. T. Howard.** 1991. Nucleotide sequence of 42 kbp of vaccinia virus strain WR from near the right inverted terminal repeat. J Gen Virol **72 (Pt 6):**1349-76.
37. **Solt, L. A., and M. J. May.** 2008. The IkappaB kinase complex: master regulator of NF-kappaB signaling. Immunol Res **42:**3-18.
38. **Sonnberg, S., B. T. Seet, T. Pawson, S. B. Fleming, and A. A. Mercer.** 2008. Poxvirus ankyrin repeat proteins are a unique class of F-box proteins that associate with cellular SCF1 ubiquitin ligase complexes. Proc Natl Acad Sci U S A **105:**10955-60.
39. **Sood, C. L., J. M. Ward, and B. Moss.** 2008. Vaccinia virus encodes I5, a small hydrophobic virion membrane protein that enhances replication and virulence in mice. J Virol **82:**10071-8.
40. **Spencer, E., J. Jiang, and Z. J. Chen.** 1999. Signal-induced ubiquitination of IkappaBalpha by the F-box protein Slimb/beta-TrCP. Genes Dev **13:**284-94.
41. **Stack, J., I. R. Haga, M. Schroder, N. W. Bartlett, G. Maloney, P. C. Reading, K. A. Fitzgerald, G. L. Smith, and A. G. Bowie.** 2005. Vaccinia virus protein A46R targets multiple Toll-like-interleukin-1 receptor adaptors and contributes to virulence. J Exp Med **201:**1007-18.
42. **Tait, S. W., E. B. Reid, D. R. Greaves, T. E. Wileman, and P. P. Powell.** 2000. Mechanism of inactivation of NF-kappa B by a viral homologue of I kappa b alpha. Signal-induced release of i kappa b alpha results in binding of the viral homologue to NF-kappa B. J Biol Chem **275:**34656-64.
43. **Traenckner, E. B., S. Wilk, and P. A. Baeuerle.** 1994. A proteasome inhibitor prevents activation of NF-kappa B and stabilizes a newly phosphorylated form of I kappa B-alpha that is still bound to NF-kappa B. EMBO J **13:**5433-41.
44. **Vallabhapurapu, S., and M. Karin.** 2009. Regulation and function of NF-kappaB transcription factors in the immune system. Annu Rev Immunol **27:**693-733.

45. **van Buuren, N., B. Couturier, Y. Xiong, and M. Barry.** 2008. Ectromelia virus encodes a novel family of F-box proteins that interact with the SCF complex. J Virol **82:**9917-27.

46. **Werren, J. H., S. Richards, C. A. Desjardins, O. Niehuis, J. Gadau, J. K. Colbourne, L. W. Beukeboom, C. Desplan, C. G. Elsik, C. J. Grimmelikhuijzen, P. Kitts, J. A. Lynch, T. Murphy, D. C. Oliveira, C. D. Smith, L. van de Zande, K. C. Worley, E. M. Zdobnov, M. Aerts, S. Albert, V. H. Anaya, J. M. Anzola, A. R. Barchuk, S. K. Behura, A. N. Bera, M. R. Berenbaum, R. C. Bertossa, M. M. Bitondi, S. R. Bordenstein, P. Bork, E. Bornberg-Bauer, M. Brunain, G. Cazzamali, L. Chaboub, J. Chacko, D. Chavez, C. P. Childers, J. H. Choi, M. E. Clark, C. Claudianos, R. A. Clinton, A. G. Cree, A. S. Cristino, P. M. Dang, A. C. Darby, D. C. de Graaf, B. Devreese, H. H. Dinh, R. Edwards, N. Elango, E. Elhaik, O. Ermolaeva, J. D. Evans, S. Foret, G. R. Fowler, D. Gerlach, J. D. Gibson, D. G. Gilbert, D. Graur, S. Grunder, D. E. Hagen, Y. Han, F. Hauser, D. Hultmark, H. C. t. Hunter, G. D. Hurst, S. N. Jhangian, H. Jiang, R. M. Johnson, A. K. Jones, T. Junier, T. Kadowaki, A. Kamping, Y. Kapustin, B. Kechavarzi, J. Kim, B. Kiryutin, T. Koevoets, C. L. Kovar, E. V. Kriventseva, R. Kucharski, H. Lee, S. L. Lee, K. Lees, L. R. Lewis, D. W. Loehlin, J. M. Logsdon, Jr., J. A. Lopez, R. J. Lozado, D. Maglott, R. Maleszka, A. Mayampurath, D. J. Mazur, M. A. McClure, A. D. Moore, M. B. Morgan, J. Muller, M. C. Munoz-Torres, D. M. Muzny, L. V. Nazareth, et al.** 2010. Functional and evolutionary insights from the genomes of three parasitoid Nasonia species. Science **327:**343-8.

47. **Wilton, B. A., S. Campbell, N. Van Buuren, R. Garneau, M. Furukawa, Y. Xiong, and M. Barry.** 2008. Ectromelia virus BTB/kelch proteins, EVM150 and EVM167, interact with cullin-3-based ubiquitin ligases. Virology **374:**82-99.

48. **Zaragoza, C., M. Saura, E. Y. Padalko, E. Lopez-Rivera, T. R. Lizarbe, S. Lamas, and C. J. Lowenstein.** 2006. Viral protease cleavage of inhibitor of kappaBalpha triggers host cell apoptosis. Proc Natl Acad Sci U S A **103:**19051-6.

Chapter 4: A Large Deletion Virus Provides Additional Insights into the Function of ECTV154

The results contained within this chapter consist of unpublished material. Experiments in this chapter were performed by K. Burles. The document was written by K. Burles with a major editorial contribution made by Dr. M. Barry.

pDGloxP-VACVB4R-400L, which was used to generate VACV811ΔB4R-YFP, was cloned by Q. Wang.

4.1 BRIEF INTRODUCTION

The NFκB pathway is an important regulator of the antiviral response (28, 29, 66). The NFκB transcription factor is sequestered in the cytoplasm by its inhibitor, IκBα (33). Upon cellular stimulation, the IKK complex phosphorylates IκBα, leading to its poly-ubiquitination by the $SCF^{\beta TrCP}$ ubiquitin ligase and subsequent degradation (27, 35, 62). Left unsequestered by its inhibitor, the NFκB transcription factor is free to translocate into the nucleus, where it stimulates transcription of genes involved in the antiviral response (28, 29, 66). Activation of the NFκB pathway occurs in response to a variety of stimuli. Work in our laboratory focuses on the classical activation pathway, which is activated following the engagement of the inflammatory cytokines TNFα and IL-1β with the TNFR and IL-1R, respectively (47). Although the signaling pathways stimulated by TNFα and IL-1β use different adapter proteins and signalling molecules, they both converge at the IKK complex (59).

The *Poxviridae* are a family of large dsDNA viruses that are notorious for inhibiting the immune response and regulating cellular signalling pathways (6, 32, 45, 56). Inhibition of the NFκB pathway is crucial to the poxvirus life cycle, which is evident by the large number of NFκB inhibitors that are encoded by poxviruses (43, 49). In VACVCop, the prototypic member of the *Poxviridae*, a number of inhibitors of the NFκB pathway have been identified. Some inhibitors, including A52R, A46R, and K7L, prevent IL-1β-mediated NFκB activation by disrupting signalling complexes at the IL-1R (8, 23, 26, 55), while N1L, B14R, and K1L inhibit activation of the IKK complex by preventing its phosphorylation (12, 13, 17, 57). In addition, M2L prevents ERK2 phosphorylation and subsequent activation of IKK complex (21, 30), while E3L prevents NFκB activation induced by the PKR pathway, following recognition of viral double stranded RNA (46).

Although a number of inhibitors of the NFκB pathway have been identified in VACVCop, work in our laboratory using two large deletion vaccinia viruses, Modified Vaccinia strain

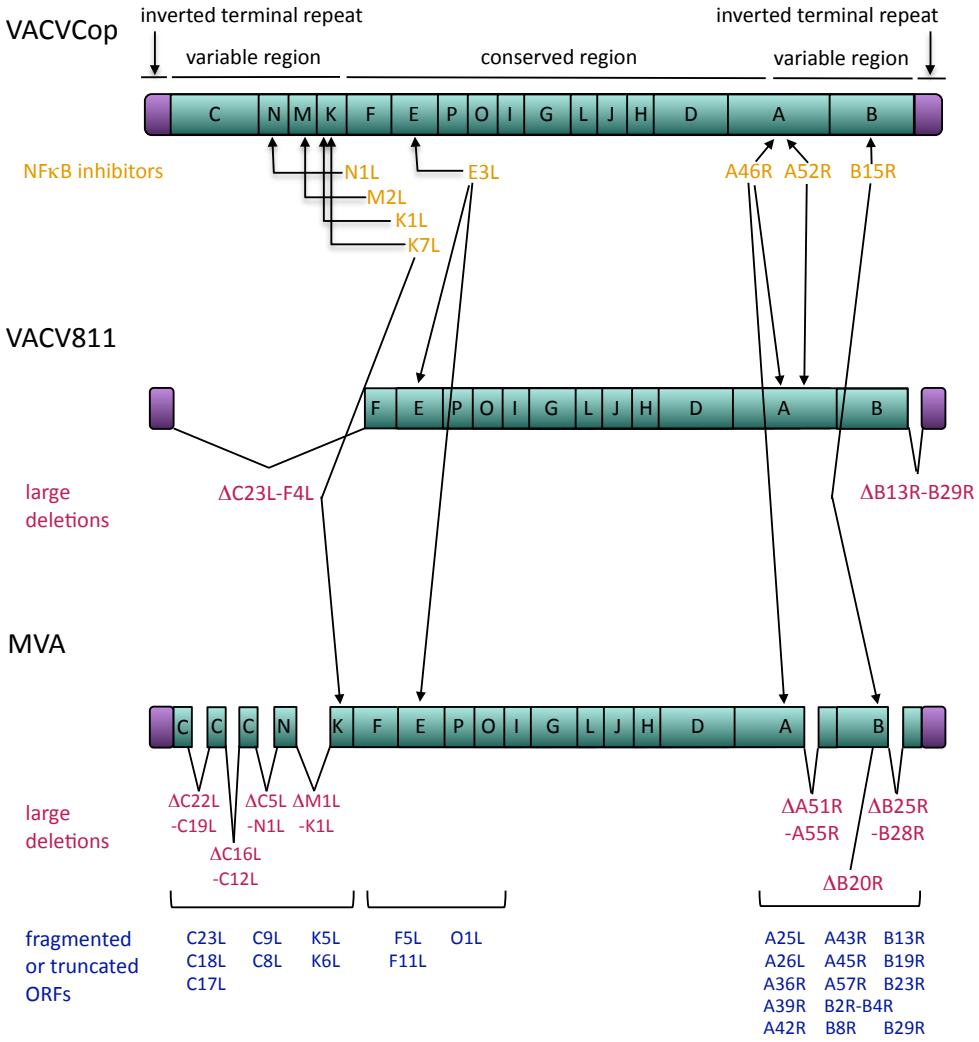

Figure 4-1. Schematic representation of VACVCop, VACV811, and MVA. The letters correspond to the genomic fragments in VACVCop that were identified by *HindIII* restriction enzyme digestion (16). Locations of the known NFκB inhibitors are indicated in orange. Large deletions in VACV811 and MVA are indicated in pink and fragmented or truncated ORFs are indicated in blue (adapted from 20).

Ankara (MVA) and VACV strain 811 (VACV811), suggests that additional inhibitors of the NFκB pathway exist in VACV (20). MVA, a virus that is unable to successfully propagate in many mammalian cell lines, was passaged in chicken embryo fibroblasts over 570 times, resulting in the several random ORF mutations and deletions (4, 42) (Figure 4-1). Infection with MVA induces degradation of IκBα and translocation of NFκB into the nucleus (38). In contrast to MVA, VACV811 was strategically engineered by progressive deletion of ORFs from VACVCop, so that the end product contained the minimal number of ORFs necessary for virus replication (48). In total, VACV811 is missing 55 ORFs; 38 from the left side (C23L to F4L) and 17 from the right side (B13R to B29R) (Figure 4-1). VACV811 is missing all known inhibitors of TNFα-induced NFκB activation, however work in our laboratory demonstrated that infection with VACV811 prevents TNFα-induced nuclear translocation of NFκB, and results in accumulation of phosphorylated IκBα in the cytoplasm (20).

Interestingly, inhibition of TNFα-induced NFκB activation is dependent on an ORF that is expressed late in infection, since IκBα is degraded in VACV811-infected cells in the presence of AraC, an inhibitor of late gene synthesis (20). By comparing the genomes of VACV811 and MVA, we identified 18 ORFs in VACV811 that are fragmented, truncated, or completely missing in MVA (Table 4-1). Of the 18 ORFs, our attention was drawn to VACVB4R, since it has an orthologue in ECTV, ECTV154. The amino acid sequence of ECTV154 and VACVB4R are 94% identical, and both ORFs encode an F-box domain at the C-terminus and have six Ank domains dispersed throughout the N-terminus (Figure 4-2). Since we have already characterized ECTV154 as an inhibitor of the NFκB pathway, we investigated whether the VACV811 mutant lacking VACVB4R, VACV811ΔB4R, still inhibited the NFκB pathway. Here, we report VACV811ΔB4R inhibited TNFα- and IL-1β-induced NFκB activation. However, deletion of VACVB4R from VACV811 decreased the ability of this virus to spread in tissue culture. Additionally, our studies revealed that deletion of VACVB4R from VACV811 did not prevent expression of late genes. Our results suggest that VACVB4R is important for mediating virus spread during infection.

a.

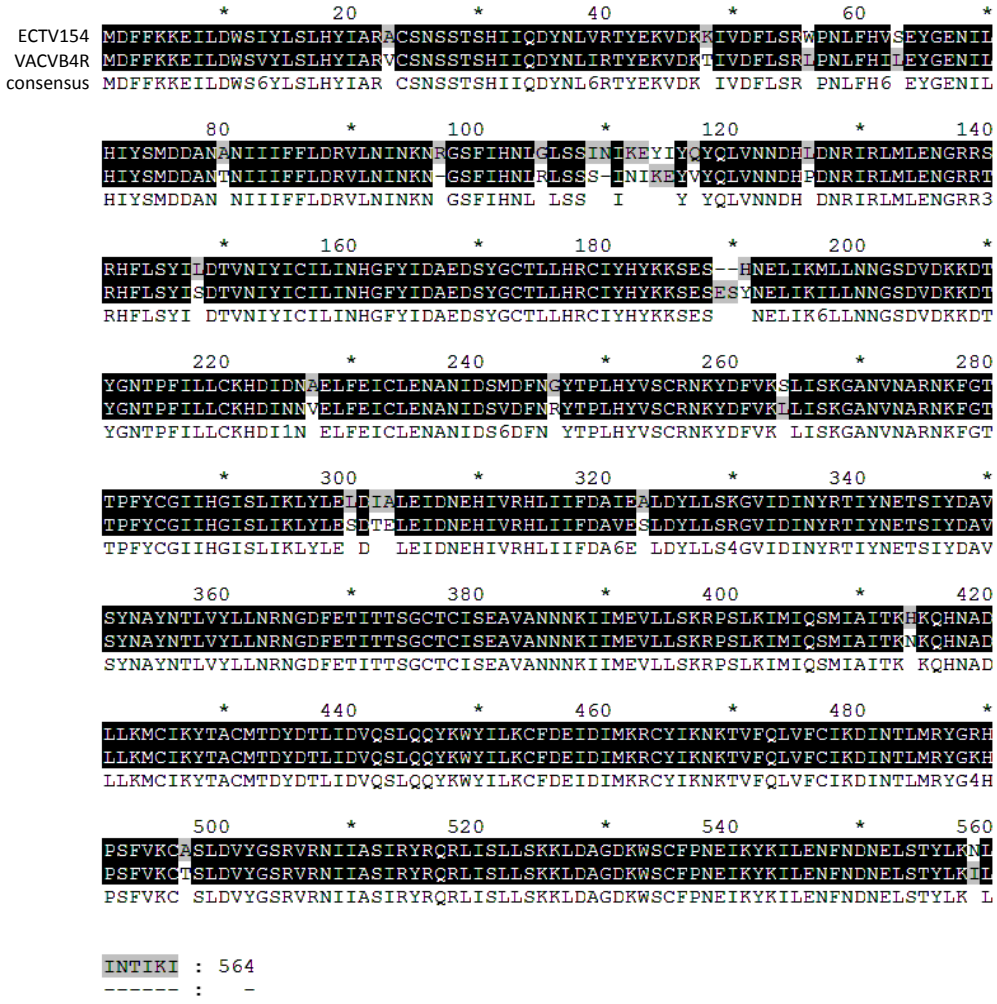

b.

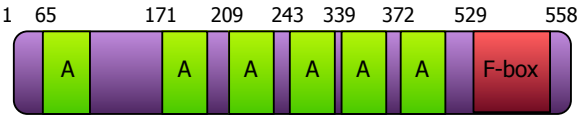

Figure 4-2. The sequence and domain organization of VACVB4R (a.) Alignment between VACVB4R and ECTV154. Amino acid sequences were aligned using ClustalW (36 and 65). Poxvirus amino acid sequences were obtained from the Poxvirus Bioinformatics Resource Center (reference 37). Residues representing 100% identity are shaded black. The sequences of VACVB4R and EVM154 are 94% identical. **(b.)** Schematic representation of VACVB4R. VACVB4R contains an F-box domain at the C-terminus, and six ankyrin (A) domains located throughout the N-terminus, which could be important for substrate recruitment.

4.2 RESULTS

4.2.1 Characterization of the growth properties of VACV811 and VACVΔB4R

In order to understand the function of VACVB4R in the context of virus infection, we generated a deletion virus, VACV811ΔB4R, that was devoid the VACVB4R ORF. We used a novel selectable and excisable marker system that relies on the Cre recombinase to delete ORFs of interest (52) (Figure 2-2). Unfortunately, we were unable to passage VACV811 through cells expressing Cre-recombinase, therefore our deletion virus still contains the *YFP*/*gpt* cassette. Since we observed that ECTVΔ154 had a small-plaque phenotype (Figures 3-12, 3-13, 3-15, 3-16), we examined the growth characteristics of VACV811ΔB4R. Our goal in this process was two-pronged; to further understand the differences in growth between VACVCop and VACV811, and to understand what effect deletion of VACVB4R had on the growth of VACV811. To understand more about the growth of these viruses in tissue culture, we performed a single-step growth curve. BGMK cells were infected at an MOI of 10 with VACVCop, VACV811, or VACV811ΔB4R. Surprisingly, VACV811 and VACV811ΔB4R replicated at comparable levels to VACVCop (Figure 4-3). While determining virus titers, we noticed that the plaques of VACV811 were slightly smaller than those of VACVCop, and the plaques of VACV811ΔB4R were much smaller than both the plaques of VACVCop and VACV811. To determine if any of these differences were significant, we used a plaque assay to compare the sizes of plaques (Figure 4-4). BGMK cells were infected with VACVCop, VACV811, or VACV811ΔB4R and plaques were photographed at the indicated times post-infection. At two days post infection, VACVCop was already producing large round plaques. Strikingly, VACV811 was just beginning to form plaques, while cells infected with VACV811ΔB4R exhibited minuscule areas of clearing (Figure 4-4). Three days post-infection, the plaques in VACVCop increased in size, and secondary plaques were beginning to form. Compared to VACVCop, VACV811 plaques were still much smaller in size, and VACV811ΔB4R plaques were just beginning to form. In contrast, at five days post-infection, all of the cells infected with VACV had been lysed, and plaques were no longer

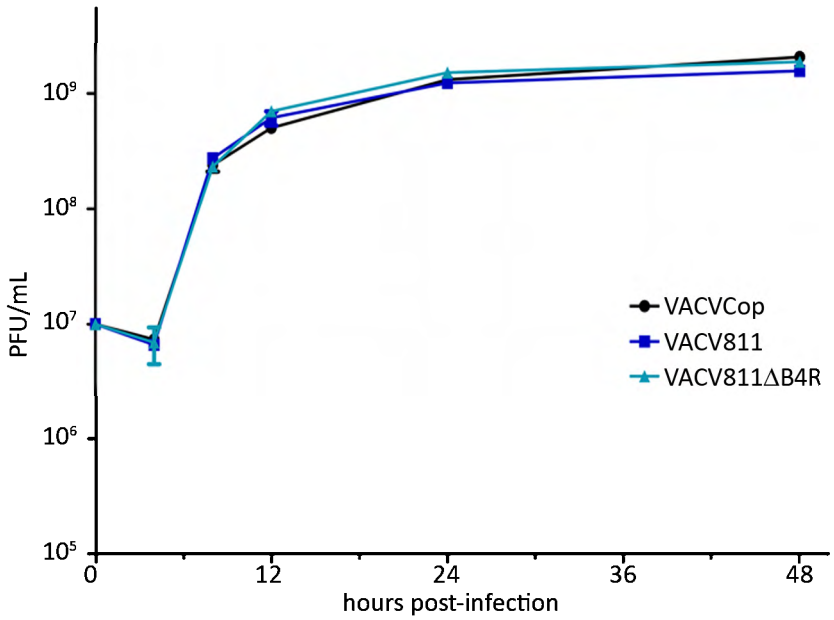

Figure 4-3. Single-step analysis of virus growth in BGMK cells indicates that VACVCop, VACV811, and VACV811ΔB4R grow equally well. BGMK cells were infected at an MOI of 10 with VACVCop, VACV811, and VACV811ΔB4R for single-step growth analysis. Infected cells were harvested up to 48 hours post-infection and lysed to release infectious virus. Serial dilutions of infectious virus were plated on BGMK cells. Infected monolayers were fixed and stained with crystal violet and plaques were counted to generate a single-step growth curve. Representative of three independent experiments with double titrations.

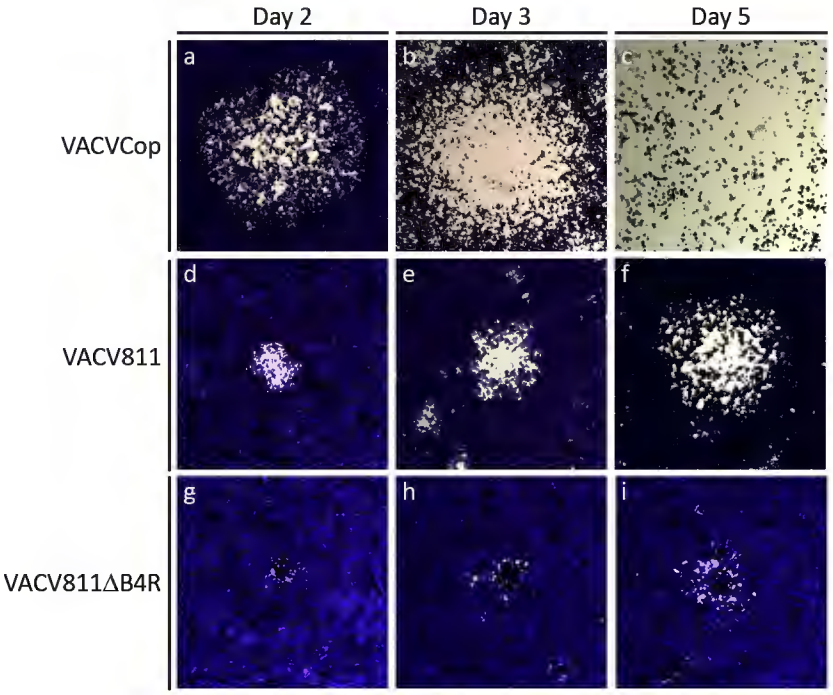

Figure 4-4. VACV811ΔB4R displays smaller plaques in BGMK cells compared to VACVCop and VACV811. BGMK cells were infected with VACVCop (a-c), VACV811 (d-f), or VACV811ΔB4R (g-i). Cells were stained with crystal violet 2 days (a, d, g), 3 days (b, e, h), or 5 days (c, f, i) post-infection.

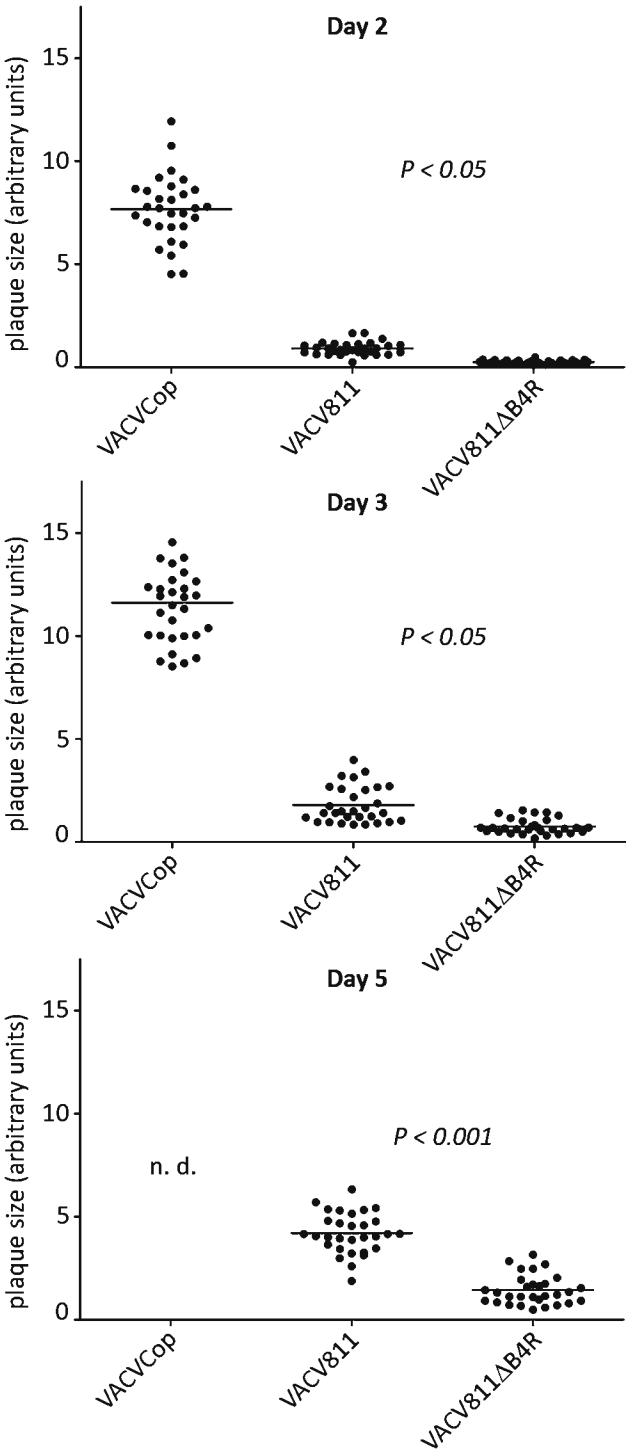

Figure 4-5. VACV811ΔB4R displays smaller plaques in BGMK cells. BGMK cells were infected and stained with crystal violet at 2, 3, and 5 days post-infection. Photographed plaques were measured using ImageJ and analyzed using GraphPad to determine significant differences in plaque size between the viruses. The difference in plaque size between VACVCop and VACV811, and VACVCop and VV811ΔB4R was significant in all cases (*P < 0.001*). Differences in plaque size between VACV811 and VACV811ΔB4R are listed above. n. d., no data.

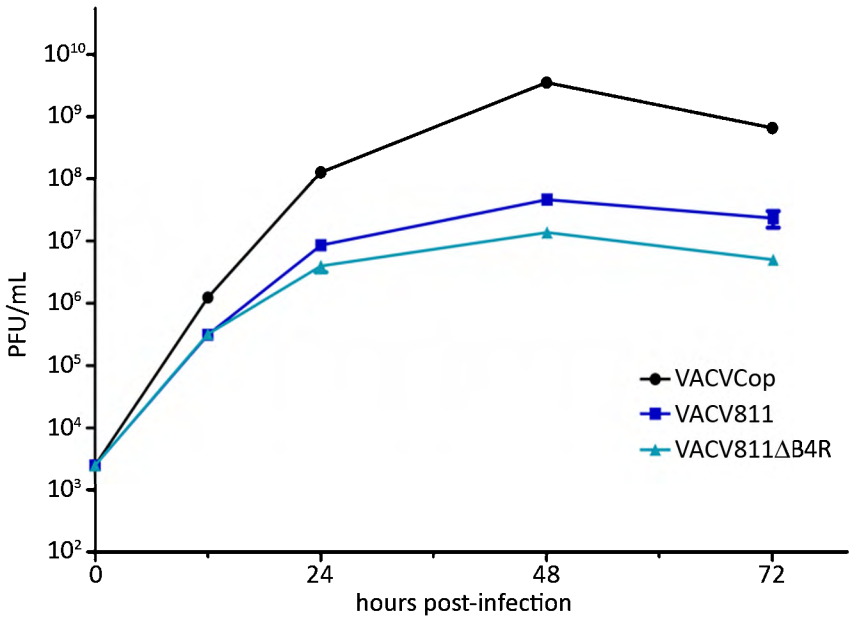

Figure 4-6. Multiple-step analysis of virus growth in BGMK cells indicates differences in growth between VACVCop, VACV811, and VACV811ΔB4R. BGMK cells were infected at an MOI of 0.01 with VACVCop, VACV811, or VACV811ΔB4R for multiple-step growth analysis. Infected cells were harvested up to 72 hours post-infection and lysed to release infectious virus. Serial dilutions of infectious virus were plated on BGMK cells. Infected monolayers were fixed and stained with crystal violet and plaques were counted to generate a multiple-step growth curve. Representative of three independent experiments with double titrations.

visible, while VACV811 had now developed large round plaques. Interestingly, plaques formed by VACV811ΔB4R were still barely visible following five days of infection. Using computer analysis we measured the plaques, and statistical testing revealed that the differences in plaque size between VACVCop and VACV811, and VACVCop and VACV811ΔB4R, were significant at all days post-infection, with a p-value of < 0.001 in all cases (Figure 4-5). The differences between VACV811 and VACV811ΔB4R at two and three days post-infection was less significant, with a p-value of < 0.05 in both cases, however at five days post-infection the differences were more significant, with a p-value of < 0.001 (Figure 4-5). To determine if the observed defect in spread affected virus replication, we performed a multiple-step growth curve (Figure 4-6). BGMK cells were infected at an MOI of 0.01 with VACVCop, VACV811, or VACV811ΔB4R. VACV811 grew to titers that were two logs lower than VACVCop, while the titers of VACV811ΔB4R were approximately half to one full log less than VACV811 (Figure 4-4). Together, these data indicated VACV811 is defective in spread compared to VACVCop, and the loss of VACVB4R from VACV811 further decreases the ability of VACV811 to spread in tissue culture.

4.2.2 VACV811ΔB4R inhibits NFκB p65 nuclear translocation

A useful approach to identify viral proteins that inhibit cell signalling pathways is to use large deletion viruses, such as VACV811 (4, 20, 48, 68). VACV811 is missing 55 ORFs that are encoded by VACVCop, and lacks known inhibitors of TNFα-induced NFκB activation, but contains A46R and A52R, which inhibit IL-1β-induced NFκB activation (43, 48). Using VACV811, our laboratory identified eighteen potential unknown inhibitors of the NFκB pathway, including VACVB4R (20). Since we have characterized ECTV154, an orthologue of VACVB4R, as in inhibitor of NFκB, we wanted to determine if deleting VACVB4R from VACV811 prevented VACV811 from inhibiting TNFα-induced NFκB activation. To do this, we used immunofluorescence microscopy to visualize the localization of the NFκB subunit p65 (Figure 4-7). HeLa cells were mock infected or infected with VACVCop, VACV811, or VACV811ΔB4R. Twelve hours post-infection, cells were stimulated with

TNFα. Cells were stained with DAPI to visualize nuclei and the DNA-rich virus factories. Staining with an antibody to NFκB p65 revealed that p65 was dispersed throughout the cytoplasm in mock-infected cells (Figure 4-7, panels a-c), whereas mock-infected cells treated with TNFα displayed dramatic accumulation of p65 in the nucleus (Figure 4-7, panels d-f) (54, 55). In contrast, cells infected with VACVCop and VACV811 displayed cytoplasmic retention of p65 following stimulation (Figure 4-7, panels g-l). Surprisingly, cells infected with VACV811ΔB4R also displayed localization of p65 in the cytoplasm following stimulation, indicating that deletion of VACVB4R did not abrogate the ability of VACV811 to inhibit NFκB activation (Figure 4-7, panels m-o). The experiment was repeated using IL-1β to stimulate the cells. Mock-infected cells that were stimulated with IL-1β displayed nuclear localization of p65 (Figure 4-8, panels d-f), while p65 remained in the cytoplasm of cells infected with VACVCop, VACV811, or VACV811ΔB4R (Figure 4-8, panels g-o).

To confirm that VACV811ΔB4R inhibited NFκB activation, we generated nuclear and cytoplasmic extracts to monitor NFκB p65 nuclear translocation. HeLa cells were mock infected, or infected VACVCop, VACV811, or VACV811ΔB4R. Twelve hours post-infection, cells were stimulated with TNFα. Nuclear and cytoplasmic extracts were immunoblotted for NFκB p65, I5L, as a control to indicate virus infection (61), and PARP and β-tubulin, as controls to indicate the purity of the nuclear and cytoplasmic fractions, respectively (39, 58). In mock-infected cells, a large amount of p65 was detected in the cytoplasm, but very low levels were detected in the nucleus (Figure 4-9). Following stimulation with TNFα, high levels of p65 were observed in the nuclear fraction, indicating that the NFκB pathway had been activated. Strikingly, infected cells subjected to stimulation with TNFα displayed minimal levels of p65 in the nuclear fraction, indicating that NFκB activation was inhibited. The experiment was repeated using IL-1β, and similar results were observed (Figure 4-10). Overall, these data indicated that deletion of VACVB4R from VACV811 does not prevent VACV811 from inhibiting TNFα and IL-1β p65 nuclear translocation.

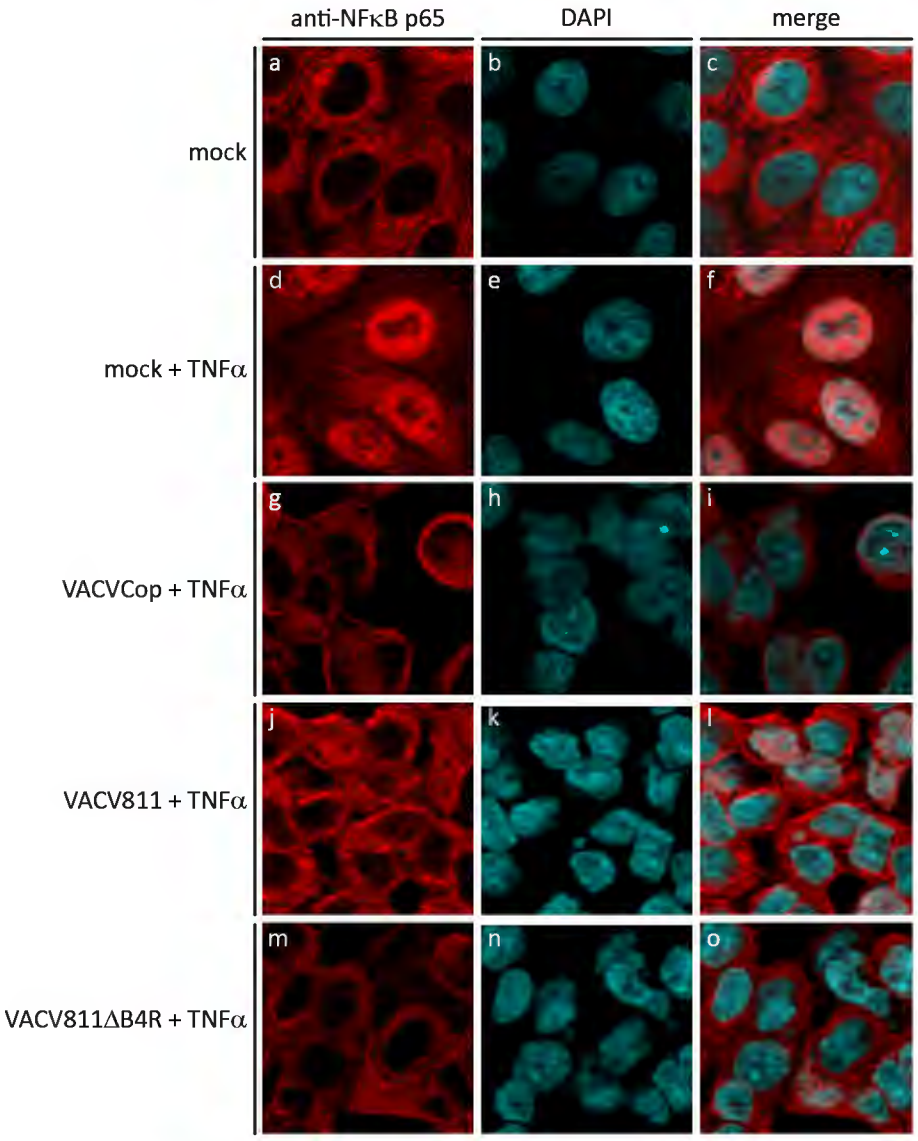

Figure 4-7. VACV811ΔB4R inhibits TNFα-stimulated NFκB p65 nuclear translocation. HeLa cells were mock-infected (a-f) or infected at an MOI of 5 with VACVCop (g-i), VACV811 (j-l), or VACV811ΔB4R (m-o). Twelve hours post-infection, cells were mock-stimulated (a-c) or stimulated with 10 ng/mL of TNFα for 20 minutes (d-o). Endogenous NFκB p65 was detected with an antibody specific for p65, and nuclei were detected with DAPI.

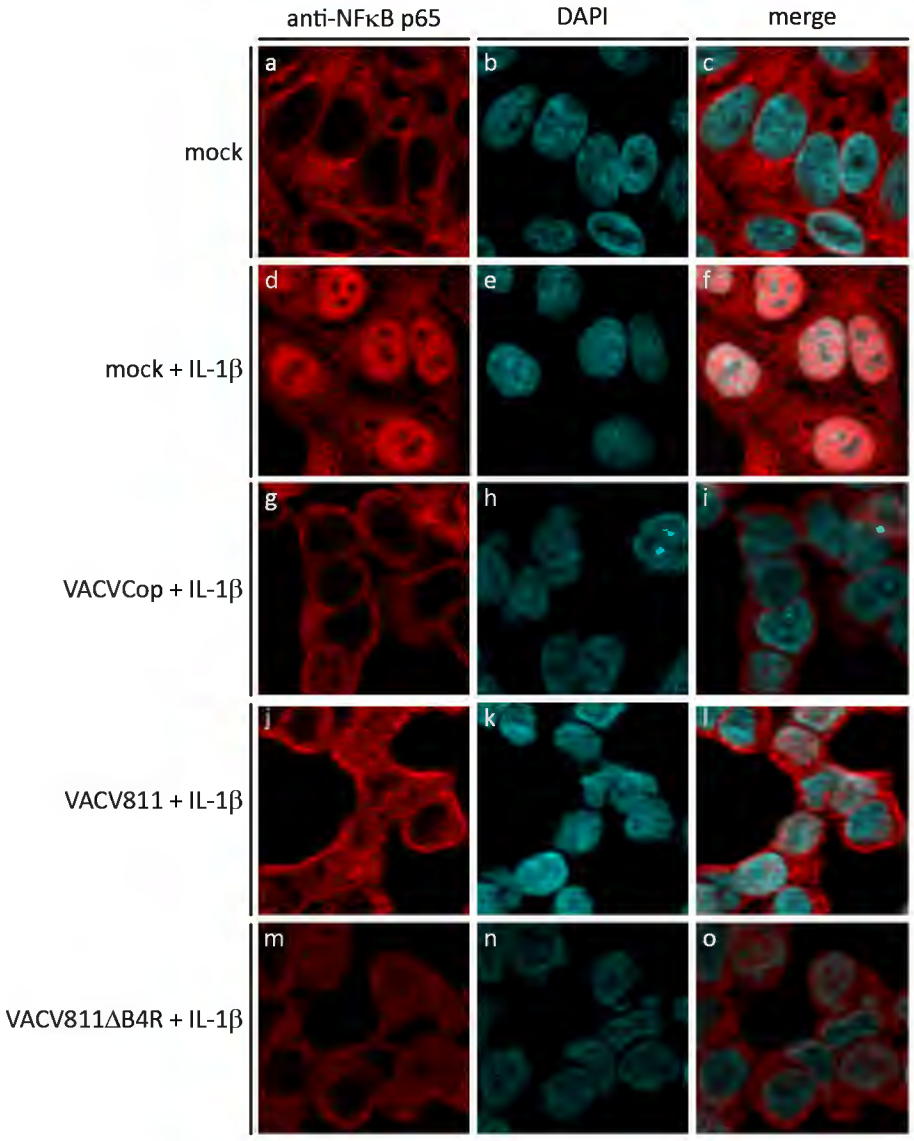

Figure 4-8. VACV811ΔB4R inhibits IL-1β-stimulated NFκB p65 nuclear translocation. HeLa cells were mock-infected (a-f) or infected at an MOI of 5 with VACVCop (g-i), VACV811 (j-l), or VACV811ΔB4R (m-o). Twelve hours post-infection, cells were mock-stimulated (a-c) or stimulated with 10 ng/mL of IL-1β for 20 minutes (d-o). Endogenous NFκB p65 was detected with an antibody specific for p65, and nuclei were detected with DAPI.

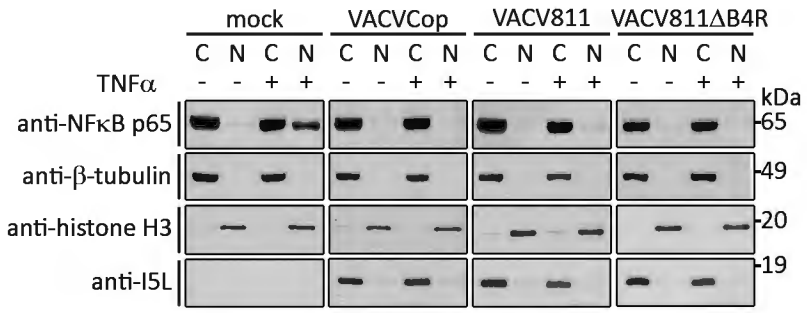

Figure 4-9. VACV811ΔB4R inhibits TNFα-induced NFκB p65 nuclear translocation. HeLa cells were mock infected or infected at an MOI of 5 with VACV, VACV811, or VACV811ΔB4R. Twelve hours post-infection, cells were mock stimulated or stimulated with 10 ng/mL of TNFα for 20 minutes. Cytoplasmic and nuclear extracts were immunoblotted for endogenous NFκB p65, β-tubulin as a control for cytoplasmic extracts, histone H3 as a control for nuclear extracts, and I5L as a control to indicate that infection had occured.

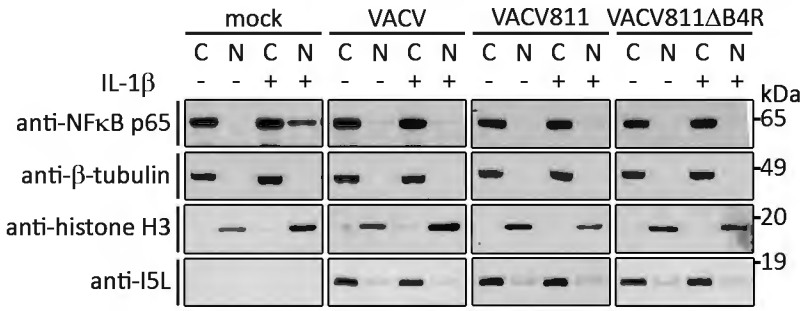

Figure 4-10. VACV811ΔB4R inhibits IL-1β-induced NFκB p65 nuclear translocation. HeLa cells were mock infected or infected at an MOI of 5 with VACV, VACV811, or VACV811ΔB4R. Twelve hours post-infection, cells were mock stimulated or stimulated with 10 ng/mL of IL-1β for 20 minutes. Cytoplasmic and nuclear extracts were immunoblotted for endogenous NFκB p65, β-tubulin as a control for cytoplasmic extracts, histone H3 as a control for nuclear extracts, and I5L as a control to indicate that infection had occured.

4.2.3 Deletion of VACVB4R from VACV811 does not prevent late gene expression

Ank/F-box proteins have been characterized in a number of poxviruses (10, 11, 63, 67). The large deletion virus MVA is an attenuated form of VACV that is growth restricted in many human and mammalian cell lines (18, 42). MVA only possesses one Ank/F-box protein, 68k-ank, which is an orthologue of ECTV165. Interestingly, deleting 68k-ank from MVA results in decreased production of intermediate and late viral proteins, suggesting that the presence of 68k-ank is important for productive infection (63). Since VACV811 only possesses one Ank/F-box protein, VACVB4R, we investigated whether deletion of VACVB4R affected production of intermediate and late viral proteins. To monitor levels of late protein expression following infection, we used immunoblotting (Figure 4-11). RK13 cells were infected with VACVCop, VACV811, or VACV811ΔB4R and whole cell lysates were collected at the indicated times post-infection. Samples were immunoblotted for E3L, a VACVCop protein that is expressed early during infection, and B5R, A34R, and I5L, which are expressed late during infection (5, 9). In cells infected with VACV and VACV811, E3L accumulated almost immediately, and the late proteins B5R, A34R, and I5L began accumulating 3 hours post-infection (Figure 4-11). In cells infected with VACV811ΔB4R, patterns of protein accumulation were similar to those of VACV and VACV811, indicating that deletion of VACVB4R does not affect late protein expression (Figure 4-11).

4.3 DISCUSSION

The NFκB pathway is an important regulator of the antiviral response (28, 29, 66). Importantly, a number of inhibitors of the NFκB pathway have been identified in poxviruses, including A52R, A46R, K7L, N1L, B14R, K1L, M2L, and E3L (43, 49). However, recent data from our lab suggests that VACV, the prototypic poxvirus, encodes additional inhibitors of the NFκB pathway (20) (Table 4-1). Of the eighteen potential inhibitors that we identified, we chose to focus on VACVB4R, since we had previously demonstrated that its orthologue in ECTV, ECTV154, inhibits NFκB activation (Chapter

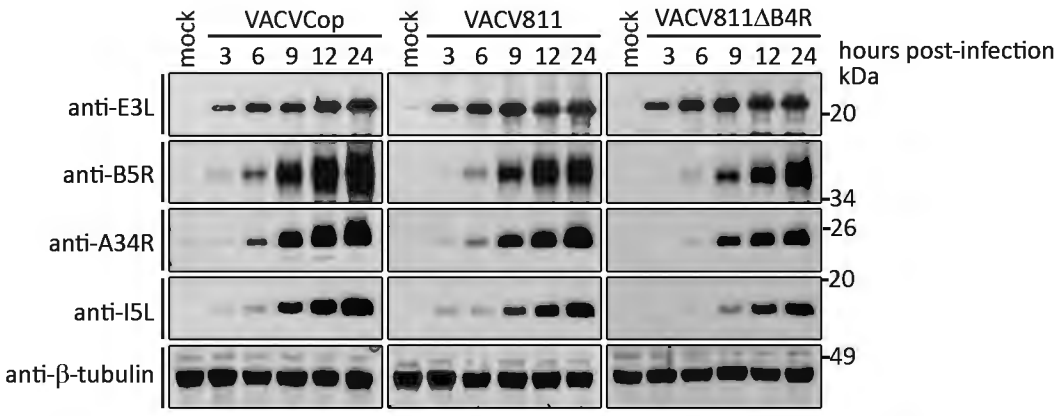

Figure 4-11. Expression of late proteins occurs during VV811ΔB4R infection. RK13 cells were infected with VACVCop, VACV811, or VACV811ΔB4R at an MOI of 5. Whole cell lystates were harvested at the indicated times post-infection and immunoblotted for the early protein E3L, the late proteins B5R, A34R, and I5L, and b-tubulin as a loading control.

Table 4-1. Open reading frames present in VACV811 and absent from MVA

ORF	Expression	Characteristics	Putative Function	Reference
F11L	Early	Binds RhoA	Involved in viral transcription and elongation; inhibits RhoA signalling; involved in morphogenesis and cell motility;	(34, 39)
F5L	Early	Membrane protein	Major membrane protein	(53)
O1L	Early	Contains leucine zipper and nuclear target sequence	Unknown	(22)
A25R	Unknown	Pseudogene	Cowpox A-type inclusion protein	None available
A26R	Late	Structural protein; present in IMV	Involved in IMV movement within the cell; may be involved in morphogenesis and dissemination	(14, 41)
A39R	Late	Semaphorin-like; secreted glycoprotein	Immune modulator; induces IL-6 and IL-8 secretion	(15)
A40R	Early	C-type lectin-like type II membrane protein	Unknown	(69)
A42R	Late	Profilin homolog, present in IMV	Possibly involved in phosphoinositide metabolism	(7, 14, 39, 58)
A43R	Late	Type I transmembrane protein; localizes to Golgi and plasma membranes	Unknown; reduced size of skin lesions in mice infected with A43R knockout	(60)
A45R	Late	Superoxide dismutase homolog; present in IMV core	Unknown; inactive Cu-Zn superoxide dismutase	(3, 58)
A51R	Unknown	Unknown	Unknown	None available
A53R	Gene Fragment	Secreted TNFR-like protein	Non-functional TNFR homolog	(1)
A54R	Early	Unknown	Unknown	None available
A55R	Early	BTB-Kelch protein; interacts with functional cullin-3 based ubiquitin ligase	Unknown	(70)
A57R	Early/late	Guanylate kinase homolog	Unknown	(58)
B2R	Early	Schlafen homolog	Unknown, may be involved in regulation of virus virulence	(24)
B4R	Late	Ank/F-box protein; interacts with functional cullin-1 based ubiquitin ligase	Unknown	(67)
B8R	Early	Interferon gamma receptor homolog	Secreted interferon gamma receptor	(2)

RhoA, Ras homolgue gene family member A; IMV, intracellular mature virus; TNFR, tumour necrosis factor receptor; BTB, Bric-a-Brac, Tramtrack, Broad complex. (Adapted from K. Fagan-Garcia).

3). In order to understand the function of VACVB4R during virus infection, we created a deletion virus, VACV811ΔB4R, which is missing the VACVB4R ORF. Interestingly, when we used single-step growth analysis to assess synthesis of infectious virus, there was no attenuation VACV811 or VACV811ΔB4R compared to VACVCop (Figure 4-3). Since VACV811 is missing 55 ORFs, including many important modulators of the immune response, we were surprised that levels of VACV811 and VACV811ΔB4R were comparable to VACVCop. In contrast, we were less surprised to see no difference in between VACV811 and VACV811ΔB4R, since deletion of a single immune modulator from poxviruses does not typically have a detrimental effect to growth properties *in vitro* (25, 44). Perhaps if we repeated our single-step growth analysis using cells that are restrictive to VACV811 growth, we would observe decreases in the replicative capacity of VACV811 compared to VACVCop. In restrictive cell lines, poxviruses are able to enter the cell, but cell-type-specific blockages prevent the virus from completing its life cycle (40). Unfortunately, VACV can replicate in almost all cell lines with the exception of two hamster cell lines, CHO and MDBK, so finding a restrictive cell line proved difficult (31). We also assessed whether late gene expression occurred during infection with VACV811ΔB4R (Figure 4-11). A paper published by Sperling *et al* prompted us to look at late gene expression, since deletion of the Ank/F-box protein, 68k-Ank, from MVA abrogated late gene expression (63). The caveat to this experiment was that a defect in late gene expression was only observed in restrictive cell lines (63). However many cell lines are restrictive to MVA, so this was not a problem (4, 42). In contrast to MVA, very few cell lines are restrictive to VACV growth (31). In order to perform this experiment, we required a restrictive cell line. CHO cells could not be used since they are so restrictive to VACV that late gene expression does not occur (50), and MDBK cells were not available to us. Instead, we hypothesized that the rabbit cell line, RK13, might be restrictive to VACV811 since VACV811 is missing the ORF K1L, which was previously demonstrated to be important for replication of VACV in RK13 cells (51, 64). However, late gene expression did occur in RK13 cells following infection with VACV811ΔB4R, indicating that deletion of VACVB4R did not abrogate expression of late gene in RK13

cells (Figure 4-11). This data further demonstrated that VACV811ΔB4R is not defective in producing infectious virions.

Interestingly, we did observe a small plaque phenotype for VACV811 and VACV811ΔB4R, compared to VACVCop (Figures 4-4 and 4-5). The differences in plaque sizes between VACV811 and VACV811ΔB4R were also significant, suggesting that VACVB4R might be important for virion release or spread (Figures 4-4 and 4-5). The small plaque phenotypes of VACV811 and VACV811ΔB4R prompted us to perform multiple-step growth analysis, which further confirmed that VACV811 and VACV811ΔB4R have decreased efficiency in release or spread (Figure 4-6). Importantly, B5R, which is next to the VACVB4R in the VACV genome, is important for EV formation and deletion of B5R results in a small plaque phenotype (19). We were able to conclude that the decrease in plaque size in VACV811ΔB4R was not associated with decreased expression of B5R, since B5R is expressed during VACV811ΔB4R infection (Figure 4-11).

Since VACV811 is missing all of the currently known inhibitors of TNFα-induced NFκB activation (43, 48), we expected that deletion of VACVB4R would prevent VACV811 from inhibiting NFκB activation. However, VACV811ΔB4R still inhibited NFκB activation induced by TNFα (Figures 4-5 and 4-7) and IL-1β (Figures 4-6 and 4-8). Since VACV811 is missing so many inhibitors, including all of the Ank/F-box proteins, we expected a shift in NFκB inhibition by deleting VACVB4R. These data suggest that there are still additional unidentified inhibitors of the NFκB pathway in VACVCop. Preliminary data from our lab suggests that one of the 18 potential inhibitors that we identified, A55R, inhibits NFκB activation (Table 4-1). The orthologue of A55R in ECTV, ECTV150, is a BTB-Kelch protein that associates with a cullin-3-based E3 ubiquitin ligase during infection (70). Significantly, although ECTV150 inhibits p65 nuclear translocation, it is unable to prevent degradation of IκBα, suggesting that A55R is not the protein that prevents degradation of IκBα. Though we suspect that VACVB4R is responsible for blocking

degradation of IκBα, additional experiments need to be performed to confirm that there are no other proteins that prevent IκBα degradation.

In conclusion, we used the deletion virus VACV811ΔB4R to demonstrate that additional inhibitors of the NFκB pathway exist in the genome of VACVCop. We also demonstrated that deletion of VACVB4R decreases the ability of VACV811 to spread efficiently in tissue culture. Since VACVB4R did not decrease replicative capacity of VACV811 or reduce late gene expression, it is possible that VACVB4R is important for EV release or spread. Further experiments to identify potential substrates of VACVB4R, and to identify where in the VACV lifecycle VACVB4R plays a role will be important to understand more about the function of this protein.

4.4 REFERENCES

1. **Alcami, A., A. Khanna, N. L. Paul, and G. L. Smith.** 1999. Vaccinia virus strains Lister, USSR and Evans express soluble and cell-surface tumour necrosis factor receptors. J Gen Virol **80 (Pt 4):**949-59.
2. **Alcami, A., and G. L. Smith.** 1995. Vaccinia, cowpox, and camelpox viruses encode soluble gamma interferon receptors with novel broad species specificity. J Virol **69:**4633-9.
3. **Almazan, F., D. C. Tscharke, and G. L. Smith.** 2001. The vaccinia virus superoxide dismutase-like protein (A45R) is a virion component that is nonessential for virus replication. J Virol **75:**7018-29.
4. **Antoine, G., F. Scheiflinger, F. Dorner, and F. G. Falkner.** 1998. The complete genomic sequence of the modified vaccinia Ankara strain: comparison with other orthopoxviruses. Virology **244:**365-96.
5. **Assarsson, E., J. A. Greenbaum, M. Sundstrom, L. Schaffer, J. A. Hammond, V. Pasquetto, C. Oseroff, R. C. Hendrickson, E. J. Lefkowitz, D. C. Tscharke, J. Sidney, H. M. Grey, S. R. Head, B. Peters, and A. Sette.** 2008. Kinetic analysis of a complete poxvirus transcriptome reveals an immediate-early class of genes. Proc Natl Acad Sci U S A **105:**2140-5.
6. **Barry, M., N. van Buuren, K. Burles, K. Mottet, Q. Wang, and A. Teale.** 2010. Poxvirus exploitation of the ubiquitin-proteasome system. Viruses **2:**2356-80.
7. **Blasco, R., N. B. Cole, and B. Moss.** 1991. Sequence analysis, expression, and deletion of a vaccinia virus gene encoding a homolog of profilin, a eukaryotic actin-binding protein. J Virol **65:**4598-608.
8. **Bowie, A., E. Kiss-Toth, J. A. Symons, G. L. Smith, S. K. Dower, and L. A. O'Neill.** 2000. A46R and A52R from vaccinia virus are antagonists of host IL-1 and toll-like receptor signaling. Proc Natl Acad Sci U S A **97:**10162-7.
9. **Broyles, S. S.** 2003. Vaccinia virus transcription. J Gen Virol **84:**2293-303.
10. **Camus-Bouclainville, C., L. Fiette, S. Bouchiha, B. Pignolet, D. Counor, C. Filipe, J. Gelfi, and F. Messud-Petit.** 2004. A virulence factor of myxoma virus colocalizes with NF-kappaB in the nucleus and interferes with inflammation. J Virol **78:**2510-6.
11. **Chang, S. J., J. C. Hsiao, S. Sonnberg, C. T. Chiang, M. H. Yang, D. L. Tzou, A. A. Mercer, and W. Chang.** 2009. Poxvirus host range protein CP77 contains an F-box-like domain that is necessary to suppress NF-kappaB activation by tumor necrosis factor alpha but is independent of its host range function. J Virol **83:**4140-52.
12. **Chen, R. A., N. Jacobs, and G. L. Smith.** 2006. Vaccinia virus strain Western Reserve protein B14 is an intracellular virulence factor. J Gen Virol **87:**1451-8.
13. **Chen, R. A., G. Ryzhakov, S. Cooray, F. Randow, and G. L. Smith.** 2008. Inhibition of IkappaB kinase by vaccinia virus virulence factor B14. PLoS Pathog **4:**e22.

14. **Chung, C. S., C. H. Chen, M. Y. Ho, C. Y. Huang, C. L. Liao, and W. Chang.** 2006. Vaccinia virus proteome: identification of proteins in vaccinia virus intracellular mature virion particles. J Virol **80:**2127-40.
15. **Comeau, M. R., R. Johnson, R. F. DuBose, M. Petersen, P. Gearing, T. VandenBos, L. Park, T. Farrah, R. M. Buller, J. I. Cohen, L. D. Strockbine, C. Rauch, and M. K. Spriggs.** 1998. A poxvirus-encoded semaphorin induces cytokine production from monocytes and binds to a novel cellular semaphorin receptor, VESPR. Immunity **8:**473-82.
16. **DeFilippes, F. M.** 1982. Restriction enzyme mapping of vaccinia virus DNA. J Virol **43:**136-49.
17. **DiPerna, G., J. Stack, A. G. Bowie, A. Boyd, G. Kotwal, Z. Zhang, S. Arvikar, E. Latz, K. A. Fitzgerald, and W. L. Marshall.** 2004. Poxvirus protein N1L targets the I-kappaB kinase complex, inhibits signaling to NF-kappaB by the tumor necrosis factor superfamily of receptors, and inhibits NF-kappaB and IRF3 signaling by toll-like receptors. J Biol Chem **279:**36570-8.
18. **Drexler, I., K. Heller, B. Wahren, V. Erfle, and G. Sutter.** 1998. Highly attenuated modified vaccinia virus Ankara replicates in baby hamster kidney cells, a potential host for virus propagation, but not in various human transformed and primary cells. J Gen Virol **79 (Pt 2):**347-52.
19. **Engelstad, M., and G. L. Smith.** 1993. The vaccinia virus 42-kDa envelope protein is required for the envelopment and egress of extracellular virus and for virus virulence. Virology **194:**627-37.
20. **Fagan-Garcia, K., and M. Barry.** 2011. A vaccinia virus deletion mutant reveals the presence of additional inhibitors of NF-kappaB. J Virol **85:**883-94.
21. **Gedey, R., X. L. Jin, O. Hinthong, and J. L. Shisler.** 2006. Poxviral regulation of the host NF-kappaB response: the vaccinia virus M2L protein inhibits induction of NF-kappaB activation via an ERK2 pathway in virus-infected human embryonic kidney cells. J Virol **80:**8676-85.
22. **Goebel, S. J., G. P. Johnson, M. E. Perkus, S. W. Davis, J. P. Winslow, and E. Paoletti.** 1990. The complete DNA sequence of vaccinia virus. Virology **179:**247-66, 517-63.
23. **Graham, S. C., M. W. Bahar, S. Cooray, R. A. Chen, D. M. Whalen, N. G. Abrescia, D. Alderton, R. J. Owens, D. I. Stuart, G. L. Smith, and J. M. Grimes.** 2008. Vaccinia virus proteins A52 and B14 Share a Bcl-2-like fold but have evolved to inhibit NF-kappaB rather than apoptosis. PLoS Pathog **4:**e1000128.
24. **Gubser, C., R. Goodbody, A. Ecker, G. Brady, L. A. O'Neill, N. Jacobs, and G. L. Smith.** 2007. Camelpox virus encodes a schlafen-like protein that affects orthopoxvirus virulence. J Gen Virol **88:**1667-76.
25. **Gubser, C., S. Hue, P. Kellam, and G. L. Smith.** 2004. Poxvirus genomes: a phylogenetic analysis. J Gen Virol **85:**105-17.
26. **Harte, M. T., I. R. Haga, G. Maloney, P. Gray, P. C. Reading, N. W. Bartlett, G. L. Smith, A. Bowie, and L. A. O'Neill.** 2003. The poxvirus protein A52R targets Toll-like receptor signaling complexes to suppress host defense. J Exp Med **197:**343-51.

27. **Hatakeyama, S., M. Kitagawa, K. Nakayama, M. Shirane, M. Matsumoto, K. Hattori, H. Higashi, H. Nakano, K. Okumura, K. Onoe, and R. A. Good.** 1999. Ubiquitin-dependent degradation of IkappaBalpha is mediated by a ubiquitin ligase Skp1/Cul 1/F-box protein FWD1. Proc Natl Acad Sci U S A **96:**3859-63.
28. **Hayden, M. S., and S. Ghosh.** 2012. NF-kappaB, the first quarter-century: remarkable progress and outstanding questions. Genes Dev **26:**203-34.
29. **Hayden, M. S., and S. Ghosh.** 2008. Shared principles in NF-kappaB signaling. Cell **132:**344-62.
30. **Hinthong, O., X. L. Jin, and J. L. Shisler.** 2008. Characterization of wild-type and mutant vaccinia virus M2L proteins' abilities to localize to the endoplasmic reticulum and to inhibit NF-kappaB activation during infection. Virology **373:**248-62.
31. **Hruby, D. E., D. L. Lynn, R. C. Condit, and J. R. Kates.** 1980. Cellular differences in the molecular mechanisms of vaccinia virus host range restriction. J Gen Virol **47:**485-8.
32. **Johnston, J. B., and G. McFadden.** 2003. Poxvirus immunomodulatory strategies: current perspectives. J Virol **77:**6093-100.
33. **Karin, M., and Y. Ben-Neriah.** 2000. Phosphorylation meets ubiquitination: the control of NF-[kappa]B activity. Annu Rev Immunol **18:**621-63.
34. **Kato, S. E., F. A. Greco, C. R. Damaso, R. C. Condit, and N. Moussatche.** 2004. An alternative genetic method to test essential vaccinia virus early genes. J Virol Methods **115:**31-40.
35. **Kroll, M., F. Margottin, A. Kohl, P. Renard, H. Durand, J. P. Concordet, F. Bachelerie, F. Arenzana-Seisdedos, and R. Benarous.** 1999. Inducible degradation of IkappaBalpha by the proteasome requires interaction with the F-box protein h-betaTrCP. J Biol Chem **274:**7941-5.
36. **Larkin, M. A., G. Blackshields, N. P. Brown, R. Chenna, P. A. McGettigan, H. McWilliam, F. Valentin, I. M. Wallace, A. Wilm, R. Lopez, J. D. Thompson, T. J. Gibson, and D. G. Higgins.** 2007. Clustal W and Clustal X version 2.0. Bioinformatics **23:**2947-8.
37. **Lefkowitz, E. J., C. Upton, S. S. Changayil, C. Buck, P. Traktman, and R. M. Buller.** 2005. Poxvirus Bioinformatics Resource Center: a comprehensive Poxviridae informational and analytical resource. Nucleic Acids Res **33:**D311-6.
38. **Lynch, H. E., C. A. Ray, K. L. Oie, J. J. Pollara, I. T. Petty, A. J. Sadler, B. R. Williams, and D. J. Pickup.** 2009. Modified vaccinia virus Ankara can activate NF-kappaB transcription factors through a double-stranded RNA-activated protein kinase (PKR)-dependent pathway during the early phase of virus replication. Virology **391:**177-86.
39. **Machesky, L. M., N. B. Cole, B. Moss, and T. D. Pollard.** 1994. Vaccinia virus expresses a novel profilin with a higher affinity for polyphosphoinositides than actin. Biochemistry **33:**10815-24.
40. **McFadden, G.** 2005. Poxvirus tropism. Nat Rev Microbiol **3:**201-13.

41. **McKelvey, T. A., S. C. Andrews, S. E. Miller, C. A. Ray, and D. J. Pickup.** 2002. Identification of the orthopoxvirus p4c gene, which encodes a structural protein that directs intracellular mature virus particles into A-type inclusions. J Virol **76:**11216-25.
42. **Meyer, H., G. Sutter, and A. Mayr.** 1991. Mapping of deletions in the genome of the highly attenuated vaccinia virus MVA and their influence on virulence. J Gen Virol **72 (Pt 5):**1031-8.
43. **Mohamed, M. R., and G. McFadden.** 2009. NFkB inhibitors: strategies from poxviruses. Cell Cycle **8:**3125-32.
44. **Moss, B.** 2007. *Poxviridae:* The Viruses and Their Replication. *In* D. M. K. a. P. M. Howley (ed.), Fields Virology 5ed.
45. **Moss, B., and J. L. Shisler.** 2001. Immunology 101 at poxvirus U: immune evasion genes. Semin Immunol **13:**59-66.
46. **Myskiw, C., J. Arsenio, R. van Bruggen, Y. Deschambault, and J. Cao.** 2009. Vaccinia virus E3 suppresses expression of diverse cytokines through inhibition of the PKR, NF-kappaB, and IRF3 pathways. J Virol **83:**6757-68.
47. **Osborn, L., S. Kunkel, and G. J. Nabel.** 1989. Tumor necrosis factor alpha and interleukin 1 stimulate the human immunodeficiency virus enhancer by activation of the nuclear factor kappa B. Proc Natl Acad Sci U S A **86:**2336-40.
48. **Perkus, M. E., S. J. Goebel, S. W. Davis, G. P. Johnson, E. K. Norton, and E. Paoletti.** 1991. Deletion of 55 open reading frames from the termini of vaccinia virus. Virology **180:**406-10.
49. **Rahman, M. M., and G. McFadden.** 2011. Modulation of NF-kappaB signalling by microbial pathogens. Nat Rev Microbiol **9:**291-306.
50. **Ramsey-Ewing, A., and B. Moss.** 1995. Restriction of vaccinia virus replication in CHO cells occurs at the stage of viral intermediate protein synthesis. Virology **206:**984-93.
51. **Ramsey-Ewing, A. L., and B. Moss.** 1996. Complementation of a vaccinia virus host-range K1L gene deletion by the nonhomologous CP77 gene. Virology **222:**75-86.
52. **Rintoul, J. L., J. Wang, D. B. Gammon, N. J. van Buuren, K. Garson, K. Jardine, M. Barry, D. H. Evans, and J. C. Bell.** 2011. A selectable and excisable marker system for the rapid creation of recombinant poxviruses. PLoS One **6:**e24643.
53. **Roseman, N. A., and M. B. Slabaugh.** 1990. The vaccinia virus HindIII F fragment: nucleotide sequence of the left 6.2 kb. Virology **178:**410-8.
54. **Salminen, A., T. Paimela, T. Suuronen, and K. Kaarniranta.** 2008. Innate immunity meets with cellular stress at the IKK complex: regulation of the IKK complex by HSP70 and HSP90. Immunol Lett **117:**9-15.
55. **Schroder, M., M. Baran, and A. G. Bowie.** 2008. Viral targeting of DEAD box protein 3 reveals its role in TBK1/IKKepsilon-mediated IRF activation. EMBO J **27:**2147-57.
56. **Seet, B. T., J. B. Johnston, C. R. Brunetti, J. W. Barrett, H. Everett, C. Cameron, J. Sypula, S. H. Nazarian, A. Lucas, and G. McFadden.** 2003. Poxviruses and immune evasion. Annu Rev Immunol **21:**377-423.

57. **Shisler, J. L., and X. L. Jin.** 2004. The vaccinia virus K1L gene product inhibits host NF-kappaB activation by preventing IkappaBalpha degradation. J Virol **78:**3553-60.
58. **Smith, G. L., Y. S. Chan, and S. T. Howard.** 1991. Nucleotide sequence of 42 kbp of vaccinia virus strain WR from near the right inverted terminal repeat. J Gen Virol **72 (Pt 6):**1349-76.
59. **Solt, L. A., and M. J. May.** 2008. The IkappaB kinase complex: master regulator of NF-kappaB signaling. Immunol Res **42:**3-18.
60. **Sood, C. L., and B. Moss.** 2010. Vaccinia virus A43R gene encodes an orthopoxvirus-specific late non-virion type-1 membrane protein that is dispensable for replication but enhances intradermal lesion formation. Virology **396:**160-8.
61. **Sood, C. L., J. M. Ward, and B. Moss.** 2008. Vaccinia virus encodes I5, a small hydrophobic virion membrane protein that enhances replication and virulence in mice. J Virol **82:**10071-8.
62. **Spencer, E., J. Jiang, and Z. J. Chen.** 1999. Signal-induced ubiquitination of IkappaBalpha by the F-box protein Slimb/beta-TrCP. Genes Dev **13:**284-94.
63. **Sperling, K. M., A. Schwantes, C. Staib, B. S. Schnierle, and G. Sutter.** 2009. The orthopoxvirus 68-kilodalton ankyrin-like protein is essential for DNA replication and complete gene expression of modified vaccinia virus Ankara in nonpermissive human and murine cells. J Virol **83:**6029-38.
64. **Sutter, G., A. Ramsey-Ewing, R. Rosales, and B. Moss.** 1994. Stable expression of the vaccinia virus K1L gene in rabbit cells complements the host range defect of a vaccinia virus mutant. J Virol **68:**4109-16.
65. **Thompson, J. D., D. G. Higgins, and T. J. Gibson.** 1994. CLUSTAL W: improving the sensitivity of progressive multiple sequence alignment through sequence weighting, position-specific gap penalties and weight matrix choice. Nucleic Acids Res **22:**4673-80.
66. **Vallabhapurapu, S., and M. Karin.** 2009. Regulation and function of NF-kappaB transcription factors in the immune system. Annu Rev Immunol **27:**693-733.
67. **van Buuren, N., B. Couturier, Y. Xiong, and M. Barry.** 2008. Ectromelia virus encodes a novel family of F-box proteins that interact with the SCF complex. J Virol **82:**9917-27.
68. **Wasilenko, S. T., T. L. Stewart, A. F. Meyers, and M. Barry.** 2003. Vaccinia virus encodes a previously uncharacterized mitochondrial-associated inhibitor of apoptosis. Proc Natl Acad Sci U S A **100:**14345-50.
69. **Wilcock, D., S. A. Duncan, P. Traktman, W. H. Zhang, and G. L. Smith.** 1999. The vaccinia virus A4OR gene product is a nonstructural, type II membrane glycoprotein that is expressed at the cell surface. J Gen Virol **80 (Pt 8):**2137-48.
70. **Wilton, B. A., S. Campbell, N. Van Buuren, R. Garneau, M. Furukawa, Y. Xiong, and M. Barry.** 2008. Ectromelia virus BTB/kelch proteins, EVM150 and EVM167, interact with cullin-3-based ubiquitin ligases. Virology **374:**82-99.

Chapter 5: Discussion

5.1 SUMMARY OF RESULTS

Current evidence indicates that poxviruses exploit the ubiquitin-proteasome system (6). A number of modulators of the ubiquitin-proteasome system have been identified in poxviruses; however, this project focused on characterizing a family of substrate adapter proteins for the SCF ubiquitin ligase. Previously, our lab demonstrated that four Ank/F-box proteins in ECTV, ECTV002, ECTV005, ECTV154, and ECTV165, associate with the SCF ubiquitin ligase (91). Here, we have shown the ECTV Ank/F-box proteins inhibit nuclear translocation of the NFκB subunit p65. Inhibition is dependent on the F-box domain, suggesting that ECTV002, ECTV005, ECTV154, and ECTV165 inhibit NFκB through modulation of the SCF ubiquitin ligase. We also demonstrated that expression of the ECTV Ank/F-box proteins prevents degradation of IκBα. Together, our data suggest that ECTV002, ECTV005, ECTV154, and ECTV165 inhibit IκBα degradation and NFκB activation via regulation of the ubiquitin-proteasome system. In addition, we demonstrated that deleting a single Ank/F-box protein from ECTV did not affect the ability of the virus to inhibit NFκB activation, indicating that many NFκB inhibitors are present in ECTV. To study ECTV154 in a context where all known inhibitors of TNFα-induced NFκB activation are absent, including all of the Ank/F-box proteins, we used the large deletion virus VACV811. We deleted the orthologue of ECTV154, VACVB4R, from VACV811 and assessed the ability of the virus to inhibit NFκB activation. We demonstrated that VACV811ΔB4R still inhibited NFκB activation, indicating that additional unidentified inhibitors of the NFκB pathway exist in VACV. Interestingly, we observed that ECTV and VACV811 missing ECTV002 or ECTV154/VACVB4R exhibit a small plaque phenotype, suggesting that ECTV002 and ECTV154/VACVB4R might be important for virion release or spread.

5.2 POXVIRUS MODULATION OF THE UBIQUITIN-PROTEASOME SYSTEM

One of the most notable features of poxviruses is their ability to manipulate cell signalling pathways (6, 47, 68, 79). Significantly, a number of regulators of the ubiquitin-proteasome system have been identified in poxviruses, including poxvirus-encoded

ubiquitin molecules, ubiquitin ligases, and substrate adapter proteins (6). Since poxviruses modulate the ubiquitin-proteasome system in so many ways, it is clear that these viruses rely heavily on the ubiquitin-proteasome system during infection. To corroborate this, the ubiquitin-proteasome system is fully functional during infection with VACV (30). Furthermore, poxviruses require a functional ubiquitin-proteasome system for productive infection, since inhibition of the proteasome during orthopoxvirus infection results in a block in DNA replication and late gene synthesis (77, 88). This section will describe the ubiquitin modulators encoded by poxviruses. Notably, the functions of many of these ubiquitin modulators are undetermined, highlighting the importance of studying poxvirus-encoded ubiquitin molecules, ubiquitin ligases, and substrate adapter proteins.

A few members of the *Poxviridae* family, including canarypox virus, *Melanoplus sanguinipes*, and *Amsacta moorei*, encode homologues of cellular ubiquitin (2, 8, 89). However, the importance of ubiquitin molecules encoded by poxviruses has not been determined. A virus-encoded ubiquitin gene has also been indentified *Autographa californica* nuclear polyhedrosis (AcNPV), a member of the *Baculoviridae* family of dsDNA viruses that infect insects (75). Disruption of the ubiquitin gene in AcNPV has no effect on virus viability; however, a decrease in virion budding and total infectious particles is observed (75). Whether poxvirus-encoded ubiquitin molecules are required for production of infectious particles remains to be determined. Although most poxviruses do not encode their own ubiquitin genes, ubiquitin is associated with the virion. Proteomic analysis of VACV indicates that ubiquitin accounts for approximately 3% of total virion protein (22). Additionally, a lipid-modified form of ubiquitin is associated with several viruses (37, 75, 92). For example, AcNPV, African swine fever virus, herpes simplex virus, and VACV incorporate lipid-modified ubiquitin in their envelopes (22, 37, 75, 92). Previous analysis of AcNPV demonstrated that the lipid-modified ubiquitin was host derived (75). Scavenging ubiquitin from the host may represent another strategy used by poxviruses to increase the levels of ubiquitin

available during infection. Alternatively, lipid-modified ubiquitin may exist in cell membranes for a cellular function, such as autophagosome formation, and the virus simply acquires it passively during envelope acquisition. Whether other poxviruses have lipid-modified ubiquitin incorporated into their envelopes has not been studied. Alternatively, viral-encoded ubiquitin homologues might be present to inhibit the ubiquitin-proteasome system. The ubiquitin molecule encoded by AcNPV is a chain terminator for K48-linked polyubiquitination (39). As such, it is possible that poxvirus-encoded ubiquitin may also act as chain terminators to inhibit degradation of certain substrates. At present, the reason that only a few members of the poxvirus family encode ubiquitin homologues remains unclear.

Poxviruses also encode a family of proteins that function as RING domain-containing ubiquitin ligases, called the p28 family. Members of the p28 family contain a DNA-binding domain at the N-terminus and a RING domain at the C-terminus. The DNA-binding domain, known as the KilA-N domain, is largely uncharacterized; however, it is important for the localization of p28 to the DNA-rich virus factories during infection (70). In contrast to KilA-N, the catalytic RING domain confers ubiquitin ligase activity to p28 (6, 43, 70). Interestingly, p28 is expressed in a number of chordopoxviruses, including the *Avipoxvirus, Lepripoxvirus,* and *Orthopoxvirus* genera (6). Amongst the orthopoxviruses, viruses such as ECTV and VARV encode functional p28 proteins; however, many culture-adapted strains of VACV have truncated or missing p28 genes (43). In fact, the only version of p28 in VACV that is capable of ubiquitin ligase activity is encoded by the IHD-W strain (43). The function of p28 remains to be determined. The VARV orthologue of p28 associates with Ubc13, which is an E2 that aids in formation of K63-linked polyubiquitin chains (43). Work in our lab has also demonstrated that p28 targets K48-linked polyubiquitin chains to the virus factory. Together, these data indicate that p28 mediates ubiquitination in the virus factory. Perhaps, p28-mediated ubiquitination contributes to the suggested role for p28 of inhibiting apoptosis and contributing to virulence (17, 18, 80).

Poxviruses also encode a second family of proteins that function as modified RING-domain containing ubiquitin ligases, called the MARCH (membrane-associated RING-CH) family. The MARCH family of proteins contains a modified RING domain that includes a transmembrane sequence responsible for membrane localization (69). This family is limited to certain poxvirus genera, including the *Capripoxvirus, Leporipoxvirus, Suipoxvirus,* and *Yatapoxvirus* genera (6). Interestingly, substrates have been identified for the MARCH E3s, making this family unique among poxviral ubiquitin ligases. M153R, encoded by MYXV, is the most extensively studied poxviral MARCH E3 ubiquitin ligase. M153 downregulates MHC class I from the cell surface, thus circumventing recognition of virally infected cells by $CD8^+$ T cells (7, 38). In addition to MHC class I, poxviral MARCH E3 ubiquitin ligases have been implicated in downregulation of other cell surface molecules, including CD95, CD66, and CD4 (7, 38, 58).

In addition to encoding functional E3 ubiquitin ligases, poxviruses encode a family of RING proteins with sequence similarity to the RING domain of the APC11 subunit in the anaphase promoting complex/cyclosome (APC/C) (6, 61). The APC/C is composed of twelve subunits, making it the largest cellular ubiquitin ligase that has been identified (73). A number of components of APC/C are responsible for substrate recruitment, thus contributing the ability of the APC/C to regulate mitosis, induction of anaphase, exit from mitosis, and DNA replication (73). It is thought that the APC/C evolved from the SCF ubiquitin ligase, since it contains subunits possessing cullin and RING domains (73). Similar to the architecture of the SCF ubiquitin ligase, the cullin domain-containing protein APC2 acts as a molecular scaffold that binds to APC11, a RING domain-containing protein that recruits the E2 conjugating-enzyme to the APC/C (55, 87).

APC11 homologues have been identified in the *Parapoxvirus* and *Molluscipoxvirus* genera, and in crocodilepox virus and squirrelpox virus (6). However, only the APC11 homologue poxvirus APC/cyclosome regulator (PACR) in Orf virus, a member of the *Parapoxvirus* genus, has been characterized (61). PACR associates with the APC/C in a

similar manner to APC11; however, PACR is mutated in the RING domain, thus preventing association of the E2 enzyme, and subsequent ubiquitination of substrates (61). Substrates of the APC/C include cellular ribonucleotide reductase and thymidine kinase, both of which contribute to free nucleotide supplies in the cell. Interestingly, most poxviruses encode their own ribonucleotide reductase and thymidine kinase proteins. However, genes encoding ribonucleotide reductase and thymidine kinase are absent from Orf virus, as well as other members of the *Poxviridae* that encode APC11 homologues. Perhaps some poxviruses encode APC11 in order to prevent substrate recruitment to the APC/C. Through this mechanism, poxviruses that do not encode ribonucleotide reductase and thymidine kinase genes can still promote synthesis of free nucleotides, thus increasing efficiency of their lifecycle.

Some members of the *Poxviridae* also encode substrate adapter proteins, such the BTB/Kelch family, which recruits substrates to cullin-3 based E3 ubiquitin ligases (33, 96). BTB/Kelch proteins interact cullin-3 through the Bric-a-Brac, Tramtrack, Broad complex (BTB) domain, and mediate substrate recruitment through the Kelch domain (1, 96). ORFs that encode BTB/Kelch proteins are found in the genomes of most members of the *Poxviridae* (6). In contrast to other poxviral modulators of the ubiquitin-proteasome system, which are encoded by one or two ORFs in the genome, up to six ORFs that encode BTB/Kelch substrate adapter proteins are present in the genomes of many poxviruses (81). There are two possible mechanisms by which poxviruses use BTB/Kelch proteins to modulate cullin-3-based ubiquitin ligases: they could recruit substrates to the ubiquitin ligase complex to alter the cellular environment, or they could sequester cullin-3-based ubiquitin ligases, thus preventing ubiquitination of their target substrates. The presence of multiple ORFs in poxviral genomes that each encode BTB/Kelch proteins with different numbers and locations of the Kelch repeats suggests that each BTB/Kelch protein recruits unique substrates to the cullin-3 based ubiquitin ligase, as opposed to sequestering the ligases and preventing them from functioning. Currently, substrates have not been identified for poxviral BTB/Kelch proteins; however,

deletion of ORFs encoding BTB/Kelch proteins from VACV, CPXV, and sheeppox virus results in decreased virulence of the viruses, indicating that BTB/Kelch proteins are important during infection (5, 9, 32, 52, 74). Similar to the BTB/Kelch proteins, the substrates for many other poxviral modulators of the ubiquitin-proteasome have not been identified, so the functions of these poxviral proteins are not well understood. Substrate identification will be crucial for advancing our knowledge in this field, and this is discussed more in section 5.5.

5.3 POXVIRAL ANK/F-BOX SUBSTRATE ADAPTER PROTEINS

Poxviral Ank/F-box proteins are a newly identified family of substrate adapter proteins for the SCF ubiquitin ligase (60). Given the importance of the ubiquitin-proteasome system during poxvirus infection, it seems likely that Ank/F-box proteins also play a key role during the poxvirus lifecycle (77, 88). The Ank domain is composed of a 33 amino acid sequence that forms a helix-loop-helix structure (66). Since its identification in the cytoskeleton protein Ankyrin (66), the Ank domain has been extensively studied, and it is one of the most common protein-protein interaction motifs that exists (14). Proteins containing Ank domains are present in bacteria, archeobacteria, and eukaryotes; however, with the exception of poxviruses, Ank domain-containing proteins are extremely uncommon in viruses (60). Interestingly, in contrast to other viruses, Ank domain-containing proteins represent the largest protein family encoded by poxviruses (83). All but one genus of poxviruses, the *Molluscipoxvirus* genus, contain proteins that possess Ank domains (60). Most poxviruses encode four to five Ank domain-containing proteins; however, members of the *Avipoxvirus* genus encode upwards of fifty Ank domain-containing proteins (89). Poxvirus proteins containing Ank domains are large proteins, and many range from 400 to 650 amino acids in length. Typically, they contain five to ten Ank domains clustered towards the N-terminus.

Usually, Ank domain-containing proteins exist in conjunction with other functional domains, including those important for ion transport and protein kinase activity (3). However in poxviruses, Ank domain-containing proteins exist instead with an F-box domain (60). In fact, depending on the poxvirus, 80 to 100% of its Ank domain-containing proteins exist in conjunction with an F-box domain (60). The F-box domain is necessary for interaction with Skp1 in the SCF ubiquitin ligase, and cellular F-box proteins recruit substrates to the SCF to be ubiquitinated (50). Proteins containing F-box domains recruit proteins for ubiquitination through their substrate binding domains, which include WD40 and LRR domains (51). Strikingly, the combination of multiple Ank domains in conjunction with a C-terminal F-box was thought to be unique to poxviruses (60), until recently when Ank/F-box proteins were identified in the parasitoid wasp, *Nasonia* (94). In poxviral Ank domain-containing proteins the F-box has been renamed the Pox proteins repeats of ankyrin C-terminal (PRANC) domain; however, our lab continues to refer to it as the F-box domain. Poxviral Ank/F-box proteins differ from cellular F-box proteins in three ways; first, the F-box is located at the C-terminus, in contrast to being located at the N-terminus in cellular F-box proteins, and, second, cellular F-box proteins do not exist in conjunction with Ank domains (60). Thirdly, the F-box domain, which is normally composed of three alpha helices, is truncated in poxviruses and is missing the third alpha helix (60, 82).

Ank/F-box proteins have been identified in many poxviruses (6). However, with the exception of the CPXV protein CP77, and the MYXV proteins MNF (M150) and M-T5, many poxviral Ank/F-box proteins remain uncharacterized (6, 10, 19, 21, 48, 93). This project focused on characterizing Ank/F-box proteins in ECTV. Using a bioinformatics screen, our lab identified seven Ank domain-containing proteins in ECTV, four of which contained F-box domains (91). Orthologues of ECTV002, ECTV005, ECTV154, and ECTV165 are present in many orthopoxviruses. Orthologues of ECTV002 are found in CMPV (CMLV003), CPXV (CPXV006), horsepox virus (HSPV004), MPXV (MPXV003), taterapox virus (TATV006), and VARV (G1R). With the exception of G1R, all of these

ORFs are present in two copies per genome, as one copy located in each ITR region. In contrast, G1R is located only at the right end of the genome. Unlike ECTV002, there is only one orthologue of ECTV005 and it exists in CPXV (CPX011). Many orthologues of ECTV154 exist and they are found in CMPV (CMLV182), CPXV (CPXV204), horsepox virus (HSPV206), MPXV (MPXV172), rabbitpox virus (RPXV168), taterapox virus (TATV187), VACV (VACVB4R), and VARV (VARV176). Finally, a number of orthologues of ECTV165 also exist within the *Orthopoxvirus* genus, including CPXV (CPXV217), horesepox virus (HSPV220), rabbitpox virus (RPXV180), VACV (B18R), and VARV (VARV197).

5.4 REGULATION OF NFκB BY POXVIRAL ANK/F-BOX PROTEINS

Our data indicate that the ECTV Ank/F-box proteins associated with the SCF ubiquitin ligase and prevented degradation of IκBα and nuclear translocation of NFκB p65. We did not determine whether VACVB4R associated with the SCF ubiquitin ligase, or prevented IκBα degradation and p65 nuclear translocation; however, given the high level of amino acid sequence identity between ECTV154 and VACVB4R, we suspect that VACVB4R functions in a similar manner to ECTV154. Since the proteasome is active during poxvirus infection (30), we suspect that ECTV002, ECTV005, ECTV154/VACVB4R, and ECTV165 prevent ubiquitination of IκBα by interfering with the SCF ubiquitin ligase. In uninfected cells, the cellular F-box protein βTrCP recruits phosphorylated IκBα to the SCF ubiquitin ligase, and IκBα becomes ubiquitinated (41, 53, 84). We expect that the Ank/F-box proteins may compete with βTrCP for available Skp1 in the SCF ubiquitin ligase. With less available Skp1 in the cell, the interaction between βTrCP and the SCF ubiquitin ligase would be diminished, thereby preventing IκBα ubiquitination and subsequent degradation. This is not an uncommon mechanism, since the HIV protein Vpu also prevents IκBα degradation by disrupting binding to βTrCP and preventing the interaction between Skp1 and βTrCP (15). During this project, we attempted to determine if βTrCP and Skp1 still interact during infection with ECTV or VACV; however, our attempts were unsuccessful. Another possibility is that the Ank/F-box proteins

target βTrCP for degradation. This mechanism is used by the NSP1 protein family, a member of which is encoded by some rotaviruses (35). Unfortunately, we had difficulties detecting βTrCP, so we were unable to determine whether βTrCP is degraded during infection with ECTV or VACV.

5.5 VIRUSES MISSING CERTAIN ANK/F-BOX PROTEINS EXHIBIT SMALL PLAQUE PHENOTYPE

Poxviruses produce two forms of infectious virion, MVs and EVs (23, 67). Most MVs are released during cell lysis. However, through a process mediated by the VACVCop ORFs A27L, B5R, and F13L, some MVs are transported away from virus factories to endosomes and the trans-Golgi network, where they acquire two additional lipid membranes to become WVs (11, 26, 46, 78). Following acquisition of additional membranes, WVs are transported along microtubules to the cell surface, a process that is mediated by the VACVCop ORFs A36R, F11L, F12L, and E2L (4, 25, 42, 65). Once WVs reach the cell surface, they fuse with the plasma membrane and lose one of the additional two membranes to become EVs. Some EVs are released immediately, while others remain associated with the outside of the plasma membrane and activate actin polymerization and are propelled to infect adjacent cells (13, 24). The VACVCop ORFs A33R, A34R, A36R, and B5R mediate a signalling cascade that results in actin polymerization (20, 49, 59). Interestingly, VACV811 contains all of the currently known ORFs that are important for release and spread (Table 5-1). Yet compared to VACVCop, VACV811 produces small plaques and was shows decreased growth in a multiple-step growth curve, indicating that additional ORFs in the VACVCop genome must be important for virion release and spread. There are a number of uncharacterized ORFs in the VACVCop genome that are missing in VACV811, and it would be interesting to determine what, if any, role these ORFs play in release and spread (Table 5-1). Notably, all of the ORFs missing from VACV811 are located in the variable regions of the genome. Variable regions encode many non-essential ORFs that regulate cellular signalling

Table 5-1. Open reading frames present in VACV and absent from VACV811

ORF	Characteristics
Deletions from the left side of the genome	
C23L	Chemokine binding protein
C22L	Pseudogene; TNFα receptor
C21L	Contains Ank repeats
C20L	Contains Ank repeats
C19L	Contains Ank repeats
C18L	Pseudogene; contains Ank repeats
C17L	Pseudogene; contains Ank repeats
C16L	Unknown
C15L	Unknown
C14L	Unknown
C13L	Unknown
C12L	Serine protease inhibitor
C11R	Epidermal growth factor
C10L	IL-1R antagonist
C9L	Contains Ank repeats
C8L	Unknown
C7L	Host-range factor
C6L	Unknown
C5L	Unknown
C4L	Il-1R antagonist
C3L	Secreted complement binding protein
C2L	Kelch-like protein
C1L	Homology to Bcl-2 family; function unknown
N1L	Homology to Bcl-2 family; inhibits apoptosis and NFκB
N2L	Alpha amantin sensitivity protein
M1L	Contains Ank repeats
M2L	Inhibits NFκB
K1L	Contains Ank repeats; inhibits NFκB
K2L	Serine protease inhibitor
K3L	eIF-2 decoy; competes for phosphorylation with cellular eIF-2; prevents PKR-induced IFN response
K4L	Nicking and joining enzyme
K5L	Possibly a monoglyceride lipase
K6L	Possibly a monoglyceride lipase
K7R	Unknown
F1L	Inhibits apoptosis
F2L	dUTPase
F3L	Kelch-like protein
F4L	Ribonucleotide reductase small subunit

Table 5-1. Continued…

Deletions from the right side of the genome	
B13R	Serine protease inhibitor
B14R	Pseudogene; serine protease inhibitor
B15R	Unknown
B16R	IL-1β receptor
B17L	Unknown
B18R	Contains Ank repeats
B19R	IFNα receptor
B20R	Pseudogene; contains Ank repeats
B21R	Unknown
B22R	Unknown
B23R	Pseudogene; contains Ank repeats
B24R	Pseudogene; contains Ank repeats
B25R	Contains Ank repeats
B26R	Contains Ank repeats
B27R	Contains Ank repeats
B28R	Pseudogene
B29R	Chemokine binding protein

VACV811 is missing 55 ORFs compared to the VACVCop. TNFα, tumour necrosis factor alpha; Ank, ankyrin; IL-1R, interleukin-1 receptor; Bcl-2, B-cell lymphoma 2; NFκB, nuclear factor kappa-light-chain enhancer of activated B cells; eIF-2, eukaryotic initiation factor 2; PKR, dsRNA-dependent protein kinase; IFN, interferon; IL-1β, interleukin-1 beta.

pathways and the host immune response, so it is surprising that an ORF dedicated to virion release or spread would be located in this region (47, 62, 79). However, a few essential genes are also located in the variable ends of the genome, so the potential for a gene involved in release or spread to be located in the variable regions is not completely unlikely (67). Further characterization of the ORFs with unknown functions missing from VACV811 will be interesting.

In addition to the ORFs that are absent from VACV811, we also identified an ORF encoded by VACV811 that we suspect might mediate release or spread. Though we originally deleted VACVB4R from VACV811 to study additional inhibitors of the NFκB pathway, we observed that VACV811ΔB4R produces smaller plaques than even VACV811. VACV811ΔB4R was also defective in spread, as assessed by multiple-step growth analysis. Additionally, deletion of the orthologue of VACVB4R, ECTV154, from ECTV resulted in a small plaque phenotype. Notably, deletion of ECTV002 from ECTV also resulted in a small plaque phenotype. Typically, small plaque phenotypes are observed upon deletion of a gene that is important for virus morphogenesis, release, or spread. For instance, deletion of the VACVCop genes A33R, A34R, A36R, B5R, F12L, F13L, or E2L (12, 26, 27, 72, 76, 95, 97), results in a small plaque phenotype. Consequently, our data suggest that ECTV002 and ECTV154/VACVB4R may play a role in virion release or spread. We ruled out the possibility that ECTV002 and ECTV154/VACVB4R might be important for MV morphogenesis, since single-step growth analysis revealed that the deletion viruses synthesized infectious virions as well their parental viruses. Thus, we believe that diminished virus spread could be due to either a block in production or release of EV, or reduced efficiency of secondary infection by released EVs.

Unfortunately, we did not explore the mechanism by which ECTV002 and ECTV154/VACVB4R might contribute to release and spread. However, in the future, a number of experiments would be useful to try to understand more about why the small-

plaques are formed by viruses missing ECTV002 or ECTV154/VACVB4R. Cesium chloride density gradients could be used to determine if EVs are released during infection with ECTVΔ002, ECTVΔ154, or VACV811ΔB4R (29). In this process, viral DNA in infected cells is isotopically labeled following infection. Twenty-four hours post-infection, virions contained within the cell and released virions are purified using a cesium chloride gradient, and the number of virus particles in each fraction is determined using a scintillation counter. Cesium chloride density gradients were used to determine whether EVs were released following deletion of B5R from VACV (29). If the results indicate that EVs are not released in the absence of ECTV002 or ECTV154/VACVB4R, electron microscopy can be used to determine at what stage EV release is being prevented. Using electron microscopy, all stages of morphogenesis, including the formation of virus factories, lipid crescents, IVs, and MVs, can be detected (27). WVs can also be detected along microtubules leading from the trans-Golgi network to the cell membrane and at the cell membrane where they are fusing and being released as EVs at the surface of infected cells. Images generated by electron microscopy would be very helpful for determining whether WVs are even produced, and if they are, at what step in the pathway to becoming an EV they are blocked. Electron microscopy was used to determine that deletion of A34R prevented formation of WV (27). Finally, if cesium chloride density gradients instead reveal that EVs are released, assays to determine whether the structure of the actin cytoskeleton is modified during infection could be performed (45). Confocal microscopy could be used to compare formation of actin stress fibres and actin projectiles in cells infected with ECTVΔ002, ECTVΔ154, and VACV811ΔB4R, to cells infected with ECTV or VACV811. Visualization of actin by confocal micrscopy was used to demonstrate that F11L remodels actin (64).

Many poxviral proteins that are important for release and spread are packaged into the virion, however VACVB4R has not been identified in the VACVCop virion (67). No work has been done to characterize the ECTV virion, so whether ECTV002 or ECTV154 are packaged is unknown. Considering that ECTV154 is the orthologue of a protein that isn't

contained within the VACVCop virion, we speculate that ECTV154 is not packaged in the ECTV virion. Since ECTV002 and ECTV154/VACVB4R are Ank/F-box proteins, we suspect that they inhibit virion release or spread by recruiting unique substrates to the SCF ubiquitin ligase. To date, ubiquitin ligases have not been implicated in virion release or spread; however as described in section 5.2, ubiquitination may be important for VACVCop release or spread. Importantly, some poxviral proteins that mediate release and spread require post-translational modifications in order to function. For instance, F13L is palmitoylated, and A34R is glycosylated (16, 36). Potentially, some poxviral proteins that are important for virion release and spread might require processing by the proteasome, an event that could be mediated by ECTV002 or ECTV154/VACVB4R. Unfortunately, with the exception of the GRR signal that mediates processing of the NFκB precursors p100 and p105, proteasomal processing motifs are not well characterized (56). Consequently, it is difficult at this point to screen the poxviral proteins to determine if any of them contain proteasomal-processing signals.

5.6 SUBSTRATE IDENTIFICATION COULD YIELD CLUES TO THE FUNCTION OF ANK/F-BOX PROTEINS

Though we have compelling evidence suggesting that the Ank/F-box proteins inhibit the NFκB pathway, it is possible that NFκB inhibition is a non-specific effect of viral hijacking of the SCF ubiquitin ligase. Additionally, the dual role of ECTV002 in NFκB activation (63), and our observation that ECTV002 and ECTV154/VACVB4R might regulate virion release or spread, suggests that each of the Ank/F-box proteins recruits unique substrates to the SCF ubiquitin ligase. Substrate identification is an elusive process in the ubiquitin field; however, identifying potential interacting partners for the Ank/F-box proteins will give us great insight into the biological roles of ECTV002, ECTV005, ECTV154/VACVB4R, and ECTV165. A previous student in our lab, Dr. Nick van Buuren, made a number of attempts to identify interacting partners of ECTV005. Dr. van Buuren immunoprecipitated Flag-ECTV005 and used SDS-PAGE and silver staining to excise a

number of bands, which were analyzed by mass spectrometry (91). Unfortunately, his attempts to identify substrates for EVM005 were unsuccessful. However, of the 69 cellular F-box-containing proteins, substrates for only nine of these proteins have been identified, signifying the difficulty of substrate identification for F-box-containing proteins (31).

There are many options for substrate identification that our lab has not explored. A promising option would be to employ the stable isotope labeling with amino acids in culture (SILAC) technique for substrate identification. SILAC has been developed within the last ten years, and although it is a new technique it is being used quite extensively by the bioinformatics community (57). Using SILAC, the entire set of proteins expressed by a cell's genome, called the proteome, is metabolically labeled with "heavy" non-radioactive isotopic amino acids. To identify potential substrates of the Ank/F-box proteins, cells can be infected with ECTVΔ002, ECTVΔ005, ECTVΔ154, ECTVΔ165, VACV811ΔB4R, or their parental viruses ECTV or VACV811. Prior to infection, cells to be infected with the knockout viruses would be grown for five rounds of cell division in medium containing the "heavy" amino acid to ensure cellular proteins have incorporated the labeled amino acid (71). Twelve hours post-infection, the two infected cell populations (those infected with the parental and those infected with the knockout virus) would be mixed together, and their proteomes extracted and analyzed using mass spectrometry. Peptides that have incorporated the "heavy" amino acid will have a known mass shift relative to unlabeled peptides, and this will allow the proteomes from cells infected with the ECTV or VACV811 parental viruses and the knockout viruses to be distinguished from each other. For each peptide, the result will be a pair in the mass spectra, with the peptide labeled with the "heavy" amino acid from the cells infected with the knockout viruses having the higher mass. Equal peak intensities of the two mass spectra will indicate that there is no difference in protein levels in each of the infected cell populations, while a difference in peak intensities will indicate a difference in abundance of proteins. Observed differences in protein abundance should be

indicative of proteins that are potentially regulated by the Ank/F-box proteins. SILAC is an extremely sensitive technique, and upwards of 1500 potential substrates can be identified using this approach.

SILAC has been used to quantify changes in the proteome of the nucleolus after infection with Influenza A virus (28) and Adenovirus (54)**.** Though SILAC is a promising technique for substrate identification, there are potential pitfalls to this approach, including the inability to distinguish between proteins that are directly ubiquitinated by Ank/F-box proteins and those whose abundance in the cell are increased as a result of either degradation of their regulators or of indirect effect of virus modulation of other pathways. In addition, this approach would only identify cellular proteins ubiquitinated by the Ank/F-box proteins, since peptides are labeled before infection. As well, it is possible that the changes in abundance of peptides may not be significant enough to identify proteins whose expression is regulated by the Ank/F-box proteins. An alternative approach would be to use the 2D difference in gel electrophoresis (DIGE) system. DIGE would be useful for identifying any viral proteins that are regulated by the Ank/F-box proteins. The DIGE approach is similar to SILAC, except protein samples are labeled after infection has occurred, using cyanine dyes. Samples infected with parental or knockout virus are labeled with a different fluorescent cyanine dye, each of which are matched for charge and size, so they co-migrate on the 2D gel (90). Increased fluorescence of one dye or the other would be indicative of differences in protein abundance between the two protein samples. Protein spots of interest would be extracted from the 2D gel and analyzed by mass spectrometry, potentially allowing us to identify substrates for the Ank/F-box proteins. As alluded to previously, substrate identification will be crucial for understanding more about the role of poxvirus Ank/F-box proteins during infection.

5.7 OTHER POTENTIAL ROLES OF THE ANK/F-BOX PROTEINS

To get an idea of the potential functions of the Ank/F-box proteins, we used PBR BLAST analysis to identify cellular proteins in *Homo sapiens* and *Mus musculus* with similar protein sequences to the Ank domain-containing N-termini of ECTV002, ECTV005, ECTV154/VACVB4R, and ECTV165 (www.poxvirus.org) (Table 5-2). The idea was that if we identified proteins with similar sequences to the Ank/F-box proteins, we could learn about the roles of these proteins in the cell and potentially generate a hypothesis as to what the Ank/F-box proteins might do. Using this technique, we identified some hypothetical roles for ECTV002, and ECTV154/VACVB4R that might be interesting to explore (Table 5-2). For instance, when we looked for proteins with similar sequences to ECTV002, and ECTV154/VACVB4R, we identified the protein ankyrin repeat domain 44. Ankyrin repeat domain 44 is a protein that is hypothesized to regulate the protein phosphatase 6 (PP6) through an unknown mechanism. Interestingly, PP6 dephosphorylates IκBε following TNFα stimulation, thus preventing NFκB activation (85, 86). It is unlikely that ECTV002 or ECTV154/VACVB4R would target PP6 for degradation, since that would allow NFκB to remain activated. However, ECTV002 or ECTV154/VACVB4R might target a negative regulator of PP6 for degradation. Another interesting protein with sequence homology to ECTV154/VACVB4R that we identified was tankyrase. Tankyrase is a regulator of the Wnt signalling pathway, which controls the expression of genes involved in cell proliferation (34, 44). An important component of the Wnt pathway is the effector protein β-catenin. In the absence of a Wnt signal, β-catenin is ubiquitinated following phosphorylation, targeting it for degradation. Phosphorylation of β-catenin, is mediated by casein kinase 1α (CK1α) and glycogen synthase kinase 3β (GSK3β) (40). Importantly, axin is a component of a scaffold that brings β-catenin into close proximity with CK1α and GSK3β (40). However upon Wnt stimulation, tankyrase ribosylates axin resulting in its degradation (44). Thus, during Wnt stimulation β-catenin is not degraded, and it enters the nucleus where it associates with transcriptional activators facilitating the expression of various gene targets

Table 5-2. Cellular proteins with sequence homology to the Ank/F-box proteins

Protein	e value	% Identity	% Similarity	Characteristics	Accession	References
ECTV002						
Ankyrin repeat domain 44	2e-006	23.1	39.72	Putative regulatory subunit of PP6; PP6 dephosphorylates IκBε	AAH16985	(85, 86)
ECTV005						
N/A	N/A	N/A	N/A	N/A	N/A	N/A
ECTV154/VACVB4R						
Ankyrin repeat domain 44	2e-011	24.27	45.63	Putative regulatory subunit of PP6; PP6 dephosphorylates IκBε	AAH16985	(85, 86)
TNNI3K	4e-008	22.81	42.97	Serine/threonine protein kinase	AAH32865	None available
tankyrase	1e-007	24.52	45.19	poly-ADP-ribosylating enzymes; ribosylates axin leading to its degradation	BAD92576	(44)
ECTV165						
Hypothetical protein	7e-008	22.42	39.39	unknown	CAI56716	None available

Proteins in the *Homo sapien* and *Mus musculus* genomes with sequence homology to ECTV002, ECTV004, ECTV154/VACVB4R, and ECTV165 were identified using PBR blast (www.poxvirus.org). Anything with an e value greater than 1e-006 was rejected. Duplicate hits of the same protein with different sequence accession were also rejected. PP6, protein phosphatase 6; IκBε, IkappaB kinase epsilon; ADP, adenosine diphosphate.

involved in cell proliferation (34). Since ECTV154/VACVB4R exhibit sequence similarity to tankyrase, it is possible that they might target axin for degradation. Through this mechanism, expression of cellular proteins that aid in the poxviruses lifecycle might be synthesized, thus increasing lifecycle efficiency. As described in section 5.2, some poxviruses manipulate the APC/C to increase expression of the ribonucleotide reductase and thymidine kinase genes. This manipulation promotes synthesis of free nucleotides, thus increasing efficiency of the lifecycle of those. Thus, the idea of poxvirus manipulation of Wnt signalling might be reasonable. Unfortunately, using this approach did not provide insight into the function of ECTV005 or ECTV165 (Table 5-2).

5.8 CONCLUSIONS

This project characterized four Ank/F-box proteins encoded by ECTV, ECTV002, ECTV005, ECTV154, and ECTV165. We demonstrated that ECTV002, ECTV005, ECTV154, and ECTV165 prevent degradation of IκBα and nuclear translocation of the NFκB subunit p65. The ability of the ECTV Ank/F-box proteins to inhibit p65 nuclear translocation is dependent on the F-box domain, suggesting that interaction with the SCF ubiquitin ligase is important for NFκB inhibition. Using deletion viruses that were missing the Ank/F-box proteins, we demonstrated that deletion of a single Ank/F-box protein is not enough to abrogate the ability of ECTV or VACV811 to inhibit NFκB activation. An additional observation was that viruses lacking ECTV002, or ECTV154/VACVB4R exhibit small plaque phentoypes, suggesting that these Ank/F-box proteins might be important for virion release or spread. Though we can use BLAST analysis to speculate what other roles the Ank/F-box proteins might have during infection, substrate identification will be crucial for advancing our knowledge on ECTV002, ECTV005, ECTV154/VACVB4R, and ECTV165.

5.9 REFERENCES

1. **Adams, J., R. Kelso, and L. Cooley.** 2000. The kelch repeat superfamily of proteins: propellers of cell function. Trends Cell Biol **10:**17-24.
2. **Afonso, C. L., E. R. Tulman, Z. Lu, E. Oma, G. F. Kutish, and D. L. Rock.** 1999. The genome of Melanoplus sanguinipes entomopoxvirus. J Virol **73:**533-52.
3. **Al-Khodor, S., C. T. Price, A. Kalia, and Y. Abu Kwaik.** 2010. Functional diversity of ankyrin repeats in microbial proteins. Trends Microbiol **18:**132-9.
4. **Arakawa, Y., J. V. Cordeiro, and M. Way.** 2007. F11L-mediated inhibition of RhoA-mDia signaling stimulates microtubule dynamics during vaccinia virus infection. Cell Host Microbe **1:**213-26.
5. **Balinsky, C. A., G. Delhon, C. L. Afonso, G. R. Risatti, M. V. Borca, R. A. French, E. R. Tulman, S. J. Geary, and D. L. Rock.** 2007. Sheeppox virus kelch-like gene SPPV-019 affects virus virulence. J Virol **81:**11392-401.
6. **Barry, M., N. van Buuren, K. Burles, K. Mottet, Q. Wang, and A. Teale.** 2010. Poxvirus exploitation of the ubiquitin-proteasome system. Viruses **2:**2356-80.
7. **Bartee, E., M. Mansouri, B. T. Hovey Nerenberg, K. Gouveia, and K. Fruh.** 2004. Downregulation of major histocompatibility complex class I by human ubiquitin ligases related to viral immune evasion proteins. J Virol **78:**1109-20.
8. **Bawden, A. L., K. J. Glassberg, J. Diggans, R. Shaw, W. Farmerie, and R. W. Moyer.** 2000. Complete genomic sequence of the Amsacta moorei entomopoxvirus: analysis and comparison with other poxviruses. Virology **274:**120-39.
9. **Beard, P. M., G. C. Froggatt, and G. L. Smith.** 2006. Vaccinia virus kelch protein A55 is a 64 kDa intracellular factor that affects virus-induced cytopathic effect and the outcome of infection in a murine intradermal model. J Gen Virol **87:**1521-9.
10. **Blanie, S., J. Gelfi, S. Bertagnoli, and C. Camus-Bouclainville.** 2010. MNF, an ankyrin repeat protein of myxoma virus, is part of a native cellular SCF complex during viral infection. Virol J **7:**56.
11. **Blasco, R., N. B. Cole, and B. Moss.** 1991. Sequence analysis, expression, and deletion of a vaccinia virus gene encoding a homolog of profilin, a eukaryotic actin-binding protein. J Virol **65:**4598-608.
12. **Blasco, R., and B. Moss.** 1991. Extracellular vaccinia virus formation and cell-to-cell virus transmission are prevented by deletion of the gene encoding the 37,000-Dalton outer envelope protein. J Virol **65:**5910-20.
13. **Blasco, R., and B. Moss.** 1992. Role of cell-associated enveloped vaccinia virus in cell-to-cell spread. J Virol **66:**4170-9.
14. **Bork, P.** 1993. Hundreds of ankyrin-like repeats in functionally diverse proteins: mobile modules that cross phyla horizontally? Proteins **17:**363-74.
15. **Bour, S., C. Perrin, H. Akari, and K. Strebel.** 2001. The human immunodeficiency virus type 1 Vpu protein inhibits NF-kappa B activation by interfering with beta TrCP-mediated degradation of Ikappa B. J Biol Chem **276:**15920-8.

16. **Breiman, A., and G. L. Smith.** 2010. Vaccinia virus B5 protein affects the glycosylation, localization and stability of the A34 protein. J Gen Virol **91:**1823-7.
17. **Brick, D. J., R. D. Burke, A. A. Minkley, and C. Upton.** 2000. Ectromelia virus virulence factor p28 acts upstream of caspase-3 in response to UV light-induced apoptosis. J Gen Virol **81:**1087-97.
18. **Brick, D. J., R. D. Burke, L. Schiff, and C. Upton.** 1998. Shope fibroma virus RING finger protein N1R binds DNA and inhibits apoptosis. Virology **249:**42-51.
19. **Camus-Bouclainville, C., L. Fiette, S. Bouchiha, B. Pignolet, D. Counor, C. Filipe, J. Gelfi, and F. Messud-Petit.** 2004. A virulence factor of myxoma virus colocalizes with NF-kappaB in the nucleus and interferes with inflammation. J Virol **78:**2510-6.
20. **Chan, W. M., and B. M. Ward.** 2010. There is an A33-dependent mechanism for the incorporation of B5-GFP into vaccinia virus extracellular enveloped virions. Virology **402:**83-93.
21. **Chang, S. J., J. C. Hsiao, S. Sonnberg, C. T. Chiang, M. H. Yang, D. L. Tzou, A. A. Mercer, and W. Chang.** 2009. Poxvirus host range protein CP77 contains an F-box-like domain that is necessary to suppress NF-kappaB activation by tumor necrosis factor alpha but is independent of its host range function. J Virol **83:**4140-52.
22. **Chung, C. S., C. H. Chen, M. Y. Ho, C. Y. Huang, C. L. Liao, and W. Chang.** 2006. Vaccinia virus proteome: identification of proteins in vaccinia virus intracellular mature virion particles. J Virol **80:**2127-40.
23. **Condit, R. C., N. Moussatche, and P. Traktman.** 2006. In a nutshell: structure and assembly of the vaccinia virion. Adv Virus Res **66:**31-124.
24. **Cudmore, S., P. Cossart, G. Griffiths, and M. Way.** 1995. Actin-based motility of vaccinia virus. Nature **378:**636-8.
25. **Dodding, M. P., T. P. Newsome, L. M. Collinson, C. Edwards, and M. Way.** 2009. An E2-F12 complex is required for intracellular enveloped virus morphogenesis during vaccinia infection. Cell Microbiol **11:**808-24.
26. **Domi, A., A. S. Weisberg, and B. Moss.** 2008. Vaccinia virus E2L null mutants exhibit a major reduction in extracellular virion formation and virus spread. J Virol **82:**4215-26.
27. **Duncan, S. A., and G. L. Smith.** 1992. Identification and characterization of an extracellular envelope glycoprotein affecting vaccinia virus egress. J Virol **66:**1610-21.
28. **Emmott, E., H. Wise, E. M. Loucaides, D. A. Matthews, P. Digard, and J. A. Hiscox.** 2010. Quantitative proteomics using SILAC coupled to LC-MS/MS reveals changes in the nucleolar proteome in influenza A virus-infected cells. J Proteome Res **9:**5335-45.
29. **Engelstad, M., and G. L. Smith.** 1993. The vaccinia virus 42-kDa envelope protein is required for the envelopment and egress of extracellular virus and for virus virulence. Virology **194:**627-37.
30. **Fagan-Garcia, K., and M. Barry.** 2011. A vaccinia virus deletion mutant reveals the presence of additional inhibitors of NF-kappaB. J Virol **85:**883-94.

31. **Frescas, D., and M. Pagano.** 2008. Deregulated proteolysis by the F-box proteins SKP2 and beta-TrCP: tipping the scales of cancer. Nat Rev Cancer **8:**438-49.
32. **Froggatt, G. C., G. L. Smith, and P. M. Beard.** 2007. Vaccinia virus gene F3L encodes an intracellular protein that affects the innate immune response. J Gen Virol **88:**1917-21.
33. **Geyer, R., S. Wee, S. Anderson, J. Yates, and D. A. Wolf.** 2003. BTB/POZ domain proteins are putative substrate adaptors for cullin 3 ubiquitin ligases. Mol Cell **12:**783-90.
34. **Giles, R. H., J. H. van Es, and H. Clevers.** 2003. Caught up in a Wnt storm: Wnt signaling in cancer. Biochim Biophys Acta **1653:**1-24.
35. **Graff, J. W., K. Ettayebi, and M. E. Hardy.** 2009. Rotavirus NSP1 inhibits NFkappaB activation by inducing proteasome-dependent degradation of beta-TrCP: a novel mechanism of IFN antagonism. PLoS Pathog **5:**e1000280.
36. **Grosenbach, D. W., D. O. Ulaeto, and D. E. Hruby.** 1997. Palmitylation of the vaccinia virus 37-kDa major envelope antigen. Identification of a conserved acceptor motif and biological relevance. J Biol Chem **272:**1956-64.
37. **Guarino, L. A., G. Smith, and W. Dong.** 1995. Ubiquitin is attached to membranes of baculovirus particles by a novel type of phospholipid anchor. Cell **80:**301-9.
38. **Guerin, J. L., J. Gelfi, S. Boullier, M. Delverdier, F. A. Bellanger, S. Bertagnoli, I. Drexler, G. Sutter, and F. Messud-Petit.** 2002. Myxoma virus leukemia-associated protein is responsible for major histocompatibility complex class I and Fas-CD95 down-regulation and defines scrapins, a new group of surface cellular receptor abductor proteins. J Virol **76:**2912-23.
39. **Haas, A. L., D. J. Katzung, P. M. Reback, and L. A. Guarino.** 1996. Functional characterization of the ubiquitin variant encoded by the baculovirus Autographa californica. Biochemistry **35:**5385-94.
40. **Hart, M. J., R. de los Santos, I. N. Albert, B. Rubinfeld, and P. Polakis.** 1998. Downregulation of beta-catenin by human Axin and its association with the APC tumor suppressor, beta-catenin and GSK3 beta. Curr Biol **8:**573-81.
41. **Hatakeyama, S., M. Kitagawa, K. Nakayama, M. Shirane, M. Matsumoto, K. Hattori, H. Higashi, H. Nakano, K. Okumura, K. Onoe, and R. A. Good.** 1999. Ubiquitin-dependent degradation of IkappaBalpha is mediated by a ubiquitin ligase Skp1/Cul 1/F-box protein FWD1. Proc Natl Acad Sci U S A **96:**3859-63.
42. **Herrero-Martinez, E., K. L. Roberts, M. Hollinshead, and G. L. Smith.** 2005. Vaccinia virus intracellular enveloped virions move to the cell periphery on microtubules in the absence of the A36R protein. J Gen Virol **86:**2961-8.
43. **Huang, J., Q. Huang, X. Zhou, M. M. Shen, A. Yen, S. X. Yu, G. Dong, K. Qu, P. Huang, E. M. Anderson, S. Daniel-Issakani, R. M. Buller, D. G. Payan, and H. H. Lu.** 2004. The poxvirus p28 virulence factor is an E3 ubiquitin ligase. J Biol Chem **279:**54110-6.

44. **Huang, S. M., Y. M. Mishina, S. Liu, A. Cheung, F. Stegmeier, G. A. Michaud, O. Charlat, E. Wiellette, Y. Zhang, S. Wiessner, M. Hild, X. Shi, C. J. Wilson, C. Mickanin, V. Myer, A. Fazal, R. Tomlinson, F. Serluca, W. Shao, H. Cheng, M. Shultz, C. Rau, M. Schirle, J. Schlegl, S. Ghidelli, S. Fawell, C. Lu, D. Curtis, M. W. Kirschner, C. Lengauer, P. M. Finan, J. A. Tallarico, T. Bouwmeester, J. A. Porter, A. Bauer, and F. Cong.** 2009. Tankyrase inhibition stabilizes axin and antagonizes Wnt signalling. Nature **461:**614-20.
45. **Irwin, C. R., and D. H. Evans.** 2012. Modulation of the myxoma virus plaque phenotype by vaccinia virus protein f11. J Virol **86:**7167-79.
46. **Isaacs, S. N., E. J. Wolffe, L. G. Payne, and B. Moss.** 1992. Characterization of a vaccinia virus-encoded 42-kilodalton class I membrane glycoprotein component of the extracellular virus envelope. J Virol **66:**7217-24.
47. **Johnston, J. B., and G. McFadden.** 2003. Poxvirus immunomodulatory strategies: current perspectives. J Virol **77:**6093-100.
48. **Johnston, J. B., G. Wang, J. W. Barrett, S. H. Nazarian, K. Colwill, M. Moran, and G. McFadden.** 2005. Myxoma virus M-T5 protects infected cells from the stress of cell cycle arrest through its interaction with host cell cullin-1. J Virol **79:**10750-63.
49. **Katz, E., B. M. Ward, A. S. Weisberg, and B. Moss.** 2003. Mutations in the vaccinia virus A33R and B5R envelope proteins that enhance release of extracellular virions and eliminate formation of actin-containing microvilli without preventing tyrosine phosphorylation of the A36R protein. J Virol **77:**12266-75.
50. **Kipreos, E. T., and M. Pagano.** 2000. The F-box protein family. Genome Biol **1:**REVIEWS3002.
51. **Kobe, B., and A. V. Kajava.** 2001. The leucine-rich repeat as a protein recognition motif. Curr Opin Struct Biol **11:**725-32.
52. **Kochneva, G., I. Kolosova, T. Maksyutova, E. Ryabchikova, and S. Shchelkunov.** 2005. Effects of deletions of kelch-like genes on cowpox virus biological properties. Arch Virol **150:**1857-70.
53. **Kroll, M., F. Margottin, A. Kohl, P. Renard, H. Durand, J. P. Concordet, F. Bachelerie, F. Arenzana-Seisdedos, and R. Benarous.** 1999. Inducible degradation of IkappaBalpha by the proteasome requires interaction with the F-box protein h-betaTrCP. J Biol Chem **274:**7941-5.
54. **Lam, Y. W., V. C. Evans, K. J. Heesom, A. I. Lamond, and D. A. Matthews.** 2010. Proteomics analysis of the nucleolus in adenovirus-infected cells. Mol Cell Proteomics **9:**117-30.
55. **Leverson, J. D., C. A. Joazeiro, A. M. Page, H. Huang, P. Hieter, and T. Hunter.** 2000. The APC11 RING-H2 finger mediates E2-dependent ubiquitination. Mol Biol Cell **11:**2315-25.
56. **Lin, L., and S. Ghosh.** 1996. A glycine-rich region in NF-kappaB p105 functions as a processing signal for the generation of the p50 subunit. Mol Cell Biol **16:**2248-54.

57. **Mann, M.** 2006. Functional and quantitative proteomics using SILAC. Nat Rev Mol Cell Biol **7:**952-8.
58. **Mansouri, M., E. Bartee, K. Gouveia, B. T. Hovey Nerenberg, J. Barrett, L. Thomas, G. Thomas, G. McFadden, and K. Fruh.** 2003. The PHD/LAP-domain protein M153R of myxomavirus is a ubiquitin ligase that induces the rapid internalization and lysosomal destruction of CD4. J Virol **77:**1427-40.
59. **McIntosh, A. A., and G. L. Smith.** 1996. Vaccinia virus glycoprotein A34R is required for infectivity of extracellular enveloped virus. J Virol **70:**272-81.
60. **Mercer, A. A., S. B. Fleming, and N. Ueda.** 2005. F-box-like domains are present in most poxvirus ankyrin repeat proteins. Virus Genes **31:**127-33.
61. **Mo, M., S. B. Fleming, and A. A. Mercer.** 2009. Cell cycle deregulation by a poxvirus partial mimic of anaphase-promoting complex subunit 11. Proc Natl Acad Sci U S A **106:**19527-32.
62. **Mohamed, M. R., and G. McFadden.** 2009. NFkB inhibitors: strategies from poxviruses. Cell Cycle **8:**3125-32.
63. **Mohamed, M. R., M. M. Rahman, J. S. Lanchbury, D. Shattuck, C. Neff, M. Dufford, N. van Buuren, K. Fagan, M. Barry, S. Smith, I. Damon, and G. McFadden.** 2009. Proteomic screening of variola virus reveals a unique NF-kappaB inhibitor that is highly conserved among pathogenic orthopoxviruses. Proc Natl Acad Sci U S A **106:**9045-50.
64. **Morales, I., M. A. Carbajal, S. Bohn, D. Holzer, S. E. Kato, F. A. Greco, N. Moussatche, and J. Krijnse Locker.** 2008. The vaccinia virus F11L gene product facilitates cell detachment and promotes migration. Traffic **9:**1283-98.
65. **Morgan, G. W., M. Hollinshead, B. J. Ferguson, B. J. Murphy, D. C. Carpentier, and G. L. Smith.** 2010. Vaccinia protein F12 has structural similarity to kinesin light chain and contains a motor binding motif required for virion export. PLoS Pathog **6:**e1000785.
66. **Mosavi, L. K., D. L. Minor, Jr., and Z. Y. Peng.** 2002. Consensus-derived structural determinants of the ankyrin repeat motif. Proc Natl Acad Sci U S A **99:**16029-34.
67. **Moss, B.** 2007. *Poxviridae:* The Viruses and Their Replication. *In* D. M. K. a. P. M. Howley (ed.), Fields Virology 5ed.
68. **Moss, B., and J. L. Shisler.** 2001. Immunology 101 at poxvirus U: immune evasion genes. Semin Immunol **13:**59-66.
69. **Nathan, J. A., and P. J. Lehner.** 2009. The trafficking and regulation of membrane receptors by the RING-CH ubiquitin E3 ligases. Exp Cell Res **315:**1593-600.
70. **Nerenberg, B. T., J. Taylor, E. Bartee, K. Gouveia, M. Barry, and K. Fruh.** 2005. The poxviral RING protein p28 is a ubiquitin ligase that targets ubiquitin to viral replication factories. J Virol **79:**597-601.
71. **Ong, S. E., B. Blagoev, I. Kratchmarova, D. B. Kristensen, H. Steen, A. Pandey, and M. Mann.** 2002. Stable isotope labeling by amino acids in cell culture, SILAC, as a simple and accurate approach to expression proteomics. Mol Cell Proteomics **1:**376-86.

72. **Parkinson, J. E., and G. L. Smith.** 1994. Vaccinia virus gene A36R encodes a M(r) 43-50 K protein on the surface of extracellular enveloped virus. Virology **204:**376-90.
73. **Peters, J. M.** 2006. The anaphase promoting complex/cyclosome: a machine designed to destroy. Nat Rev Mol Cell Biol **7:**644-56.
74. **Pires de Miranda, M., P. C. Reading, D. C. Tscharke, B. J. Murphy, and G. L. Smith.** 2003. The vaccinia virus kelch-like protein C2L affects calcium-independent adhesion to the extracellular matrix and inflammation in a murine intradermal model. J Gen Virol **84:**2459-71.
75. **Reilly, L. M., and L. A. Guarino.** 1996. The viral ubiquitin gene of Autographa californica nuclear polyhedrosis virus is not essential for viral replication. Virology **218:**243-7.
76. **Roper, R. L., L. G. Payne, and B. Moss.** 1996. Extracellular vaccinia virus envelope glycoprotein encoded by the A33R gene. J Virol **70:**3753-62.
77. **Satheshkumar, P. S., L. C. Anton, P. Sanz, and B. Moss.** 2009. Inhibition of the ubiquitin-proteasome system prevents vaccinia virus DNA replication and expression of intermediate and late genes. J Virol **83:**2469-79.
78. **Schmelz, M., B. Sodeik, M. Ericsson, E. J. Wolffe, H. Shida, G. Hiller, and G. Griffiths.** 1994. Assembly of vaccinia virus: the second wrapping cisterna is derived from the trans Golgi network. J Virol **68:**130-47.
79. **Seet, B. T., J. B. Johnston, C. R. Brunetti, J. W. Barrett, H. Everett, C. Cameron, J. Sypula, S. H. Nazarian, A. Lucas, and G. McFadden.** 2003. Poxviruses and immune evasion. Annu Rev Immunol **21:**377-423.
80. **Senkevich, T. G., E. V. Koonin, and R. M. Buller.** 1994. A poxvirus protein with a RING zinc finger motif is of crucial importance for virulence. Virology **198:**118-28.
81. **Shchelkunov, S. N., P. F. Safronov, A. V. Totmenin, N. A. Petrov, O. I. Ryazankina, V. V. Gutorov, and G. J. Kotwal.** 1998. The genomic sequence analysis of the left and right species-specific terminal region of a cowpox virus strain reveals unique sequences and a cluster of intact ORFs for immunomodulatory and host range proteins. Virology **243:**432-60.
82. **Sonnberg, S., S. B. Fleming, and A. A. Mercer.** 2009. A truncated two-alpha-helix F-box present in poxvirus ankyrin-repeat proteins is sufficient for binding the SCF1 ubiquitin ligase complex. J Gen Virol **90:**1224-8.
83. **Sonnberg, S., B. T. Seet, T. Pawson, S. B. Fleming, and A. A. Mercer.** 2008. Poxvirus ankyrin repeat proteins are a unique class of F-box proteins that associate with cellular SCF1 ubiquitin ligase complexes. Proc Natl Acad Sci U S A **105:**10955-60.
84. **Spencer, E., J. Jiang, and Z. J. Chen.** 1999. Signal-induced ubiquitination of IkappaBalpha by the F-box protein Slimb/beta-TrCP. Genes Dev **13:**284-94.
85. **Stefansson, B., and D. L. Brautigan.** 2006. Protein phosphatase 6 subunit with conserved Sit4-associated protein domain targets IkappaBepsilon. J Biol Chem **281:**22624-34.

86. **Stefansson, B., T. Ohama, A. E. Daugherty, and D. L. Brautigan.** 2008. Protein phosphatase 6 regulatory subunits composed of ankyrin repeat domains. Biochemistry **47:**1442-51.
87. **Tang, Z., B. Li, R. Bharadwaj, H. Zhu, E. Ozkan, K. Hakala, J. Deisenhofer, and H. Yu.** 2001. APC2 Cullin protein and APC11 RING protein comprise the minimal ubiquitin ligase module of the anaphase-promoting complex. Mol Biol Cell **12:**3839-51.
88. **Teale, A., S. Campbell, N. Van Buuren, W. C. Magee, K. Watmough, B. Couturier, R. Shipclark, and M. Barry.** 2009. Orthopoxviruses require a functional ubiquitin-proteasome system for productive replication. J Virol **83:**2099-108.
89. **Tulman, E. R., C. L. Afonso, Z. Lu, L. Zsak, G. F. Kutish, and D. L. Rock.** 2004. The genome of canarypox virus. J Virol **78:**353-66.
90. **Unlu, M., M. E. Morgan, and J. S. Minden.** 1997. Difference gel electrophoresis: a single gel method for detecting changes in protein extracts. Electrophoresis **18:**2071-7.
91. **van Buuren, N., B. Couturier, Y. Xiong, and M. Barry.** 2008. Ectromelia virus encodes a novel family of F-box proteins that interact with the SCF complex. J Virol **82:**9917-27.
92. **Webb, J. H., R. J. Mayer, and L. K. Dixon.** 1999. A lipid modified ubiquitin is packaged into particles of several enveloped viruses. FEBS Lett **444:**136-9.
93. **Werden, S. J., J. Lanchbury, D. Shattuck, C. Neff, M. Dufford, and G. McFadden.** 2009. The myxoma virus m-t5 ankyrin repeat host range protein is a novel adaptor that coordinately links the cellular signaling pathways mediated by Akt and Skp1 in virus-infected cells. J Virol **83:**12068-83.
94. **Werren, J. H., S. Richards, C. A. Desjardins, O. Niehuis, J. Gadau, J. K. Colbourne, L. W. Beukeboom, C. Desplan, C. G. Elsik, C. J. Grimmelikhuijzen, P. Kitts, J. A. Lynch, T. Murphy, D. C. Oliveira, C. D. Smith, L. van de Zande, K. C. Worley, E. M. Zdobnov, M. Aerts, S. Albert, V. H. Anaya, J. M. Anzola, A. R. Barchuk, S. K. Behura, A. N. Bera, M. R. Berenbaum, R. C. Bertossa, M. M. Bitondi, S. R. Bordenstein, P. Bork, E. Bornberg-Bauer, M. Brunain, G. Cazzamali, L. Chaboub, J. Chacko, D. Chavez, C. P. Childers, J. H. Choi, M. E. Clark, C. Claudianos, R. A. Clinton, A. G. Cree, A. S. Cristino, P. M. Dang, A. C. Darby, D. C. de Graaf, B. Devreese, H. H. Dinh, R. Edwards, N. Elango, E. Elhaik, O. Ermolaeva, J. D. Evans, S. Foret, G. R. Fowler, D. Gerlach, J. D. Gibson, D. G. Gilbert, D. Graur, S. Grunder, D. E. Hagen, Y. Han, F. Hauser, D. Hultmark, H. C. t. Hunter, G. D. Hurst, S. N. Jhangian, H. Jiang, R. M. Johnson, A. K. Jones, T. Junier, T. Kadowaki, A. Kamping, Y. Kapustin, B. Kechavarzi, J. Kim, B. Kiryutin, T. Koevoets, C. L. Kovar, E. V. Kriventseva, R. Kucharski, H. Lee, S. L. Lee, K. Lees, L. R. Lewis, D. W. Loehlin, J. M. Logsdon, Jr., J. A. Lopez, R. J. Lozado, D. Maglott, R. Maleszka, A. Mayampurath, D. J. Mazur, M. A. McClure, A. D. Moore, M. B. Morgan, J. Muller, M. C. Munoz-Torres, D. M. Muzny, L. V. Nazareth, et al.** 2010. Functional and evolutionary insights from the genomes of three parasitoid Nasonia species. Science **327:**343-8.

95. **Wolffe, E. J., S. N. Isaacs, and B. Moss.** 1993. Deletion of the vaccinia virus B5R gene encoding a 42-kilodalton membrane glycoprotein inhibits extracellular virus envelope formation and dissemination. J Virol **67:**4732-41.
96. **Xu, L., Y. Wei, J. Reboul, P. Vaglio, T. H. Shin, M. Vidal, S. J. Elledge, and J. W. Harper.** 2003. BTB proteins are substrate-specific adaptors in an SCF-like modular ubiquitin ligase containing CUL-3. Nature **425:**316-21.
97. **Zhang, W. H., D. Wilcock, and G. L. Smith.** 2000. Vaccinia virus F12L protein is required for actin tail formation, normal plaque size, and virulence. J Virol **74:**11654-62.

Appendix

A.1 INTRODUCTION

Poxvirus infection activates a potent immune response that includes both innate and adaptive immunity (17, 23, 29). During the initial stages of viral infection, pattern recognition receptors sense various viral molecules and initiate the innate immune response (34). During innate immunity, genes important for inflammation and initiation of the adaptive immune response are upregulated. One such gene that becomes upregulated is pro-IL-1β, which is an important antiviral cytokine that is responsible for inducing the inflammatory response (9). Pro-IL-1β is cleaved into its active form, IL-1β, in the cytoplasm by the inflammasome (5, 13, 15, 22). Inflammasomes are large multi-protein complexes that assemble following recognition of dsDNA in the cytoplasm by members of the AIM2-like receptor (ALR) family of pattern recognition receptors (5, 13, 15, 22) (Figure A-1). Clustering of AIM2 on multiple DNA binding sites triggers formation of the inflammasome scaffold, resulting in recruitment of the adaptor protein ASC via its pyrin domain. ASC recruits pro-caspase-1 to the inflammasome, and the close proximity of the pro-caspases results in an auto-cleavage reaction to activate caspase-1. Activated caspase-1 subsequently cleaves pro-IL-1β to IL-1β (24).

Pyrin domains are present in a number of cellular proteins that mediate signaling cascades in inflammation, immunity, cell differentiation, apoptosis and cancer (30). The cellular pyrin domain-containing proteins, cPOP1 and cPOP2, are highly homologous to the pyrin domain of ASC, and negatively regulate inflammasome activation by binding ASC and preventing its interaction with ALRs (10, 32) (Figure A-1). Since dsDNA is a product of poxvirus infection, it is not surprising that a number of poxviruses encode pyrin domain-containing proteins that are similar to cPOP1 and cPOP2 which potentially regulate the inflammasome (11). Proteins containing pyrin domains have been identified in MYXV (M013L), Shope Fibroma virus (gp013L), swinepox virus (SPV14L), Yaba-like disease virus (YLDV18L) and deer poxvirus (DPV024) (11); however, only M013L and gp013L have been demonstrated to inhibit the inflammasome (11, 16).

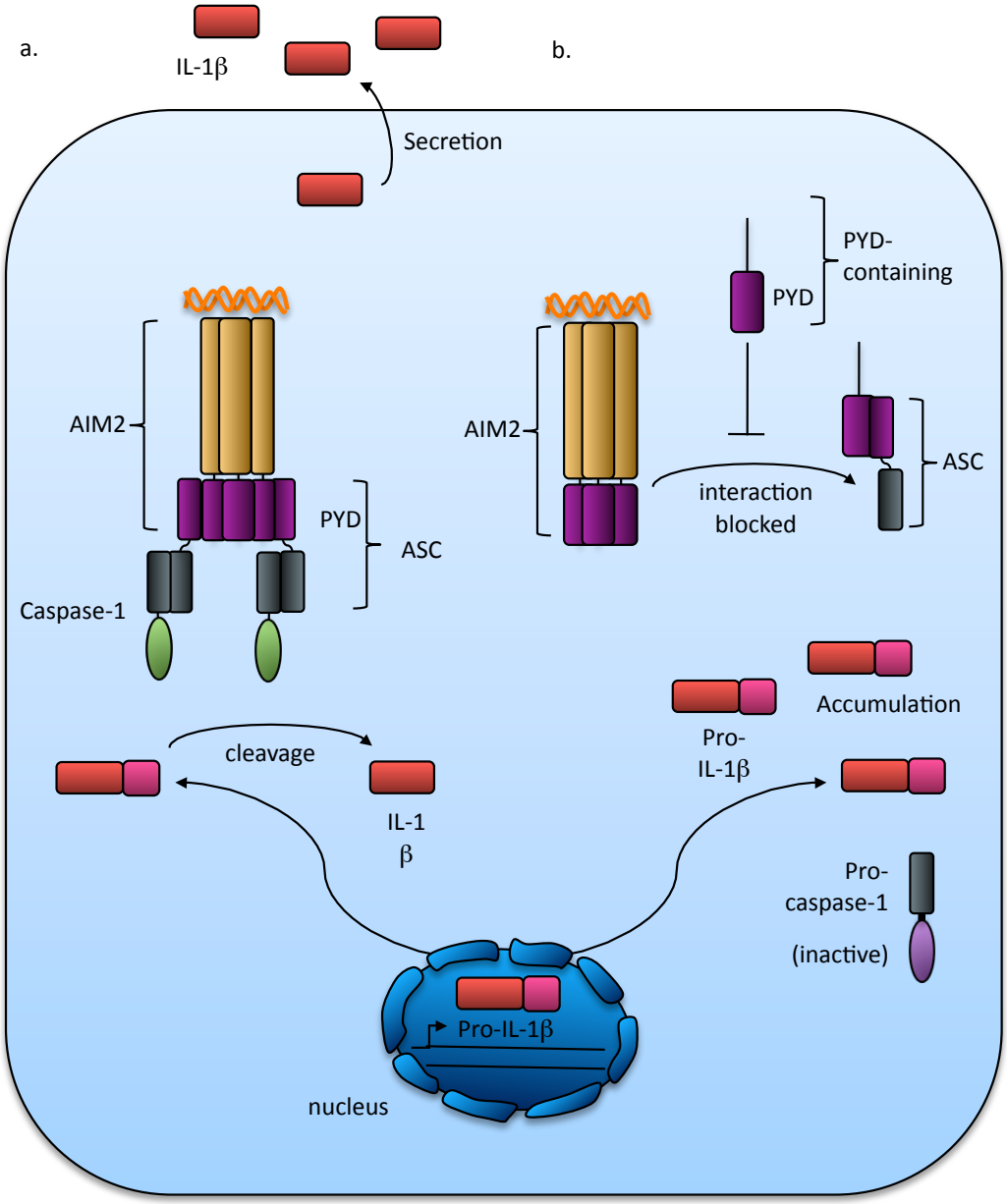

Figure A-1. The AIM2 inflammasome regulates IL-1β activation. In healthy cells, pro-IL-1β is expressed at low levels, and remains in the cytoplasm in its inactive "pro" form. **(a.)** When dsDNA is in the cytoplasm, the sensor AIM2 binds DNA at multiple sites, and the adapter protein ASC is recruited to AIM2 via pyrin-pyrin interactions. ASC recruits pro-caspase-1, and the close proximity of pro-caspases results in an autocleavage reaction that activates caspase-1, so that it can cleave pro-IL-1β into its active form. IL-1β is secreted and stimulates the NFκB and pro-inflammatory pathways in neighboring cells. **(b.)** Proteins containing pyrin domains can negatively regulate inflammasome assembly by binding to the ASC adapter via pyrin-pyrin interactions. This prevents ASC from binding AIM2 and recruiting caspase-1. Pro-IL-1β accumulates in the cell.

Recently, it has also been shown that M013L inhibits NFκB activation through its pyrin domain (25).

Our sequence analysis of the ORF VACVC1L has revealed that VACVC1L contains a putative pyrin domain at the N-terminus (Figure A-2), and a Bcl-2-like fold at the C-terminus (Figure A-3). Recently, our data was confirmed when Gonzalez *et al.* used sequence alignments to demonstrate that VACVC1L fits into the Bcl-2-like family of proteins encoded VACV (14). Proteins containing pyrin domains regulate inflammasome activation via a homotypic interaction with other pyrin domain-containing proteins as discussed above, and the NFκB pathway via heterotypic interactions with proteins in the NFκB cascade (31). Proteins possessing Bcl-2 folds are most often involved in the regulation of apoptosis, but it seems that VACV encodes a subset of Bcl-2-like proteins, A46R, A52R, B15R, K7L and N1L, that are capable of inhibiting NFκB activation (8, 23). Interestingly, anti-apoptotic activity has only been reported for N1L, though these data remain controversial (1, 2, 7). Currently, no function has been assigned to VACVC1L. Given that both pyrin domains and Bcl-2-like domains inhibit the NFκB pathway, and pyrin domains inhibit inflammasome activation, we hypothesized that VACVC1L modulates innate immune signalling.

A.2 MATERIALS AND METHODS

A.2.1 Plasmids

Table A-1 summarizes the plasmids used in this study. pGEM-T (Promega) was used as a subcloning vector for sequencing PCR and restriction enzyme digestion products. Sequencing was performed prior to cloning the products into the final vector, using the T7 and SP6 primer sites that flank the multiple cloning site in pGEM-T. DNA sequences preceded by a Flag sequence were cloned into pcDNA3 (Invitrogen). pEGFP-C2 (Clontech) was used for generating proteins with an N-terminal GFP fusion. pEGFP-N3 (Clontech) was used for generating proteins with C-terminal GFP fusion.

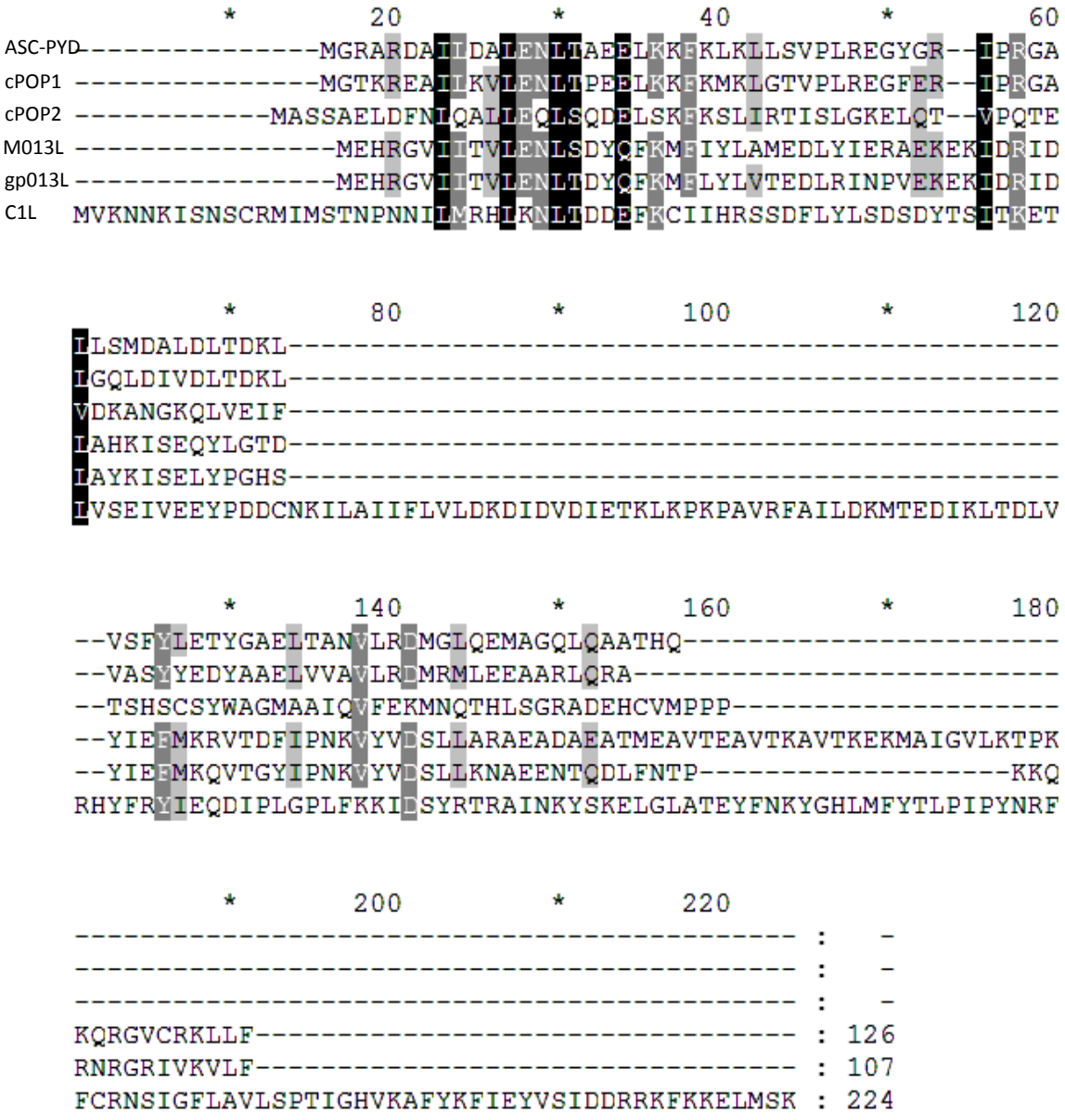

Figure A-2. The N-terminus of C1L aligns with pyrin domain-containing proteins. C1L was aligned with ASC, the pyrin-domain containing inflammasome adapter protein, cPOP1 and cPOP2, two negative regulators of the inflammasome, and myxoma virus M013L and Shope fibroma virus gp103L, two poxvirus pyrin domain-containing proteins that inhibit inflammasome activation. Amino acid sequences were aligned using ClustalW (references 19 and 33).

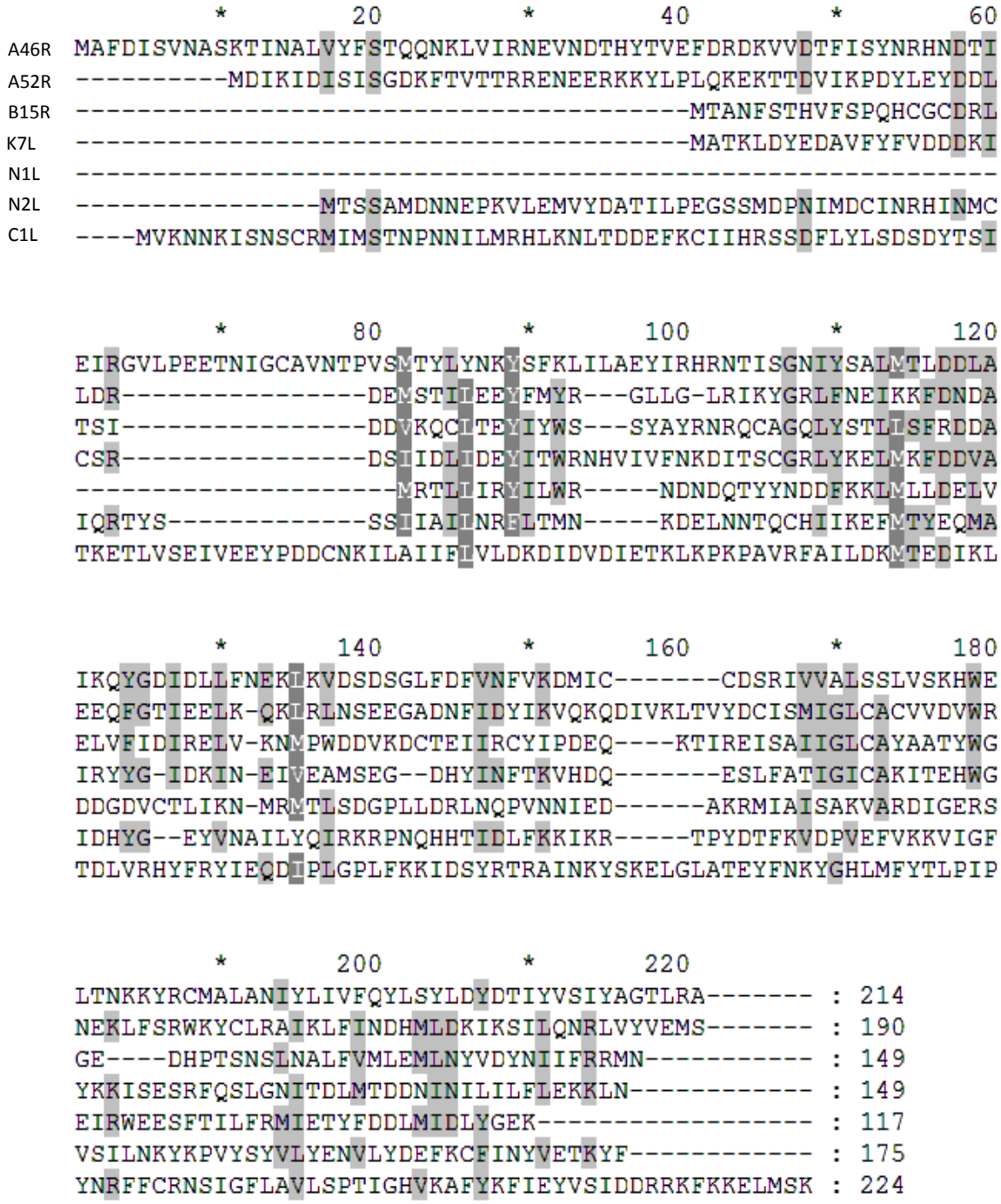

Figure A-3. The C-terminus of C1L aligns with the Bcl-2 family encoded by vaccinia virus. C1L was aligned with members of the vaccinia virus Bcl-2 family. Amino acid sequences were aligned using ClustalW (references 19 and 33). Poxvirus amino acid sequences were obtained from the Poxvirus Bioinformatics Resource Center (reference 20).

A.2.2 Cloning

A.2.2.1 Codon optimization of VACVC1L. Since poxviruses replicate in the cytoplasm, ORFs are not subjected to the RNA processing machinery that exists in the nucleus. As such, many poxvirus ORFs contain cryptic splice sites that are recognized in the nucleus during transient expression, resulting in degradation of the ORF in the nucleus (3). In order to increase the efficiency of transient expression of VACVC1L, we used codon optimization (3). A vector containing CO-VACVC1L was designed to remove cryptic splice sites, and optimize the expression of the ORF in *Homo sapiens* by increasing the guanine and cytosine content in the sequence of the ORF. In addition, vectors were designed for easy cloning into pcDNA3.1 and pEGFP-C2 and pEGFP-N3, in order to generate Flag-tagged and GFP-tagged versions of the ORFs. pMK-RQ-CO-VACVC1L purchased from GENEART and contains from 5' to 3': a *HindIII* cut site, a Flag sequence, the CO-VACVC1L sequence, and a *BamHI* cut site. pMK-RQ-CO-VACVC1L also carries resistance to kanamycin. pMK-RQ-CO-VACVC1L was designed to contain an *EcoRI* cut site between the Flag-sequence and CO-VACVC1L, however there was an error during ordering of the vector, and the *EcoRI* cut site was removed.

A.2.2.2 Generation of pcDNA3-Flag-CO-VACVC1L. In order to generate VACVC1L with a Flag-tag at the N-terminus, pMK-RQ-Flag-CO-VACVC1L was digested with *HindIII* and *BamHI* and the fragment was ligated into pcDNA3.1 (Table A-1) using the *HindIII* and *BamHI* restriction sites.

A.2.2.3 Generation of pcDNA3-CO-VACVC1L-Flag. In order to generate VACVC1L with a Flag-tag at the C-terminus, pMK-RQ-Flag-CO-VACVC1L was used as PCR template with the following primers: CO-VACVC1L-Flag Forward (Table A-2) and CO-VACVC1L-Flag Reverse (Table A-2). The PCR product was subcloned into pGEM-T to generate pGEM-T-CO-VACVC1L-Flag (Table A-1). pcDNA3-CO-VACVC1L-Flag was generated by digesting pGEM-T-COVACVC1L-Flag with *EcoRI* and *BamHI* and ligating the fragment into pcDNA3.1 (Table A-1) using the *EcoRI* and *BamHI* restriction sites.

A.2.2.4 Generation of pEGFP-N-CO-VACVC1L. In order to generate VACVC1L with a GFP-tag at the N-terminus, pMK-RQ-Flag-CO-VACVC1L was used as PCR template with the

Table A-1. Plasmids used in this study

Plasmid	Description	Source
pMK-RQ-CO-VACVC1L	Codon optimized; N-terminal Flag sequence followed by sequence of VACVC1L; *HindIII* at N-terminus and *BamHI* at C-terminus	GENEART
pGEM-T	Subcloning vector; CMV promoter	Promega
pGEM-T-Flag-CO-VACVC1L	Codon optimized; N-terminal Flag sequence; flanked by *EcoRI* and *BamHI*	This study
pGEM-T-CO-VACVC1L-Flag	Codon optimized; C-terminal Flag sequence; flanked by *EcoRI* and *BamHI*	This study
pGEM-T-G-CO-VACVC1L	Codon optimized; VACVC1L sequence followed by a stop codon; flanked by *EcoRI* and *BamHI*	This study
pGEM-T-CO-VACVC1L-G	Codon optimized; start codon followed by VACVC1L sequence; flanked by *EcoRI* and *BamHI*	This study
pcDNA3.1	T7 and CMV promotor	Invitrogen
pcDNA3-Flag-CO-VACVC1L	Codon optimized; N-terminal Flag sequence	This study
pcDNA3-CO-VACVC1L-Flag	Codon optimized; C-terminal Flag sequence	This study
pcDNA3-Flag-CO-ECTV002	Codon optimized; N-terminal Flag	N. van Buuren
pCDNA3-Flag-CO-VACVF1L	Codon optimized; N-terminal Flag	K. Veugelers
pcDNA3-Flag-CO-VACVN1L	Codon optimized; N-terminal Flag	K. Veugelers
pcDNA3-Flag-Bak	N-terminal Flag-tag	G. Shore
pcDNA3-HA-Bax	N-terminal HA-tag	G. McFadden
pEGFP-C2	GFP sequence upstream of the multiple cloning site	Clontech
pEGFP-N-CO-VACVC1L	Codon optimized; N-terminal GFP sequence	This study
pEGFP-N3	GFP sequence downstream of the multiple cloning site	Clontech
pEGFP-C-CO-VACVC1L	Codon optimized; C-terminal GFP sequence	This study
pEGFP-VACVF1L	N-terminal GFP-tag	S. Wasilenko
pRK5-Flag-VACVA52R	N-terminal Flag-tag	A. Bowie

Table A-2. Primers used in this study

Primer name	Primer Sequence (5' to 3')	Restriction Site	Description
CO-VACVC1L-Flag Forward	GAA TTC ATG GTG AAG AAC AAC AAG ATC AGC	*EcoRI*	Used to generate pcDNA3-CO-VACVC1L-Flag
CO-VACVC1L-Flag Reverse	GGA TCC TCA TTT GTC GTC GTC GTC CTT GTA GTC CTT GCT CAT CAG TTC TTT	*BamHI*	Used to generate pcDNA3-CO-VACVC1L-Flag
GFP-CO-VACVC1L Forward	GAA TTC GTG AAG AAC AAC AAG ATC AGC	*EcoRI*	Used to generate pEGFP-N-CO-VACVC1L
GFP-CO-VACVC1L Reverse	GGA TCC TCA CTT GCT CAT CAG TTC TTT	*BamHI*	Used to generate pEGFP-N-CO-VACVC1L
CO-VACVC1L-GFP Forward	GAA TTC ATG GTG AAG AAC AAC AAG ATC AGC	*EcoRI*	Used to generate pEGFP-C-CO-VACVC1L
CO-VACVC1L-GFP Forward	GGA TCC CTT GCT CAT CAG TTC TTT	*BamHI*	Used to generate pEGFP-C-CO-VACVC1L

following primers: GFP-CO-VACVC1L Forward (Table A-2) and GFP-CO-VACVC1L Reverse (Table A-2). The PCR product was subcloned into pGEM-T to generate pGEM-T-G-CO-VACVC1L (Table A-1). pEGFP-N-CO-VACVC1L was generated by digesting pGEM-T-G-CO-VACVC1L with *EcoRI* and *BamHI* and ligating the fragment into pEGFP-C2 (Table A-1) using the *EcoRI* and *BamHI* restriction sites.

A.2.2.5 Generation of pEGFP-C-CO-VACVC1L. In order to generate VACVC1L with a GFP-tag at the C-terminus, pMK-RQ-Flag-CO-VACVC1L was used as PCR template with the following primers: CO-VACVC1L-GFP Forward (Table A-2) and CO-VACVC1L-GFP Reverse (Table A-2). The PCR product was subcloned into pGEM-T to generate pGEM-T-C-CO-VACVC1L (Table A-1). pEGFP-C-CO-VACVC1L was generated by digesting pGEM-T-C-CO-VACVC1L with *EcoRI* and *BamHI* and ligating the fragment into pEGFP-N3 (Table A-1) using the *EcoRI* and *BamHI* restriction sites.

A.2.3 Antibodies

For immunoblots, mouse anti-EGFP (Covance) and mouse anti-FlagM2 (Sigma-Aldrich) were used at a concentration of 1:5000, and the secondary antibody Peroxidase-conjugated AffiniPure goat anti-mouse (Jackson Laboratories) was used at a concentration of 1:25000. For immunofluorescence assays, antibodies used were mouse anti-FlagM2 (Sigma-Aldrich) and rabbit anti-NFκB p65 (Santa Cruz Biotechnology). Both antibodies were used at a concentration of 1:200. Secondary antibodies for immunofluorescence were goat anti-mouse AlexaFlour 488 (Invitrogen) and goat anti-rabbit AlexaFlour 546 (Invitrogen). Both antibodies were used at a concentration of 1:400.

A.2.4 Assays

A.2.4.1 Immunoblots to detect expression of VACVC1L constructs

293T cells (1×10^6) were mock transfected, or transfected with 2μg of pcDNA-Flag-CO-ECTV002, pcDNA3-Flag-CO-VACVC1L, or pcDNA3-CO-VACVC1L-Flag. Eighteen hours post-transfection, whole cell lysates were generated and immunoblotted with mouse

anti-FlagM2. Alternatively, 293T cells (1 x 10^6) were mock transfected, or transfected with 0.5 μg of pEGFP-C2, 2 μg of pEGFP-CO-N-VACVC1L, or 2 μg of pEGFP-CO-C-VACVC1L. Whole cell lysates were generated 18 hours post-transfection and immunoblotted with mouse anti-EGFP.

A.2.4.2 Immunofluorescence microscopy

HeLa cells (2 X 10^5) were seeded on coverslips and mock transfected or transfected with 2 μg pRK5-Flag-VACVA52R or pcDNA3-Flag-CO-VACVC1L. Fourteen hours post-transfection, cells were stimulated with 10 ng/mL of TNFα (Roche) for 20 minutes. Following stimulation, cells were fixed with 2% w/v paraformaldehyde (Sigma-Aldrich) in PBS for 10 minutes, permeabilized with 1% v/v NP-40 (Sigma-Aldrich) in PBS for 5 minutes, and blocked with 30% v/v goat serum (Invitrogen) in PBS for 15 minutes. Cells were incubated overnight with mouse anti-FlagM2 and rabbit anti-NFκB p65. The cells were stained with goat anti-mouse Alexaflour 488 and goat anti-rabbit Alexaflour 546. The cover slips were mounted in 50% v/v glycerol containing 4 mg/mL N-propyl-gallate (Sigma-Aldrich) and 250 μg/mL 4,6-diamino-2-phenylindole (DAPI) (Invitrogen) to visualize nuclei. Cells were visualized using the 40x oil immersion objective of a Ziess Axiovert 200M fluorescent microscope outfitted with an ApoTome 10 optical sectioning device (Carl Zeiss, Inc).

A.2.3.3 Flow cytometry to detect apoptosis

HeLa cells (1 x 10^6) were mock transfected, transfected with 0.5 μg of pEGFP-C2, or transfected with 0.5 μg of pEGFP-C2 in conjunction with 2 μg of pcDNA3-Flag-CO-VACVF1L, 2 μg of pcDNA3-Flag-CO-VACVN1L or 2 μg of pcDNA3-Flag-CO-VACVC1L. Alternatively, cells were transfected with 0.5 μg of pEGFP-C2, 2 μg of pEGFP-VACVF1L, 2 μg of pEGFP-N-CO-VACVN1L or 2 μg of pEGFP-C-CO-VACVC1L and the assay was performed as described above. Apoptosis was induced by stimulating cells with 10 ng/mL of TNFα and 5 μg/mL of cycloheximide (Signma-Aldrich) at 37°C for 4 hours, or by transfecting cells with 2 μg of pcDNA3-HA-Bax or 2 μg of pcDNA3-Flag-Bak for 18 hours.

Following treatment or transfection, cells were stained 37°C for 30 minutes with 0.2 μM of tetramethylrhodamine ethyl ester (TMRE) (Invitrogen) to assess mitochondrial membrane potential (12). Cells were washed twice with PBS containing 1% v/v HI-FBS, and analyzed by measuring through the FL-1 channel with a 489 nm filter (42 nm band-pass filter) and FL-2 channel with a 585 nm filter (42 nm band-pass filter). Data were collected using a FACSan flow cytometer (Bectin Dickinson).

A.3 RESULTS

In order to study VACVC1L, we generated four constructs, pcDNA3-Flag-CO-VACVC1L, pcDNA3-CO-VACVC1L-Flag, pEGFP-N-CO-VACVC1L, and pEGFP-C-CO-VACVC1L (Table A-1 and Figure A-4). Since VACVC1L is a smaller protein, we tagged it at each end in order to ensure that we could study each domain of VACVC1L while limiting the potential for the protein tag to interfere with the structure of function of VACVC1L. pcDNA3-Flag-CO-VACVC1L has an N-terminal Flag-tag and pcDNA3-CO-VACVC1L-Flag is tagged at the C-terminus. pEGFP-N-CO-VACVC1L is tagged with GFP at the N-terminus and pEGFP-C-CO-VACVC1L is tagged at the C-terminus. With the exception of C1L-Flag, expression of the constructs could be detected by immunoblot (Figure A-4).

Since we expected that VACVC1L might inhibit NFκB activation, we used immunofluorescence to assess the location of NFκB p65 following stimulation with TNFα (Figure A-5). HeLa cells were mock transfected or transfected with pRK5-Flag-VACVA52R, or pcDNA3-Flag-CO-VACVC1L. Twelve hours post-transfection, cells were stimulated with TNFα. Nuclei were detected with DAPI, and transfected cells were detected using an antibody for Flag. Staining with an antibody to NFκB p65 revealed that p65 was dispersed throughout the cytoplasm in mock-transfected cells (Figure A-5, panels a-c), whereas mock-transfected cells treated with TNFα displayed dramatic accumulation of p65 in the nucleus (26, 28) (Figure A-5, panels d-f). A52R was used as a negative control since it has been shown to inhibit IL-1β-induced NFκB activation but

a.

pcDNA3-Flag-CO-VACVC1L

pcDNA3-CO-VACVC1L-Flag

pEGFP-N-CO-VACVC1L

a.

pEGFP-C-CO-VACVC1L

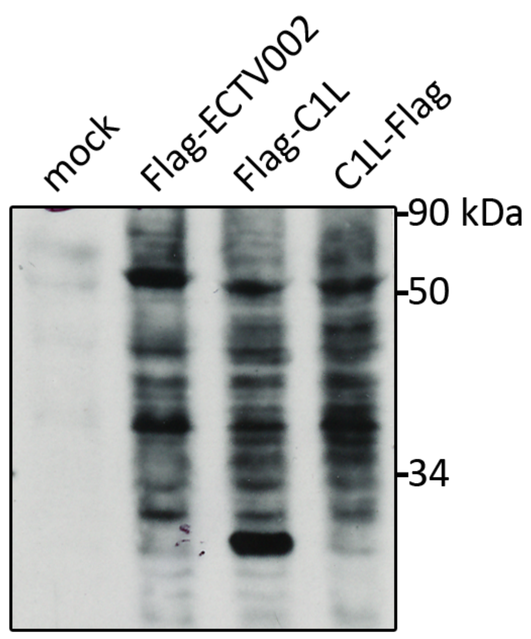

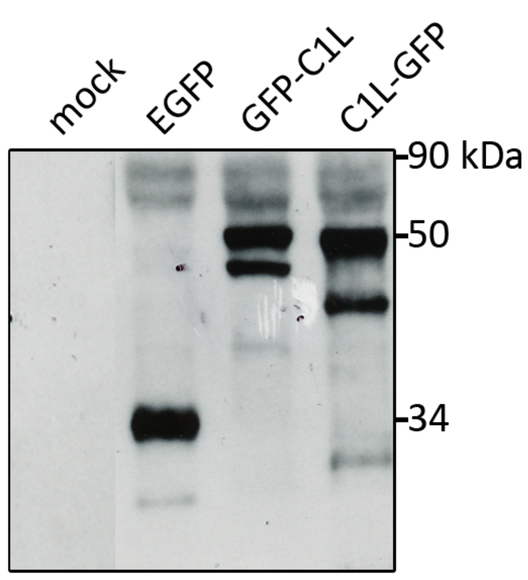

Figure A-4. C1L constructs generated during this study. (a.) Schematic diagram of the four consructs generated in order to study the function of C1L. **(b.)** Detection of expression of C1L constructs by immunoblot. 293T cells were mock transfected or transfected with pcDNA3-Flag-CO-ECTV002, pcDNA3-Flag-CO-VACVC1L, pcDNA3-CO-VACVC1L-Flag, pEGFP-C2, pEGFP-CO-N-VACVC1L, or pEGFP-C-CO-VACVC1L. Eighteen hours post-transfection, whole cell lysates were harvested and immunoblotted with antibodies for Flag or GFP.

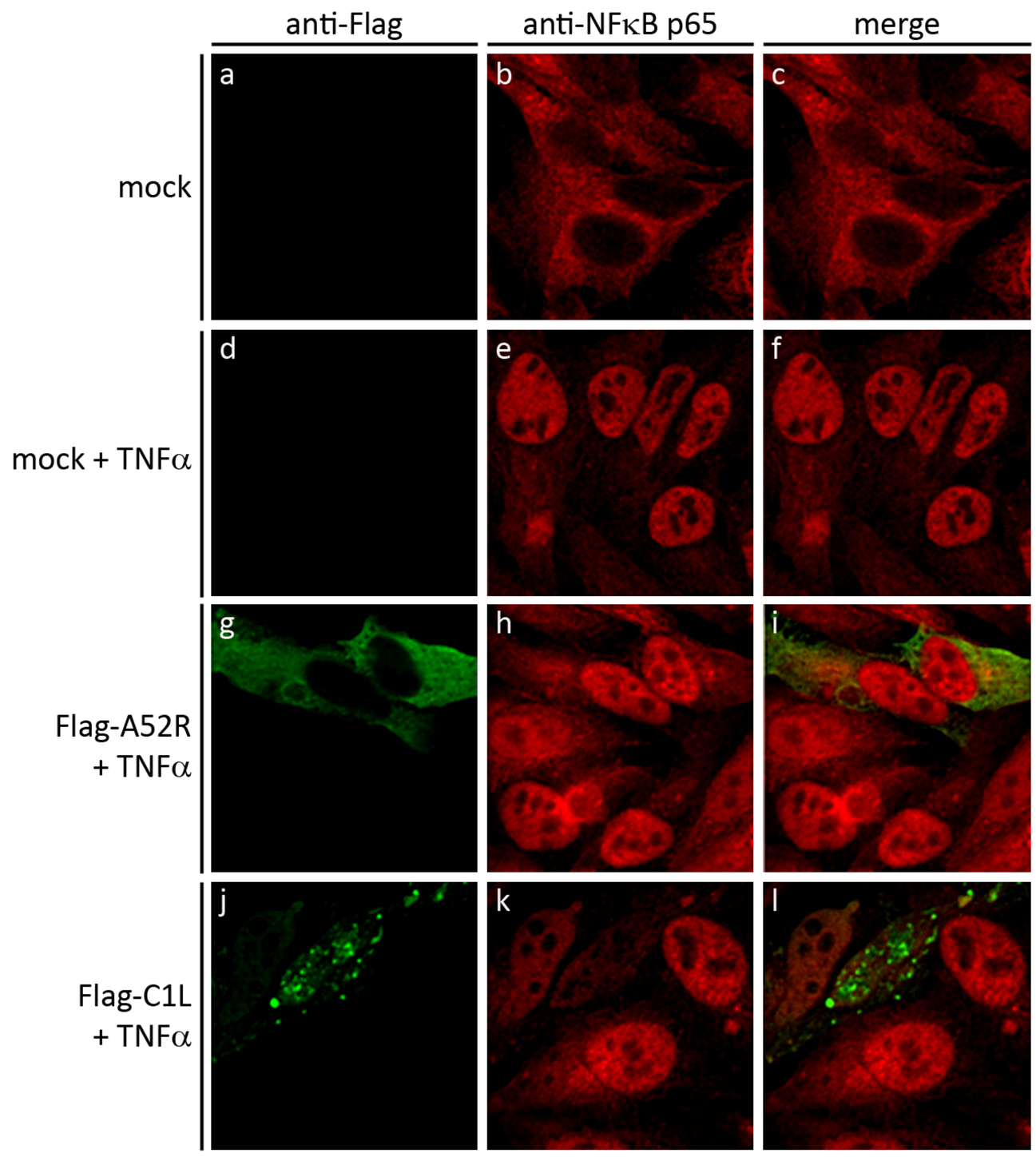

Figure A-5. Expression of C1L does not prevent TNFα-induced NFκB p65 nuclear translocation. HeLa cells were mock transfected (a-f) or transfected with pRK-Flag-VACVA52R (g-i) or pcDNA3-Flag-CO-VACVC1L (j-l). Twelve hours post-transfection, cells were mock stimulated (a-c) or stimulated with 10 ng/mL of TNFα for 20 minutes (d-l). Endogenous p65 was detected with an antibody specific for p65, and nuclei were detected with DAPI.

not TNFα-induced NFκB activation (4). As expected, A52R did not prevent nuclear translocation of p65 (Figure A-5, panels g-i). Interestingly, cells expressing Flag-C1L also displayed nuclear translocation of p65, indicating that VACVC1L does not inhibit TNFα-induced NFκB activation (Figure A-5, panels j-l). Notably, Flag-C1L localized to punctuate structures in the cytoplasm, a phenotype that is often observed with proteins that possess pyrin domains (5, 13). To quantify the percentage of cells displaying p65 nuclear translocation, experiments were performed in triplicate, and p65 nuclear translocation was quantified by counting greater than 150 cells (Figure A-6). Approximately 95% of cells stimulated with TNFα displayed nuclear accumulation of p65 (Figure A-6). In cells transfected with the A52R and Flag-C1L, p65 accumulated in the nuclei of 85% and 60% of cells treated with TNFα, respectively (Figure A-6). Overall, the data indicated that expression of VACVC1L does not prevent NFκB activation during TNFα stimulation.

Since VACVC1L possesses a Bcl-2 domain at the C-terminus (14), we used flow cytometry to determine if expression of VACVC1L could inhibit apoptosis. HeLa cells were transfected with pEGFP-C2 as a negative control, or transfected with pEGFP-C2 in conjunction with pcDNA3-Flag-CO-VACVC1L, or pcDNA3-Flag-CO-VACVF1L or pcDNA3-Flag-CO-VACVN1L as positive controls since they inhibit apoptosis (1, 7, 35). Eighteen hours post-transfection, cells were treated with TNFα and the protein synthesis inhibitor cycloheximide for four hours. TMRE was used to examine mitochondrial membrane potential, and a drop in TMRE corresponded to a drop in membrane potential, which was indicative of apoptosis. Results were displayed as percent death (Figure A-7). Flow cytometry revealed that expression of F1L blocked the loss of membrane potential induced by TNFα and cycloheximide, since only 4% death was observed (Figure A-7). In contrast, EGFP, N1L, and Flag-C1L did not block induction of apoptosis, since cells transfected with pEGFP-C2, pcDNA3-Flag-CO-VACVN1L, or pcDNA3-Flag-CO-VACVC1L, displayed 43%, 42%, and 39% death, respectively. To further demonstrate these data, we repeated the assay using the GFP-tagged VACVC1L constructs and transfected Hela cells with pEGFP-C2, pEGFP-VACVF1L, pEGFP-N-CO-

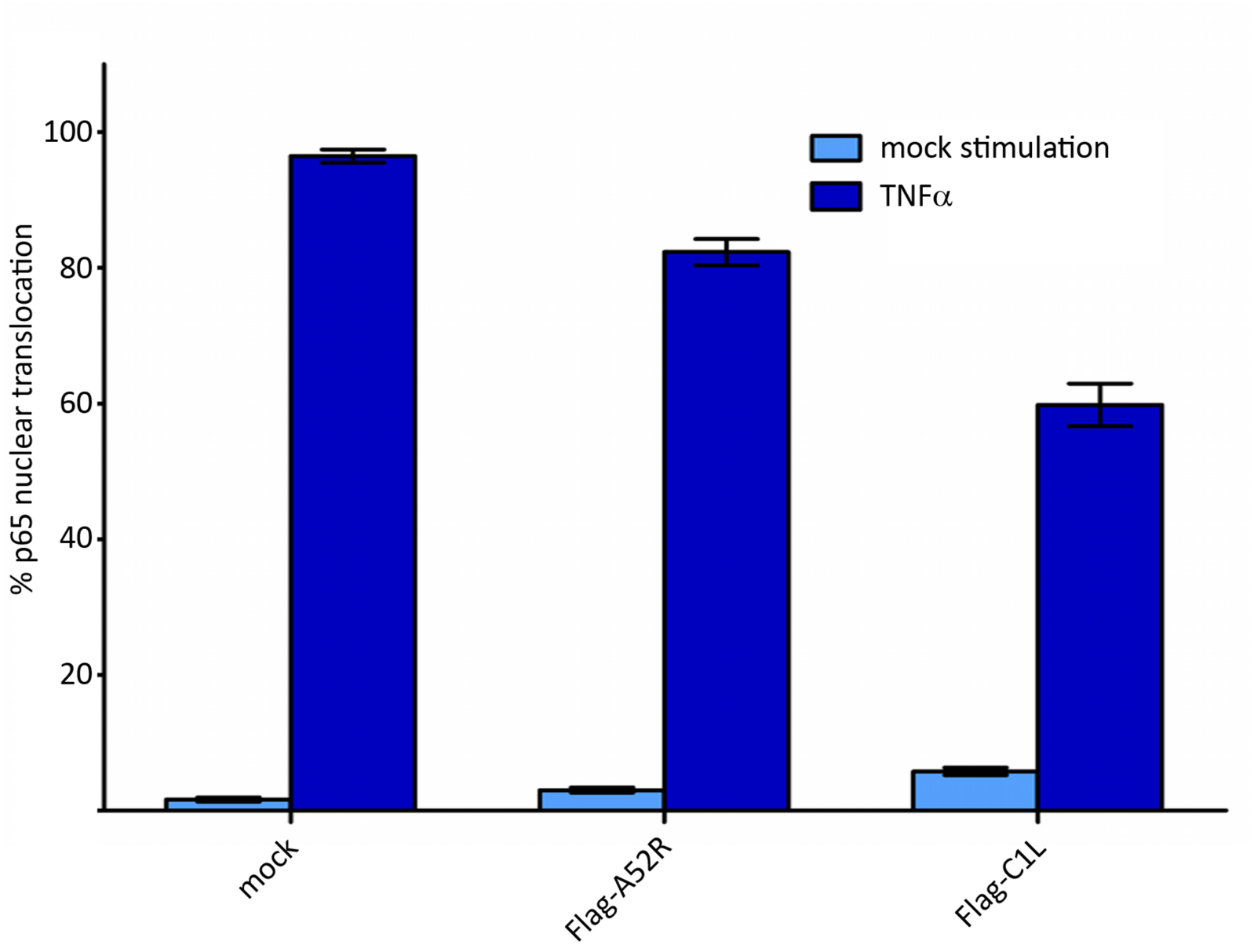

Figure A-6. C1L does not inhibit NFκB p65 nuclear translocation. To quantify NFκB p65 nuclear translocation, a total of 150 cells were counted from three independent experiements and the percentage of cells exhibiting NFκB p65 in the nucleus was calculated.

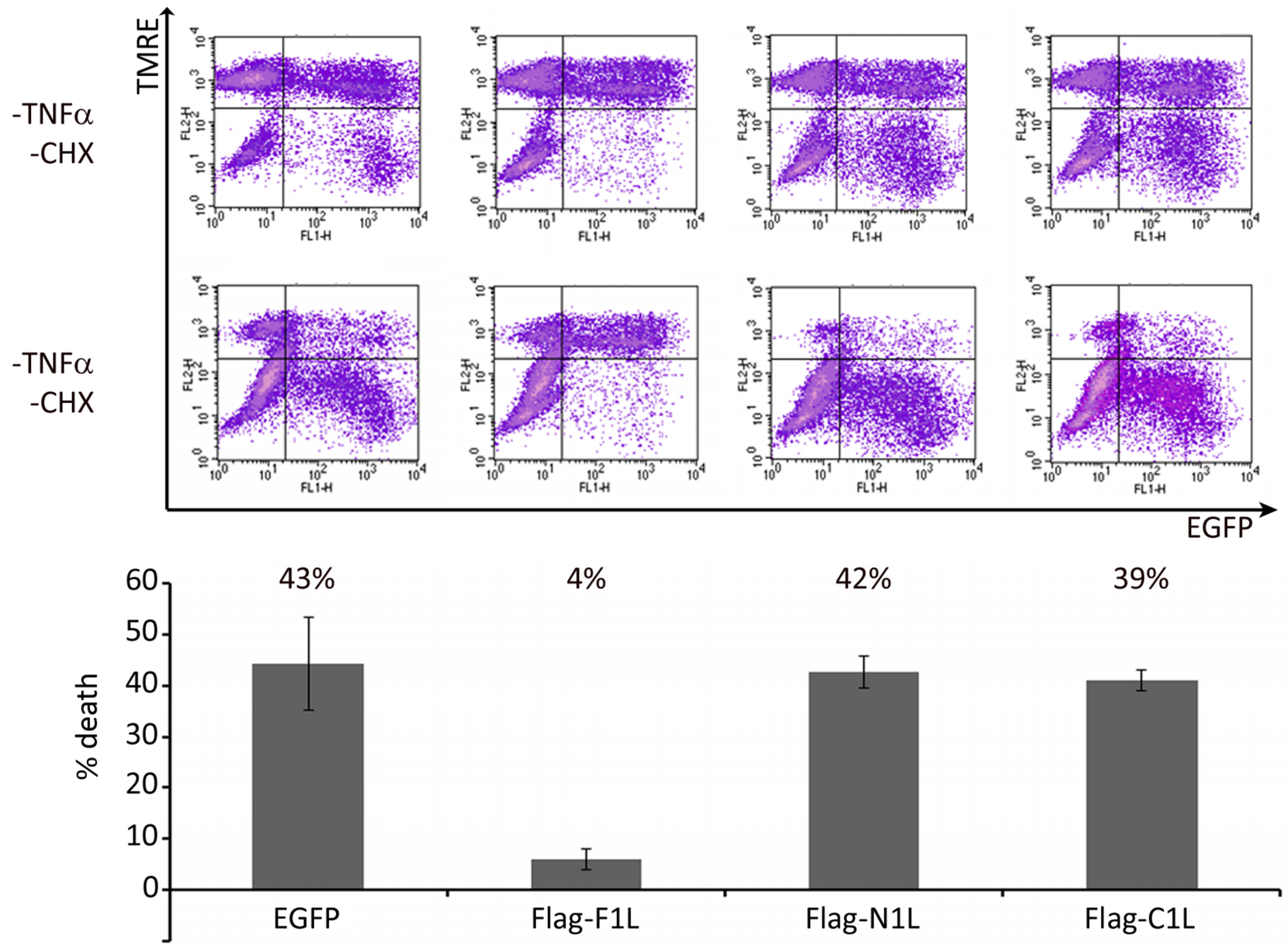

Figure A-7. C1L does not inhibit TNFα-induced apoptosis. HeLa cells were transfected with 0.5 µg of pEGFP-C2, or co-transfected with 0.5 µg of pEGFP-C2 and 2 µg of pCDNA3-Flag-CO-F1L, pcDNA3-Flag-CO-N1L, or pcDNA3-Flag-CO-C1L. Sixteen hours post-transfection, cells were mock stimulated or stimulated with 10 ng/mL of TNFα and 5 µg/mL of cycloheximide (CHX) for 4 hours to induce apoptosis. Cells were stained with TMRE to assess mitochondrial membrane potential and flow cytometry was used to analyze TMRE fluorescence. Three independent experiments, each analysing 20, 000 cells, were performed and representative plots are displayed. The percentage of cells displaying loss of mitochondrial membrane potential after induction of apoptosis was calculated and is diplayed as % death.

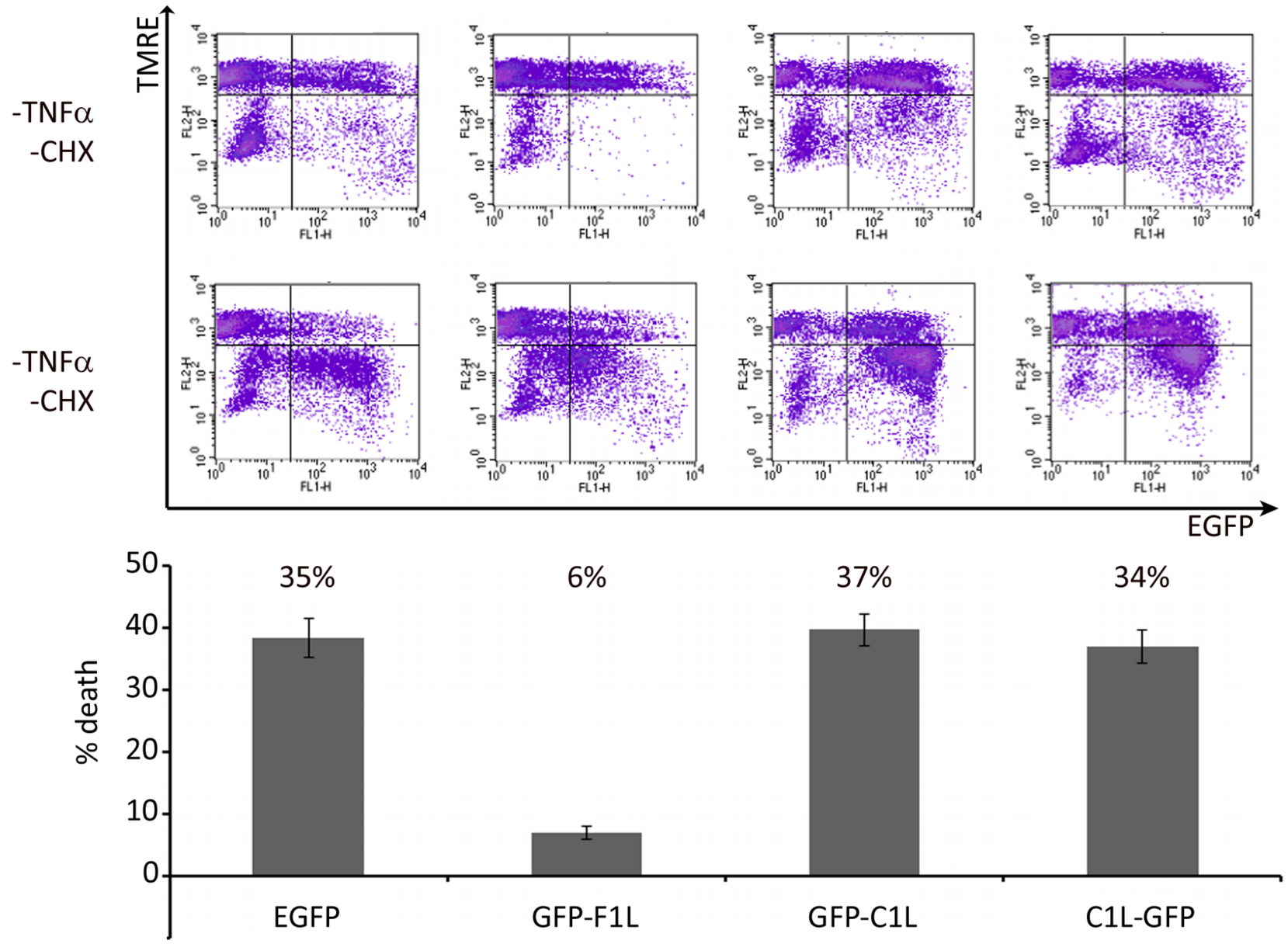

Figure A-8. C1L does not inhibit TNFα-induced apoptosis. HeLa cells were transfected with 0.5 μg of pEGFP-C2, or 2 μg of pEGFP-VACVF1L, pEGFP-N-CO-VACVC1L, or pEGFP-C-CO-VACVC1L. Eighteen hours post-transfection, cells were mock stimulated or stimulated with 10 ng/mL of TNFα and 5 μg/mL of cycloheximide (CHX) for 4 hours to induce apoptosis. Cells were stained with TMRE to assess mitochondrial membrane potential and flow cytometry was used to analyze TMRE fluorescence. Three independent experiments, each analysing 20, 000 cells, were performed and representative plots are displayed. The percentage of cells displaying loss of mitochondrial membrane potential after induction of apoptosis was calculated and is diplayed as % death.

VACVN1L or pEGFP-C-CO-VACVC1L (Figure A-8). Not surprisingly, cells expressing F1L displayed 6% death, and cells expressing EGFP, GFP-C1L, or C1L-GFP displayed 35%, 37%, and 34% death, respectively. Overall, these data indicated that VACVC1L does not protect against TNFα-induced apoptosis.

Apoptosis can be induced by a number of stimuli, including permeabilisation of the outer mitochondrial membrane by the pro-apoptotic proteins Bax or Bak (6, 21, 27, 36). To determine if VACVC1L could inhibit Bax-induced apoptosis, we again used flow cytometry (Figure A-9). HeLa cells were mock transfected or transfected with pEGFP-C2, pEGFP-VACVF1L, pEGFP-N-CO-VACVN1L or pEGFP-C-CO-VACVC1L, with or without pcDNA3-HA-Bax, which induces apoptosis. Eighteen hours post-transfection, cells were stained with TMRE to assess mitochondrial membrane potential. In mock-transfected cells, expression of Bax induced apoptosis in 60% of cells (18) (Figure A-9). Interestingly, apoptosis was also induced in cells expressing the negative control EGFP, and the positive control F1L, since 56% and 65% of cells had undergone death, respectively (Figure A-9). Expression of VACVC1L did not prevent Bax-induced apoptosis, since cells expressing GFP-C1L and C1L-GFP displayed 48% and 29% death, respectively. Interestingly, VACVC1L seemed capable of protecting against Bax-induced apoptosis better than F1L could, however F1L did not present as a valid control in this experiment. Finally, we repeated the assay using transfection of pcDNA3-Flag-Bak as the apoptotic stimuli (Figure A-10). Over-expression of Bak-induced apoptosis in 52% of mock-transfected cells (6), and 50% of cells transfected with the positive control, EGFP (Figure A-10). Apoptosis was induced in 30% of cells expressing the positive control F1L, and in 49% and 30% of cells expressing GFP-C1L and C1L-GFP, respectively. Whether VACV C1L inhibited apoptosis is debatable, since the percentage of death in cells expressing F1L and C1L-GFP was the same. F1L has been used as a control for inhibition of Bak-induced apoptosis before, and the percentage of cell death was less than 5%; however, we could not repeat this data so it is difficult to draw conclusions from this data (2).

Together, the data indicate the VACVC1L does not inhibit TNFα-induced NFκB activation, or apoptosis induced by TNFα. Unfortunately, we did not investigate whether VACVC1L could inhibit activation of the inflammasome.

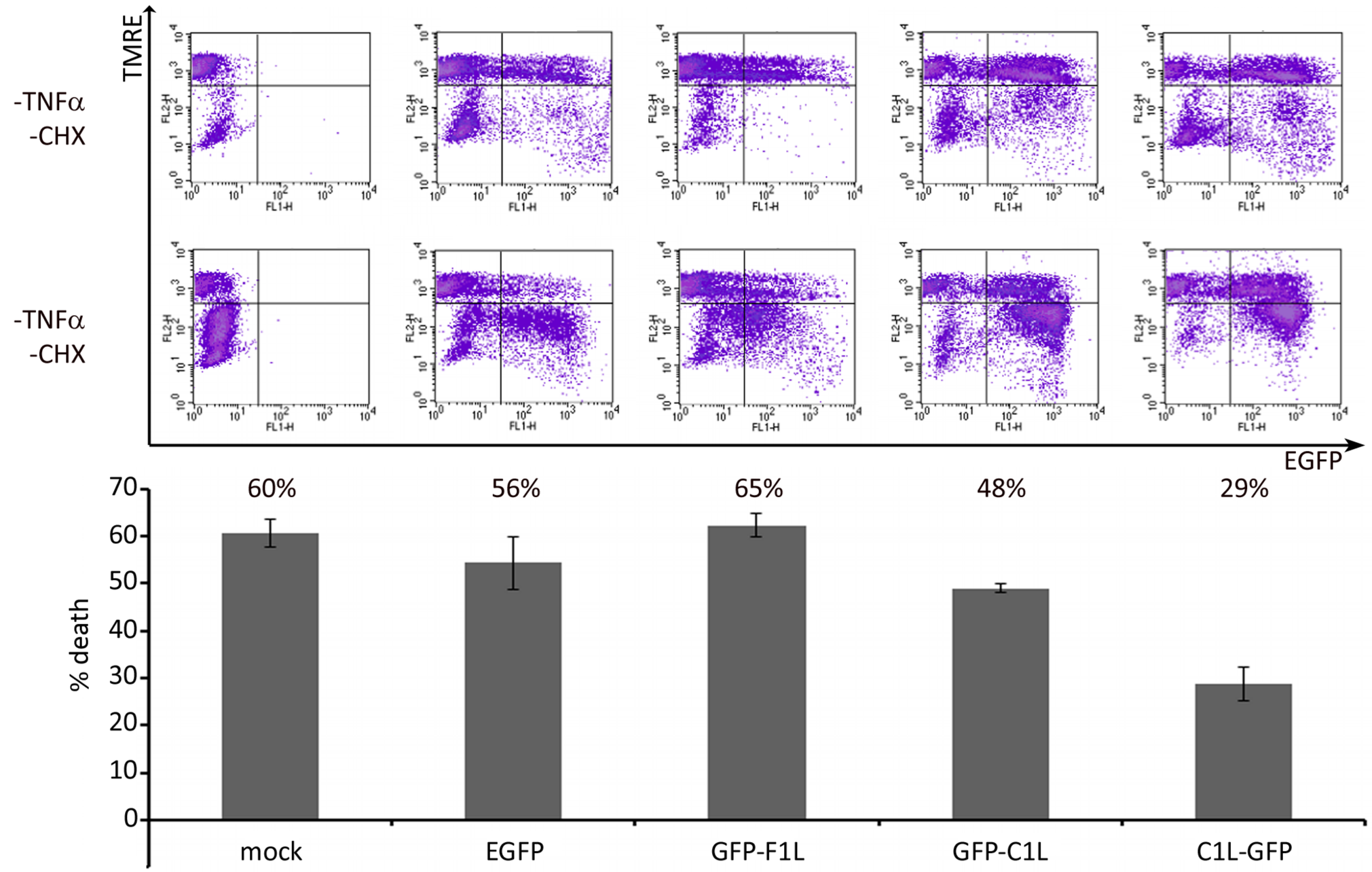

Figure A-9. C1L does not inhibit Bax-induced apoptosis. HeLa cells were mock-transfected, co-transfected with 0.5 µg pcDNA3-HA-Bax and 0.5 µg of pEGFP-C2, or co-transfected with 0.5 µg pcDNA3-HA-Bax and 2 µg of pEGFP-VACVF1L, pEGFP-N-CO-VACVC1L, or pEGFP-C-CO-VACVC1L. Eighteen hours post-transfection, cells were stained with TMRE to assess mitochondrial membrane potential and flow cytometry was used to analyze TMRE fluorescence. Three independent experiments, each analyzing 20, 000 cells, were performed and representative plots are displayed. The percentage of cells displaying loss of mitochondrial membrane potential after induction of apoptosis was calculated and is diplayed as % death.

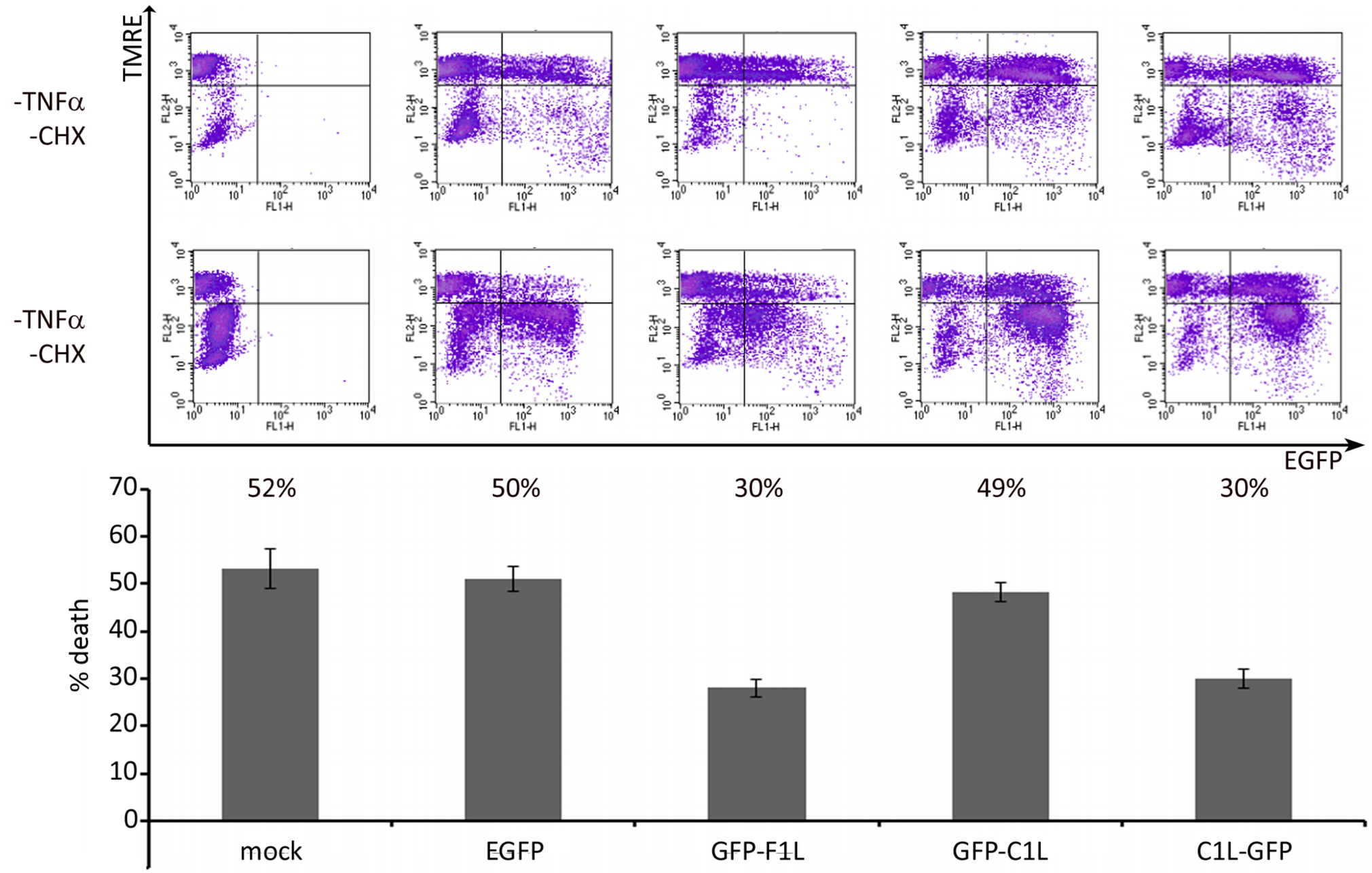

Figure A-10. C1L does not inhibit Bak-induced apoptosis. HeLa cells were mock-transfected, co-transfected with 0.5 µg pcDNA3-HA-Bax and 0.5 µg of pEGFP-C2, or co-transfected with 0.5 µg pcDNA3-Flag-Bak and 2 µg of pEGFP-VACVF1L, pEGFP-N-CO-VACVC1L, or pEGFP-C-CO-VACVC1L. Eighteen hours post-transfection, cells were stained with TMRE to assess mitochondrial membrane potential and flow cytometry was used to analyze TMRE fluorescence. Three independent experiments, each analyzing 20, 000 cells, were performed and representative plots are displayed. The percentage of cells displaying loss of mitochondrial membrane potential after induction of apoptosis was calculated and is diplayed as % death.

A.4 REFERENCES

1. **Aoyagi, M., D. Zhai, C. Jin, A. E. Aleshin, B. Stec, J. C. Reed, and R. C. Liddington.** 2007. Vaccinia virus N1L protein resembles a B cell lymphoma-2 (Bcl-2) family protein. Protein Sci **16:**118-24.
2. **Banadyga, L., K. Veugelers, S. Campbell, and M. Barry.** 2009. The fowlpox virus BCL-2 homologue, FPV039, interacts with activated Bax and a discrete subset of BH3-only proteins to inhibit apoptosis. J Virol **83:**7085-98.
3. **Barrett, J. W., Y. Sun, S. H. Nazarian, T. A. Belsito, C. R. Brunetti, and G. McFadden.** 2006. Optimization of codon usage of poxvirus genes allows for improved transient expression in mammalian cells. Virus Genes **33:**15-26.
4. **Bowie, A., E. Kiss-Toth, J. A. Symons, G. L. Smith, S. K. Dower, and L. A. O'Neill.** 2000. A46R and A52R from vaccinia virus are antagonists of host IL-1 and toll-like receptor signaling. Proc Natl Acad Sci U S A **97:**10162-7.
5. **Burckstummer, T., C. Baumann, S. Bluml, E. Dixit, G. Durnberger, H. Jahn, M. Planyavsky, M. Bilban, J. Colinge, K. L. Bennett, and G. Superti-Furga.** 2009. An orthogonal proteomic-genomic screen identifies AIM2 as a cytoplasmic DNA sensor for the inflammasome. Nat Immunol **10:**266-72.
6. **Chittenden, T., E. A. Harrington, R. O'Connor, C. Flemington, R. J. Lutz, G. I. Evan, and B. C. Guild.** 1995. Induction of apoptosis by the Bcl-2 homologue Bak. Nature **374:**733-6.
7. **Cooray, S., M. W. Bahar, N. G. Abrescia, C. E. McVey, N. W. Bartlett, R. A. Chen, D. I. Stuart, J. M. Grimes, and G. L. Smith.** 2007. Functional and structural studies of the vaccinia virus virulence factor N1 reveal a Bcl-2-like anti-apoptotic protein. J Gen Virol **88:**1656-66.
8. **Danial, N. N., A. Gimenez-Cassina, and D. Tondera.** 2010. Homeostatic functions of BCL-2 proteins beyond apoptosis. Adv Exp Med Biol **687:**1-32.
9. **Dinarello, C. A.** IL-1: discoveries, controversies and future directions. Eur J Immunol **40:**599-606.
10. **Dorfleutner, A., N. B. Bryan, S. J. Talbott, K. N. Funya, S. L. Rellick, J. C. Reed, X. Shi, Y. Rojanasakul, D. C. Flynn, and C. Stehlik.** 2007. Cellular pyrin domain-only protein 2 is a candidate regulator of inflammasome activation. Infect Immun **75:**1484-92.
11. **Dorfleutner, A., S. J. Talbott, N. B. Bryan, K. N. Funya, S. L. Rellick, J. C. Reed, X. Shi, Y. Rojanasakul, D. C. Flynn, and C. Stehlik.** 2007. A Shope Fibroma virus PYRIN-only protein modulates the host immune response. Virus Genes **35:**685-94.
12. **Ehrenberg, B., V. Montana, M. D. Wei, J. P. Wuskell, and L. M. Loew.** 1988. Membrane potential can be determined in individual cells from the nernstian distribution of cationic dyes. Biophys J **53:**785-94.
13. **Fernandes-Alnemri, T., J. W. Yu, P. Datta, J. Wu, and E. S. Alnemri.** 2009. AIM2 activates the inflammasome and cell death in response to cytoplasmic DNA. Nature **458:**509-13.

14. **Gonzalez, J. M., and M. Esteban.** 2010. A poxvirus Bcl-2-like gene family involved in regulation of host immune response: sequence similarity and evolutionary history. Virol J **7:**59.
15. **Hornung, V., A. Ablasser, M. Charrel-Dennis, F. Bauernfeind, G. Horvath, D. R. Caffrey, E. Latz, and K. A. Fitzgerald.** 2009. AIM2 recognizes cytosolic dsDNA and forms a caspase-1-activating inflammasome with ASC. Nature **458:**514-8.
16. **Johnston, J. B., J. W. Barrett, S. H. Nazarian, M. Goodwin, D. Ricciuto, G. Wang, and G. McFadden.** 2005. A poxvirus-encoded pyrin domain protein interacts with ASC-1 to inhibit host inflammatory and apoptotic responses to infection. Immunity **23:**587-98.
17. **Johnston, J. B., and G. McFadden.** 2003. Poxvirus immunomodulatory strategies: current perspectives. J Virol **77:**6093-100.
18. **Kitanaka, C., T. Namiki, K. Noguchi, T. Mochizuki, S. Kagaya, S. Chi, A. Hayashi, A. Asai, Y. Tsujimoto, and Y. Kuchino.** 1997. Caspase-dependent apoptosis of COS-7 cells induced by Bax overexpression: differential effects of Bcl-2 and Bcl-xL on Bax-induced caspase activation and apoptosis. Oncogene **15:**1763-72.
19. **Larkin, M. A., G. Blackshields, N. P. Brown, R. Chenna, P. A. McGettigan, H. McWilliam, F. Valentin, I. M. Wallace, A. Wilm, R. Lopez, J. D. Thompson, T. J. Gibson, and D. G. Higgins.** 2007. Clustal W and Clustal X version 2.0. Bioinformatics **23:**2947-8.
20. **Lefkowitz, E. J., C. Upton, S. S. Changayil, C. Buck, P. Traktman, and R. M. Buller.** 2005. Poxvirus Bioinformatics Resource Center: a comprehensive Poxviridae informational and analytical resource. Nucleic Acids Res **33:**D311-6.
21. **Lindsten, T., A. J. Ross, A. King, W. X. Zong, J. C. Rathmell, H. A. Shiels, E. Ulrich, K. G. Waymire, P. Mahar, K. Frauwirth, Y. Chen, M. Wei, V. M. Eng, D. M. Adelman, M. C. Simon, A. Ma, J. A. Golden, G. Evan, S. J. Korsmeyer, G. R. MacGregor, and C. B. Thompson.** 2000. The combined functions of proapoptotic Bcl-2 family members bak and bax are essential for normal development of multiple tissues. Mol Cell **6:**1389-99.
22. **Martinon, F., A. Mayor, and J. Tschopp.** 2009. The inflammasomes: guardians of the body. Annu Rev Immunol **27:**229-65.
23. **Mohamed, M. R., and G. McFadden.** 2009. NFkB inhibitors: strategies from poxviruses. Cell Cycle **8:**3125-32.
24. **Muruve, D. A., V. Petrilli, A. K. Zaiss, L. R. White, S. A. Clark, P. J. Ross, R. J. Parks, and J. Tschopp.** 2008. The inflammasome recognizes cytosolic microbial and host DNA and triggers an innate immune response. Nature **452:**103-7.
25. **Rahman, M. M., M. R. Mohamed, M. Kim, S. Smallwood, and G. McFadden.** 2009. Co-regulation of NF-kappaB and inflammasome-mediated inflammatory responses by myxoma virus pyrin domain-containing protein M013. PLoS Pathog **5:**e1000635.
26. **Salminen, A., T. Paimela, T. Suuronen, and K. Kaarniranta.** 2008. Innate immunity meets with cellular stress at the IKK complex: regulation of the IKK complex by HSP70 and HSP90. Immunol Lett **117:**9-15.

27. **Schinzel, A., T. Kaufmann, and C. Borner.** 2004. Bcl-2 family members: integrators of survival and death signals in physiology and pathology [corrected]. Biochim Biophys Acta **1644:**95-105.
28. **Schroder, M., M. Baran, and A. G. Bowie.** 2008. Viral targeting of DEAD box protein 3 reveals its role in TBK1/IKKepsilon-mediated IRF activation. EMBO J **27:**2147-57.
29. **Seet, B. T., J. B. Johnston, C. R. Brunetti, J. W. Barrett, H. Everett, C. Cameron, J. Sypula, S. H. Nazarian, A. Lucas, and G. McFadden.** 2003. Poxviruses and immune evasion. Annu Rev Immunol **21:**377-423.
30. **Stehlik, C., and A. Dorfleutner.** 2007. COPs and POPs: modulators of inflammasome activity. J Immunol **179:**7993-8.
31. **Stehlik, C., L. Fiorentino, A. Dorfleutner, J. M. Bruey, E. M. Ariza, J. Sagara, and J. C. Reed.** 2002. The PAAD/PYRIN-family protein ASC is a dual regulator of a conserved step in nuclear factor kappaB activation pathways. J Exp Med **196:**1605-15.
32. **Stehlik, C., M. Krajewska, K. Welsh, S. Krajewski, A. Godzik, and J. C. Reed.** 2003. The PAAD/PYRIN-only protein POP1/ASC2 is a modulator of ASC-mediated nuclear-factor-kappa B and pro-caspase-1 regulation. Biochem J **373:**101-13.
33. **Thompson, J. D., D. G. Higgins, and T. J. Gibson.** 1994. CLUSTAL W: improving the sensitivity of progressive multiple sequence alignment through sequence weighting, position-specific gap penalties and weight matrix choice. Nucleic Acids Res **22:**4673-80.
34. **Thompson, M. R., J. J. Kaminski, E. A. Kurt-Jones, and K. A. Fitzgerald.** 2011. Pattern recognition receptors and the innate immune response to viral infection. Viruses **3:**920-40.
35. **Wasilenko, S. T., T. L. Stewart, A. F. Meyers, and M. Barry.** 2003. Vaccinia virus encodes a previously uncharacterized mitochondrial-associated inhibitor of apoptosis. Proc Natl Acad Sci U S A **100:**14345-50.
36. **Wei, M. C., W. X. Zong, E. H. Cheng, T. Lindsten, V. Panoutsakopoulou, A. J. Ross, K. A. Roth, G. R. MacGregor, C. B. Thompson, and S. J. Korsmeyer.** 2001. Proapoptotic BAX and BAK: a requisite gateway to mitochondrial dysfunction and death. Science **292:**727-30.